University College London

Division of Biosciences

Neuroscience

Thesis submitted for the degree of Doctor of Philosophy

Academic Year   2012

Sanusi Mohammad Bello

The Role of Cadherins and Catenins in the Segregation and Migration of Spinal Motor Neurons

Supervisor: Dr Stephen R. Price

September 2012

Declaration

I, Sanusi Mohammad Bello, do hereby declare that this thesis represents entirely my work and where any information is derived from other sources, I confirmed that this has been clearly indicated in the thesis.

Signed……………………………..

Date……………………………….

ABSTRACT

During development Spinal motor neurons are generated from their point of origin in the ventricular zone and migrate to reach their final settling position (motor pools) in the ventral spinal cord. The formation of motor pools depends on early motor column segregation; cadherins cell adhesive proteins have been implicated in the segregation of motor neurons in the spinal cord but the exact role for these cell-cell adhesion molecules in the organisation and migration of spinal motor neurons during development is not established. I show that during development expression of cadherins contribute to the organisation and migration of spinal lateral motor column (LMC) motor neurons to their final settling positions and there is close association between spinal motor neuron and radial glia. Misexpression of a dominant negative cadherin results in abnormal migration of spinal motor neurons and columnar desegregation. Similarly, expression of a dominant negative catenin (a major cytoplasmic binding partner to cadherins) results in columnar desegregation and arrest of motor neuron along their migratory route.

Perturbations of Wnt signalling have no effect on motor neurons migration indicating that the results are due to perturbation of cadherin adhesive function. Our observation that cadherin and catenins but not Wnt signalling contributes to normal migration and segregation of spinal motor neurons, suggest that cadherin may act in close association with radial glia in directing the migration of spinal motor neurons similar to the establish role of radial glia in cortical neuronal migration.

Keywords:

Cadherins, Catenins, Motor neuron, Migration, Radial Glia, Spinal cord

Acknowledgements

First of all, I wish to express my sincere gratitude and appreciation to my supervisor in person of Dr Stephen R Price for the opportunity given me to carry out this work in his laboratory and for the support and guidance throughout the period of this PhD. I will never forget the support I received from you.

I am equally grateful to past members of the Price research group notably: Dr Manisha Rajebhosale, Dr Hadas Milo, Dr Waleed Mubarak, Dr Zahra Samji, Mark Hintze, Samantha Kviklyte, Dr Robert Perry and Salma. To the present lab members namely: Dr Rosanna C G Smith, Dr Marc R Astick, and Kristina Tubby, I must say thank you for being kind, supportive and friendly throughout the period of the work leading to this thesis.

To the members of the central laboratory in the department; Mary Rahman and Pala I say thank you for offering your support. To members of the Stan laboratory namely: Sharon Boast, Dr Ali Ghanem, Sittipon, and Mathew I say thank you for the access to use some of your equipments while conducting this work. I must mention the names of members of the Jessen laboratory namely, Dr Peter Arthur Farraj, Dr Daniel Wilton, Dr Susana, Kathleen Malgapo and Lucy Carty for being friendly and supportive throughout the period of this work.

To all the supporting staff in the teaching office, admin, finance and store I say thank you for contributing in various ways to the success of this work. To Debbie Bartram, and Helen Jefferson-Brown. To Ian Blanley, Michael, and Jonathan. To all my friends in UCL and London namely: Umar Mohammed Sada, Shamsu Ibrahim Hassan ,Lawal Bello Moriki and Dr Umar Lamorde I say thank you all!

Abbreviations

ADP	Adenosine diphosphate
ALPHA-CAT	Alpha catenin
APC	Adenomatous Polyposis Coli: tumour suppressor gene
ALS	Amyotrophic Lateral Sclerosis
ANOVA	Analysis of Variance
APP	Amyloid precursor protein
ATP	Adenosine Tri-Phosphate
BrdU	Bromodeoxyuridine (5' bromo 2'-deoxyuridine)
BETA CAT	Beta (β) Catenin
BSA	Bovine Serum Albumin
BETA GAL	Beta (β) Galactosidase
CAGS	CAG promoter
CDNA	Complementary DNA
CP	Cortical Plate
CY3	Cyanine (dye) 3
CY5	Cyanine (dye) 5
CCD	Close Circuit Digital Camera
CDN	Cadherin Dominant Negative
CDK	Cyclin-dependent kinase
CNS	Central Nervous System
COREL-DRAW 13	Corel-Draw Image software
DAKO PEN	Dako Cytomation Immuno pen marker
DMEM	Dulbeco's Modified Eagle Medium

4D5	39.4D5 Islet-1 antibody
DH5-ALPHA	E.Coli strain for routine cloning applications
DRG	Dorsal Root Ganglion
EAP3	Exon Associated Protein 3
E-GFP-N3	e- Green Fluorescence Protein
E (N)	Embryonic (day)
EM	Electron Microscopy
EPLIN	Epithelial protein lost in neoplasm
ER81	ETS family transcription factor
ETS	E-twenty six family of transcription factors
FITC	Fluoresceine isothiocyanate
FGF8	Fibroblast growth factor 8
FOXP1	Forkhead box(fox) protein P1(a pan LMC transcription factor)
GFP	Green Fluorescence protein
GABA	Gama Amino Butyric Acid
GAMA CAT	Gama (γ) Catenin
GAP	GTPase activating protein
GTPASE	Guanosine triphosphate(hydrolysis enzyme)
GDNF	Glial cell derived neurotrophic factor
GDNR	Glial cell derived neurotrophic factor receptor
GFAP	Glial fibrillary acidic protein
GFRa1	Glial cell line derived neurotrophic factor receptor alpha 1
GPI	Glucose-6-phosphate Isomerase
GSK3β	Glycogen synthase kinas 3 β

HA	Haemaglutinin antibody
HB-9	Homeobox-9
HBSS	Hanks balanced salt solution
HH	Hamilton and Hamburger
5-HT	5-Hydroxytryptamine – also called serotonin
IgG1	Immunoglobulin G subclass 1
IgG2B	Immunoglobulin G subclass 2b
IPLAB	Scientific image analysis software
IRES	Internal ribosome entry site
ISLET-1	Lim/homeodomain transcription factor
ISLET-2	Lim/homeodomain transcription factor
ICV	Intracerebroventricular
IV	Interventricular
IZ	Intermediate zone
JNK	cJun N-terminal kinases pathway
K+	Potassium ion
KANAMYCIN	Kanamycin antibiotic
LB	Lysogenic broth(rich medium for growing bacteria)
LIM-1	Lim homeobox 1
LHX1	Lhx1 gene
LIM-2	Lim homeobox 2
LMC	Lateral motor column
LMCm	Lateral motor column medial
LMCl	Lateral motor column lateral

MAPK	Mitogen-activated protein kinase
MMC	Medial motor column
MMCm	Median motor column medial
MMCl	Median motor column lateral
Mg2+	Magnesium ion
MNs	Motor neurons
MN-CAD	Alternative name for Cadherin-20
MNDs	Motor neuron disease
MNR2	Homeobox protein that specify Motor neuron identity
mRNA	Messenger RNA
Myc	Myc- a transcription factor
MZ	Marginal Zone
NPRAP	Neural plakoglobin-related armadillo repeat
N-390 CAD	N-Δ390 cadherin
NCAM	Neural Cell Adhesion Molecule (also CD56)
NGF	Nerve growth factor
NJPA1	Neuron-glial junctional polypeptide antibody
NKX2.2	Homeobox protein coded by Nkx2.2 gene
NKX6	Homeobox protein coded by NKx6 gene
NO	Nitric oxide
OCT	Optimum concentrating temperature
OLIG2	Oligodendrocyte transcriptions factor 2-regulator of ventral neuroectodermal cell fate.

PB	Phosphate buffer
PBS	Phosphate buffer saline
PCR	Polymerase chain reaction
PEN-STREP	Penicillin-streptomycin antibiotic
PFA	Para formaldehyde
PG	Preganglionic
PGC	Preganglionic columns (column of Terni in chick)
P1	Buffer-P1- Resuspension buffer
P2	Buffer P2- Lysis buffer
P3	Buffer P3- Neutralization buffer
PTP1B	Phosphor-tyrosine protein phosphatase 1B
P-VALUE	Statistical significance test
QBT	Buffer QBT- Equilibration buffer
QF	Buffer QF- Elution buffer
RA	Retinoic Acid
RNA	Ribonucleic acid
SC	Spinal cord
Shh	Sonic hedgehog
SN	Spinal nerve
SOC	Super Optimal Broth with Catabolite repression
SVZ	Sub ventricular zone
T-CAD	T-cadherin
TCF	T-cell factor

TRITON X 100   Non-ionic surfactant used as a laboratory detergent

T-TEST   Statistical test of two means

WT   Wild type

TABLE OF CONTENTS

LIST OF FIGURES

LIST OF TABLES

1 Introduction

1.1 Organization of the Central Nervous System.

A fundamental tenet in the organisation of the nervous system, particularly in that of vertebrates, is that structure and function are intimately related. Functionally related neurons are most often found in similar regions of the nervous system, thus partitioning of the nervous system seems to predict function of the neurons at that location. This functional segregation of neurons in the CNS occurs along two main architectural schemes. First, in evolutionarily more recent regions of the nervous system, a prime example being the cortex, functionally related neurons tend to be stratified into layers or laminae (Rakic, 1972). Secondly, in evolutionarily more ancient regions for example the midbrain, hindbrain and cerebellum, functionally related neurons tend to be clustered into three dimensional groupings termed neuronal nuclei (Ramon y Cajal 1911). There are, of course parallels in the organisation in both regions. For example, in the dorsal spinal cord, the primary mode of organisation is in terms of layers of neurons that receive different sensory inputs. Additionally, within the layers of the cortex, adjacent neurons sub serve related functions. Examples of this "within plane" organisation are the ocular dominance columns whereby input from each eye to the primary visual cortex is segregated. Nevertheless, these two organisational schemes demarcate two distinct modes of neuronal segregation, one with a more two-dimensional nature (laminae) and one three dimensional (nuclei). The evolutionary reason for these differences may well lie in the ability of layers to pack more neurons into a given volume compared to nuclei. However, very little has been demonstrated about how and why neurons segregate in different ways in the nervous system. Indeed, whilst some strides have been made in our understanding of the mechanisms of cortical lamination, very little is understood of neuronal nucleus formation. This mode of

organisation is the focus of research in the Price lab and will form the main theme of the research in this thesis.

1.2 Cell type diversity in the nervous system.

Irrespective of the mode of organisation, the developing central nervous system generates numerous distinct subtypes of neurons both in space and time, and this emergence of neuronal diversity is critical to the assembly of functional neuronal circuits. Therefore, to understand the function of the nervous system and how this function is ultimately translated to behaviour of the organism requires that we gain greater knowledge of the molecular control of the acquisition of neuronal identity. This knowledge is also a key to uncovering the mechanisms of neurological diseases whereby developmental mechanisms may have been misappropriated for example in the pathogenesis of spina bifida. Also recent studies suggests the involvement of mutations common to both human and other animals in the genesis of developmental neuroanomalies with consequent on motor neuron identity deficiency (Shums et al., 2010, Copp et al., 2011, Robinson et al., 2012). Additionally, a greater understanding of the regulation of neuronal subtype identity may be critical to the development of treatments for the repair of damaged nervous systems. A promising approach, beyond the scope of this introductory chapter is the use of progenitor cell populations and/or stem cells in the treatment of neurodegenerative diseases.

Over the past several decades, considerable progress has been made in the area of identifying the signals and elucidating the molecular mechanisms that regulate neural cell fate (Edlund &Jessell 1999; Jessell 2000; Shirasaki & Pfaff 2002). To a good first approximation, initially uncommitted neural progenitor populations regionally restricted to locations along the rostro caudal and dorso ventral axes acquire their fate by exposure

to different types and concentrations of signals. These so-called extrinsic signals regulate sets of intrinsic, cell-specific transcription factors which specify cell fate by controlling the transcription of multiple downstream genes.

Research on the regulation of neuronal subtype identity is particularly advanced in the vertebrate spinal cord. The spinal cord essentially performs two main and critical functions for the organism; namely the transmission of peripheral sensory information and the generation of characteristic motor outputs. The neurons that process and relay sensory input are found, predominantly, in the dorsal half of the spinal cord, whereas the neurons that participate in motor output, including motor neurons (MNs), are located ventrally (Ramon y Cajal 1906). Thus, the organisation of the nervous system intimately reflects the function of the neurons at that location. This positioning is to a large extent a consequence of the developmental origin of each individual neuronal subtype. Here, I will focus on neuronal development in ventral regions of the spinal cord and discuss recent work that has shed light on the molecular mechanisms controlling the generation of these neuronal subtypes.

1.3 Organization of the Spinal cord

The spinal cord is the most caudal part of the central nervous system and arguably the most evolutionarily ancient part of the CNS. In humans, it extends from the base of the skull to the first lumbar vertebra. Its main functions are to receive sensory information from the skin, joints, and muscles of the trunk and the limbs and to control both voluntary and reflex movements via the activation of motor neurons.

Owing to the larger number of motor neurons located at limb-levels, the size and shape of the spinal cord varies along its length. Macroscopically, it is divided in to two main portions, the gray matter and surrounding white matter.

The gray matter contains the nerve cell bodies and is typically divided into ventral and dorsal horns because it appears as an "H"-shape in transverse section. The dorsal horn contains layers of orderly arranged sensory relay neurons that receive input from the skin while the ventral horn contains motor neurons that innervate specific muscles in the limbs and the trunk.

The white matter is largely composed of longitudinal tracts of myelinated axons. These tracts are composed of both ascending pathways, through which sensory information reaches the brain and descending pathway that carry motor commands and modulatory influences from the brain. Within Humans, there are 31 pairs of spinal nerves each with a sensory (dorsal root) and motor (ventral root) divisions emerging from the dorsal and ventral aspect of the spinal cord respectively. The dorsal root carries sensory information in to the spinal cord from the skin and muscles. Different axons coursing in the dorsal root mediate sensations of pain, temperature and touch which are all associated with specialised sensory receptor cells found peripherally. Activation of motor neurons in the spinal cord represents the ultimate destination of all neural activity since all higher brain levels controlling motor activity must ultimately act through these neurons in the ventral spinal cord in order to promote muscle contraction and thus movement.

The main mechanism used during development in order to set up these dorsal versus ventral characteristics of the spinal cord makes use of regionalisation of neural progenitor cells in the dorso-ventral axis. This specification of neuronal identity in the central nervous system is controlled by inductive signals secreted by embryonic organizing centres during development (Tanabe and Jessell, 1996, Lumsden and Krumlauf 1996).

Briefly, these signals define cell fate by regulating transcription factor expression (Bang and Goulding, 1996). The differentiation of motor neurons depends on signals provided by Sonic Hedgehog (Shh) that is produced from the notochord and floor plate (Tanabe et al, 1995, Ericson et al, 1996, Chiang et al, 1996).

Initially, Shh converts medial neural plate cells into a ventral progenitor population (Ericson 1996) and later it directs the differentiation of these ventral progenitors into motor neurons and interneurons respectively depending on different concentration thresholds (Roelink et al, 1995., Ericson et al, 1997). Cells in the ventral progenitor domains respond to graded Shh signalling by establishing distinct ventral progenitor domains defined through the expression of homeodomain proteins Pax6 and Nkx2.2 in the brain stem and spinal cord (Ericson et al, 1997).

Within the brainstem, these two distinct ventral progenitor populations generate distinct classes of motor neurons. Within a ventral region of the Pax6+ progenitors generate somatic motor neurons which project axons to the extra ocular eye muscles and muscles that control movement of the eye. The further ventral progenitors expressing Nkx2.2 produce visceral motor neurons, which innervate the ganglia associated with the sympathetic nervous system and also the motor neurons derived from the branchial arches, the so-called branchiomotor neurons. As they exit the cell cycle, these two progenitor populations express additional homeodomain proteins that further characterize distinct motor neuron subtypes (Tsuchida et al, 1994, Varela-Echaveria et al 1996, Ericson et al 1997). In contrast, the current belief is that spinal motor neurons are only expressed by the ventral Pax-6 domain with no, or little, contribution of the Nkx2.2 domain.

1.4 Generation of Spinal Motor neurons and a hierarchy of identity acquisition.

Motor neurons are largely unique in that they project axons out of the spinal cord in to the periphery to innervate individual targets. Additionally, motor neurons share common features such as large soma and cholinergic phenotype. Spinal MNs are generated when two inductive signals, Sonic hedgehog and retinoic acid (RA), induce the expression of the essential MN determinant, the homeodomain transcription factor Olig2, in neural progenitors (Briscoe and Novitch, 2008). The expression of Olig2 depends on the prior expression by the motor neuron progenitors of an additional homeodomain containing transcription factor of the Nkx6 sub-family. As MNs arise from Olig2+ cells, they subsequently diversify into distinct functional subtypes based on their position along the rostro caudal axis and within each body segment (Jessell, 2000; Landmesser, 2001). The first transcription factor to be expressed as motor neurons become post mitotic is the homeodomain factor Hb9/MNR2. In the chicken, forced expression of MNR2 is sufficient to change dorsal neurons into a motor neuron type. This forced expression of MNR2 results in cells of a cholinergic phenotype that project axons ventrally and out of the ventral roots. These results suggest that MNR2 is a determinant of a generic motor neuron identity.

Along the rostro-caudal axis, limb-projecting motor neurons are only found in spinal cord segments adjacent to the limb and absent in the thoracic spinal cord. This gross rostrocaudal patterning of motor neurons has been ascribed to differential expression of Hox genes regulated by paraxial mesoderm expression of retinoic acid signals. (Liu et al., 2001; Dasen et al., 2003, 2005). The mechanisms that establish the intra segmental diversification of limb-projecting motor neurons also depends on differential Hox gene expression (described below).

21

However, the positional cues that allow MNs to segregate into different classes that innervate different muscle and autonomic nervous system targets throughout the body are only beginning to be elucidated.

 MNs first organize into longitudinal columns that extend along the rostro caudal axis of the embryo to facilitate the matching of MNs with their synaptic targets (Landmesser, 1978; Jessell, 2000). At limb levels, newly born MNs separate to form a median motor column (MMC) that innervates trunk muscles, and a lateral motor column (LMC) that innervates the developing limbs (Jessell, 2000; Shirasaki and Pfaff, 2002). A similar separation occurs in the thoracic spinal cord, leading to the formation of an MMC and a different group of lateral MNs termed the preganglionic motor column (PGC; referred to as the column of Terni in chickens), which innervates the sympathetic nervous system (Jessell, 2000; Shirasaki and Pfaff, 2002). MMC and LMC motor neurons then segregate further forming medial and lateral sub-columns, also called motor neuron divisions, (MMCm, MMCl, LMCm, and LMCl) that respectively innervate the dorsal and ventral halves of the trunk and limbs (Jessell, 2000; Shirasaki and Pfaff, 2002). Superimposed on the divisional organization of the LMC, MNs subdivide into even smaller groupings, termed motor pools, which innervate the individual muscles within each target region (Romanes, 1964; Jessell, 2000; Dasen et al., 2005). Much less is known about pool organisation within the MMC, presumably owing to its composition of much fewer motor neurons.

Thus, there is a temporal sequence by which motor neurons acquire their specific positioning, reflective of the axon targets of the motor neurons. This temporal sequence represents a hierarchy of motor neuron subtype identity acquisition. Coupled to this hierarchy are the expression of distinct transcription factor profiles of the motor neurons that imbue the neurons with their different columnar, divisional and pool identities.

Recent work has begun to shed light on how distinct transcriptional networks act at post mitotic stages of differentiation to diversify MNs, particularly during the course of post mitotic MNs differentiation to establish a unique three-dimensional motor coordinate system required to steer movement.

The rostro caudal position of the motor columns is established by the functions of specific Hox transcription factors expressed along the body axis. The cross repressive actions of Hox6 and Hox9 proteins play a critical role in specifying the formation of LMC versus PGC motor columns at brachial and thoracic levels, respectively (Dasen et al., 2003), while Hox10 proteins regulate LMC formation at lumbar levels(Carpenter et al., 1997; Lin and Carpenter, 2003; Shah et al., 2004). At later times, the combinatorial expression of different Hox proteins further subdivides the columns into individual motor pools, indicating that Hox proteins can contribute to the intra segmental organization of MNs (Dasen et al., 2005). To identify novel regulators of MN diversification, an analysis of the genes that are differentially expressed in control versus Olig2 mutant spinal cord progenitors, which lack the ability to form MNs, was performed (Mukouyama et al., 2006; Briscoe and Novitch, 2008).

Through this approach, the Forkhead domain transcription factor Foxp1 was identified as a protein prominently expressed by MNs only at limb levels and absent from thoracic levels of the spinal cord; suggesting that Foxp1 might contribute to the generation of different populations of MNs within these body segments. Although Foxp1 expression has been observed in multiple regions of the central nervous system (Tamura et al., 2003), its function in neural development has just recently been examined. Loss of Foxp1 causes LMC neurons to become scrambled and adopt a more MMC-like phenotype, although they still project axons into the limb. Forced expression of Foxp1 converts MMC cells into an LMC phenotype.

Interestingly, there is an intimate link between Hox protein expression and the induction of Foxp1 only in Limb levels of the spinal cord suggesting that Foxp1 is a major determinant of LMC identity.

As the same pattern of Hox protein expression is often observed within multiple motor columns present at the same rostro caudal position (Liu et al., 2001; Dasen et al., 2005), additional mechanisms must exist to provide MNs with their intra segmental, divisional, identity. To date, the best candidates for regulating the divisional identity of MNs is members of the LIM-homeodomain (LIM-HD) transcription factor family. The specific profile of LIM-HD proteins expressed by a MN correlates with its columnar status (Tsuchida et al., 1994; Jessell, 2000; Shirasaki and Pfaff, 2002), for example the LMCm cells express islet-1 whereas the LMCl cells express Lhx1. Experimental alterations of the code of LIM-HD proteins expressed by a MN can alter its cell body settling position, axonal projections, and target specificities; loss of Lhx1 results in a randomisation of axon projections into the dorsal and ventral limbs whereas forced expression of Lhx1 redirects LMCm axons to the dorsal limb (Sharma et al., 1998, 2000; Kania et al., 2000; Kania and Jessell, 2003; Thaleret al., 2004). However, most LIM-HD proteins are broadly expressed by MNs as they are initially formed (Sharma et al., 1998; Tanabe et al., 1998), becoming restricted in their expression.

1.5 Motor pool organisation of spinal motor neurons

The typical vertebrate limb contains more than 50 muscle groups, and each of these targets is innervated by a unique pool of motor neurons. Detailed motor pool maps have been described in the middle of the last century in the developing and adult spinal cord (Romanes, 1964; Landmesser, 1978; Hollyday, 1980). Motor neurons within a motor pool share three common features: first, they project axons to the same muscle in the limb (Landmesser, 1978). Second, they all receive monosynaptic input from proprioceptive sensory neurons innervating the same muscle target (Frank et al., 1988) and finally motor neurons in the same motor pool are electrically coupled together by selective gap junction coupling (Beronwitz et al., 1983). The distinct motor neurons pools are distributed within the motor columns in the ventral spinal cord forming synapses with distinct muscles groups in a very precise fashion, thereby allowing coordinated contraction and relaxation of specific muscles (Goulding, 1998). In many cases the cell bodies of motor neurons are clustered indiscrete nuclei, although the physiological relevance to motor pool clustering is still uncertain.

Anatomical studies of the position of motor pools in the spinal cord have revealed that each motor pool occupies a stereotypical position in the spinal cord. Of note is that the topography of motor neuron position in the anterior-posterior, medial–lateral and dorsal-ventral axes of the spinal cord map onto the innervation of the limb muscles in Proximal-distal, dorsal-ventral and anterior-posterior axes of the limb. A motor pool within the LMC typically spans two to three segments of the spinal cord, and the number of motor neurons within a given pool is proportional to size of the muscle it innervates.

Much less is known of the acquisition of this topographic identity of motor neuron pools. For a restricted subset of motor neurons, Nkx6 proteins continue to be expressed within a subset of post mitotic motor neurons in a pool restricted pattern. Loss of post-mitotic Nkx6 expression results in a loss of pool specificity of those motor neurons axon projections. Further, forced expression of Nkx6 proteins seems to rewire axon projections of neurons not normally fated to project axons to those muscles. Thus, there also appears to be a transcriptional correlate of motor pool identity superimposed on the divisional identity of motor neurons.

Of particular note is the finding that members of the ETS family of transcription factors also subdivide motor columns into different pools. For example, in chicken the Adductor (LMCm) and Femorotibialis (LMCl) motor pools express Er81 and the illiotrochanterici (LMCl) motor pool expresses PEA3. Expression of these genes is also correlated to those sensory neurons that will make monosynaptic connections to ETS expressing motor pools. For example, Adductor and Femorotibialis projecting sensory neurons also express Er81. This suggests the possibility that matched ETS expression could also drive matched cell surface potentials to drive specificity of monosynaptic connection. This hypothesis has proven difficult to test as the removal of PEA3 in the mouse results in an unexpected phenotype.

Loss of PEA3 caused a failure of the axons of PEA3 motor pools to terminally arborize in their appropriate muscle. Additionally, and unexpectedly, the PEA3 motor pools also failed to form appropriate clusters in the ventral horn. This finding rather muddies the investigation of the specificity of monosynaptic connectivity in the PEA3 mutant.

However, dendritic arborisation of PEA3 motor neurons and also monosynaptic connectivity was lost in the PEA3 mutant suggesting that PEA3 may control synapse specificity either directly or through the correct positioning of motor neurons within the ventral horn (Fig 1.1).

The expression of ETS genes is dependent on signals from the limb. Removal of the limb bud of the chicken results in a loss of both Er81 and PEA3 in motor neurons. This ETS expression seems to rely on neurotrophic factor signalling from pockets of GDNF in the limb mesenchyme. Loss of the GDNR receptor GFRa1 in motor neurons reveals a concomitant loss of PEA3 expression and loss of GDNF itself causes the same phenotype. Interestingly, bath application of GDNF to a spinal cord dissected out of the GDNF mutant induced expression of PEA3 only in the appropriate motor neurons. Taken together, these results suggest that motor pool expression of ETS genes depends on neurotrophic factors permissively rather than instructively. In both the GDNF and GFRa1 mutants the cell body positions of PEA3 motor pools were also scrambled. Recent work has also revealed a scrambling of motor pools in the Foxp1 mutant mouse and interestingly a concomitant loss of specificity of monosynaptic contact to those motor neurons.

Of further note is that the sensory afferent projections into the ventral horn appeared normal. This suggests that the actions of PEA3 on monosynaptic specificity may well be due to the correct positioning of the motor neurons within the ventral horn and that this relies on extrinsic signals from the limb. How then do motor neurons achieve their correct positions within the ventral horn?

Figure 1.1 ETS protein expression by motor pools and connectivity in the spinal monosynaptic reflex circuit.

Schematic diagram of ETS protein expression in the ventral spinal cord motor neuron pools at the level of (LS2) second lumbo-sacral region and connectivity in the spinal monosynaptic reflex circuit connectivity. The coloured segments in each circle in the dorsal root ganglion (DRG) denote percentage $ER81^+$, $PEA3^+$, or $ER81^-/PEA3^-$ neurons. Specific motor pools of the LMCm and the LMCl represented in the ventral horn of the spinal cord are for LMCl: Iliotrochanterici (ITR) external femorotibialis (eF), internal femeorotibialis (iF), the Sartorius (S) and for the LMCm, the Adductor (A). Their corresponding limb muscles on the left side of the panel are connected accordingly. (Derived *from Lin et al., Cell, vol. 95, 393-407, October, 1998*)
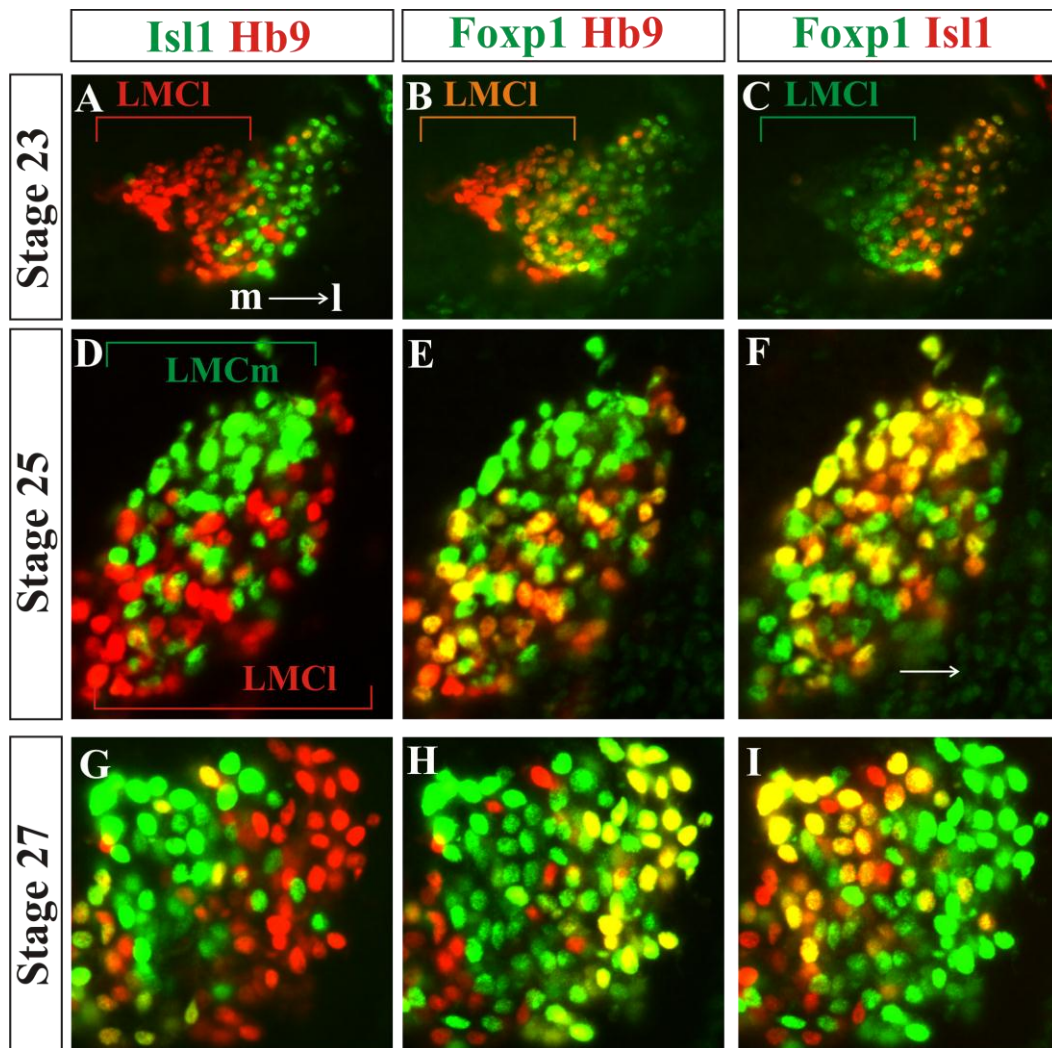
Figure 1.2 Expression profile of Foxp1 and LIM-HD protein at lumbar region of developing chick spinal cord.

Time course of motor neurons segregation showing the pan expression of foxp1 in the ventral lumbar spinal cord of chick embryo at various developmental stages. *A-G*, expression of Islet-1 and HB9. *B-I* expression of Foxp1 along the ventral lumbar spinal cord at stages 23 (*B-C*), stages 25 (*E-F*), and stages 27 (*H-I*).

1.6 Spinal motor neuron segregation

The birthdates of LMC divisions and pools occurs at subtly different times. The LMCm is born before the LMCl and within each division; individual motor pools differ in their timing by the order of several hours. The segregation of the lateral motor column motor neurons into discrete motor neuron pools begins immediately after these neurons exit the cell cycle and occurs in two phases. In one phase motor neurons segregate by means of an inside-out migration where prospective LMCl motor neurons migrate through the neurons of the LMCm to reach their final settling position (Holliday and Hamburger, 1977; Sockanathan and Jessell, 1998). Superimposed on this medio-lateral migration phase is a pool specific aggregation of motor neurons that presumably occurs in a dorso-ventral in addition to medio-lateral segregation. However, to date, time-lapse imaging of pool segregation has eluded experimental validification and so these processes are inferred from static images of the location of ETS positive motor pools during development. Thus, in the chicken, the main stages of motor neuron segregation occur from birth (around stage 17) to stage 24 or 25 whereby migration is the dominant segregation mechanism. From stage 25 to stage 29/30 motor pool segregation occurs. A similar time course of segregation also occurs in the mouse with most motor neurons born before e10.5 followed by a rapid divisional segregation, complete by e11.5 and pool specificity emerging until around e13.5.

The emergence of motor pool sorting in the chicken is driven by the differential expression of members of the type II subfamily of cadherin cell adhesion molecules. Type II cadherins are differentially expressed in lumbar and brachial motor pools and the combination of cadherins expressed within motor neurons uniquely identifies all the motor neurons of a given motor pool at a given level of the spinal cord. For example, in the second lumbar spinal segment the Adductor motor pool expresses cadherins -13, -

6b, -8 and -20. In contrast, the adjacent Femorotibialis motor pool neurons express cadherins -13, -6b and -8 such that both are identifiably distinguishable by the expression of cadherin-20 within the Adductor motor neurons. Equalisation of cadherin expression profiles between the Adductor and Femorotibialis by either the addition of cadherin-20 in the F pool or the removal of cad-20 function in the A pool resulted in a mixing of A and F motor pools. In contrast, control manipulations of cadherin expression profiles through misexpression of either cadherin-6b (expressed in both A and F motor pools) or E-cadherin (expressed in neither A nor F motor pools) resulted in no mixing of the motor neurons. These data suggested that the cadherin expression profiles of A and F neurons were both necessary and sufficient for the segregation of the motor pools (Fig 1.3).

The differential cadherin expression profiles of distinct motor pools displayed a highly dynamic time course of expression. For some motor neurons, pool specific cadherin expression was initiated after the medio-lateral migratory phase of divisional segregation. For a different set of cadherins, typified by the expression profile of cadherin-20, initially broad or pan-motor neuron expression was refined subsequent to the motor divisional segregation phase. Thus, the mature pattern of differential pool-specific cadherin expression emerged during the pool segregation phase of motor neuron organisation. This pool specific expression of cadherins required signals from the limb as limb ablation disrupted the later, but interestingly not the earlier, phase of cadherin expression. This result was very similar to that obtained for the ETS genes PEA3 and Er81 where the induction of ETS expression required limb-derived signals. Indeed, misexpression of Er81 is sufficient to induce ectopic expression of cadherin-20. Taken together, these data suggest that limb-derived signals modulate cadherin expression in motor neurons through the pool specific induction of ETS protein

31

expression (Fig 1.4). In support of this model, the PEA3, GDNF and GFRa1 mutant mice also show a perturbation of cadherin expression within motor neurons. It thus seems likely that the disruption of pool sorting in the PEA3, GDNF and GFRa1 mice is a direct result of the deregulation of cadherin expression in those mutant mice.

Recent work in the Price lab has demonstrated that differential cadherin expression is also found amongst the brainstem motor neurons that contribute axons to distinct cranial nerves. In addition, equalisation of the cadherin expression profile between two cranial motor nuclei results in those neurons comingling. Further, cadherin expression profiles are initially broadly expressed followed by a dynamic change in expression to reveal the nucleus specific expression of cadherins. This switch in cadherin expression is also associated with extrinsic signals influencing the motor neurons. In the case of the motor nuclei in the middle of the brainstem at rhombomere 5, this extrinsic signal appears to be from a local brainstem source of FGF8, which is expressed in the auditory hindbrain nuclei required for sound source localisation. Thus, the concept of an initially broad cadherin expression profile being dynamically regulated by extrinsic factors to drive neuron segregation seems to be a general mechanism for the segregation of nuclei, at least that of motor nuclei. We hypothesised that the initially broad expression profile of cadherins within spinal motor neurons could be important for the initial, early phase of LMC divisional segregation via medio-lateral migration of the motor neurons. We do indeed find that this is the case; manipulations of pan-motor neuron cadherin function results in a dramatic migration phenotype and concomitant deregulation of LMC divisional segregation (Bello et al 2012 and this thesis).

Figure 1.3 Motor pools and cadherin expression.

Pattern of cadherin expression in motor pools at the level of second lumbo sacral level of developing chick spinal cord. **Yellow** (Adductor) pool expresses cadherin 8, T-cadherin, cadherin 6b and MN cadherin. Green (Hip-Retractor) motor pool expresses high levels of cadherin 8 and low levels of cadherin 12. **Brown** (internal Femorotibialis) motor pool selectively expressed only high levels of cadherin 8. **Purple** (Sartorius) motor pool selectively expressed cadherin 10. Red (external Femorotibialis) motor pool expressed cadherin 8, cadherin 6b and T-cadherin. **Blue upper** level (Iliotrochanterici) motor pool expressed high levels of cadherin 6b, cadherin 7 and low levels of cadherin 8. **Blue lower** level (anterior Iliotibialis) motor pool expressed cadherin 6b and low levels of MN cadherin. Cadherin in brackets are expressed at low levels.

Derived from Price et al, Cell, Vol. 109, (2002) 205-216

Figure 1.4 Spinal Motor Neuron Organization and Projection Patterns of motor axon.
Above panel *(left)*, shows Motor neurons progenitor domains arise from the neural tube in response to graded concentration of sonic hedgehog along the dorso ventral axis of the neural tube. The dorsal progenitor domains are less exposed to the sonic hedgehog (**Shh**) and the more ventral progenitor domains are the most exposed. Above *(Right)*, shows schematic of motor neurons soma movements during development. First at stage 24 LMCl motor neurons generated after LMCm motor neurons and migrated through the LMCm neurons to reach their definitive lateral position in the ventral lumbar spinal cord.(red=LMCl, yellow=LMCm) arrow points to direction of migration. Second, at stage 26 superimposed on the inside-out migration of neurons that will acquire the **LMCl** and **LMCm** motor columns, motor pool formation is taking place, here, **F** represent the Femerotibialis motor pool and **A** represent the Adductor motor pool of the hind limb muscles. **Below panel** *(left)*, Schematic showing the trajectories of the **LMCm** and the **LMCl** motor axons and the expression of LIM-Homeodomain transcription factor within the columns**.** *(Right)*, motor pool specific expression of LIM-Homeodomain and ETS family transcription factors at second lumbosacral level at stage 35. The specific muscle's motor pools are for external femorotibialis (**eF**), Adductor (**A**), Hip Retractor (**HR**), Sartorious (**S**) and Iliotrochanterici (**ITR**). *(Derived from Price and Briscoe, Mechanisms of Development 121 (2004) 1103-1115)*

1.7 Neuronal Migration

All neurons need to be able to migrate away from their origins in germinal zones to their final positions in cell assemblies. Whilst migration of cell types, particularly fibroblasts and more primitive cells such as the slime mould Dictyostelium Discoideum, has been under intense investigation for a number of years, interest in neuronal migration has become more highly studied in recent years. One of the main reasons for this is that mechanisms that regulate neuronal migration have pointed to migration abnormalities in several naturally occurring genetic defects in humans.

Although neuronal migration occurs throughout the developing nervous system, it is most often studied in the forebrain and cerebellum. Two distinct modes of migration have been identified so far: radial migration and tangential migration. Radial migration is the principal mode of migration in the developing cerebral cortex. The main feature of radial migration is that neurons move orthogonal to the surface of the brain away from the proliferative zones along radially oriented glial fibres that span the entire depth of the cortex. This type of neuronal movement has also been termed gliophilic migration, because of the interactions between the migrating neurons and the glial substrate. In tangential migration, neurons move parallel to the surface of the brain along axons of other neurons. An example of this mode of migration is the movement of cortical interneurons from their origin in the ventral telencephalon to the developing cerebral cortex.

1.8 Cortical Neuronal Migration

Neuronal migration in the cerebral cortex begins when the first cohort of post mitotic neurons leaves the germinal ventricular zone (VZ) to form the preplate at the surface of the cerebral vesicles. This early-generated zone is then split by the arrival of accumulating cortical plate (CP) neurons into the superficial marginal zone (MZ) and the deeper subplate(8). [3H]-Thymidine-incorporation studies have shown that layers II–VI of the cerebral cortex are generated in an 'inside-out' sequence. Neurons that are generated early reside in the deepest layers, whereas later-born cells migrate past the existing layers to form the superficial layers; this is akin to the migration of LMC neurons in the spinal cord. Consequently, the MZ and sub-plate contain the earliest-generated neurons of the cerebral cortex. Those in the MZ (layer I) differentiate into Cajal–Retzius cells. The subplate is separated from the VZ by the intermediate zone (IZ), a layer that will eventually form the white matter containing the axons of the cortex. As the CP emerges, another layer of proliferating cells appears between the VZ and IZ. This is the so-called subventricularzone (SVZ) which contains cells, produced in the VZ, that give rise mainly to glia. As a result of electron microscope investigations of this glia and the generation of neurons, Rakic suggested that young neurons use the radially arranged processes of specialized glia (radial glia) as a scaffold to reach their positions in the developing CP.

Recently, it was discovered that the neuronal migration in other regions of the CNS particularly the cortex may be under the influence of HMG box transcription factors evident by wide expression of the family member SOX1. Its high expression by the telencephalic neurons and the absence of SOX1 was associated with migration deficit raising the possibility of neuronal migration being under control of transcription factors (Ekonomou et al., 2005).

1.9 Cortical Neuronal Radial glial migration

Once post-mitotic neurons have been generated by the ventricular zone, they detach from the ventricular surface and move their cell bodies to the cortex. Rakic's EM observation of a close neuron--glial relationship in the foetal macaque cerebral wall (Rakic 1972) indicated the presence of a differential binding affinity and suggested the existence of a 'radial-glial' mode of migration that may be mediated by adhesion molecules present on apposing neuronal and glial cell surfaces (Rakic 1981; 1990 Rakic and others 1994). Subsequent time-lapse imaging studies have confirmed the hypothesis that new-born neurons use radial glia to guide their migration (Nadrajah et al., 2003; Koster R W and Fraser Scott E., 2001). Radial glial guided migration has also been observed in a variety of mammalian species that range from rodents to human (Sidman and Rakic 1973; Kadhim and others 1988; Hatten and Mason 1990; Misson and others 1991; O'Rourke and others 1992; Noctor et al 2001; deAzevedo 2003; Zecevic 2004).

What are the cellular mechanisms, and molecules, involved in the long distance guidance of migrating neurons along radial glia? The idea of differential adhesion between migrating neurons and radial glial fibers suggested the possibility that homophilic adhesion molecules may account for this guidance (Rakic, 1981). However, there are multiple steps in cortical migration from the initial attachment of the neuron to the glia, the migration phase of the cell body and the subsequent detachment of the neuron from the glial membrane. Each of these processes involves distinct protein families. Multiple molecular species have been associated with neuronal migration that indicates the complexity of this process (e.g., Hatten and Mason 1990; Fishelland Hatten 1991; Cameron and Rakic 1994; Anton and others1996, 1997, 1999; Schmid and Anton, 2003; Rio and others 1997; Gongidi and others 2004; Xie and others 2006).

As would be predicted, most factors are membrane bound, but there are also a number of secreted diffusible molecules serving as attracting and repulsing agents that influence direction of migration and allocation of neurons into a particular structure (Wu and others1999). Factors that affect cytoskeletal remodelling are particularly important for nuclear translocation. For example, antibody perturbation of the glial membrane protein (NJPA1), localized in the plasmalemmal junction between migrating neurons and adjacent radial glial fibers (Cameron and Rakic 1994) caused withdrawal of the leading process, changes in micro tubular organization, and premature detachment of neurons from the radial glial shafts (Anton and others 1996).

Perhaps the best characterised signal involved with the radial migration of cortical neurons is that of the Reelin and Disabled pathway. Reelin is a large protein found expressed in the Cajal-Retzius cells of layer 1. It was first identified via a spontaneous mutant mouse that showed awkward gait in its movement. This so called Reeler mouse displayed severely disorganised laminae in its cortex. This disorganisation manifested itself in a relatively normal layer 1 but in the subsequent layers not being organised in an inside-out fashion but rather the reverse. The model proposed to explain this phenotype was that the Reeler mutation prevented the migrating cortical neurons from detaching from the radial glia. This seemed to be borne out when the protein Reelin was cloned as being mutated in the Reeler mouse. A similar cortical disorganisation was observed in the Disabled mouse and the cloning of Dab, the protein mutated in Disabled demonstrated that Dab and Reelin are involved in the same pathway to regulate detachment of migrating neurons. Reelin has also been shown to play a role, albeit minor, in the division and pool organisation of spinal motor neurons.

In addition to the Reeler pathway, recently members of the cadherin family, particularly N-cadherin, have also been implicated in regulating cortical neuron migration. Therefore, there is precedent for an involvement of cadherin expression in regulating neuronal migration.

Figure 1.5 Models of Cortical Neuronal Migration.

 (A) Berry and Rogers, 1965. Following cell division, the nucleus of one daughter cell moves towards the cortical plate through the long radial process, while the other cell remains in the ventricular zone. *(B)* Morest, 1970. Neuroblasts lose their ventricular attachments and translocate their somata through radially oriented processes that terminate at the pial surface. *(C)* Rakic, 1972. Post mitotic neurons use radially oriented glial fibres as a scaffold to reach their positions in the cortical plate. *(D)* Current: somal translocation (***red***) is the predominant mode of movement during early corticogenesis, whereas glia-guided migration (***blue***) is more prevalent at later stages, when the cerebral wall is considerably thicker. *(Derived from Bagirathy and Parnavelas, Nature Neuroscience, 3, 423-432 2002)*

1.10 The cadherin family.

Cell-cell interactions are crucial to all aspects of development, especially that of the highly complex nervous system. Central to this are a variety of cell-cell adhesion molecules including those of the Cadherin super family found to be differentially expressed during development and in the adult. (Hirano et al 2003). Cadherins constitute a large super family, with over one hundred members, of obligate calcium-dependent cell adhesion proteins, which play a major role in development and tissue morphogenesis (Takeichi M. 1995). In adults, interactions between cadherins on adjacent cells maintain the structural integrity of solid tissues and regulate the turnover and reorganization of tissue structures (Gumbiner BM. 1996, Gumbiner BM. 2005.). During development, cadherins direct cell segregation and the formation of distinct tissue interfaces (Takeichi M. 1991, Gonzalez-Reyes A, St Johnson D. 1998, Gumbiner BM. 2005).

1.11 Classification

The cadherin superfamily comprises at least five different subfamilies including the classical cadherins (type I), atypical (type II) protocadherins, desmosomal cadherins and cadherin-like proteins that do not fall into the other Subfamilies. The classical cadherins are the most extensively studied. Different classical cadherins are named according to the tissues from which they were first isolated. For example, E-, N-, and R-cadherins were derived from epithelial, neural, and retinal tissues, respectively. This archaic nomenclature has actually been detrimental to understanding how these cadherins function because their expression is not rigidly confined to each of the tissues they were originally cloned from. Desmosomal cadherins occur almost exclusively at desmosomal junctions in epithelial tissues and in cardiac muscle.

The protocadherins are less well characterized, but they are expressed throughout the nervous system and elsewhere (Gumbiner BM. 2005).

Membership of the cadherin superfamily is defined by having one or more cadherin repeats. Cadherin repeats are independently folding polypeptides of approximately 110 amino acids that contain motifs with the conserved sequence DRE, DXNDNAPXF, and DXD (Takeichi, 1990). The number of these cadherin repeats in each family varies between each subfamily, ranging from just one or two to more than 30. However, both type I and type II cadherins contain five extracellular cadherin repeats. Interestingly, each of the cadherin subfamilies can be delineated purely by the sequence of the first extracellular cadherin repeat. Figure 1.6 shows a list of cadherins and their phylogenetic properties.

Protein name[a]	Synonyms (or names of orthologues)	Gene symbol[a]	Species[b] (gene location[c])	GenBank Acc. No.	# Extracellular cadherin domains	HAV
BS-cadherin		BS-CDH	Bs	U61755	5	No
Cadherin-1	E-cadherin, uvomorulin, L-CAM	CDH1	Hs (16q22.1)	Z13009	5	Yes
Cadherin-2	N-cadherin	CDH2	Hs (18q12.1)	S42303	5	Yes
Cadherin-3	P-cadherin, B-cadherin[d], XB/U-cadherin[d]	CDH3	Hs (16q22.1)	X63629	5	Yes
Cadherin-4	R-cadherin, XmN-cadherin	CDH4	Hs (20q13.3)	L34059	5	Yes
Cadherin-5	VE-cadherin	CDH5	Hs (16q22.1)	X79981	5	No
Cadherin-6	K-cadherin	CDH6	Hs (5p14-15.1)	D31784	5	No
Cadherin-7		CDH7	Hs (18q22-23)	AJ007611	5	No
Cadherin-8		CDH8	Hs (16q22.1)	L34060	5	No
Cadherin-9	T1-cadherin	CDH9	Hs	AB035302	5	No
Cadherin-10	T2-cadherin	CDH10	Hs (5p13-14)	AF039747	5	No
Cadherin-11	OB-cadherin	CDH11	Hs (16q22.1)	L34056	5	No
Cadherin-12	Br-cadherin, N-cadherin-2	CDH12	Hs (5p15.1-15.2)	L34057	5	No
Cadherin-13	T- or H-cadherin	CDH13	Hs (16q24.2)	L34058	5	No
Cadherin-15	M-cadherin	CDH15	Hs (16q24.3)	D83542	5	Yes
Cadherin-16	Ksp-cadherin	CDH16	Hs (16q21-22)	AF016272	7	No
Cadherin-17	LI-cadherin, HPT-1	CDH17	Hs (8q22.1-22.3)	X83228	7	No
Cadherin-18	Cadherin-14, mouse EY-cadherin	CDH18	Hs (5p15.1-15.2)	U59325	5	No
Cadherin-19		CDH19	Hs (18q22-23)	AJ007607	5	No
Cadherin-20	F-cadherin[e], mouse "cadherin-7"[e]	CDH20	Hs (18q22-23)	AF217289	5	No
Cdh-3		CE-CDH3	Ce	L14324	19	No
Dachsous		DACHSOUS	Dm	L08811	27	No
Desmocollin-1		DSC1	Hs (18q12.1)	Z34522	5	No
Desmocollin-2		DSC2	Hs (18q12.1)	X56807	5	No
Desmocollin-3		DSC3	Hs (18q12.1)	X83929	5	No
Desmoglein-1		DSG1	Hs (18q12.1)	X56654	4	No
Desmoglein-2		DSG2	Hs (18q12.1)	Z26317	5	No
Desmoglein-3		DSG3	Hs (18q12.1)	M76482	5	No
DE-cadherin		DE-CDH	Dm	D28749	6	No
DN-cadherin		DN-CDH	Dm	AB002397	15	No
EP-cadherin	C-cadherin	EP-CDH	Xl	U04707	5	Yes
Fat		FAT	Hs (4q34)	X87241	34	No
Flamingo	Starry night (Stan)	FMI	Dm	AB028498	9	No
Flamingo1		FMI1	Mm	AB028499	8	No
HMR1		HMR1	Ce	AF016854	2	No
MEGF1	Fat2	MEGF1	Rn	AB011527	34	No
MEGF2	Celsr1	MEGF2	Rn	AB011528	8	No
Paraxial protocadherin	PAPC	PAR-PCDH	Xl	AF042192	6	No
PB-cadherin		PB-CDH	Rn	D83348	5	No
Protocadherin-α1	CNR family member	PCDH-α1	Hs (5q31-33)	AF152305	6	No
Protocadherin-β1	Protocadherin-3 family member	PCDH-β1	Hs (5q31-33)	AF152488	6	No
Protocadherin-β15	Protocadherin-3 family member	PCDH-β15	Hs (5q31-33)	AF152494	6	No
Protocadherin-γa1	Protocadherin-2 family member[f]	PCDH-γA1	Hs (5q31-33)	AF152318	6	No
Protocadherin-γb1	Protocadherin-2 family member[f]	PCDH-γB1	Hs (5q31-33)	AF152330	6	No
Protocadherin-γc3	Protocadherin-2 family member[f]	PCDH-γC3	Hs (5q31-33)	AF152337	6	No
Protocadherin-1	Protocadherin-42	PCDH1	Hs (5q31-33)	L11370	7	No
Protocadherin-4	VE-cadherin-2	PCDH4	Mm	Y08715	6	No
Protocadherin-7	BH-protocadherin, NF-protocadherin	PCDH7	Hs (4p15)	AB006755	7	No
Protocadherin-8	Arcadlin	PCDH8	Hs (13q21)	AF061573	6	No
Protocadherin-10	OL-protocadherin	PCDH10	Mm	U88549	6	No
Protocadherin-11	Protocadherin-X	PCDH11	Hs (Xq21.3/Yp11)	AB026187	7	No
Protocadherin-68		PCDH68	Hs	AF029343	6	No
Ret		RET	Hs	X12949+X15262	7	No

Figure 1.6 List of cadherins and their phylogenetic properties

(Derived from Nollet et al, J.Mol. Biol. (2000) 229, 551-572)

1.12 Structure and specificity of adhesion

Many aspects of the three-dimensional structure of cadherins and their molecular interactions have been elucidated. Most cadherins are integral surface membrane glycoproteins composed of three domains: a cytoplasmic domain, a trans-membrane domain, and a calcium-binding extracellular domain which contains the cadherin repeats. The cadherin repeat has a folding topology similar to the variable domain of immunoglobulins (Overduin et al., 1995; Shapiro et al., 1995). Ca2+ rigidifies the multi domain structure of cadherins (Pokutta et al., 1994; Nagar et al., 1996) and is essential to strong cell-cell adhesion.

Cadherins are present in the cytoplasmic membrane in both monomeric and dimeric forms. The lateral dimerization and clustering of N- and E-cadherin in a cis-configuration has been proposed to increase cadherin adhesivity and that swapping of beta-strands between cadherin monomers plays an important role in cadherin-mediated adhesion (Shapiro et al., 1995; Brieher et al., 1996; Yap et al., 1997; Tamura et al., 1998). The cis-dimers can interact with dimers located in the membrane of another cell in a Tran's configuration, thereby mediating adhesion of the two opposing membranes. Both biochemical and cell adhesion experiments and in vivo characterisation of cadherin function has demonstrated that it is the first cadherin repeat that mediates specificity of cell to cell adhesion of the cadherin family (at least of the classical cadherins).

The adhesive interfaces in the extracellular domain 1 of N-cadherin mediating trans-dimer formation is relatively large (Nose et al., 1990; Shapiro et al, 1995). Interestingly, type II cadherins display a much larger interface whilst mediating a much weaker cell adhesion indicating that factors other than just first extracellular domain interactions must determine the strength of cadherin adhesion.

Type I classic cadherins specifically bind to the same type of cadherin and do not interact at detectable levels with type II cadherins (Nose et al., 1990; Tomschy et al., 1996). For some type I classic cadherins, it has been shown that this binding specificity is mediated by relatively minor differences in the amino acid composition of the first extracellular domain (Nose et al., 1990). On the molecular level, amino acid residues in the first extracellular domain have been identified that systematically vary between different type I cadherins but are phylogenetically conserved across species (Redies and MuÈller, 1994). Interestingly, the adhesive specificity of at least some cadherins is preserved in evolution. For example, R-cadherin of chicken and mouse bind to each other but not (or less strongly) to other type I classic cadherins in either of the two species (Matsunami et al., 1993).

A detailed phylogenetic comparison of type I classic cadherins has been published (Gallin, 1998). Type II cadherins display more complicated adhesion specificity. Whilst they will not interact with type I cadherins, they appear to show little specificity of interaction within the type II family, at least in in vitro and cell-line based cell adhesion assays. However, in vivo, not least in motor neuron pool sorting, they do show specificity of action. Where this specificity arises from is currently unknown, although the first extracellular domain is critical to this specificity. For several cadherins, alternatively spliced isoforms have also been described. For example, cadherin-11 (OB cadherin), BH-cadherin and cadherin-8 are present in truncated forms with different or entirely missing cytoplasmic domains (Kido et al., 1998; Yoshida et al., 1998; Kawaguchi et al., 1999). From human osteoclast-like cells, an isoform of cadherin-6 was isolated that also shows differences in amino acid composition of the extracellular domain (Mbalaviele et al., 1998).

Finally, Wu and Maniatis (1999) described truncated proto cadherins which just consisted of the extracellular domain and the trans-membrane domain.

1.13 Molecules associated with cadherins

Intracellularly, cadherins are associated with many other types of molecules, some of which are involved in signal transduction. These associations can results in different functional states of cadherins and the ability of the cell to modulate cadherin adhesion dynamically. These states are regulated by processes (reviewed in Aberle et al., 1996; Barth et al., 1997) such as tyrosine phosphorylation of intracellular partner molecules (reviewed in Daniel and Reynolds, 1997; Loureiro and Peifer, 1998).

The cytoplasmic domain of many cadherins binds directly to a group of proteins called catenins, β-catenin and γ-catenin. These molecules establish connections with the actin cytoskeleton via their binding to α-catenin and via its interaction with EPLIN and also play a role in signal transduction (reviewed in Huber et al., 1996a). Between the subfamilies of cadherins, there are striking differences in the length and composition of the cytoplasmic domain, suggesting that the cadherin subfamilies differ in their intracellular binding partners and functions. Apart from their function in cell adhesion, catenins and related molecules are involved in several signaling pathways, e.g., the Wnt/Wingless pathway. These pathways play roles in basic cellular processes, such as migration, apoptosis and cell proliferation (Barth et al., 1997).

Some cadherin-associated molecules are predominantly expressed in the nervous system. For example, most neural cells do not express αE-catenin but a related molecule, αN-catenin (Hirano et al., 1992; Hirano and Takeichi, 1994; Uchida et al., 1994).

In the nervous system, αE-catenin is only expressed by the ependymal lining of the CNS and the choroid plexus which show an epithelial phenotype (Uchida et al., 1994). There is also a predominantly neurally expressed armadillo-related protein, called δ-catenin (Zhou et al., 1997b) or NPRAP (Levesque et al.,1999), which is predominantly expressed in the brain and interacts with presenilin-1 and β-catenin. The cadherin/catenin adhesion system seems to be well conserved throughout the metazoa. There are several examples of cadherin-like molecules identified in invertebrate species. A homologue of the β-catenin/plakoglobin/armadillo gene family has been identified in Hydra, one of the lowest metazoans with well-established epithelial cell layers and junctional complexes (Hobmayer et al., 1996).

In the Drosophila nervous system, a truncated isoform of armadillo, the Drosophila β-catenin homologue, accumulates in nerve cells. This molecule and Drosophila N-cadherin were both shown to play a role in building the axonal scaffold of the CNS (Iwai et al., 1997; Loureiro and Peifer, 1998). Another example for cadherin/catenin-associated molecules expressed in the brain is the adenomatous polyposis coli tumour suppressor protein APC (Brakeman et al., 1999). The number of cadherin-associated molecules is continuing to grow as the signal transduction pathways involving cadherins and catenins are studied in greater detail.
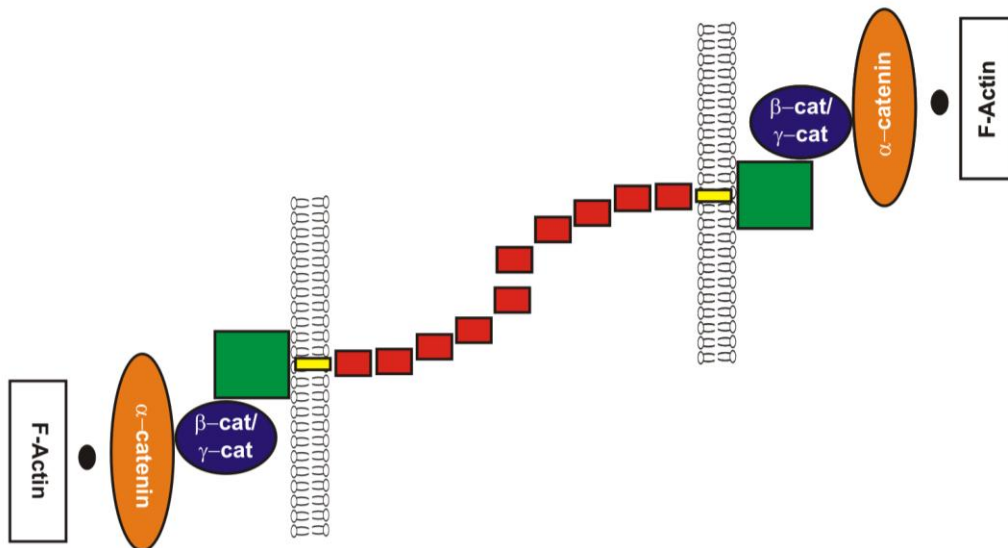
Figure 1.7 Cadherin catenin complext and interactions with the actin cytoskeleton.

The red area indicated the extra cellular cadherin domain consist of five cadherin repeats, responsible for cadherin-cadherin interaction between cells. The yellow element represents the trans-membrane domain of the cadherin responsible for linking the extracellular domain with the cytoplasmic cadherin domain indicated in green. The intracellular domain is a site for the assembly of a macromolecular complex linking the adhesion machinery to the actin cytoskeleton. α-and β-catenin play critical role in this activity. β-catenin binds to both the C-terminus of the intracellular cadherin domain and the N-terminus of α-catenin. α-catenin bind to a number of proteins as well as binding directly to F-actin which through subsequent interactions links the cadherin catenin complex with the actin cytoskeleton. The two lipid bilayer represents two neighbouring cells.

1.14 Interaction with other molecules

An additional group of molecules that interact with the cadherin/catenin complex are the protein tyrosine phosphatases, e.g. the receptor-type molecule PTPm (BradyKalnayet al., 1998). PTPm is expressed at high levels in the CNS and forms a complex with N-cadherin in retinal tissue and in the neurites of retinal ganglion cells. Down regulation of PTPm decreases N-cadherin-dependent neurite outgrowth while it has no effect on neurite outgrowth induced by laminin or L1 (Burden Gulley and Brady-Kalnay, 1999). A member of the leukocyte antigen-related protein (LAR)-related trans membrane tyrosine phosphatase family is also associated with the cadherin/catenin complex; this molecule is itself phosphorylated on tyrosine in a TrkA(a high affinity catalytic receptor for neurotrophin, nerve growth factor)-dependent manner (Kypta et al., 1996). A third example is the cytoplasmic phosphatase PTP1B which is associated with N-cadherin and dephosphorylates β-catenin (Balsamo et al., 1996).

Some protein tyrosine kinases are also associated with cadherins, e.g., p60v-src (Hamaguchi et al., 1993) and fyn (Kohmura et al., 1998). Fyn is intra cellularly associated with members of a specific subfamily of proto cadherins (CNR proto cadherins; Kohmura et al., 1998).Tyrosine phosphorylation of the cadherin/catenin complex has been implicated in several cellular processes regulated by cadherins, such as adhesiveness and tumour cell invasiveness (Daniel and Reynolds, 1997) and it is likely to play an important role also in CNS development. One receptor tyrosine kinase, the fibroblast growth factor receptor (FGFR1), is activated as a result of the stimulation of axon outgrowth by N-cadherin as well as by members of other cell adhesion molecules (e.g., NCAM and L1; Doherty and Walsh, 1996). The fibroblast growth factor receptor has also been implicated in retinal axon extension (Lom et al., 1998).

1.15 Cell Adhesion of cadherins in vitro

The best known function of cadherins is in cell-cell adhesion. The binding between cadherins is generally regarded as being type specific. Cadherin-expressing cells can sort out from each other and aggregate according to which cadherin they express. This is often demonstrated in vitro with an aggregation assay using cell lines (L-cells) transfected with cadherin cDNAs (protocol in Nakagawa et al., 1997). In the assay, cells are dispersed into a single cell suspension. The suspension is gently swirled for a few hours in a tissue culture dish so that the cells do not settle at the bottom of the dish but instead can encounter each other. Non-adherent cells remain single in the suspension. If a non-adherent parent cell is induced to express a cadherin by transfecting it with cadherin cDNAs, the derived cells adhere to each other and form aggregates.

This type of adhesiveness has been demonstrated for most classic cadherins and also a number of proto cadherins (see, e.g., Nose et al., 1988; Inuzuka et al., 1991a; Breviario et al., 1995; Kimura et al.,1995; Nakagawa and Takeichi, 1995; Sugimoto et al.,1996; Bradley et al., 1998; Hirano et al., 1999b; Yamagata et al., 1999). In the case of most cadherins studied to date, the adhesion is ``calcium-dependent'' because no aggregation of cadherin-expressing cells takes place in the absence of Ca2+, as first described by Takeichi et al. (1981).

Other classes of adhesion molecules, e.g., members of the Ig superfamily, do not depend on Ca2+ for their adhesive function. If a non-adherent parent cell line is separately transfected with two different cadherins, for example, with E-cadherin and N-cadherin, the two types of derived cells can segregate and form separate aggregates (``homotypic'' binding; Fig. 1.8D; see, e.g., Nose et al., 1988; Miyatani et al.,1989; Breviario et al., 1995; Kimura et al., 1995; Nakagawa and Takeichi, 1995; Obata et al.,

1995; Bradley et al., 1998; Kido et al., 1998; Shimoyama et al.,1999). However, aggregates of aggregates are the most commonly found scenario. Namely, that a large ball of cells composed of E-cadherin aggregates and N-cadherin aggregates will form. Thus, although the cells have 'sorted out' they do display significant cross interaction. Cells expressing other combinations of cadherins, for example, N-cadherin and R-cadherin (Inuzuka et al., 1991a) or cadherin-7 and cadherin-6B (Nakagawa and Takeichi, 1995), form mixed aggregates (``heterotypic'' binding) but, within the aggregates, the cells tend to segregate according to the cadherin they express.

With few exceptions (Murphy Erdosh et al., 1995), heterotypic binding is weaker than homotypic binding. Two cell lines expressing the same type of cadherin but in different amounts also tend to segregate from each other. The cells with the higher expression levels move to the inner part of the aggregates, while the cells with the lower expression levels form an outer shell (Steinberg and Takeichi, 1994).

Experiments with adhesive cell lines and computer simulations of cellular aggregation behaviour have shown that, depending on the mixing ratio and relative adhesive strengths of two cell populations, the cellular patterns resulting from their mixed aggregation can show considerable variations, ranging from dispersion of cells, to the formation of layered structures or mixed aggregates, to the complete segregation of the different cell types (Steinberg, 1963; Glazier and Graner, 1993; Graner, 1993; Graner and Sawada, 1993; Steinberg and Takeichi, 1994).

The qualitative and quantitative differences in cadherin-mediated cell-cell adhesion between embryonic cells are likely to form the molecular basis of the differential cell sorting and aggregation of embryonic cells observed in a variety of systems (Moscona and Moscona, 1952; Steinberg, 1963; reviewed in Steinberg, 1996; Grunwald, 1996b),

including the nervous system (Takeichi et al., 1990). There are numerous examples from different organ systems demonstrating that cell populations expressing different cadherins tend to sort out in vivo according to which cadherin they express.

Figure 1.8 Binding specifity of cadherins revealed by cell adhesion assay.

(A) In this assay, a cultured cell line is dispersed into a single cell suspension (upper part of the panels). The result of the assay is shown in lower part of the panels. Non-adherent cells (gray) remain in a single cell suspension. *(B)* If a non-adherent cell line is transfected with cDNA for a cadherin, the cells expressing the cadherin (blue) adhere to each other to form aggregates (B).*(C)* Cadherin based Cell adhesion is a calcium dependant process   since no aggregation takes place in the absence of calcium irons Ca2+ *(D)* homotypic binding results when   a cell line is transfected with two different cadherins, for example, E-cadherin (blue) and N-cadherin (red), the two types of cells segregate and form separate aggregates.*(E)* Some combinations of cadherins results in a heterotypic binding, for example N-cadherin (red) and R-cadherin (green), transfected cells form mixed aggregates (``heterotypic'' binding) but, within the aggregates, the cells segregate according to the cadherin they express. This result demonstrates that heterotypic binding is weaker than homotypic binding. *(F)* Two cell lines expressing the same type of cadherin but in different amounts also segregate from each other. The cells with the higher expression levels (dark blue) move to the interior of the aggregates while the cells with the lower expression levels (light blue) form an outer shell.

(Derived from C Redies, 2000 Prog in Neurobiology 61, 2000: 611 – 648)

1.16 Cadherin roles in cell-cell adhesion in vivo

Since the major role of cadherin is in cell-cell adhesion it is not surprising that these molecules are expressed in all cohesive tissues. In many cases multiple cadherins are expressed by a single tissue. Somitogenesis is a good example of cadherin function in adhesion in vivo. N-cadherin is expressed uniformly at the paraxial mesoderm and if its function is blocked by antibody or gene targeting, the somite structure becomes disorganized. Although cadherin 11 is also expressed in the somite, a null mutation of cadherin 11 shows a normal somite phenotype. Double knock-out mice of cadherin 11 and N-cadherin shows more severe phenotype with a complete fragmentation of somite epithelia than in N-cadherin null mutation alone. This indicates a minor role for cadherin 11 and a major role for N-cadherin. Similar roles of cadherins in histogenesis in other tissues were demonstrated experimentally in other tissues such as the lung epithelium, skin, limb cartilage, neural tube, retina, tectum and the early embryo in all cases, blocking cadherin function causes disorganization of the tissue structure.

1.17 Cadherin signalling in axon guidance

Axon path finding and target recognition are critical in the formation of neural circuits (Tessier-Lavigne M. & C.S. Goodman. 1996). At the tips of growing axons, the growth cones acts as sensors to decide the direction of axonal navigation. Except for T-cadherin, which acts as a repellent molecule, cadherins seem to provide a contact dependant adhesive mechanism and many of the classical Cadherins are expressed on growth cones (Letourneau et al, 1990) Experimental evidence for the role of cadherins in target recognition comes from role of N-cadherin in the retinotectal system of the chicken embryo (Inoue A. & J.R Sanes, 1997).

N-cadherin has been shown to regulate neurite growth in vitro and has been confirmed in vivo in Xenopus (Bixby J.L. & R. Zhang 1990).

1.18 Cadherins roles in proliferation and differentiation

Cadherin mediated adhesion can regulate cell proliferation in a positive or negative direction. For example, restoration of cadherin-mediated adhesion by exogenous alpha catenin in an alpha catenin deficient dispersed carcinoma cell line, cell proliferation is enhanced. On the other hand cell growth is supressed in various other examples of N-cadherin, VE cadherin, and P-cadherin actions. The N-cadherin mediated contact inhibition seems to involve cyclin-dependent kinase (cdk) system. In null mutants of P-cadherin, the mammary gland shows hyperplasia and dysplasia, suggesting P-cadherin to be a negative regulator of mammary gland cell growth.

Cadherin–mediated adhesion is also involved in cell differentiation. For example, N-cadherin signaling is important for muscles differentiation. In addition, E-cadherin induces enterocytes differentiation through MAPK pathway. Similarly, it has been reported that N-cadherin is involved in the differentiation of O-2A oligodendrocyte precursors.

1.19 Cadherin role in neural development

Cadherins regulate neural development at multiple stages. N-cadherin is a typical example of multiple roles of a single cadherin at different stages of neural development. First, expression of N-cadherin in the neuro epithelium is uniform and helps maintain the epithelial structure. N-cadherin expression in the mantle layer become restricted to a subset of brain nuclei, layers, and fibres, suggesting that N-cadherin is involved in the selective adhesion between particular groups of early neurons and their processes.

The cadherin-catenin complexes have also recently been reported to be involved in complex central nervous processes such as synapse formation, synapse plasticity and remodelling (Price and Salinas 2005). The synapse is the specialized adhesion site between neurons and where signals are transmitted between presynaptic and post synaptic neurons. In mature neural tissue, N-cadherin expression is restricted to specific neural circuits and becomes localized at the synapses, suggesting a role for cadherin in neural circuit formation and synaptogenesis. E-cadherin, R-cadherin and cadherin-7 as well as cadherin-11 have also been found at synapses of particular neurons (Arndt K., S. Nakagawa 1998, Fannon A. M. & D. R Colman, 1996, Uchida N., et al, 1996). Furthermore, a role for cadherin in synaptic plasticity in the mouse hippocampus has been suggested.

1.20 Cadherins in cell migration

Cadherins can also mediate multiple steps in the regulation of neural crest migration. N-cadherin is broadly expressed in the neuroepithelium but is down regulated in neural crest cells before they delaminate from the neural tube and migrate peripherally (a so-called epithelial to mesenchymal transition) (Nagakawa et al, 1995). In Chicken, cadherin-6B (cad6B) is expressed first in pre-migratory neural crest cells before the epithelial mesenchymal transition and then for a short time after delamination (Park K. S. & Gumbiner B.M, 2010).

Perturbation of cadherin-6b expression and function results in a suppression of neural crest delamination. Cadherin-7 and Cadherin-11 are also expressed in migratory neural crest cells (Kimura Y., et al, 1995). Taken together this evidence indicates multiple roles for cadherins in neural migration other than the adhesive function. N-cad, cad6B and cadherin-11 appear to have signalling functions that can generate motility. Cadherin and RhoGTPases are also critical molecular players that regulate adhesion and motility during the initial delamination of neural crest cells from the neuroepithelium (Mathew R.C., & Mary C. H., 2010).

1.21 Wnt signaling and cadherin function in development.

The Wnt signalling pathway comprises a network of proteins that function in passing signals from the cell surface receptors via the cytoplasm and ultimately to the cell's nucleus where the signalling cascade leads to the expression of target genes. It controls cell-cell communication at embryonic and adult stages; as such it is involved in the cell proliferation and differentiation during development and healing (Nusse et al., 2004).

Because β-Catenin is shared by both Wnt-signalling and Cadherin-Catenin complex as a constitutive component, there is the possibility that each system is affected by the other (Ben-Ze'ev A. & B. Geiger., 1998). In addition to its crucial role in assembling the cadherin mediated cell adhesion complex, β-catenin also has an important function in the canonical Wnt signalling pathway (Bienz M., 2000; Polakis, P., 2000).

The Wnt-signalling pathway is important in cell fate determination and patterning during development. Wnt family of signalling proteins participates in multiple developmental events during embryogenesis and has also been implicated in adult tissue homeostasis. Wnt signals have effects that include mitogenic stimulation, cell fate specification, and differentiation. Wnt-signalling also plays a role in neural induction, determination of the neural crest, synapse formation and brain patterning (Patapoutian A. & L.F. Reichardt., 2000). Two important pathways of Wnt signalling are the canonical and the non-canonical Wnt signalling pathway. Canonical is β-catenin dependant and non-canonical is β-catenin independent. Both signalling pathways have been extensively studied.

The canonical (β-catenin dependant) Wnt pathway involve a series of events that occur when Wnt proteins bind to cell-surface receptors of the Frizzled family, causing the receptors to activate Dishevelled family proteins and ultimately leading to a change in the amount of β-catenin that reaches the nucleus. Dishevelled (DSH) is a key component of a membrane-associated Wnt receptor complex, which, when activated by Wnt binding, inhibits a second complex of proteins that includes axin, GSK-3, and the protein APC (Fig 1.9).

The axin/GSK-3/APC complex normally promotes the proteolytic degradation of the β-catenin intracellular signaling molecule. After inhibition of the "β-catenin destruction complex", a pool of cytoplasmic β-catenin stabilizes, and some β-catenin, is able to enter the nucleus and interact with TCF/LEF family transcription factors to promote specific gene expression. Cell surface Frizzled (FRZ) proteins usually interact with a transmembrane protein called LRP (Wehrli et al 2000). LRP can bind to Frizzled, Wnt, and axin and may stabilize the Wnt/Frizzled/LRP/Dishevelled/axin complex at the cell surface. In vertebrates, several secreted proteins have been described that can modulate Wnt signaling by either binding to Wnt (Kawano et al., 2003) or binding to a Wnt receptor protein. For example, Sclerostin can bind to LRP and inhibit Wnt signaling (Li X et al., 2005).

The part of the pathway linking the cell surface Wnt-activated Wnt receptor complex to the prevention of β-catenin degradation is still under investigation. There is evidence that trimeric G proteins can function downstream from Frizzled (Katanaev et al 2005). It has been suggested that Wnt-activated G proteins participate in the disassembly of the axin /GSK3 complex (Liu X, et al., 2005).

Several protein kinases and protein phosphatases have been associated with the ability of the cell surface Wnt-activated Wnt receptor complex to bind axin and disassemble the axin/GSK3 complex (Nusse R., 2005). Phosphorylation of the cytoplasmic domain of LRP by CK1 and GSK3 can regulate axin binding to LRP. The protein kinase activity of GSK3 appears to be important for both the formation of the membrane-associated Wnt/FRZ/LRP/DSH/Axin complex and the function of the Axin/APC/GSK3/β-catenin complex. Phosphorylation of β-catenin by GSK3 leads to the destruction of β-catenin. The glycogen synthase kinases (GSK3β), MAPK, Casein kinase2, are reported to be involved in modulation of Cadherin-based adhesion (Aberle et al, 1997, Sheibani et al, 2000, Lickert et al, 2000) further indicating the possibility of crosstalk between cadherin/ catenin signalling and the canonical Wnt pathway.

There are many non-canonical pathways, but the two best-studied pathways are the: Planar Cell Polarity (PCP) and Wnt/Calcium Pathways.

The most distinctive differences between the canonical and non-canonical pathways include the specific ligands activating each pathway, β-catenin, LRP5/6 co-receptor, and Dsh-DEP domain independence, and the ability of the non-canonical pathway to inhibit the canonical pathway. Ligands that activate the non-canonical pathways are Wnt4, Wnt5a, and Wnt11 (Michael Kuehl, 2008, Komiya et al., 2008). Expression of Wnt5a was shown to be increased in prostate cancer; (Wang et al., 2010) the mechanism of this increase in Wnt5a protein expression was proposed to be increase in Wnt5a gene transcription due to hypomethylation of Wnt5a promoter region (Michael Kuehl 2005, Wang et al., 2007).

In the PCP pathway, ligand binding to the receptor recruits Dishevelled (Dsh), which forms a complex with Daam1. Daam1 then activates the small G-protein Rho through guanine exchange factor. Rho activates ROCK (Rho-associated kinase), which is one of the major regulators of the cytoskeleton. Dsh also forms a complex with rac1 and mediates profilin binding to actin. Rac1 activates JNK and can also lead to actin polymerization. Profilin binding to actin can result in restructuring of the cytoskeleton.

In the Wnt/Calcium pathway (Fig 1.10), Wnt5a and Frizzled regulate intracellular calcium levels. Ligand binding causes the coupled G-protein to activate PLC, leading to the generation of DAG and IP3. When IP3 binds to its receptor on the ER, intracellular calcium concentration increases. Ligand binding also activates cGMP-specific phosphodiesterase (PDE), which depletes cGMP and further increases calcium concentration. Increased concentrations of calcium and DAG can activate Cdc42 (cell division control protein 42) through PKC. Cdc42 is an important regulator of cell adhesion, migration, and tissue separation (Komiya et al., 2008).

Increased calcium also activates calcineurin and CamKII (calcium/calmodulin-dependent kinase). Calcineurin induces activation of transcription factor NFAT, which regulates ventral patterning (Komiya et al., 2008). CamKII activates TAK1 and NLK kinase, which can interfere with TCF/ß-Catenin signaling in the canonical pathway (Sugimura et al., 2010).

In the Wnt/GSK3 pathway, Wnt inhibition of GSK-3 activates mTOR without involvement of ß-Catenin, such that rapamycin can inhibit Wnt-induced cell growth and cancer formation (Inoki et al., 2006)

Figure 1.9 The canonical Wnt signaling pathway.

(*Left panel*), in cells not exposed to a Wnt signal, β-catenin is degraded through interactions with Axin, APC, and the protein kinase GSK-3. (***Right panel***), Wnt proteins bind to the Frizzled/LRP receptor complex at the cell surface. These receptors transduce a signal to Dishevelled (Dsh) and to Axin, which may directly interact (*dashed lines*). As a result of the degradation, β-catenin is inhibited, and this protein accumulates in the cytoplasm and nucleus. Subsequently, β-catenin interacts with TCF to control transcription. Negative regulators in black, while the positively acting components are coloured outlines.

(Derived from Vanderbilt, Annu. Rev. Cell. Dev. Biol. 2004. 20:781-810)

Figure 1.10 Schematic representation of the Wnt signal transduction cascade.

(a) For the canonical pathway, signaling through the Frizzled (Fz) and LRP5/6 receptor complex induces the stabilization of β-catenin via the DIX and PDZ domains of Dishevelled (Dsh) and a number of factors including Axin, glycogen synthase kinase 3 (GSK3) and casein kinase 1 (CK1). β-catenin translocates into the nucleus where it complexes with members of the LEF/TCF family of transcription factors to mediate transcriptional induction of target genes. β-catenin is then exported from the nucleus and degraded via the proteosomal machinery. **(b)** For non-canonical or planar cell polarity (PCP) signaling, Wnt signaling is transduced through Frizzled independent of LPR5/6. Utilizing the PDZ and DEP domains of Dsh, this pathway mediates cytoskeletal changes through activation of the small GTPases Rho and Rac. **(c)** For the Wnt-Ca2+ pathway, Wnt signaling via Frizzled mediates activation of heterotrimeric G-proteins, which engage Dsh, phospholipase C (PLC; not shown), calcium-calmodulin kinase 2 (CamK2) and protein kinase C (PKC). This pathway also uses the PDZ and DEP domains of Dsh to modulate cell adhesion and motility. Note that for the PCP and Ca2+ pathways Dsh is proposed to function at the membrane, whereas for canonical signaling Dsh has been proposed to function in the cytoplasm.

(Derived from Habas and Dawid Journal of Biology 2005 4:2 doi: 10.1186/jbiol22)

1.2 Rationale of this study.

Differential cadherin expression is acquired during motor neuron pool formation and this is critical to the segregation of motor neurons. However, this expression is highly dynamic, being moulded by extrinsic signals from the limb. The initial cadherin expression has a more pan-motor neuron character, all motor neurons either expressing a given cadherin or not expressing it. As this initial phase of motor neuron cadherin expression coincides with the inside out migration of motor neurons during divisional segregation, I asked whether early cadherin expression could be influential in the migration of motor neurons. I perturbed pan-motoneurons cadherin function using both dominant negative cadherin and dominant negative catenin approaches and demonstrate a dramatic perturbation of divisional segregation and motor neuron migration. I also manipulated a single cadherin, cadherin-7 that is expressed only during motor neuron migration and show a similar, albeit weaker phenotype to that of the either manipulations. I also demonstrate that motor neuron migration may occur on radial glia in the spinal cord. My results suggest a prolonged role for cadherin expression in all phases of motor neuron organisation within the ventral horn of the spinal cord.

2 Materials and Methods

2.1 Materials

2.1.1 Laboratory reagents

Laboratory reagents and chemicals used in this study were supplied by Sigma-Aldrich® Ltd, UK and Invitrogen® Limited UK, apart from the following reagents supplied by other suppliers:

Agarose, Magnesium Chloride ($MgCl_2$) and paraformaldehyde were supplied by Fisher Scientific Ltd, Loughborough, UK. Sodium Chloride (NaCl), Sodium Dihydrogen Orthophosphate-1-hydrate ($NaH_2PO.H_2O$) and Disodium Hydrogen Phosphate (Na_2HPO_4) were supplied by VWR international Ltd, UK.

Sodium Hydroxide (NaOH) was supplied by Fluka BioChemika, Buchs, Switzerland. Molecular biology grade H_2O was supplied by Eppendorf, Cambridge, UK.

2.1.2 Laboratory solutions

The laboratory solutions used in the experiments were prepared based on the standard laboratory protocols and are categorized as follows:

2.1.3 Tissue preparation and protection solutions

1Molar Phosphate Buffer: Prepared by dissolving 32g of sodium Dihydrogen orthophosphate-1-hydrate and 109.47 g of Dihydrogen sodium orthophosphate in sterile H_2O and made up the solution to 1L to the correct concentration of 0.77M of Na_2HPO_4 and 0.23M $NaH_2PO_4.H_2O$.

Phosphate Buffer Saline: Prepared from 30 ml of 5M NaCl solution; 100 ml of 1M PB and 870 ml of sterile water to the correct concentration of 0.1M PB and 0.15M NaCl.

PB fixative (4% PFA): Prepared from 4% paraformaldehyde w/v, 45 ml of ultra-pure H$_2$O, 3.8µl of 10 M NaOH and 5ml of 1M PB to the correct concentration of 0.076M NaOH, and 0.1M PB.

Block solution in PBS: 1% Foetal calf serum w/v and 0.1% Triton-X 100

Cryoprotection solution: Prepared from 150g of 99.5% sucrose, 50 ml of 1M PB, and ultra-pure H$_2$O 350 ml to the correct concentration of 30% sucrose w/v and 0.1M PB.

LB broth: 20 g of LB medium in 1L of sterile water and autoclaved for 90 minutes.

LB Agar: 35 g of LB medium in 1L of sterile water and autoclaved for 90 minutes.

2.1.4 Insitu Hybridization solutions:

Hybridization solution: 50% Formamide, 5xSSC, 5 x Denharts solution, 250µg/mL Baker's yeast tRNA, 500µg/mL Salmon sperm DNA, Phosphate Buffer (PB), pH 7.4

1M Tris-HCl Buffers: 242.2 g of TrisBase, 120-125 ml HCl adjusted to pH 7.5

Tris-HCl Buffer (pH9.5): 1M (242.2 g) TrisBase, 120-125ml (12M) HCl, adjusted to pH 9.5 **Acetylation Buffer:** 0.1M Thriethanolamine, 58 mM HCl, 26mM Acetic anhydride. **Proteinase K solution:** Proteinase K 1µg/ml in 50mM Tris-HCl pH 7.5 and 5mM EDTA 400 ml.

Buffer B1: 100 ml of 1M Tris, 30 ml of 5M NaCl to 1 L of ultra-pure H$_2$O (PBS/0.1M Tris-HCl, pH 7.5, 0.15M NaCl)

Buffer B3: 0.1M Tris-HCl, pH 9.5, 0.1M NaCl and 50 mM MgCl$_2$20 x SSC: 3M NaCl, 300 mM Sodium citrate, citric acid adjusted to pH 7.0

2.2   **Chick Embryo Preparation**

Fertilized White leghorn chicken (*Gallus domesticus*) eggs obtained from a local supplier (Henry Stuart and Company) stored in a specialized incubator (LMS cool incubator) at 15.6^0C before incubation. When incubation is desired eggs are transferred out of the special incubator and kept on the bench at room temperature for approximately 30 minutes to 1 hour to warm to room temperature, during this period of temperature equilibration eggs were clean with 70% ethanol solution to prevent contamination of the incubator, allowed to further warm on table at room temperature with five mills of albumin withdrawn before incubation.

Eggs were incubated in a force draft humidified electric incubator at 37- 38^0C *(*Lyon electric Inc., USA), allowed to develop to desired (HH) stage (Hamburger and Hamilton 1951). For the purpose of this work embryos between stages 12-32 were used for the experiments with stages 12-18 for the electroporation. All embryos were treated in accordance with the University College London procedures on the use of animals as well as the Animals (Scientific Procedures) Act of 1986, UK.

After a period of 72 hours of incubation eggs were removed out of the incubator and place on the table at room temperature, surfaces wiped with tissue paper soaked in 70% alcohol solution to further reduce contamination during process of electroporation and allowed to air dry on table for 5 - 10 minutes. Five (5) ml albumin is withdrawn by means of 18G size needle (BD plats reg) thus allowing the embryo to settle down the egg shell and further reduce the risk of injury to the developing embryo. By means of small size dissecting forceps eggs were cut opened carefully. Using dissecting microscope (Leica Galen) and the Hamburger and Hamilton atlas of chick development the exact developmental stage of the embryos is determined and properly labelled.

2.3   In-Ovo Electroporation:

Expressions of cDNAs were achieved by in ovo electroporation. Using a 1.0 mm glass capillary needle (Harvard Apparatus) the desired plasmid mixed approximately 0.1µl of DNA constructs i.e. 1-10µg/µl in molecular biology grade H_2O with 0.1% Fast Green (Sigma) was pressure injected in to the central canal of the developing spinal cord. Embryo positioned in a dorso-ventral position and the spinal cord focused on and positioned between the two electrodes.

By means of Electro Square Porator ECM 830 (BTX Inc.), five (5) electric square pulses of 50 milliseconds duration spaced over 5seconds period at 30 volts were applied by placing electrodes adjacent to each side of the developing spinal cord and thus the desired ventral aspect of the spinal cord electroporated. Embryos observed for about 10-15 seconds to established heart beat and its viability following the procedure. Further five (5) mills of albumin is withdrawn and a few drops of antibiotic penicillin-streptomycin 10,000 units/ml (Invitrogen Corporation) applied and the eggs is closed using electric tape or thin film (Pechiney Plastic, Chicago).

Eggs are clearly marked indicating the stage of electroporation and the DNA used (for data collection purposes), returned to rack and incubated at 38^0C to the desired stage of development (HH 25-32) for dissection. Embryos were electroporated at Hamburger and Hamilton stages 12-18 and analyzed between HH stages 25-32.

2.3.1   Staging and Dissection

The exact stage of development of the chick embryo is critical in the series of experiments carried out throughout this work because the developmental stage of the embryo forms the basis on which the subsequent experiments and analysis are based. Staging of the embryos is done on the third day post electroporation or the seventh day

of embryologic development (E7) eggs were cut opened using small butterfly scissors and the developing embryos were staged according to Hamburger and Hamilton (HH) stages of development (Hamilton and Hamburger 1952, revised 1992).

Throughout the study, the revised edition of the Hamburger and Hamilton atlas of the normal stages in chick embryo development was used for the purpose of establishing the stage of development.

The parameters used in staging are the days of incubation, the head formation, wings, limb, and visceral arches development as well as the developing eye ball, beak and head and neck flexures. For proper staging of development, stages 1-46 were clearly indicated with stage 1 being the pre-streak stage and stage 46 being the newly hatched chick; however in the conduct of this work no embryo exceeds the stage 32 of development in keeping with the duration of generation and maturation of spinal motor neurons.

2.3.2 Embryo Dissection

The lumbosacral section of the developing spinal cord is dissected out using dissecting microscope and dissecting/ butterfly scissors. Embryos were removed from the egg shell on to a Dulbecco's Modified eagle Medium DMEM (Sterilin Ltd UK) dishes containing chilled phosphate buffer solution and placed on ice.

The lower segment of the abdominal wall of the developing embryos incised and the rib cage cut opened, the incision is then extended downward to the pelvic area thereby exposing the whole thoracic and abdominal contents. The thoracic and abdominal content were carefully evacuated and thus exposing the posterior abdominal wall. The ribs served as a reference frame for the exact point of dissection of the spinal cord.

The lower abdominal part of the spinal cord is separated from the upper part of the spinal cord, using the lower two ribs as a guide. The dissected spinal cords with the remnants of the lower thoracic spinal segments are carefully dissected further separating it from the hind limbs and the sacrococoygeal segments using the dissecting forceps and scissors. The lumber spinal segments are then placed in a chilled PBS solution on ice at room temperature for about 10 minutes. The segments are clearly labelled indicating the number of sections, embryological stage of development, the construct used in the electroporation and the date of the dissection.

Using a 15mls or 50mls falcon tubes the embryos are then immersed in preformed 4% Para formaldehyde solution to fix the tissues for one hour at room temperature on ice or in the refrigerator at 4^0C.

Following the one hour of tissue fixation, the embryos are then washed twice each for 30 minutes in PBS solution to remove the fix solution using the blood tube rotator machine SB1 (Stuart Scientific, UK). On the final wash, the PBS is gently decanted off the embryos. 10-15 mils of chilled 30% sucrose in 0.1 molar PB were added to the embryos for overnight dehydration at 4^0C.

Following dehydration, embryos were brought out for second series of fine micro dissection using the dissecting microscope to finally select the exact anatomical level lower lumber (L2 -L4) of the spinal cord to be mounted in mounting medium frozen and ready for Cryosectioning.

Lumber segments of spinal cord were then placed on to a Dulbecco's Modified eagle Medium DMEM (Sterilin Ltd UK) containing the mounting medium optimum concentrating temperature (OCT, Tissue-Tek® Ltd Netherland) and covered with the medium after taking off any remnant of the sucrose solution on them.

By way of a fine needle the sectioned spinal segments were arranged in set of two or more depending on the number of the tissues to be mounted in one block. They are transferred in to the pyramidal 22mm x 12 mm size peel-a-way® plastic tissue embedding mould (Agar Scientific Ltd, UK) containing 3-5 mils of the medium and well labelled for identification purposes.

The embryos are placed in an upside down position with the cranial part facing down and the ventral aspect facing forward (the experimenter) the position is manoeuvred to attain an erect position in the medium and carefully placed on granules of carbon dioxide (CO_2) i.e. dry ice at -80^0C in a container and covered for 15- 30 minutes to be frozen, for final Cryosectioning.

2.3.3 Cryosectioning

Tissue sections were obtained by mounting the frozen tissue block on to the cryostat (Bright Instrument Ltd, UK) following equilibration for 15-20 minutes in the cryostat machine at -24^0C. Held by a clamp in an anterior posterior position, alternate section of 15μm thickness were obtained on to an electrically (positively) charged and carefully labelled surface of 25x75x0.1mm glass slides (Super Frost®Plus, VWR International) Slides were air dried at room temperature for 30-45 minutes and stored frozen in -80^0C freezers for immunohistochemistry.

2.3.4 Immunohistochemistry:

Slides were air dried at room temperature for 10-15 minutes, labelled and marked by means of an immuno pen marker (Dako-Cytomation, Denmark A/S) to prevent spillage of added solutions on to the slides. Then 0.5 to 1.0 ml of PBS wash for 10 minutes to dissolve the OCT and to give a clear view of the of the spinal cord sections.

Block solution is added on to the slides for 30 minutes by means of 0.5 -1.0 ml of antibody block solution.

Primary antibodies diluted in block were added on to the slides for 12 to 16 hours or overnight incubation at 4^0C. Following this incubation, three (3) washes in PBS each for 5 minutes before secondary antibodies diluted in fresh block were applied for 1 hour, this followed by three washes in PBS each for 5 minutes duration, followed by two (2) drops of Vectashield® H-1000 mounting medium for fluorescence (Vector Laboratories Inc., USA) cover slipped, gently dabbed, cleaned ready for imaging.

2.3.5 **Table (2.1)** Summary of the primary antibodies used the organism in which they were raised, their specificity and concentrations.

Specifity	Organism	Supplier	Concentration
Gfp	Rabbit	Invitrogen	1:1000µl
Islet	Mouse	Hybridoma Bank	1:100µl
Lim-1	Mouse	DSHB	1:100µl
Lim-2	Mouse	DSHB	1:100µl
B-Galactosidase	Goat	Zymed	1:1000µl
Engrailed-1	mouse	DSHB	1:1000µl
Chox-10	Mouse	DSHB	1:1000µl
Conexin-43	Mouse	DSHB	1:1000µl
Hb9	Mouse	DSHB	1:50µl
Transitin	Mouse	DSHB	1:500µl
Transitin	Rat	DSHB	1:500µl
Z01	Rabbit	DSHB	1:100µl
HRP	Rabbit	Jackson	1:1000µl
HA	Rat	Roche	1:50µl
BrdU	Mouse	Roche	1:50µl
Foxp1	Guinea pig	Jackson	1:200µl
Pax6	Mouse	DSHB	1:1000 µl
β-catenin	Rabbit	Sigma	1:1000µl
γ-catenin	Mouse	BD Biosciences	1:100 µl

2.3.6 **The secondary antibodies**

The following secondary antibodies were used: Goat anti-Mouse IgG2b Cy5 (1:500),Goat anti-Rabbit IgG (1:1000 Alexafluor®), Goat anti- Mouse IgG1 Cy3 (1:1000μl), Donkey anti-Goat (1:1000μl Alexafluor®), Donkey anti-Rabbit (1:1000 Alexafluor®), Donkey anti- Mouse (1:1000 Alexafluor® 594), Goat anti-Rat (1 :1000), Donkey anti-Chick-FITC (1:250), Donkey anti-Guinea Pig Cy5 (1:500). These antibodies were supplied by either Invitrogen or Jackson Immunolaboratories.

2.4 **Generation of Constructs**

Plasmids DNAs used in this study were extracted using the maxi preps protocol (maxi kit, QIAGEN®) from competent bacterial cells (*Escherichia coli*) culture. Reprecipitation of DNAs was done using Ethanol (70-100%) and 5M NaCl. Final concentrations of the DNAs in μg/μl were determined using ND-1000 Spectrophotometer (NanoDrop®).

2.4.1 **Analysis of constructs used:**

Full-length cDNAs for the chick γ-catenin was cloned from an E3 chick cDNAs library screening and γ-catenin L127A point mutation was generated (by Dr Price) using the Quick-change kit (Stratagene) in accordance with manufacturers guidelines. Green fluorescence protein CMVeGFPN$_3$ (Invitrogen), γ-catenin and γ-catenin (L127A) cDNAs were cloned into pCAGGS vector containing an internal ribosome entry sequence followed by a cDNA encoding nuclear localization sequence tagged β-galactosidase (pCAGGS inlz). Fig 2.1. Similarly, cadherin dominant-negative (CDN) cDNAs were cloned into pCAGGS vector containing an internal ribosome entry sequence followed by a CDNA encoding nuclear localization sequence tagged β-galactosidase (pCAGGS inlz). Fig 2.2

Transposase integrated doxycycline inducible *N*-cadherin Δ390 (Kawakami and Noda, 2004; Tanabe et al., 2006; Sato et al., 2007; Watanabe et al., 2007). Cadherin-7ShRNA knock down, control cadherin-7ShRNA, and *N*-Cadherin + Cadherin 7-ShRNA (described, tested, and characterized in Barnes et al. (2010), these constructs follow the method described by Das et al. (2006), pCAGGSinlz, and CMV eGFP (Invitrogen).

Other constructs used are Haemaglutinin(HA) tagged constructs and include: HA-tagged β-catenin ΔARM, HA-tagged β-cat-1-ins, HA-tagged dominant-negative glycogen synthase kinase (GSK-DN-HA), HA-tagged wild-type glycogen synthase kinase (Wt-GSK-HA), HA-tagged pCS2-β-cat (PCS2-β-cat-HA), HA-tagged constitutively active glycogen synthase kinase (CA-GSK-HA), and HA-tagged dominant-negative T-Cell Factor (DN-TCF-HA). These constructs were tested and their results described in Bello et al. (2012) and this thesis. Other constructs used in this work are the connexin family of gap junctions proteins although their results are excluded from this thesis include: connexin 43(CX 43), connexin 43(CX 9443) and connexin 43-(CX 916).
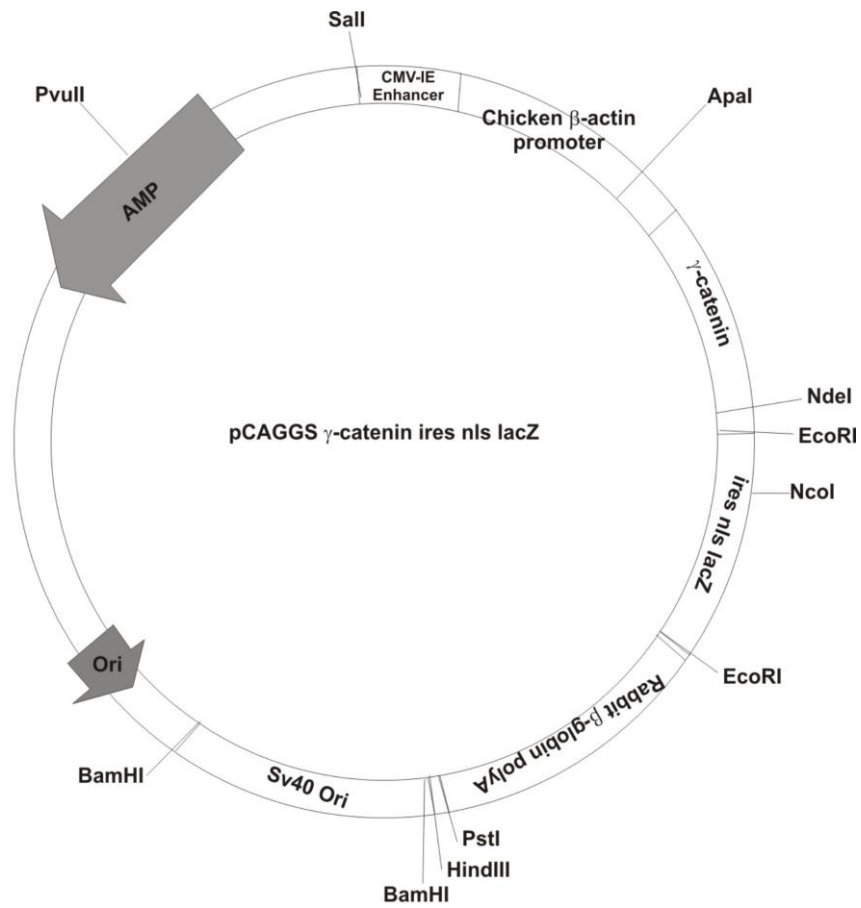
Figure 2.1 Map of γ-catenin (L127A) constructs

The γ-catenin (L127A) construct cDNAs cloned in to a pCAGGS vector containing an internal ribosome entry sequence tagged β-galactosidase pCAGGS γ-catenin ires nls lacZ.
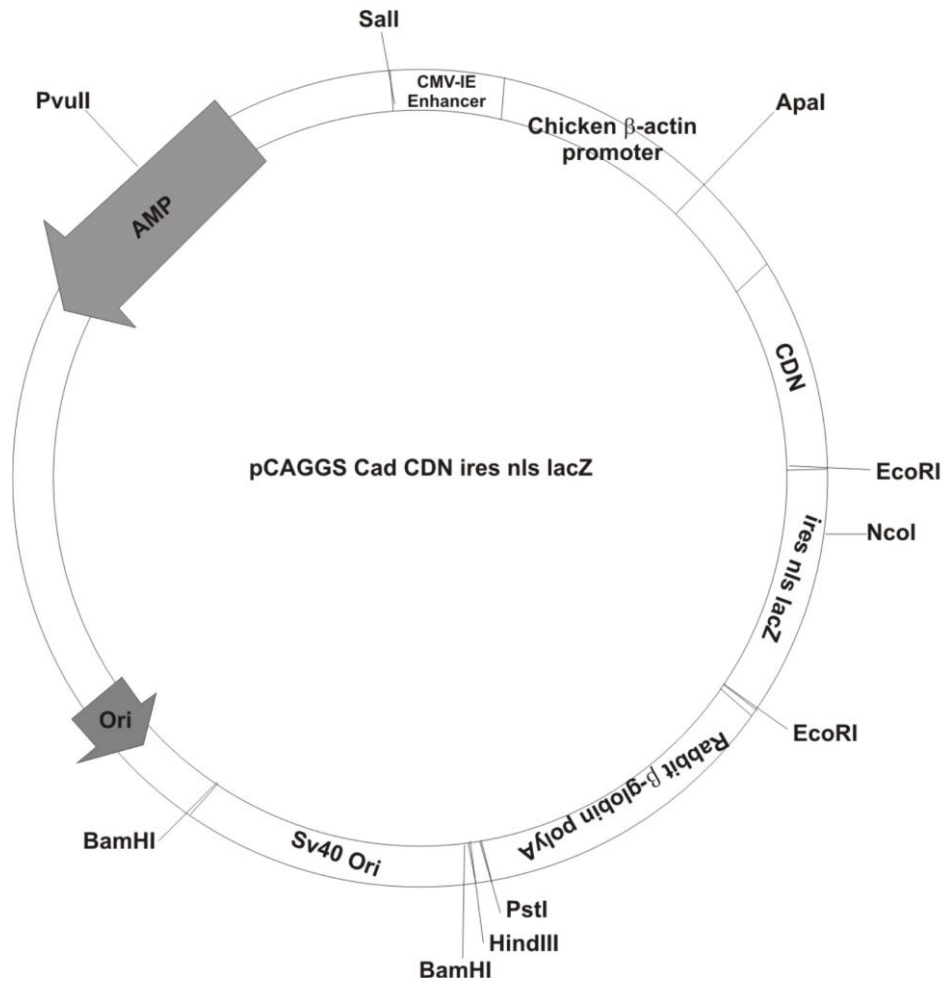
Figure 2.2 Map of cadherin dominant negative CDN construct

Cadherin dominant negative (CDN) construct cDNAs cloned in to a pCAGGS vector containing an internal ribosome entry sequence tagged β-galactosidase pCAGGS cad CDN ires nls lacZ.

2.4.2 **Bacterial transfection**

Ampicicline resistant competent bacterial cells (*Escherichia. coli*) were transfected with the DNA plasmid of choice constructs, resulting in bacterial colonies grown to harvest the DNA plasmid for subsequent in ovo electroporation or in the preparation of antisense RNA probes for insitu hybridization. The resulting plasmid DNA is extracted (maxi kit, QIAGEN$^®$).

100µl of competent bacteria were thawed on ice for 30 minutes followed by addition of 1µl of previously prepared plasmid and left on ice for further 30 minutes. The bacteria are then subjected to brief heat shock treatment for 40 seconds at 42^0C water bath and then returned to ice to cool. 500µl of LB broth was added to the plasmid and shaken at 300 rpm for 30 - 45 minutes at 37^0C. 100µl of cell suspension was spread on a pre-prepared Ampicillin agar plate (100µg ml^{-1} Ampicillin in LB agar) fully labelled and incubated at 37^0C overnight for the Ampicillin resistant bacteria to grow colonies overnight.

2.4.3 **Plasmid extraction from transfected bacteria**

2.4.3.1 Harvesting Cells

A single colony from a freshly streaked plate was carefully picked and a starter culture of 10 ml LB medium with 100µg/ml of ampicillin is inoculated. Incubated for 8 hours with vigorous shaking at 300 rpm approximately or until the starter culture become turbid. Following the incubation, the starter culture was diluted from 1:500 to 1: 1000 into 150 ml of LB medium with 500µg/ml of ampicillin and incubated for 12 to 16

77

hours or overnight at 37^0C. Cells were harvested by centrifuging at 4000 x g for 15 minutes at 4^0C.

2.4.3.2 Alkaline Lysis

Following centrifuge, the pellets were re-suspended in 10 ml of chilled Buffer P1 in which was added RNase A. Large vessels was used to ensure complete mixing of lysis buffer and incubated at room temperature (15-25^{0}C) for five minutes. This is followed by addition of 10 ml of Buffer P2 and mixed vigorously and thoroughly by inverting the sealed tube about 4-6 times and incubates at room temperature for 5 minutes the lysate appearing clear and avoiding lysis reaction exceeding the 5 minutes. Immediately, pre-chilled 10 ml of Buffer P3 was added to the lysate and mixed immediately and thoroughly by vigorously inverting 4-6 times until it becomes clear.

2.4.3.3 Lysate Clearing

The lysate is poured in to the barrel of the Qiagen QIAfilter Cartridge and incubated at room temperature for not more than 10 minutes at room temperature. For optimal performance of the QIAfilter the plunger is not inserted at this stage. The QIGEN-tip 500 is equilibrated by applying 10 ml of Buffer QBT and allowed to drain completely. The cap of the QIAfilter cartridge is then removed and the plunger inserted thus filtering the cell lysate in to the previously equilibrated QIAGEN-tip.

The filtered lysate was applied on to the QIAGEN-tip and allowed to drain by gravity flow. The DNA is held in the resin of the QIAGEN-tip-500. The QIAGEN-tip is then washed with 2x30 ml of **Buffer QC**, DNA eluted with 15 ml of **Buffer QF** and sample collected in a 15 ml falcon's tube.

2.4.4 **Precipitation of DNA**

The eluted DNA was precipitated by adding 0.7 (10.5 ml) volumes of isopropanol (2-propanol) at room temperature mixed and centrifuge immediately at 11,000 x g at 4^0C for 30 minutes, then removing the isopropanol supernatant. The DNA pellets are then washed with 5 ml of 70% ethanol at room temperature and centrifuge at 11,000 x g for 15 minutes. The pellets were air dried for 5-10 minutes at room temperature and redissolved in a 300µl of molecular biology grade H_2O(MB grade). The concentration of the plasmid was determined using the NanoDrop spectrophotometer (Thermo Scientific, Waltham, US) and concentration greater than 1µg per ml were considered suitable for the purpose of further precipitation and subsequent electroporation.

2.4.4.1 Preparation of Plasmid for in ovo electroporation

For the purpose of electroporation, higher concentrations of DNA are needed in the region of approximately 10µg/µl this is done by ethanol precipitation. For ethanol precipitation, 50 µl of each of the DNA plasmid used in the study was used. To this volume was added 0.1 volume of 5 M NaCl and mixed, this is followed by adding 2.5 volume of absolute ethanol (100%) to the volume of the mixture of DNA and 5 M NaCl. The volume was mixed and centrifuged for 20 minutes at 14,000 x g at 4^0C. The supernatant was removed and the resultant DNA pellets washed in 1 ml of 70 % ethanol by centrifuging at 14,000 x g, at 4^0C for 10 minutes. The DNA pellets were air dried and redissolved in 15µl of molecular biology grade H_2O (MB grade) and 1µl of Fast green was added ready to use for electroporation.

2.5 Retrograde Labelling of Migrating Motor Neurons

To retrograde labelled migrating motor neuron in the ventral spinal cord, Horse radish Peroxidase (HRP; Roche) 50% solution in PBS with 1% Lysolecithin (Sigma) was pressured injected in to the dorsal limb by means of 1.0 mm capillary tube (Harvard apparatus) as described in Lin et al. (1998). The retrograde labelling of migrating neuron using Horse radish Peroxidase is a two day protocol involving key stages as follows:

2.5.1 Day I:

The slides were brought out of the -82^0C freezer and air dried at room temperature for about 5-10 minutes, and are marked with immuno pen (Dako-Cytomation Denmark A/S) to prevent spillage of the antibody solution and clearly labelled. This is followed by wash in PBS for 5 minutes and 1 ml of block solution was applied on to the slides to block the sections for 30 minutes at room temperature. The blocked solution was decanted and immediately followed by application of 0.5 mls of primary antibodies diluted in block and incubated fir 12-16 hours in a humidified chamber at4^0C or overnight. The primary antibodies used in this protocol are: Dilight-488-Rabit anti Horse radish Peroxidase (1:250μl, Roche), Mouse anti Transitin-EAP3 (1:50μl, DSHB), and Mouse anti Islet-4D5 (1:25, DSHB).

2.5.2 Day II:

Slides were placed on the bench and the overnight incubated primary antibodies diluted in block solution were carefully decanted off the slides and immediately followed by three washes with 0.5 mls of PBS each for 5 minutes. Whilst the process of washing is going on, fresh block solution was prepared and secondary antibodies diluted in block were added in the following concentrations; Goat anti Mouse IgG1-Cy3 (1:1000μl,)

Goat anti Mouse IgG2b-Cy5 (1:500µl,). The slides were then incubated at room temperature in a humidified chamber for 1 hour. After 1 hour of incubation, the secondary antibodies were decanted and slides washed with 0.5 mls PBS three times each lasting 5 minutes. The PBS is then carefully decanted and two drops of Vectashield 1000 (Vecta lab Inc., USA) mounting medium carefully applied and gently cover slipped, dabbed and ready for imaging.

2.5.3 BrdU Labelling (BrdU Protocol)

Bromodeoxyuridine (5-bromo-2´- deoxyuridine, BrdU) is a synthetic nucleoside that is an analogue of thymidine. BrdU is commonly used in the detection of proliferating cells in living tissues. It can be incorporated in to the newly synthesized DNA of the replicating cells during the S-phase of the cell cycle substituting for thymidine during DNA replication and thus can be detected using specific antibodies.

BrdU (200µl, 1mM; Sigma) was injected under the developing embryo and the eggs are sealed off and returned to the forced draft incubator at 38^0C to continue incubation till the desired stage of development. Following embryo staging, dissection, and tissue preparation followed by sectioning, the sections were subjected to full BrdU protocol as described below.

2.5.4 BrdU protocol day I:

Slides were brought out of the -82^0C and allowed to air dried at room temperature for about 5–10 minutes, marked with immuno pen (Dako-Cytomation) and then washed with 0.5 mls of PBS for 5 minutes at room temperature. Block solution was prepared fresh and slides blocked with 0.5 mls of block solution for 30 minutes at room temperature in a humidified chamber. The block solution is then decanted gently and carefully 0.5 mls of primary antibodies diluted in block was applied on to the slides at

these concentrations respectively. Chick anti-β-gal (1:1000, AbCAM), Guinea pig anti-Foxp1 (1:32,000. The slides were incubated for 12 – 16 hours at 4^0C in a humidified chamber or incubated overnight.

2.5.4.1 BrdU protocol day II:

Following overnight incubation at 4^0C in a humidified chamber, the slides were brought out to room temperature and the primary antibodies decanted. This is followed by three washes with PBS) each for 5 minutes. Whilst these washes are going on a fresh block solution is prepared for secondary antibody staining. Following washes, 0.5 mls of secondary antibodies diluted in block were applied on to the slides and incubated at room temperature for 1 hour in a humidified chamber.

After the incubation, the secondary antibodies are decanted and 1 ml of 4% Para formaldehyde in PBS solution was applied and allowed to incubate for 5-10 minutes. This is followed by a brief wash (2 minutes approximately) in PBS. The slides were then immersed in a solution of 4M HCl, 0.1% Triton-X 100 for 5 minutes at room temperature. Slides were then removed and followed by three washes with PBS each for 5 minutes and left in PBS for further 5 minutes at room temperature.

About 1 ml freshly prepared block solution was applied on to the slides and allowed to incubate at room temperature in a humidified chamber for 45 minutes. The block solution is decanted and mouse anti-BrdU antibody (1:50μl) diluted in block solution was added on to the slides and incubated for overnight in the humidified chamber at 4^0C.

2.5.4.2 BrdU protocol day III:

Following overnight incubation at 4^0C, the anti BrdU antibody are decanted and preserved in -20^{0}C for subsequent use. This is followed by three washes in PBS each for 5 minutes. Donkey anti-mouse Alexa 594 (IgG mouse, 1:1000) diluted in bock solution was applied on to the slides and allowed to incubate in a humidified chamber at room temperature for 30 minutes to 1 hour. This is followed by three washes in PBS each for 5 minutes. PBS decanted and two drops of Vecta shield 1000 (Vecta lab Inc., USA) were applied on to the slides and carefully cover slipped and dabbed ready for imaging.

2.6   In Situ Hybridisation Histochemistry

For insitu hybridisation histochemistry, Digoxigenin (DIG) labelled anti sense cRNA probes were used on the alternate 15µm thick cryostat spinal cord sections as described in Price et al. (2002). Dual insitu hybridisation histochemistry with BrdU labelling was done. The three to four day protocol is divided in three key stages as described below:

2.6.1   Tissue Preparation and hybridization (Day I)

Slides were fixed in 4% Para formaldehyde in 0.1M PB for 10 minutes at room temperature, followed by three washes with PBS at three minutes per wash. Proteinase K-treatment, 1µg/ml in 50 mM, Tris-Cl pH 7.5, 6mM EDTA for 5 minutes at room temperature. This solution must be thawed and vigorously vortexed before use and mix just before slides were added. This is followed by three washes in PBS for three minutes per wash. Slides were fixed in 4% Para formaldehyde in 0.1M PB for 5 minutes at room temperature. Acetylating for 10 minutes at room temperature in (5.3ml Thriethanolamine, 0.7mL glacial HCl, 1 ml acetic anhydride in 400 ml final volume) with acetic anhydride added last and the bath stirred at all times through the incubation period. Slides were washed three times in PBS for minutes per wash and removed

individually from the last PBS wash, edges dabbed to remove excess PBS and quickly hybridization solution was added.

This is followed by pre-hybridization in 500 λ hybridization solution for >1hour at room temperature. The pre-hybridization solution is replaced with 130λ hybridization solution with probe. Solution must be mixed on the slide and carefully cover slipped. Hybridization overnight at 72^0C in chamber humidified with 5xSSC + 50% Formamide, one probe per humid chamber as probes can cross reacts if care is not taken. The probes can be either FITC or DIG labelled cRNA probes and in this study the DIG probes were used.

2.6.2 Washes and antibody staining (Day II)

Slides are washed in 5xSSC pre-heated to 72^0C and cover slips removed. Two washes at 40 minutes per wash in 0.2xSSC at 72^0C by means of immersing the slide troughs in the water bath at 72^0C as the incubator is not always reliable. Slides were equilibrated in 0.2xSSC for 5 minutes at room temperature, followed by equilibration in B1 buffer (0.1M Tris pH 7.5, 0.15M NaCl) for 5 minutes at room temperature. This is followed by block in B1 with 10% Heat Inactivated Goat Serum (HINGS) for 30 minutes to 1 hour at room temperature. Finally slides block was removed, and incubated with antibody in B1 buffer with 1% HINGS overnight at 4^0C; sheep anti-DIG-AP (Roche) at 1:5000 concentration was used.

2.6.3 Detection (Day III)

On the third day three washes in B1 buffer each for 5 minutes at room temperature was done, followed by equilibration for 10 minutes in 0.1M Tris-Cl pH 9.5, 0.1M NaCl, 0.05M $MgCl_2$. The vector NBT/BCIP product in the above buffer in addition to 0.1% Tween-20 detergent, using 500λ per slide kept in a humidified chamber in the dark.

The reaction is stopped when the desired intensity is achieved by rinsing the slide in water. The slides were air dried and mounted. The hybridization buffer is: 50% Formamide, 5xSSC, 5xDenharts, and 250µg/mL Baker's yeast tRNA, 500µg/mL salmon sperm DNA, phosphate buffer, pH 7.4.

2.6.4 Double insitu hybridization with antibody staining:

The same protocol was followed as in the insitu hybridization but with some alteration in the key stages of the protocol.

2.6.4.1 Stage I: Tissue preparation and hybridization

In this stage the slides were not treated with Proteinase K instead are permeabilized for 30 minutes in 1% Triton X-100 (Invitrogen) at room temperature following acetylation and PBS(30 mls 5M NaCl, 100 mls 0.1M PB, 900 mls distilled water) washes.

2.6.4.2 Stage II: Washes and antibody staining

Here slides are incubated overnight with the required primary antibody, which can be anti Hb9 (1:100, DSHB) or anti-Islet 1 (1:50, DSHB) in B1 Buffer containing 1% HINGS at 4^0C.

2.6.4.3 Stage III: Primary antibody detection

Following three washes for 5 minutes per wash in B1 buffer, the slides are incubated in B1 buffer containing 1% Goat serum plus Donkey anti mouse (1:500) at room temperature for 30 minutes. Then three washes in B1 buffer for 5 minutes each. Slides are then incubated with 0.5ml of vector IMMPACT DAB substrate until the desired immunogen staining is achieved. This is followed by blocking the sections in B1 buffer containing 10% Heat Inactivated Goat Serum (HINGS) for 30 minutes to 1 hour at room temperature, to be followed by overnight incubation with sheep anti-DIG

conjugated to Alkaline Phosphatase (1:5000, Roche) in B1 buffer containing 1% HINGS at 4^0C.

2.6.4.4 Stage IV: In situ detection

The insitu detection was performed as in normal insitu hybridization with three washes for 5 minutes at room temperature in B1 buffer followed by equilibration for 10 minutes in 0.1M Tris-Cl pH 9.5, 0.1M NaCl, 0.05M $MgCl_2$. The reaction can be stopped when the desired staining intensity is achieved by rinsing the slide in water for 10 minutes at room temperature. The slides were air dried and mounted with cover slips using Dako Glyceryl Mounting Medium (Invitrogen)

2.7 **Image acquisition and analysis:**

Following immunohistochemistry, serial transverse lumbar spinal cord sections of 15µm thickness were observed using a Nikon Eclipse E80i fluorescence microscope equipped with Nikon DS5M and Hamamatsu OCRA-ER closed circuit digital camera. Fluorescent images were capture using varying exposure times and processed by means of IP-Lab software for windows (Scanalytics). Cell counts and measurements of neuronal migration lengths as well as arrested migration from the ventricular zone to the final settling position in the ventral spinal cord was obtained by means of Image J software version 4 (NIH, USA), and data collated and stored in excel spread sheet for further analysis.

2.8   Data generation and analysis

Green Fluorescence Protein (gfp) fluorescence was used as a marker of good electroporation in the ventral lumber spinal cord as well as ventral axons (segmental in nature).This is followed by good fluorescence of the various motor neuron markers and other markers for radial glia and proliferating cells respectively. More than 50% gfp fluorescence is required to classify a cell well electroporated and the nucleus of the cells clearly fluorescent for Islet, Lhx-1/Lim1, and Hb9 marker for motor neurons, transitin for radial glial and BrdU for proliferating cells respectively.

Following good electroporation evidenced by good fluorescence, the serial spinal cord section were carefully observed and analysed based on the total number Islet and Hb9 positive cells in the ventral lumber spinal cord of the control (internal control) and the electroporated (observed) hemi sections of the lumber spinal cord. Similarly, the total numbers of cells in the motor columns of the control and electroporated side were determined as well as their distribution.

 Migratory path arrest of immunostained cells along the ventral motor columns in the lumbar spinal cord of experimental side were analysed compared to the control. Stacking of positive motor neurons in the ventricular zone was analysed in the different constructs used in this study. Neuronal mixing of the experiment side compared to control were analysed for the entire construct at different stages of spinal motor neuron development.

2.9   Divisional Neuronal Mixing Index

The divisional neuronal mixing index is conducted as previously described by Price et al; 2002. We identified a single lateral motor column lateral (LMC_L) cell and count the number of positive lateral motor column medial (LMC_M) cells that are directly close to or adjacent to it in both the electroporated and the control side. The control side of the spinal cord compared to the electroporated side shows no mixing of the LMC_L with the LMC_M. These observations were carried out the serial sections of at least 7 embryos and the procedure is carried out for the entire different construct used in this study. The data generated was analyzed at various stages of development using excel, sigma plot and presented as described in Price et al; 2002.

2.9.1   Motor Neuron Quantification

Throughout the course of this work the total numbers of the entire motor neurons per section per construct were determined against the developmental stages of the embryos. Total number of motor neurons positive for Islet-1 and Hb9 were quantified from the 15μm thin sections of the lumbar spinal cord at intervals of 100μm along the rostrocaudal axis of the developing lumbar region of the spinal cord.

The number of the motor neurons with respect to their position along the medio-lateral extent of the spinal cord sections was also determined and the cells in aberrant location also calculated and their percentage from the total motor neurons present based on the count of immunoreactivity for Hb9 and Islet-1 cells on the thin sections was determined by dividing the number of the cells from the total number of all motor neurons per section. Similar approach was used to determine the percentage of   abnormally located motor neurons from the total number of motor neurons on both the control and experimental side.

The number of and percentages of cells in the ventricular zone was also determine using immunoreactivity for the different markers for LMCl and LMCm respectively. The distance travelled by the motor neurons along the medio-lateral extent of the ventral spinal cord along their migratory path was also determined essentially as in Bello et al., 2012. Also the measure of dispersion of cells evidence by the increase in the area of the LMCl and LMCm in both the control and experimental side was determined. In all cases the student's t-test was applied in the analysis to determine the statistical significance between the experimental side and the control sides.

3 Developmental Profile of Spinal LMC Neurons.

3.1 Time course of Segregation of spinal Motor Neurons.

I first characterized the stage specific time course of events from the generation, migration and segregation of the lateral motor column (LMC) neurons in the ventral horn of the spinal cord at the lumbar region during development. I conducted immunohistochemistry on wild type chick spinal cord sections from HH stages 18-30 (Hamburger and Hamilton 1992), a period during which spinal motor neuron migration would normally have been completed. I analysed the timing of expression of transcription factors that are known to delineate the divisions within the motor columns in the developing ventral spinal cord.

At the levels of the ventral lumbar spinal cord, expression of pan LMC transcription factor; Forkhead domain transcription factor foxp1 identified the LMC (Dasen et al 2008). Also immunohistochemistry shows that the expression of the LIM homeodomain transcription factor Islet-1 delineates the neurons of the medial division of the lateral motor column LMC_M which project axons to the ventral aspect of the limb (Tsuchida et al., 1994), whilst another LIM homeodomain protein Hb9 identified the neurons of the lateral division of the lateral motor column LMC_L neurons which project axons to the dorsal aspect of the limb within the LMC respectively (William et al., 2003).

The combined expression of Islet-1 and Hb9 in the ventral spinal cord allowed identification of three distinct classes of spinal motor neurons early in development. Three columns identified by Islet1 and Hb9 namely lateral motor column lateral LMC_L (Hb9), lateral motor column medial LMC_M (Islet1) and medial motor column MMC were clearly distinct at the end of normal spinal motor neuron segregation in the ventral lumbar spinal cord. In addition to this, neuron of the medial motor column MMC which

90

projects to the trunk muscles expresses both Islet-1 and Hb9 respectively but do not expresses the pan LMC transcription factor foxp1 known to influence identification of the LMC (Dasen et al., 2008; Rousso et al., 2008). The expression of these transcription factors persist throughout the migratory phase of the spinal LMC neurons (Fig.3.3A-H).

3.2 Migration and Columnar Segregation of Spinal Lmc Neurons

The majority of the spinal LMC neurons (about 95%) are generated during a 24 hour window period before HH stage 23 (Hamburger and Hamilton 1992). The generation of spinal LMC neurons reaches its peak between HH stage 18-20 for LMC_M and HH stages 20-21 for LMC_L respectively (Hollyday and Hamburger 1977, whitelaw and Hollyday 1983) and by stage 28-30 neurons have reached their final settling positions in the developing ventral spinal cord. Therefore, I analysed the time course for spinal motor neuron generation, segregation and migration from the progenitor-rich ventricular zone to their final settling position in the ventral horn of the spinal cord from stages 18-30 and analysed the data for stages 19 – 28 (Fig.3.1 and Fig.3.2).

I found that LMC_M neurons populate the ventral horn early between stages 23-24 during development; this is consistent with previous observations from earlier works on neuronal segregation in the developing spinal cord (Lin et al., 1998; Socknathan and Jessell 1998; William et al., 2003). The potential LMC_L neurons begin their migratory phase at stage 24 and by stage 27-28 reached their definitive settling position in the ventral spinal cord by passing through the earlier born LMC_M neurons in a process closely similar to the "inside out" lamination of the developing cortex.

Analysis of the total number of immunofluorescent cells positive for Islet-1 and Hb9 was conducted at every stage of development under observation from stages HH18-28 (Hamburger and Hamilton 1992) and the total number both Islet-1 positive and Hb9

positive cells quantitated between stages 28-30. The total Islet-1positive cells for the two hemi sections of the developing spinal cord shows no significant difference (Figure 3.1) student *t*-test measurement *p* value= 0.5037. The total number of the Hb9 cells also shows no significant difference (Figure 1) measurements using student *t*-test *p* value=0.0860. Similarly, I next analysed the total number of Hb9 positive cells and compared it to the Islet-1 positive cells value, the overall total number of Islet-1 positive cells and Hb9 positive cells shows no statistically significant difference (Figure 2) using student *t*-test *p* value = 0.2967. These observations revealed a highly ordered and efficient normal generation process of the developing lumbar spinal motor neurons.
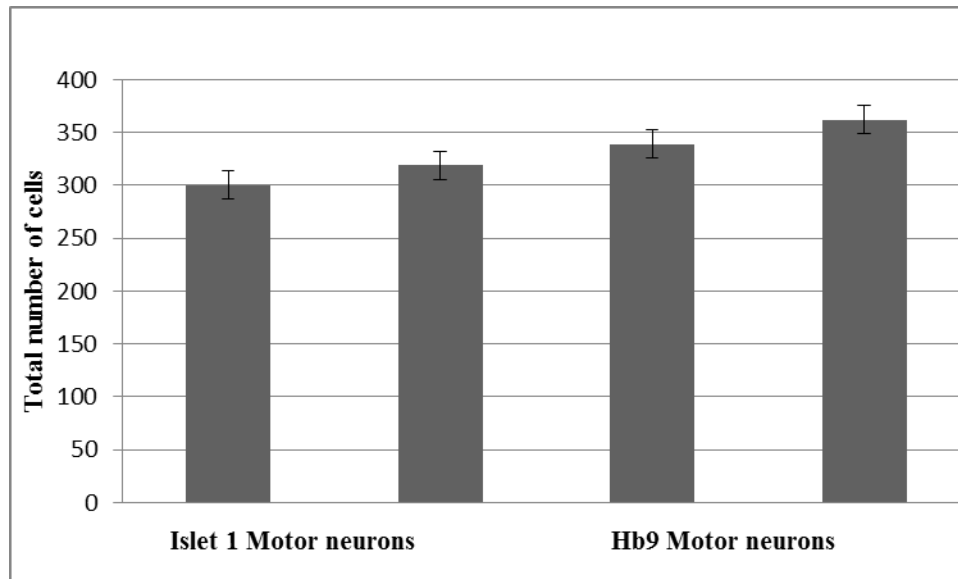
Figure 3.1 Quantitation of the total number of spinal motor neurons at stage 28**.**

Quantification of the total number of the Islet-1 and Hb9 positive cells to stage 28 wild

type embryos. HH28 wild type embryos at lumbar level of developing spinal cord.

Series 1 and 2 shows the total number of Islet-1 positive cells in the ventral hemi

sections of the lumbar spinal cord while series 3 and 4 shows the total number of Hb9

positive cells in the hemi sections of the ventral aspect of the developing lumbar spinal

cord. Student t-test p value =0.5037 and 0.0860 respectively for Islet-1 and Hb9 positive

cells. Error bars are standard error of means SEM.
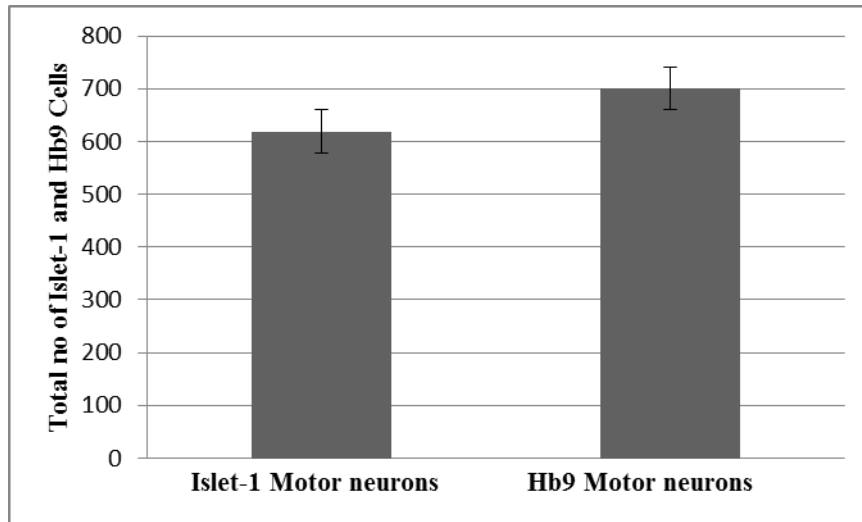
Figure 3.2 Quantitation of the number of Islet-1 and Hb9 Motor neurons to stage 28. quantification of the total number of motor neurons Islet-1 and Hb9 positive cells to stage HH28 wild type embryos at the lumbar level of developing spinal cord: 1; Islet-1 motor neuron 2; Hb9 motor neurons in the developing ventral lumbar spinal cord, student t-test p value= 0.2967 and error bars are Standard Error of Means SEM
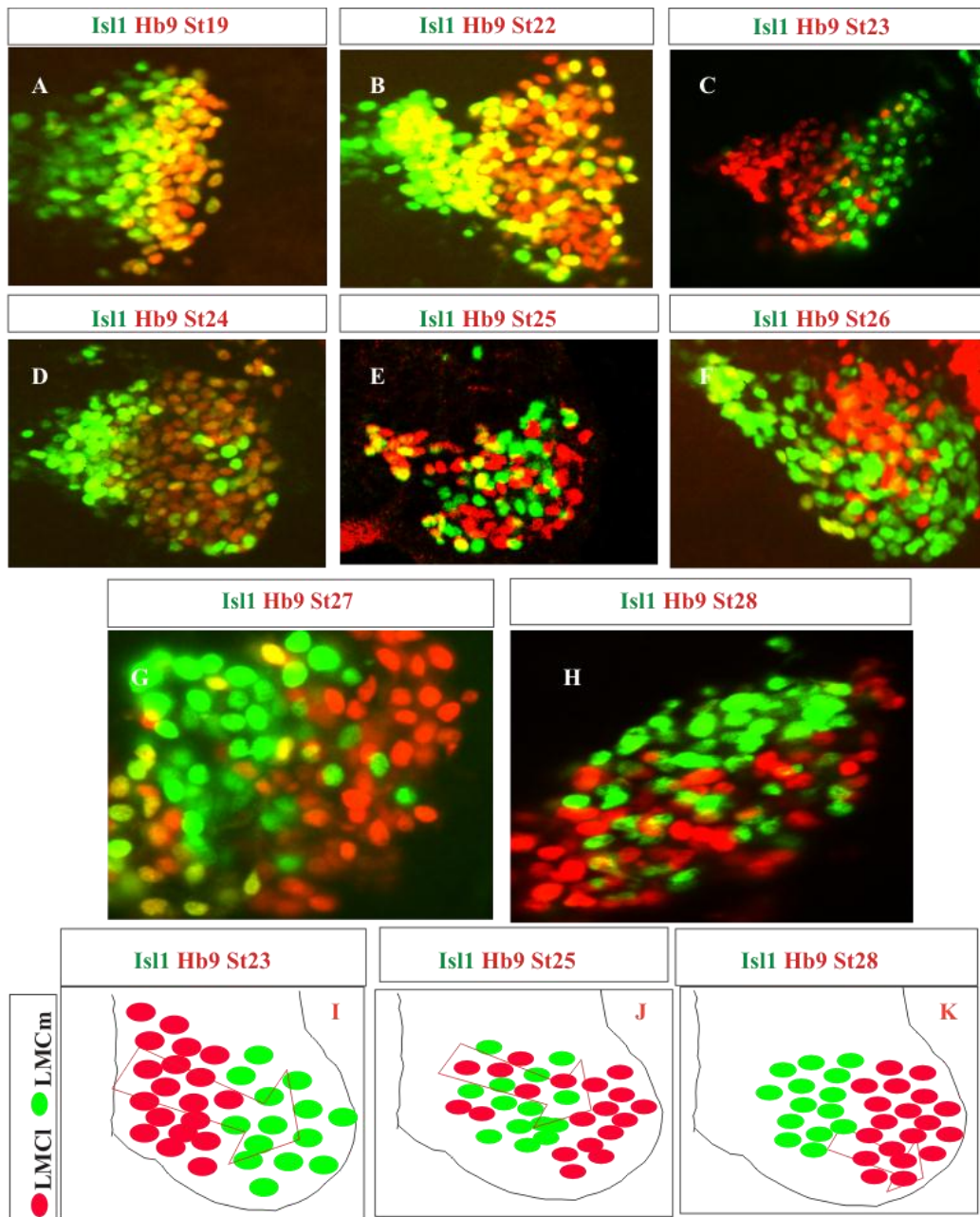
Figure 3.3 Developmental Time Course of Divisional Segregation of Spinal LMC Neurons.

Developmental Time course of divisional segregation of LMC, from HH stage 19 to 28. (A), Expression of Islet-1 and Hb9 in stage 19 embryo showing early phase of migration from the ventricular zone to ventro lateral lumbar region. (B), Expression of Hb9 and Islet-1 in the ventral horn of HH stage 22 embryos showing active segregation. (C), Hb9 and Islet-1 showing segregation of the LMC in stage 23embryo (D), Hb9 and Islet-1 expression showing LMC segregation at an advanced level with few LMCm cells within the LMCl domain in stage 24 embryo. (E), expression of Hb9 and Islet-1 in a stage 25 embryo. (F), expression of Hb9 and Islet-1 showing early part of the final phase of segregation with the LMCm and LMCl taking their final definitive position in the ventral lumbar spinal cord of stage 26 embryos. (G), Segregation almost complete by the expression of Islet-1 and Hb9 cells in a stage 27 embryo. (H), columnar segregation is complete by stage 28 during development. (I, J and K) Shows schematic summary of events in the migration of the LMCl neurons to their final settling position through the LMCm neurons in the ventral lumbar spinal cord during divisional segregation at stage 23(I), stage 25 (J), and st28 (K).
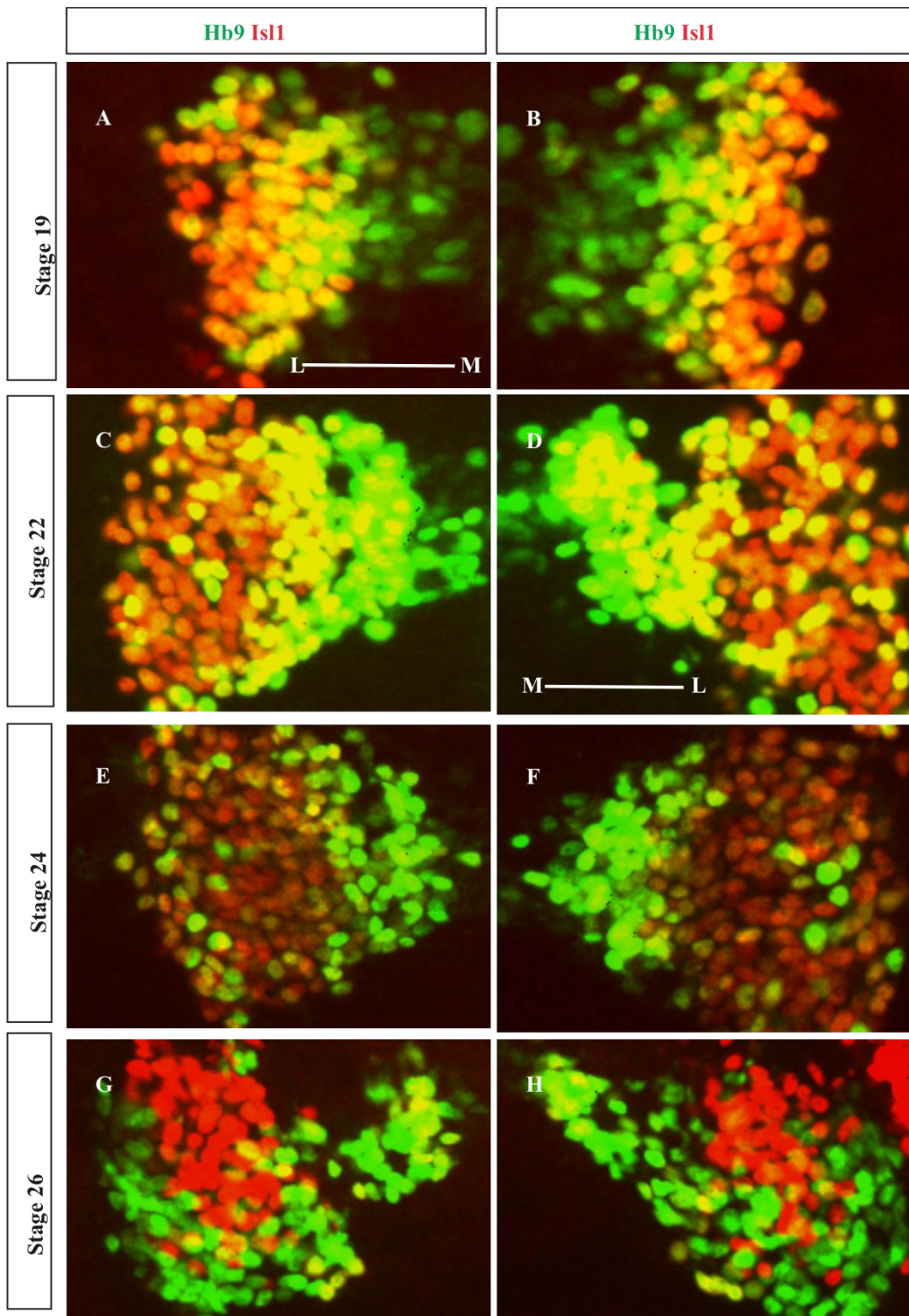
Figure 3.4 Pattern of Spinal LMC Neurons Segregation in Lumbar region of Developing Spinal Cord.

(A-B) Two hemi sections of the ventral spinal cord expressing islet-1 and Hb9 positive cells showing the initial migration of LMC neurons. The LMC neurons begin segregation in a medio-lateral direction (M-L). (C-D), segregation of LMC by LMCl intermingling with LMCm neurons along their migratory path to their final settling position in the ventral spinal cord at stage 22 of development. (E-F), beginning the final phase of segregation with few LMCl cells reaching their final settling position in stage 24 embryo. (G-H), clear and near complete columnar segregation of the LMC with distinct LMCm and LMCl visible in stage 26 embryo.

3.3 Transitin Labelled Radial Glia Fibres Directs Spinal Motor Neuron Migration

In the developing cortex, neurons migrate from the point of their generation to their final position via radial glia. Since radial glia are thought to act as a scaffold for migrating neurons in developing cortex, I next asked what guided the orderly migratory phase of the developing spinal motor neurons in general and in particular the LMC neurons in the ventral spinal cord. Previous work in developing mammalian cortex identified the expression of Nestin, an intermediate filament protein by radial glia. In chickens, the avian homologue of nestin is a nestin related intermediate filament protein called transitin (Cole and Lee, 1997) which is expressed by neural progenitors and can be induced in Muller glial cells in the chicken retina (Fisher A.J and Omar G. 2005) It is expressed by midline radial glial cells structure, by several commissural axons, and Bergmann glial cells of the developing cerebellum (Yuan et al, 1997).

I thus asked whether migrating spinal motor neurons were closely apposed to transitin radial fibres, an obligate requirement if transitin fibres identify pathways for motor neuron migration. I identified subsets of LMCl motor neurons through injection of the retrograde axonal tracer, HRP, into the dorsal limb mesenchyme at stage 25 followed by incubation with the tracer for 5 hours, a time found to be sufficient for retrograde transport of HRP from the periphery to motor neuron cell bodies. Migrating motor neurons were identified by their location within the islet-1 expressing LMCm domain at the time of analysis. In the majority of HRP positive neurons analysed within the LMCm, I found that migrating motor neurons were closely apposed to transitin expressing radial fibres (Fig.3.5B-C). This suggests the possibility that transitin radial fibres mark the pathways of LMCl neuron migration.

3.4   Transitin Labelled Radial Glia Expressed Beta Catenin in Ventral Lumber Spinal Cord

I conducted immunofluorescence staining first with transitin alone to analysed the nature of it expression in the ventral spinal cord, and then transitin and β-catenin on wild type spinal cord sections between HH stages 18-30 (Hamburger and Hamilton) a period characterised by migration and segregation of motor neurons and by the end of which LMC neurons would have reached their final settling position in the ventral spinal cord. Visualization of transitin by immunofluorescence revealed a pattern of radial fibres traversing the spinal cord from the progenitor rich ventricle to the white matter in a medio-lateral direction, characteristic of the migratory route for the developing LMC neurons. Analysis of these transitin positive fibres revealed a higher density in the dorsal spinal cord compared to the ventral spinal cord and this is constant irrespective of the stage of development analysed. Within the ventral horn an average of 14 (modal value; range 12 to 15) transitin labelled fibres could be identified (Fig.3.4B-C, E-F and Fig3.5A-F).

I further carried out staining with transitin and β-catenin in the developing spinal cord between stages 21 -28 to establish the development of the expression pattern of transitin and β-catenin along the end-feet of radial glia and the radial glial fibres. The transitin staining shows radial glial fibre labelling, and β-catenin shows labelling of the ventricular zone and transitin fibres. (Fig.3.6A-F). I found no instances of labelling of a transitin fibre that was not also β-catenin positive. Additionally, there did not appear to be significant expression of β-catenin within the ventral horn that was not associated with the transitin fibres. This suggests that β-catenin and transitin are co-localised in the ventral horn.
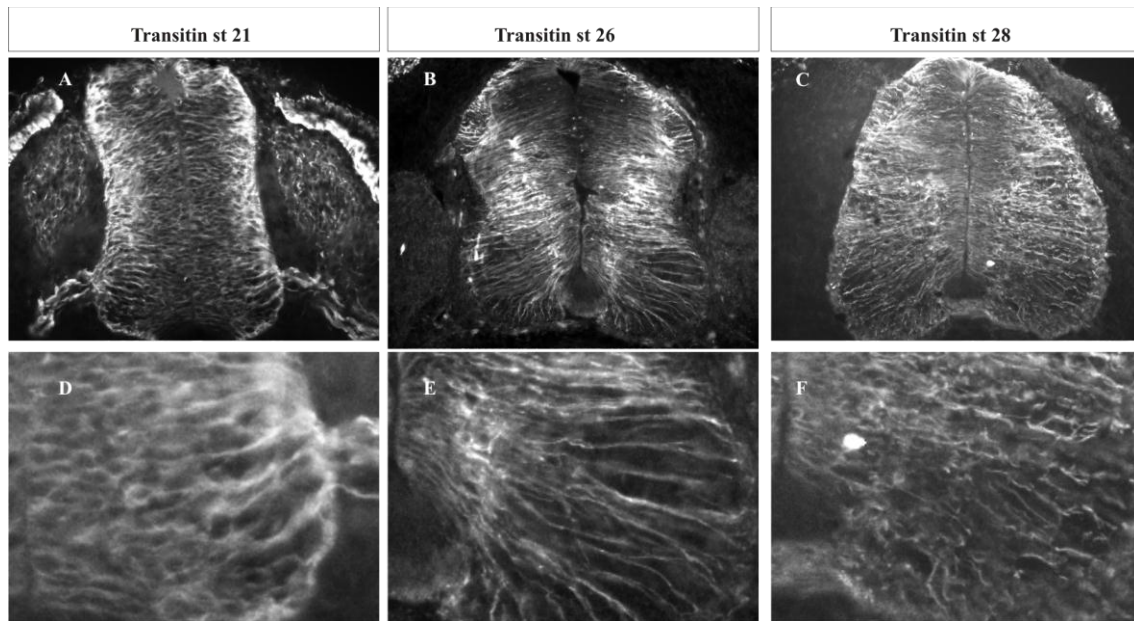
Figure 3.4 Pattern of expression of transitin in radial glia in the ventral lumbar spinal cord.

A, expression of transitin by ventral radial glia in a stage 21 embryo. Immunoreactivity for transitin labelled the ventral axons on either sides of the spinal cord. *B,* more refined expression pattern following immunoreactivity for transitin in the ventral and dorsal spinal cord at stage 26, note that there is more concentration of the transitin positive fibres in the dorsal half than the ventral half, but the fibres in the ventral half can be clearly determined in terms of numbers. *C*, at advanced stage the expression pattern remains constant with more fibres concentrated on the dorsal half of the spinal cord. *D-F* magnified areas of the right hemi section of the ventral lumbar spinal cord showing immunoreactivity for transitin at stage 21(*D*), 26(*E*), and 28 (*F*).

Transitin st 26	Transitin HRP	Transitin HRP
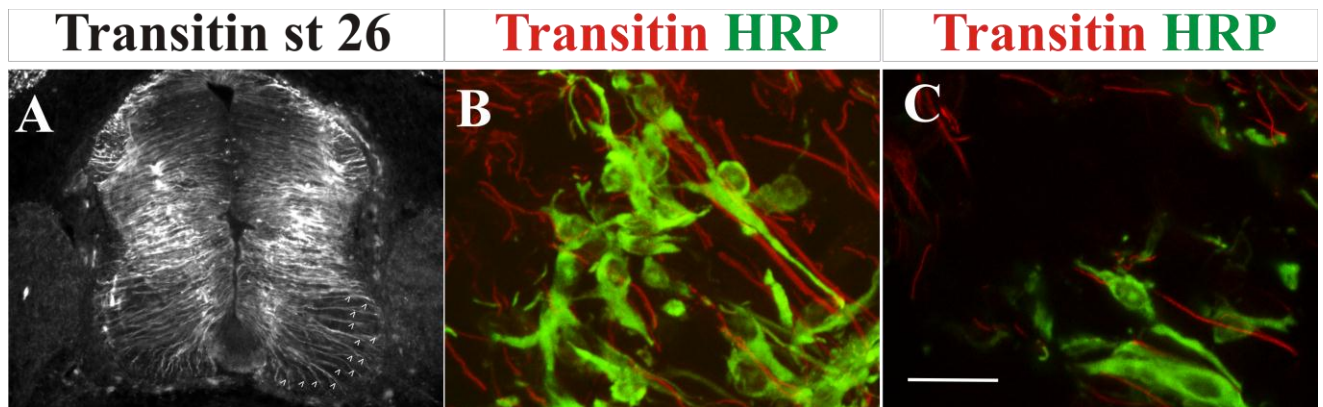
Figure 3.5 transitin labelled radial glia direct spinal motor neuron migration.

A, immunoreactivity for transitin in a stage 26 wild-type lumbar spinal cord fibres more concentrated in the dorsal half than in the ventral lumbar region, with average of 14 fibres traversing in a medio-lateral direction from the ventricular zone to the ventral horn (arrow heads point to individual fibres). *B*. immunofluorescence for transitin in red and horse radish peroxidase (HRP) labelling of spinal motor neurons shows close positioning of the migrating motor neurons and the transitin labelled radial glia in the ventral spinal cord. *C*, other examples of close relationship of radial glia and the motor neurons.
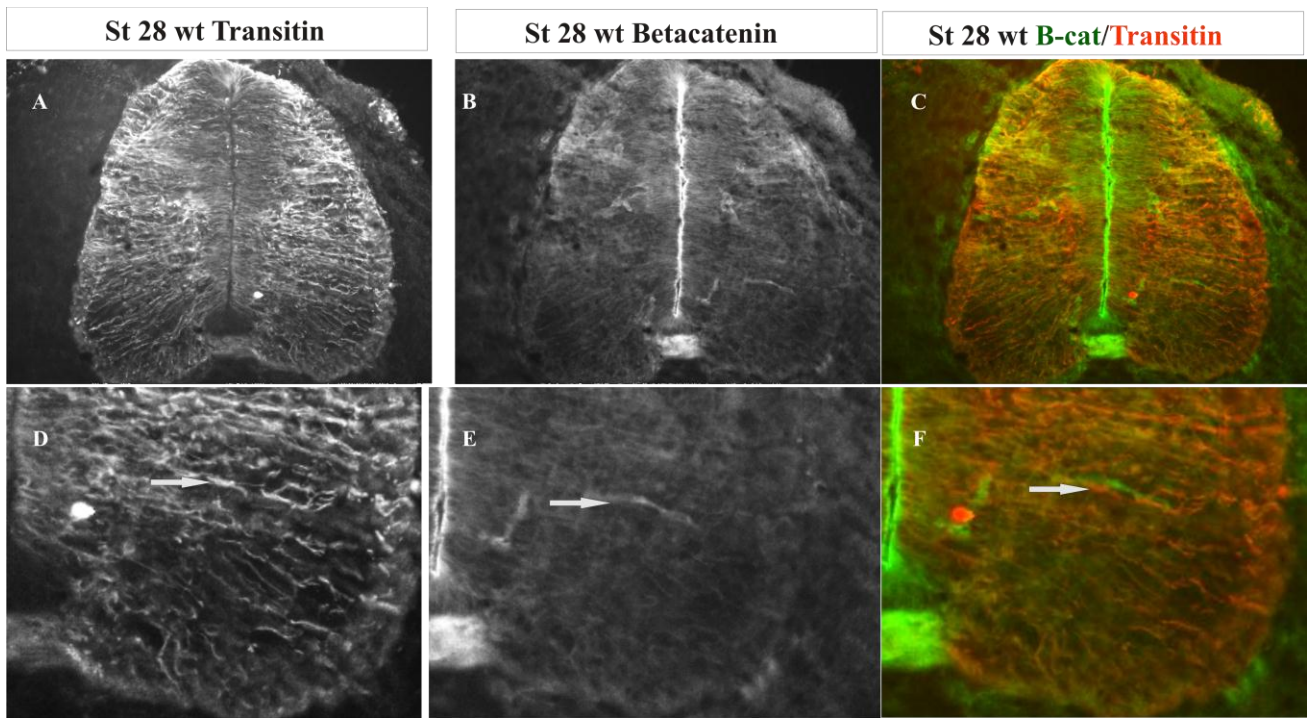
Figure 3.6 transitin labelled ventral radial glia fibres co express β-catenin.

A, transitin immunoreactivity in a stage 28 lumbar spinal cord showing that radial glia fibre labelling is more concentrated in the dorsal region than the ventral. *B*, expression of β-catenin along the ventricular zone and in radial glia fibres at stage 28. *C*, merged immunofluorescence for β-catenin and transitin showing some fibres co-labelling with both transitin and β-catenin in the ventral half of the spinal cord. *D-F*, magnification for the area in *D* (the ventral horn of the left side), *E* the ventricular zone and the ventral horn of the right side of lumbar spinal cord in *B* showing expression of β-catenin. *F* merged area in *C* arrows shows co-labelled fibres for both transitin and β-catenin.

4 Expression Profile of Catenins during Normal Development of Spinal Motor Neurons

4.1 Expression Pattern of Catenins during Normal Development of Spinal Motor Neurons

I next characterised the expression of classical cadherin signalling components during the stages of motor neuron segregation and migration (Butz et al., 1992; Zhurinsky et al., 2000; Uemura et al., 2006). Catenins are crucial to the adhesive function of cadherins and form part of the cadherin catenin complex. They are also known to be expressed in the developing central nervous system. I therefore focussed on the cytoplasmic binding partners for classical cadherins that have been shown to play roles critical to cadherin function in cell adhesion and migration. I first conducted immunohistochemistry on wild type chick spinal cord section at the lumbar level to establish their expression profile. Thus, I analysed the expression of α-catenin, β-catenin and γ-catenin by immunofluorescence. I found that α-catenin appears to be expressed in most neurons in the spinal cord and is expressed in the majority of spinal neurons, including the LMC, at all stages analysed (HH stage 22 to HH stage 27) Fig 4.1A-D. However, I observed striking differences in the expression patterns for β-catenin and γ-catenin. Double immunofluorescence of γ-catenin with Foxp1 indicated that γ-catenin is expressed in the majority of LMC neurons (Fig 4.2G). Additionally, γ-catenin immunofluorescence was observed in motor axons of the ventral root. This expression was found in the majority of LMC neurons from the time of their first generation to at least HH stage 32 (Fig 4.3I-L). In contrast, β-catenin was detected at the ventricular surface and in radial fibres projecting in the ventral horn, but appeared excluded from neurons of the LMC.

As shown before, these radial fibres express transitin. The cytoplasmic and cell surface staining of β-catenin and γ-catenin makes determination of the relative number and position of cells that express them difficult to assess by immunofluorescence. Thus, in situ hybridisation using antisense probes for β-catenin and γ-catenin was conducted. Consistent with immunofluorescence results, γ-catenin was found to be expressed in the majority of cells within the ventral horn but was excluded from cells close to the ventricular surface- the presumptive progenitor cells (Fig.4.2A-H). In contrast, β-catenin was not detected in the ventral horn but was instead expressed in a number of cells (~14 per section) in a line roughly parallel to the ventricular surface within the ventral part of the spinal cord that encompassed the extent of the ventral horn (Fig 4.1A-F, G-L). Within more dorsal regions of the spinal cord, β-catenin was detected in the majority of these presumptive progenitor cells. I therefore asked whether the ventral cells expressing β-catenin were undergoing mitosis. To address this, a 2-hour pulse of BrdU was applied to embryos at HH stage 22 and subsequent immunohistochemistry for BrdU and in situ hybridisation for β-catenin was performed. The result revealed about ~20% of BrdU+ve cells were co-labelled with β-catenin- indicating that β-catenin expressing cells are undergoing mitosis but that only a subset of cycling progenitor cells express detectable levels of β-catenin (Fig 4.1F). In keeping with previous findings that β-catenin fibres within the ventral horn express transitin, this suggests that transitin fibres within the ventral horn represent a subset of progenitor cells located within the motor neuron progenitor domain. Thus, I believe that β-catenin and γ-catenin are expressed in different cell types in the ventral horn of the spinal cord.
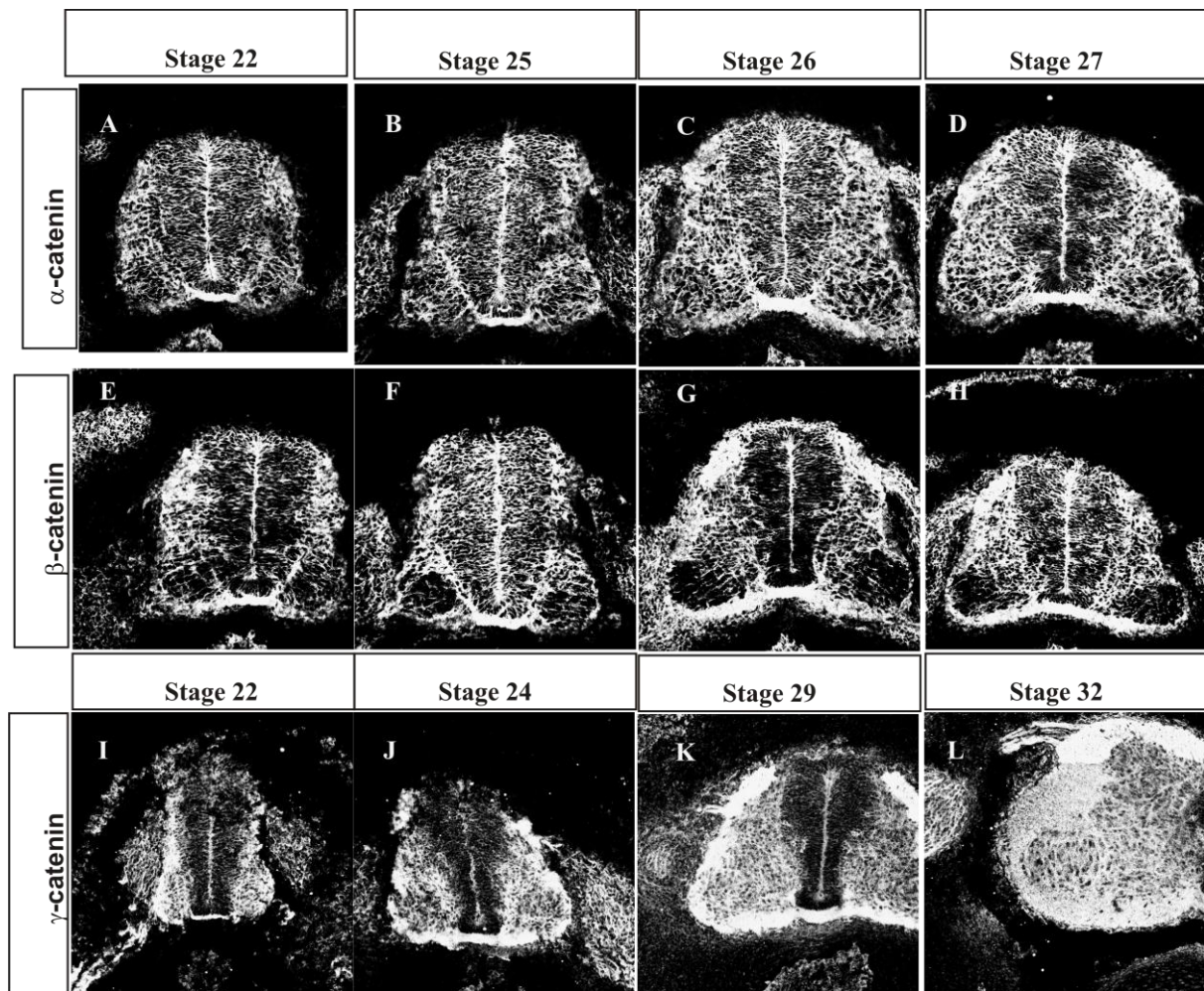
Figure 4.1 Expression profiles of Catenins during development.

The upper panel shows the expression profile for α-catenin from HH stage 22 to 27 (*A-D*) α-catenin immunoreactivity across the whole spinal cord. The middle panel shows the immunoreactivity expression profile for β-catenin from HH stage 22 to 32(*E-H*), β-catenin is found at the ventricular surface and in the radial fibres projecting in the ventral horn and appears to be excluded for the LMC neurons. The lower panel shows the expression profile for γ-catenin (*I-L*), γ-catenin is expressed by the majority of LMC neurons.
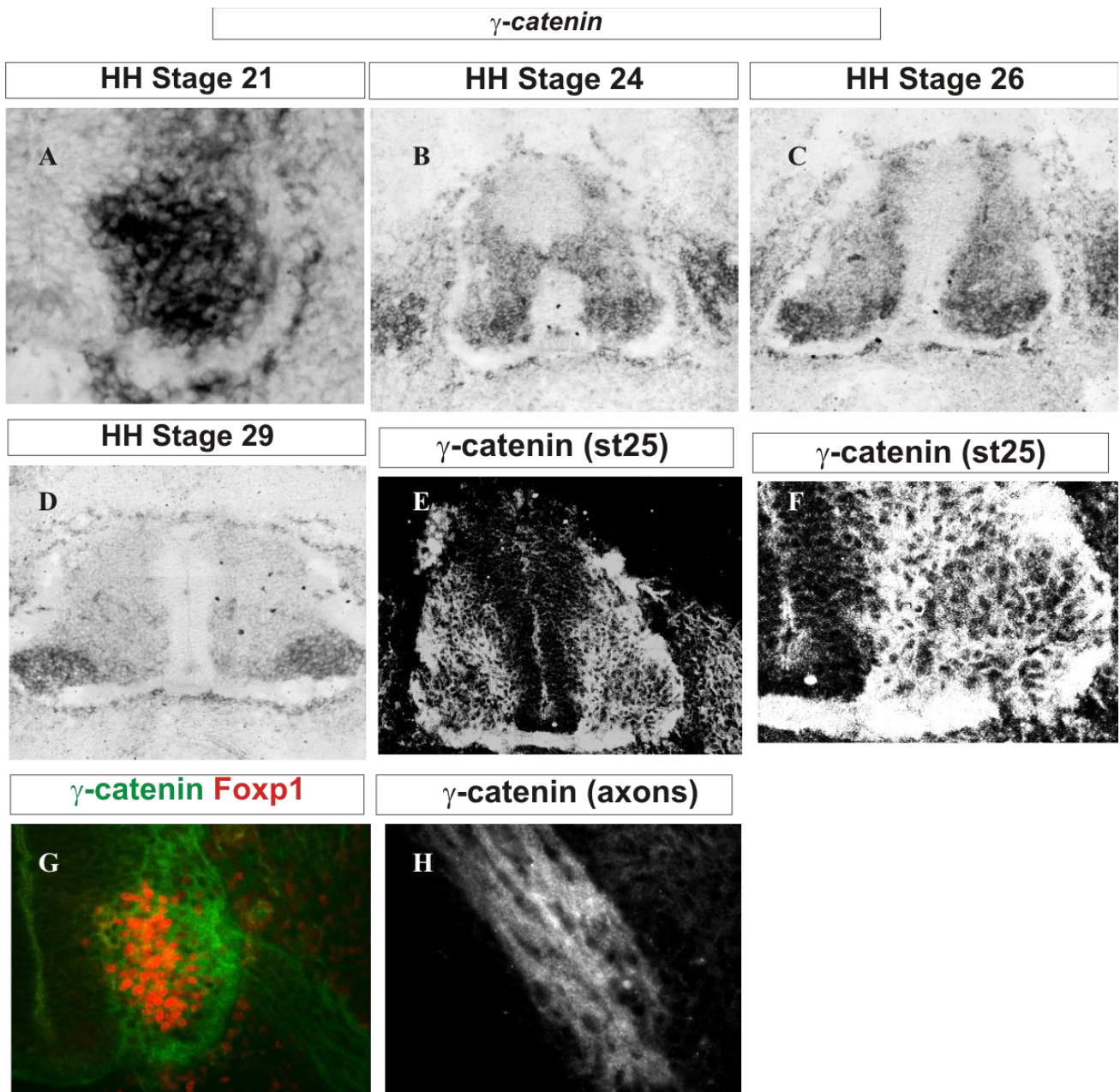
Figure 4.1 γ-Catenin is expressed In the LMC during Motor Neuron Migration.

A, γ-catenin transcript expression in the ventral horn of stage 21 lumbar spinal cord. Lumbar spinal cord expression of γ-catenin transcript at HH stage 24 (*B*), HH stage 26 (*C*), and HH stage 29 (*D*). Immunofluorescence of γ-catenin in the lumbar spinal cord at HH stage 25. The whole spinal cord is shown in *E*. the ventral horn is shown in *F* medial is to the left encompassing the ventricular zone. *G*, γ-catenin is expressed in the LMC as marked by Foxp1 expression. *H*, γ-catenin immunofluorescence in ventral motor axons.
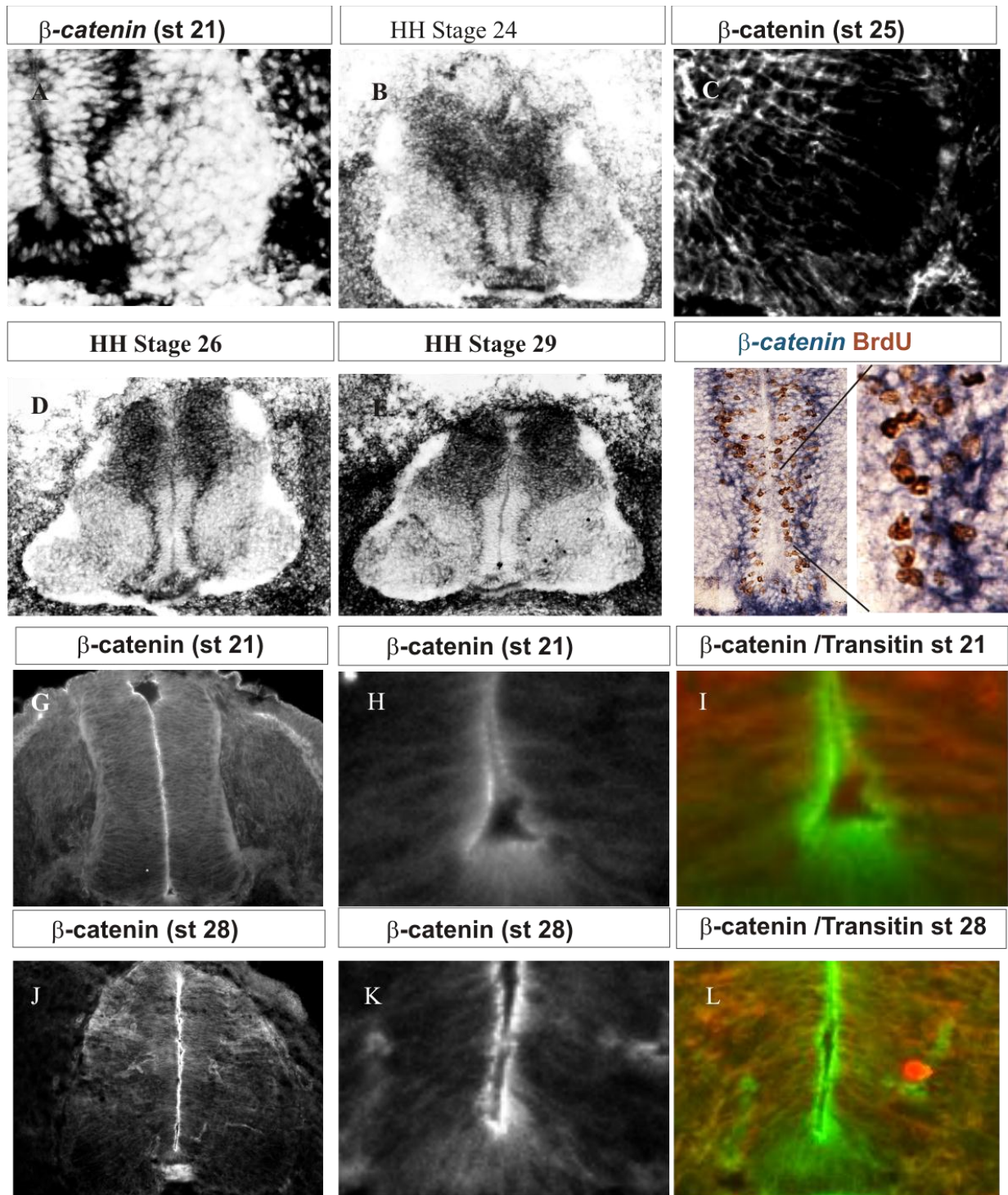
Figure 4.3 β-catenin expression in transitin radial glia.

(*A*), β-Catenin transcript expression in HH stage 21 ventral spinal cords, (*B*) stage 24, (D) stage 26 and (E) stage 29 lumbar spinal cords. (C), β-catenin immunoreactivity in the ventral horn of HH stage 25 lumbar spinal cords. (*F*), BrdU expression (brown) with β-catenin (blue) after 1 hour pulse application of BrdU to a HH stage 23 embryos. Right of F, magnification of the area pointed by the black lines. (G-I), immunoreactivity for β-catenin and transitin at HH stage 21. G, whole spinal cord, H, β-catenin alone and I, β-catenin and transitin. (J-L) Immuno reactivity at stage 28, J, whole spinal cord at HH 28, K, β-catenin alone and L, β-catenin and transitin at HH stage 28.

5 Expression profile of cadherins during Normal Development of Spinal Motor Neurons

5.1 Expression Pattern of Cadherin during Normal Development of Spinal Motor Neurons

To address the potential role of cadherin in the spinal LMC neurons segregation and migration, I characterised the expression pattern of type I cadherins and type II cadherins in the ventral lumbar spinal cord during the time of motor neuron migration.

Within spinal motor neurons, the mature pattern of differential expression of type II cadherins within spinal motor pools occurs through an extrinsic signal mediated refinement of temporal cadherin expression (Price et al., 2002; Patel et al., 2006). For example, within the chick spinal cord, a sub-group of cadherins expressed in a late, motor pool specific pattern are expressed in most, if not all, early-generated motor neurons and this expression is refined through signals present in the limb. Similarly, recent evidence in the mouse spinal cord suggests that this cadherin refinement may be due to limb-derived neurotrophic factors acting on neurotrophic factor receptors expressed within the spinal motor neuron (Livet et al., 2002; Haase et al., 2002). I therefore conducted immunohistochemistry on wild type chick spinal cord sections at various stages of development to establish the expression pattern for the type I cadherins during spinal motor neurons migration from the progenitor rich ventricular region to their final settling position in the ventral horn of the developing spinal cord. Using an antibody that recognises all type I cadherins I observed the expression of type I cadherins span from early in the development at the beginning migration up to the end

107

of their migration in the ventral spinal cord (Fig.5.1A). I next asked which of the type I cadherins could be expressed within the spinal cord.

Neurite outgrowth is critical for formation of functional connections between neurons and hence migration and segregation. The role of N-cadherin has been shown to include regulation of neurite outgrowth in vitro, induction of retinal ganglion cells neurite outgrowth (Bixby J.L. and R. Zhang., 1990). N-cadherin is also up regulated during the regeneration of peripheral nerves and may have a critical role in myelination (Shibuya Y., et al., 1995). Thus, I reasoned that N-cadherin may have a specific role in the segregation and migration of chick spinal motor neurons and thus, using immuno histochemical techniques, I characterized the expression of N-cadherin in the developing ventral lumbar spinal cord from early to late stages of spinal motor neurons development. My results suggest that N-cadherin expression overlaps completely with that of the pan-cadherin antibody. They also suggest the exclusion of N-cadherin form the LMC neurons which instead are found in the radial fibres in the ventral horn (Fig. 5.1B-D). I next characterised the expression of several type II cadherins during early motor neuron development. In contrast to type I cadherins, type II cadherins including cadherin-7, cadherin-12 and cadherin-20 were expressed in the majority of LMC neurons at early stages in development (Fig.5.2A-D, and Fig.5.3A-D) (Luo et al., 2006). Cadherin-7 protein was predominantly expressed during LMC divisional segregation and is down regulated in the majority of LMC neurons after divisional segregation (stage 28 Fig5.2A-D). To establish the expression of cadherin-12 and cadherin-20, in situ hybridization for cadherin-12 and cadherin-20 was conducted. In contrast to expression profile of cadherin-7, the expression profile shows strong expression in many LMC neurons even after the end of the LMC divisional segregation (Fig.5.3A-D) (Price et al., 2002).
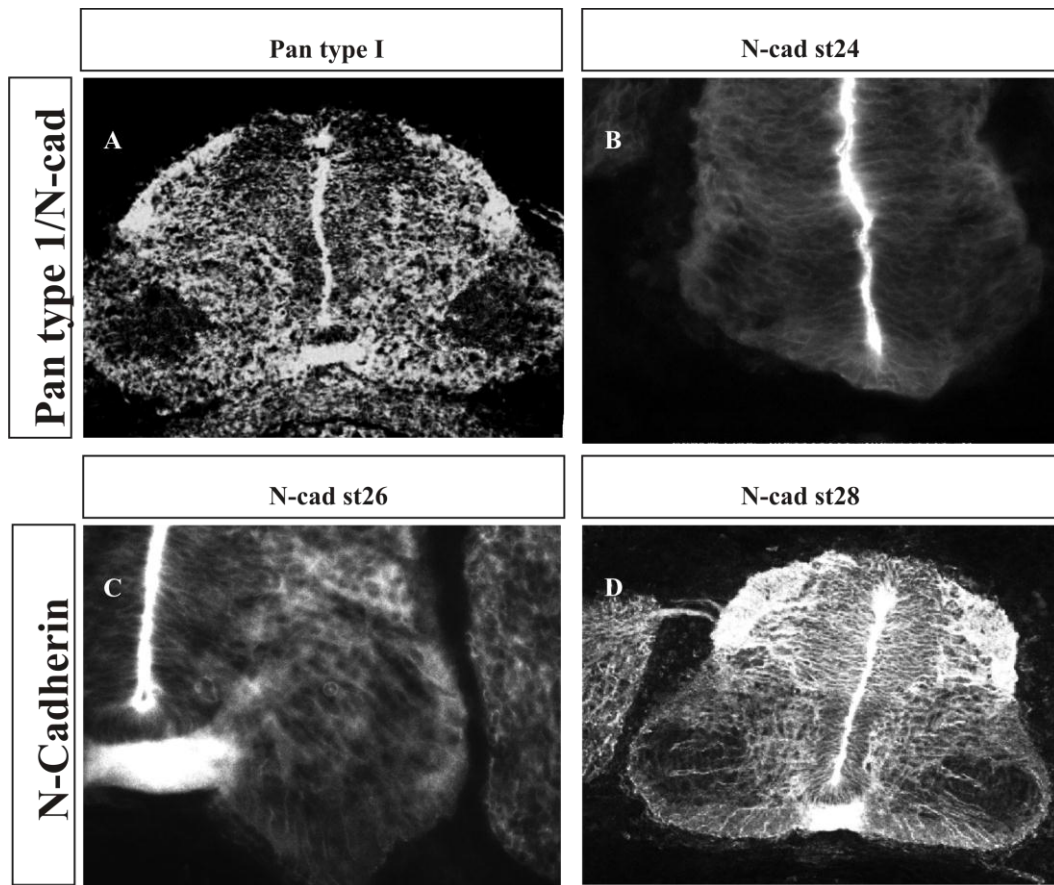
Figure 5.1 Pattern of type 1 and N-cadherins expressions in development**.**

A, Pan type I cadherin immunolabelling at HH stage 28 in the ventral lumbar spinal cord. *B*, N-cadherin immunoreactivity at HH stage 24. *C*, N-Cadherin immunoreactivity at HH stage 26 and *D*, at HH stage 28
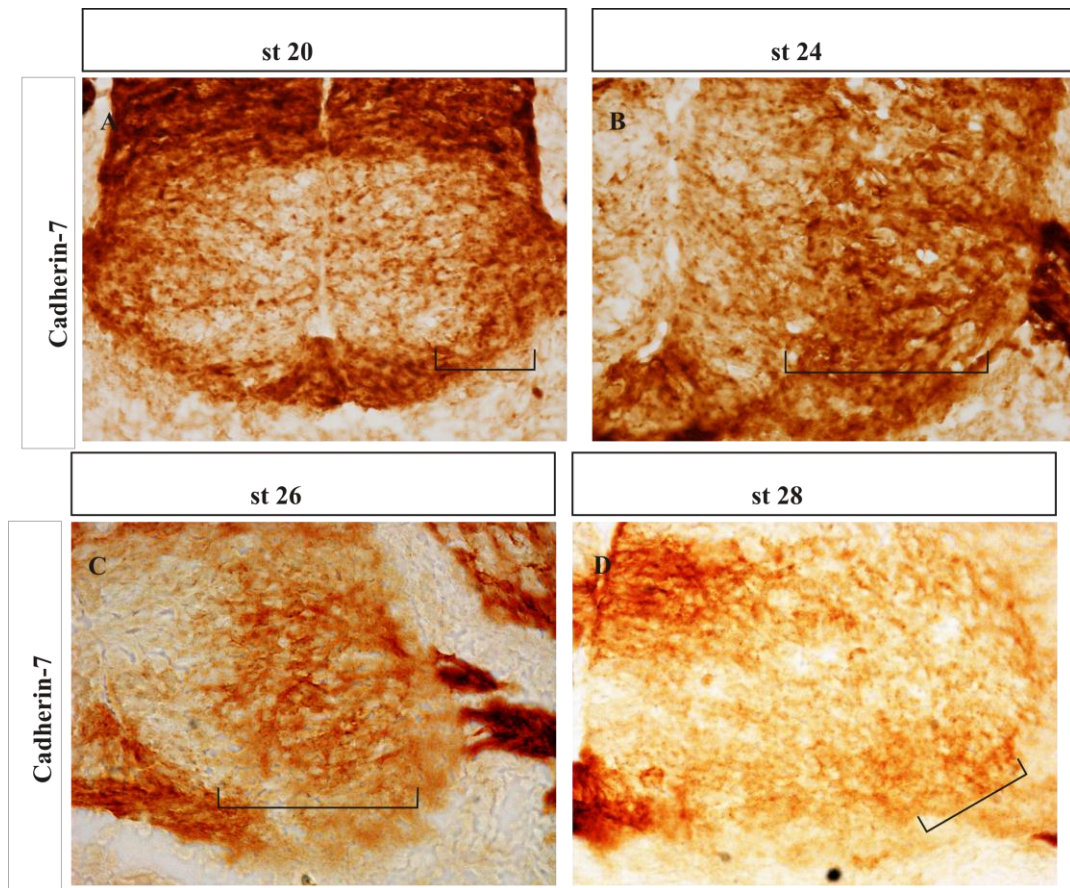
Figure 5.2 Expression of cadherin 7 in the ventral lumbar spinal cord at various stages of development.

A, Cadherin 7 immunohistochemistry in the ventral lumbar spinal cord at stage 20, *B* cadherin 7 immunohistochemistry in the ventral horn of lumbar spinal cord at stage 24 (*C*) at HH stage 26, and (*D*) at HH stage 28. Cadherin-7 appears to be expressed by the majority of LMC neurons early in development during their migratory phase (*A-C*). This expression is markedly reduced and restricted to small subset of motor neurons at the advanced stage of development (*D*).
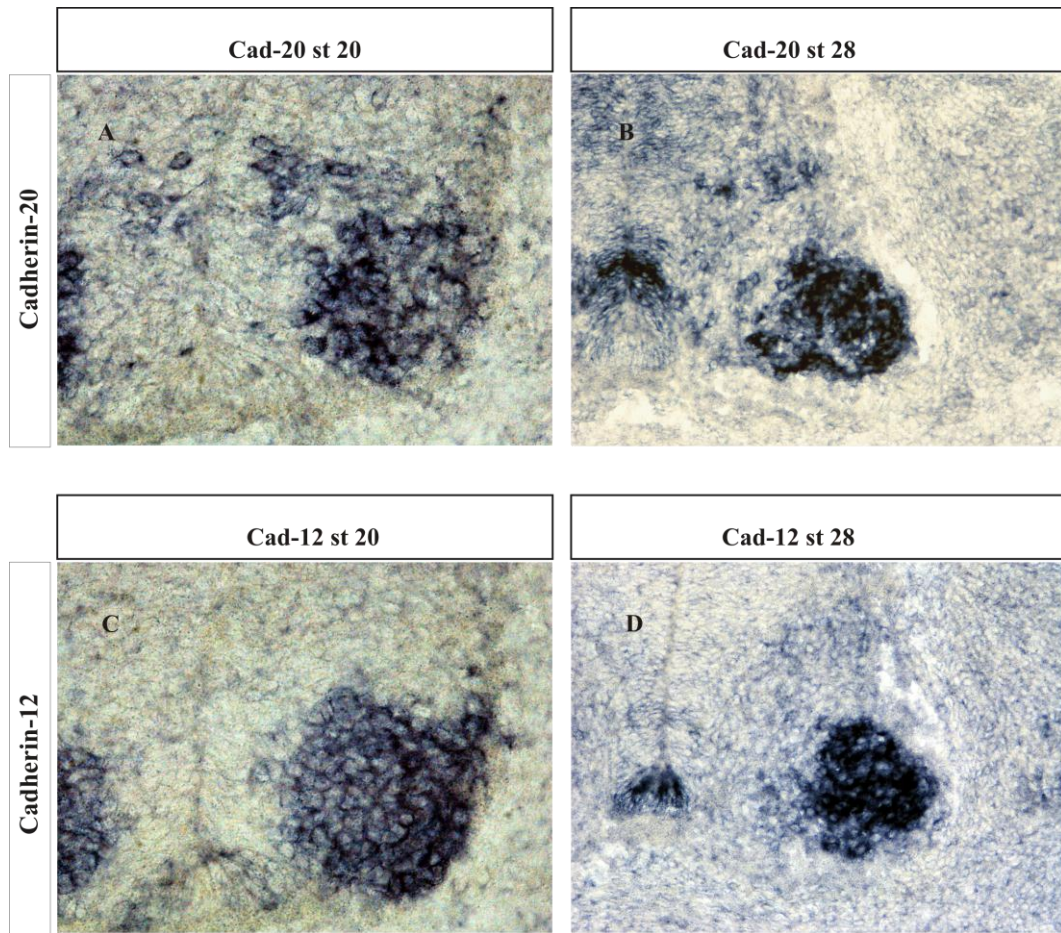
Figure 5.3 cadherin 20 and cadherin12 in situ hybridization in the ventral lumbar spinal cord.

A, cadherin-20 in situ hybridization at HH stage 20 in the ventral horn and *B*, at HH stage 28 at caudal lumbar regions of the developing spinal cord. *C*, Cadherin-12 in situ hybridization in the ventral horn at HH stage 20 and *D*, at HH stage 28 at the caudal level of the developing spinal cord.

6   Control Constructs Expressions and LMC Motor Neuron Segregation and Migration.

6.1   eGFPN3 Expressions and LMC Motor Neuron Segregation and Migration.

With its wide molecular biology application, *gfp* is a fluorescent marker with extensive use that includes but not restricted to as a reporter gene, cell marker, and fusion tag to host proteins to monitor their localization and fate (Tsien; 1998). Other applications include study of host-pathogen interactions (Valdivia et al; 1996).

EGFPN3 was used as a maker of electroporation and to follow cells for the expression of the various cadherins and catenins constructs used in this study. To determine the contribution of eGFP-N3 in motor neuron segregation in the ventral spinal cord; a control experiment eGFP-N3 misexpression was conducted. Embryos incubated to desired developmental stage (Hamburger and Hamilton 1992) HH 16-18 were electroporated with eGFPN3 and were allowed to develop to desired stages of development and dissected between stages (Hamburger and Hamilton 1992) HH25-32, sections were immunostained for Hb9, Islet-1, and gfp expression to confirm electroporation. I considered an embryo well electroporated with potentially majority of cells acquired the construct if more than 50% of the ventral spinal cord neurons were hit during electroporation and thus are gfp fluorescence positive as well as being Islet1 and Hb9 positive respectively (Fig. 6.1A-E).

I next analysed the data with respect to the number of motor neurons in the ventral spinal cord on both the experimental side and the control side. Data from the well electroporated ventral lumbar spinal cord sections were quantitated and the total number of Islet-1 positive cells and Hb9 positive cells in both control and experiment side of the

ventral spinal cord revealed no significant difference. The total number of Islet1 positive cells between the electroporated side and the control side was counted and student *t-test* measurements revealed no statically significant difference between the experiment side and the control (student *t-test P*= 0.3250). Similarly the total number of Hb9 positive cells between the electroporated side and the control side were measured and no statistically significant difference was observed (student *t-test P*=0.9805) Fig.6.2

This observation was repeated throughout the various stages of development of the observed number of embryos. Interestingly, there was no observed migration or segregation deficit of the LMC neuron at various stages of experiment. Thus, eGFPN3 expression on its own did not alter the segregation and migration of spinal LMC motor neurons.

| Gfp | Hb9 Islet-1 (Control) | Hb9 Islet-1(experiment) |
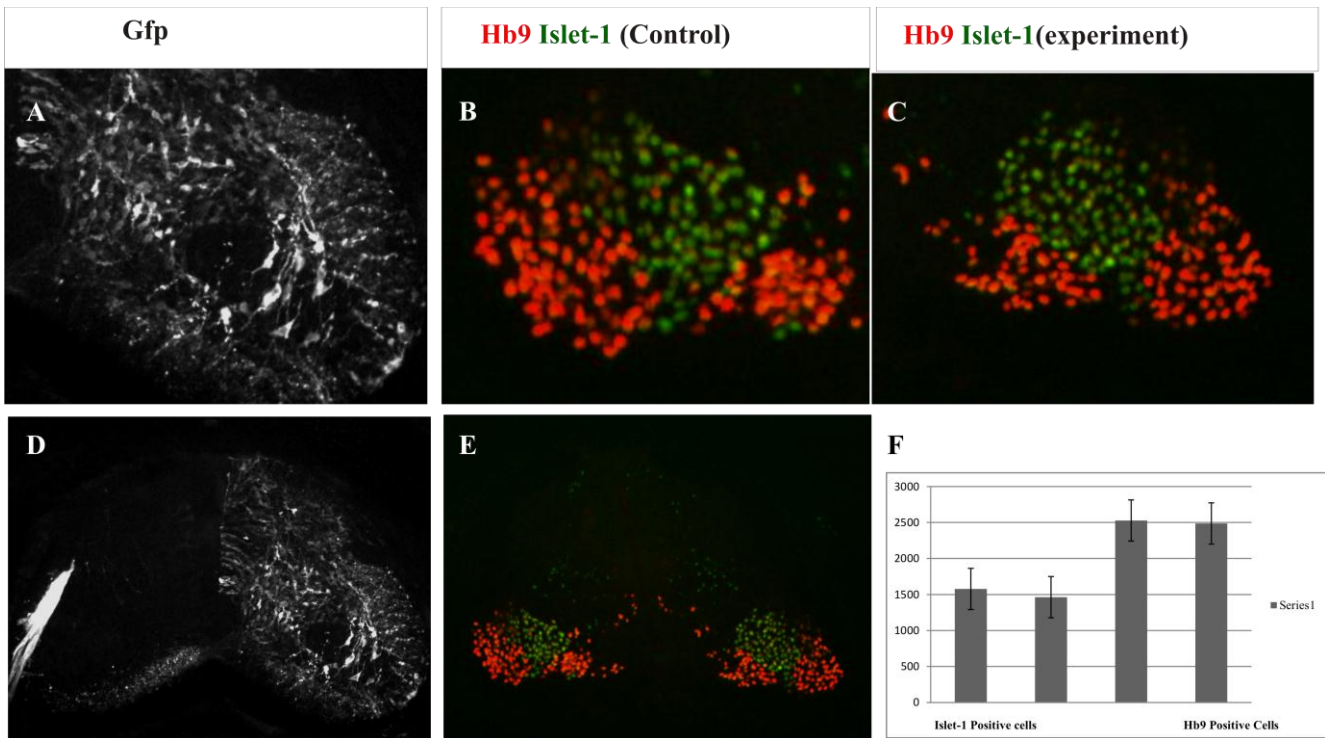
Figure 6.1 eGFPN3 expression lacks effects on the number, segregation and migration of LMC Neurons.

A, gfp fluorescence *B*, control side of the ventral lumbar spinal cord, C experimental side of the ventral spinal cord, *D*, gfp of whole section showing both the control and electroporated side, **E**, Hb9 Islet-1 showing both electroporated and control side, *F* quantification of the result of total number of Islet-1 and Hb9 positive cells shows no significant difference between the control and experimental side of three embryos to stage 28. Student t-test p value= 0.3250. Error bars are Standard Error of Means SEM

6.2 β-galactosidase Misexpression shows no effect on Neuronal Segregation

β-galactosidase is an exoglycosidase which hydrolyzes β-glycosidic bonds. It is used frequently in genetics, molecular biology and other life sciences. In *E.coli*, the gene for β-gal is the lacZ gene. Beta galactosidase is commonly used in molecular biology as a reporter to monitor gene expression. Since this enzyme is use as a reporter in this study (similar to eGFPN3), I asked whether β-galactosidase has any effect on LMC neuron segregation and migration. To determine the contribution of β-galactosidase (β-gal) in motor neuron segregation in the ventral spinal cord, a control experiment with β-galactosidase misexpression was conducted. Embryos incubated to desired developmental stage HH 16-18, electroporated with β-gal and allowed to develop to stages of development when the LMC neuron segregation and migration have been completed and wild type lumbar spinal cord sections were recovered between stages HH25-28. Immunohistochemistry for Lim-1/Lhx-1, Islet-1, and β-gal expression was conducted. To confirm LMC neurons acquisition of the reporter, more than 50 % of the ventral spinal cord should be positive for β-galactosidase immunoreactivity following electroporation. Again, I considered an embryo well electroporated if a majority of the ventral LMC neurons were β-galactosidase positive.

I observed that in relatively well electroporated sections of the lumbar spinal cord, the β-galactosidase fluorescence extends from the ventricular zone medially and to the most lateral extent of the ventral horn. Similarly β-galactosidase fluorescence was observed to extend dorsally on the electroporated side. Thus, analysis of the data for the well electroporated ventral lumber spinal cord sections were made and the total number of Islet-1 positive and Lim-1/Lhx-1 positive cells in both control and experiment side of the ventral spinal cord revealed no significant difference (data not

115

shown). This observation was consistent throughout the various stages of the migratory phase of LMC neurons.

Consistent with previous observations of the outcome of eGFPN3 expression on columnar segregation, the integrity of divisional segregation as well as the migration of LMC neurons was not compromised (Fig.6.3A-C). There was no observed migration deficit of the LMC neuron at various stages of development. Thus this ruled out any contribution of β-galactosidase to divisional segregation and migration of spinal LMC motor neurons. Therefore β-galactosidase misexpression shows no effect on the LMC neuronal segregation.

| β-gal | Islet-1 | Lhx-1 |
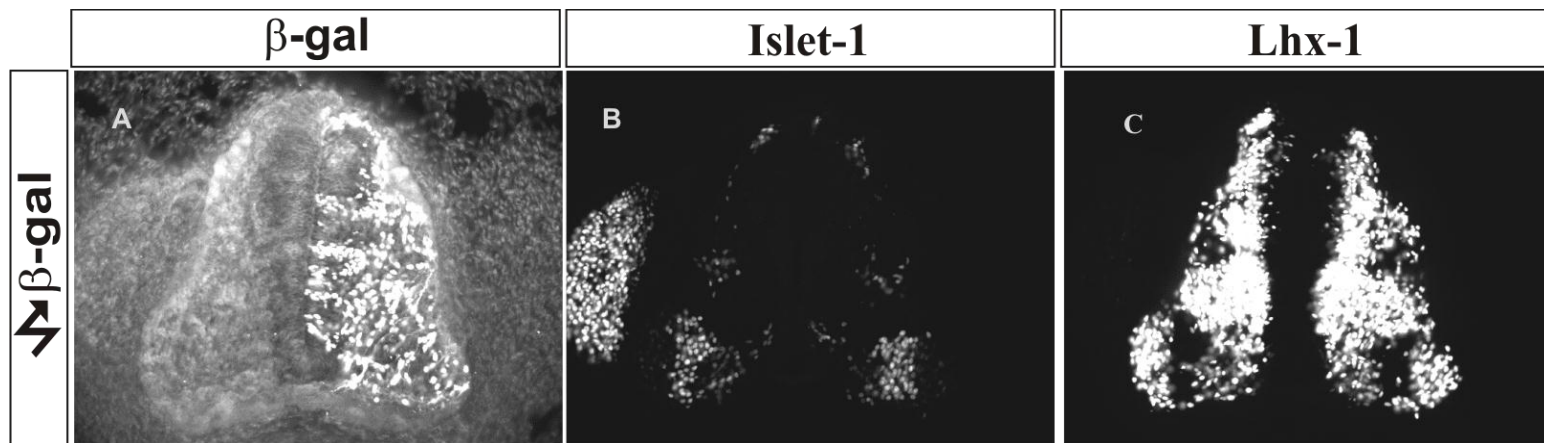
Figure 6.2 Expression of β-galactosidase shows normal segregation and migration of spinal motor neurons in the ventral lumbar spinal cord.

A- Beta galactosidase fluorescence in the ventral spinal cord of the electroporated side, the β-gal immunoreactivity extending from the medial to the most lateral extent of the ventral lumbar spinal cord, indicative of acquisition of the construct by most of the LMCm and LMCl neurons.. *B*- Islet-1 immuno histochemistry following expression of β-gal on the electroporated side, Islet-1 immunoreactivity is more in the LMCm than in the LMCl domain on the electroporated side as well as the control. *C* Lhx-1 immuno histochemistry following expression of β-gal with no observable difference in the organization of the LMC.

7 Manipulations of catenin functions and its effects on LMC Neuron Segregation and Migration.

Catenins are the major associated and direct binding partners to cadherins; they regulate the cadherin based adhesion by directly or indirectly interacting with the cytoplasmic domain of classic cadherins (Steinberg M.S. and P.M.McNutt. 1999) of the six members;(α, β, γ, δ, p120, and ARVCF) β-catenin and γ-catenin bind competitively to the C-terminal region of the classic Cadherins (Zhurinsky J. Et al, 2000).

There is a well-established predominant expression pattern of catenin by motor neurons and of particular importance is γ- catenin since it is well expressed by virtually all motor neurons. I therefore asked whether the expression of γ- catenin has any effect on the divisional segregation of spinal motor neurons. To address this I expressed a wild-type γ- catenin through in ovo electroporation and confirmed its expression along the ventricular zone, apical regions and the ventral spinal cord (Momose et al., 1999). I observed that over expression of γ- catenin visualized by β-galactosidase immunoreactivity had no observable effects on the organization of the LMC neurons, migration of the LMC neurons or the number of the spinal motor neurons (Fig7.1A-D).

To establish the role of γ-catenin in the segregation and migration of spinal motor neurons in the developing chick spinal cord, I expressed an L141A (γ-14) and L127A (γ-18) point mutants of γ-catenin (γ-14 and γ-18 respectively) generated in the Price lab. Each of these has been shown to bind to the cadherin cytoplasmic domain but not to alpha catenin. Therefore, I hypothesised that they would act   in a dominant negative fashion to uncouple cadherin function from binding to alpha catenin. I misexpressed γ-catenin γ-18 in the developing spinal cord at HH stage 16-18 and dissected at HH 28-30, a stage when motor neurons would have completed their migration and have settled in

their final settling position in the ventral lumbar spinal cord. First, I analysed the effect of γ-(L127A) expression on the localisation of β-catenin and ZO-1 proteins. Each of these proteins has prominent expression in the end feet of radial glia which are believed to depend on adherens junction formation. I reasoned that the predicted effects of γ-(L127A) expression would disrupt adherens junction formation. Following γ-(L127A) expression I found that apical end-feet localisation of both β-catenin and ZO-1 was perturbed, consistent with the predicted mode of action of the γ-(L127A) point mutation (Figure 7.2A-D).

To follow its effect in the segregation and migration of spinal motor neurons, I conducted immunohistochemistry on sections obtained using β-galactosidae immunofluorescence to follow cells that acquired the construct, for Islet-1, Lim-1/Lhx-1 and Hb9 respectively. I observed a very strong phenotype compared to wild type, showing desegregations of LMC motor neurons, arrest of migration and stacking of cells in close proximity to the ventricular zone, a position not normally known to contain motor neurons at that stage in development. Fig7.3A-D shows misexpression of gamma catenin point mutant γ-(L127A). Analysis of number of LMC neurons was done and shows no significant difference between the experiment and control (*n=5*), *P-value* (0.97). I next analyzed the nature of the effects of the construct on the organization of the LMC by using Hb9 and islet-1 immunofluorescence. I observed that the LMC domain on the experimental side covers an area approximately twice the size of the LMC domain on the contralateral side (Fig7.3A). In addition to the increase in area there was observable evidence of LMC cells in close position to the ventricular zone on the experimental side compared to the control side. Analysis of the number of LMC cells found close to the ventricular zone was done and the percentage determined to be approximately 5-6.1% (Fig 7.4). I also found that the LMCm and LMCl divisions of the

lateral motor column appeared to be mixed. In order to quantitate this phenotype, I partitioned the ventral spinal cord including the ventral horn into three equally sized bins labelled I, II and III (medially to laterally). I quantitated the number of LMCm and LMCl cells in each bin comparing electroporated and control sides of the spinal cord. I found that when γ (L127A) was expressed there was a significant alteration in the percentage of LMCl cells in bins I and II compared to the control (Fig 7.4A). This indicated to me that the LMCl cells were located more medially than the control a situation consistent with the neurons having failed to properly migrate into the ventral horn (Figure 7.3A).

However, an alternative hypothesis could be that γ-(L127A) expression caused a delay in the formation of LMC cells, which then migrated normally but did not have enough time to reach the ventral horn before my analysis. I therefore misexpressed γ-(L127A) and applied BrdU from stage 23 to the analysis at stage 28. I found that no LMC cells (observed by Foxp1 immunofluorescence) were co-labelled with BrdU (Fig7.5A-B). This indicates that following γ-(L127A) expression all motor neurons had been born by stage 23, as is found in normal embryo development. Thus, the actions of γ-(L127A) expression do not appear to be to delay LMC generation and instead more likely act on LMC neuron migration.

I next asked what the nature of the cells found close to the ventricular zone was. I first analysed the position of cells expressing Lhx-1/Lim-1, which labels the LMCl cells and also the majority of interneurons in the spinal cord. I found that following γ-(L127A) expression a large number of ventral Lhx-1/Lim-1 cells were found close the ventricular one. This number of cells was larger than the number of LMC cells found in the ventricular zone suggesting that these cells also contain a number of ventral

Lhx-1/Lim-1 interneurons. However, I never observed any similar phenotype in the dorsal spinal cord (Fig 7.6 A-C).

In order to assess whether these cells were actually within the ventricular zone itself, I next analysed the expression of Pax6 and Nkx2.2, two markers of ventral progenitor domain cells. I found completely normal location and number of Nkx2.2 cells. However, following γ(L127A) expression, the Pax6 domain appeared highly disrupted in that the ventral extent of the domain appeared to be folded dorsally and medially (Figure 7.6D,E, F, F'). The position of the Lim-1/Lhx1 cells close to the ventricle fitted between the folded Pax6 domain and the ventricle itself. Thus, the Lim-1/Lhx1 cells close to the ventricle are actually not within the ventricular zone, as defined by progenitor homeodomain transcription factor expression. I next analysed the ventricle itself by observing transitin expression in the radial glia of the ventral spinal cord following γ-(L127A) expression. I found that transitin expression still persisted at the ventricle surface and that the projection of these cells still persisted into the ventral horn (Fig7.7A-E). The pathways of LMC cells following γ-(L127A) expression still appeared to be closely associated with this transitin expression. This suggests that even though the ventricular zone has curled upwards, the LMC cells still followed a relatively normal pathway as marked by transitin expression.
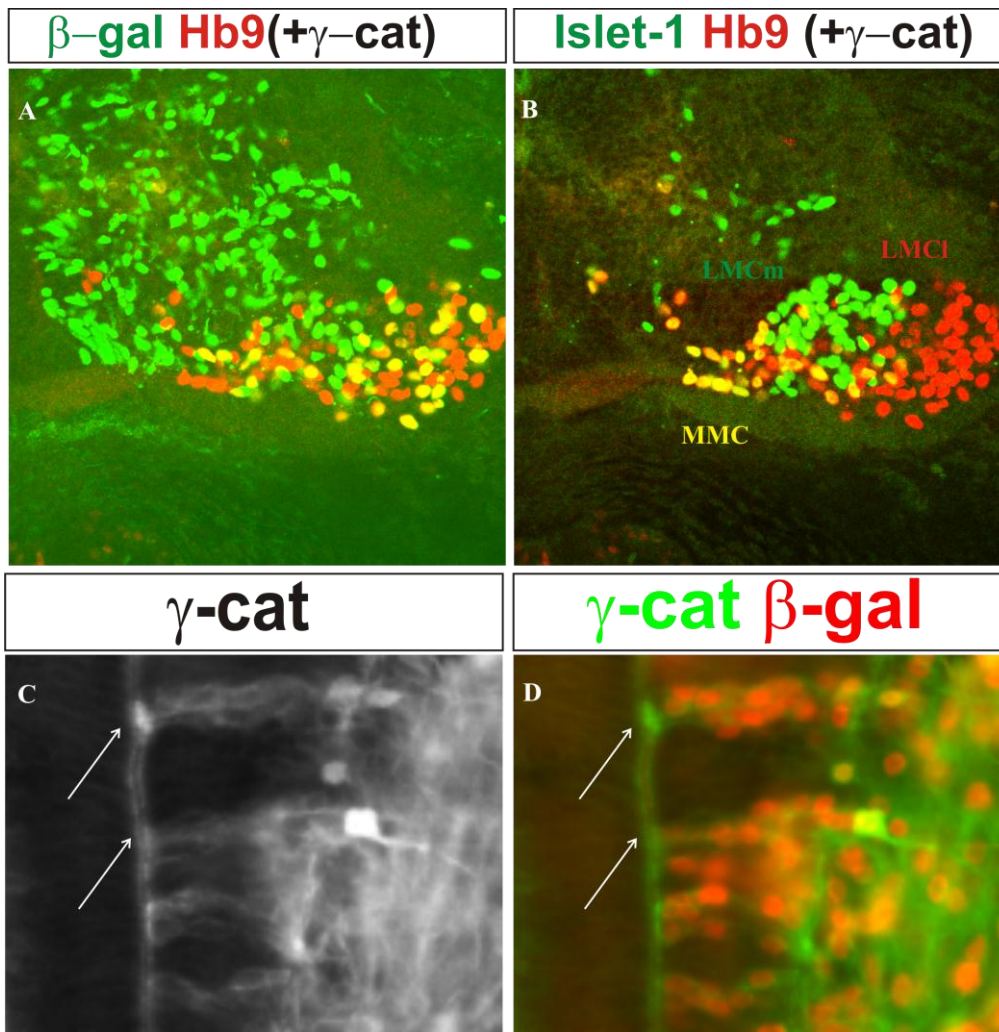
Figure 7.1 Lack of effects of γ-catenin overexpression on the LMC divisional segregation.

A, and B, lack of effect of γ-catenin overexpression on divisional segregation in the ventral spinal cord to stage 29. Electroporated cells that acquired the construct are marked by β-gal immunoreactivity in green (A). Islet-1 and Hb9 (A, B) marked the LMCl and LMCm in the ventral spinal cord. C, and D, expression of γ-catenin (L127A) visualized by immunoreactivity for γ-catenin (L127A) β-gal immunofluorescence marked the cells that acquired the construct following electroporation (D, red). The arrows indicate expression of γ-catenin at the apical region of the ventricular surface.
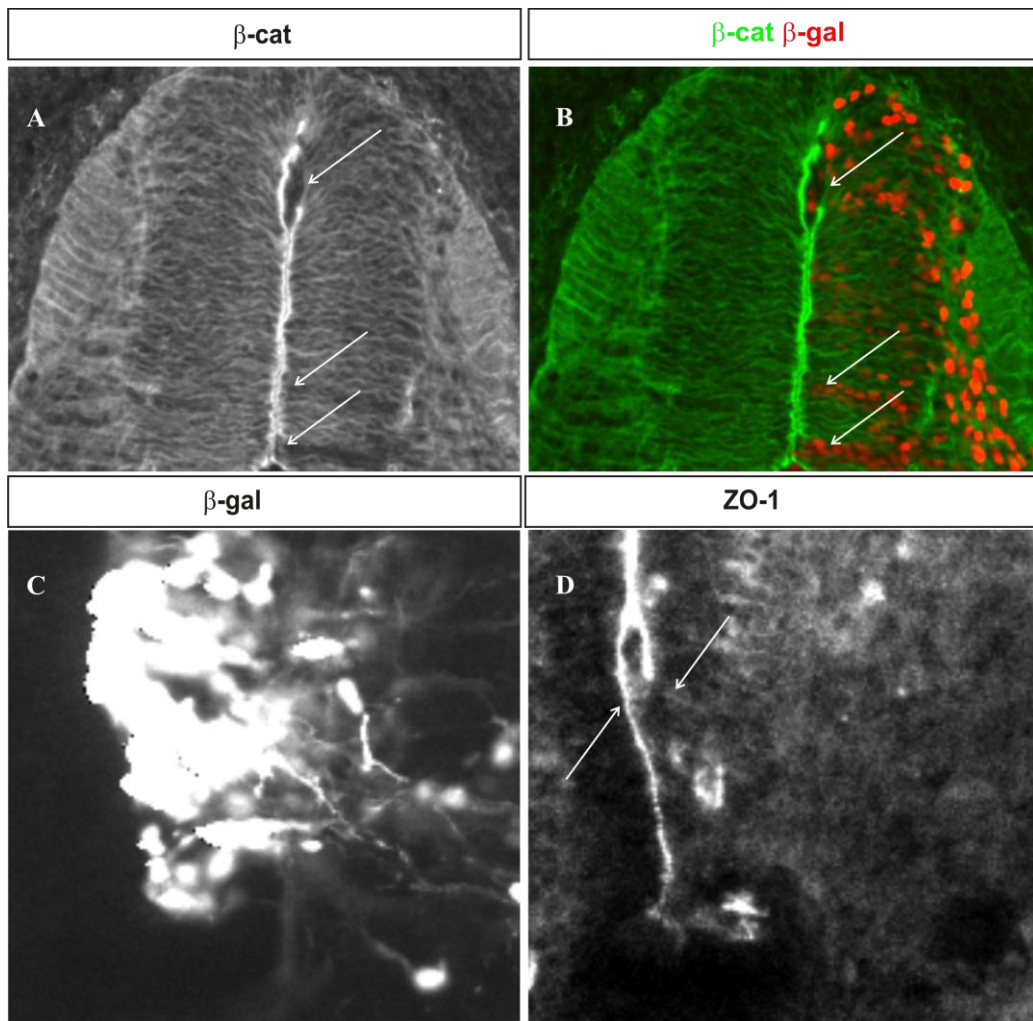
Figure 7.2 γ-catenin(L127A) disrupt apical loaclization of β-catenin along the ventricular surface.

A, immunoreactivity for β-catenin following the expression of γ-catenin (L127A) construct visualized by immunofluorescence for β-gal in B, shows disruption of apical localization of β-catenin. B, merged immunoreactivity for β-catenin and β-gal (in red) arrows shows the area of disruption of β-catenin localization. C, β-gal immunoreactivity following expression of γ-catenin (L127A). D, Disruption of Z01 apical expression following expression of γ-catenin (L127A). The left arrow on the contralateral side shows normal localization of Z01 compared to the right arrow on the experimental side showing the extent of z01 disruption.
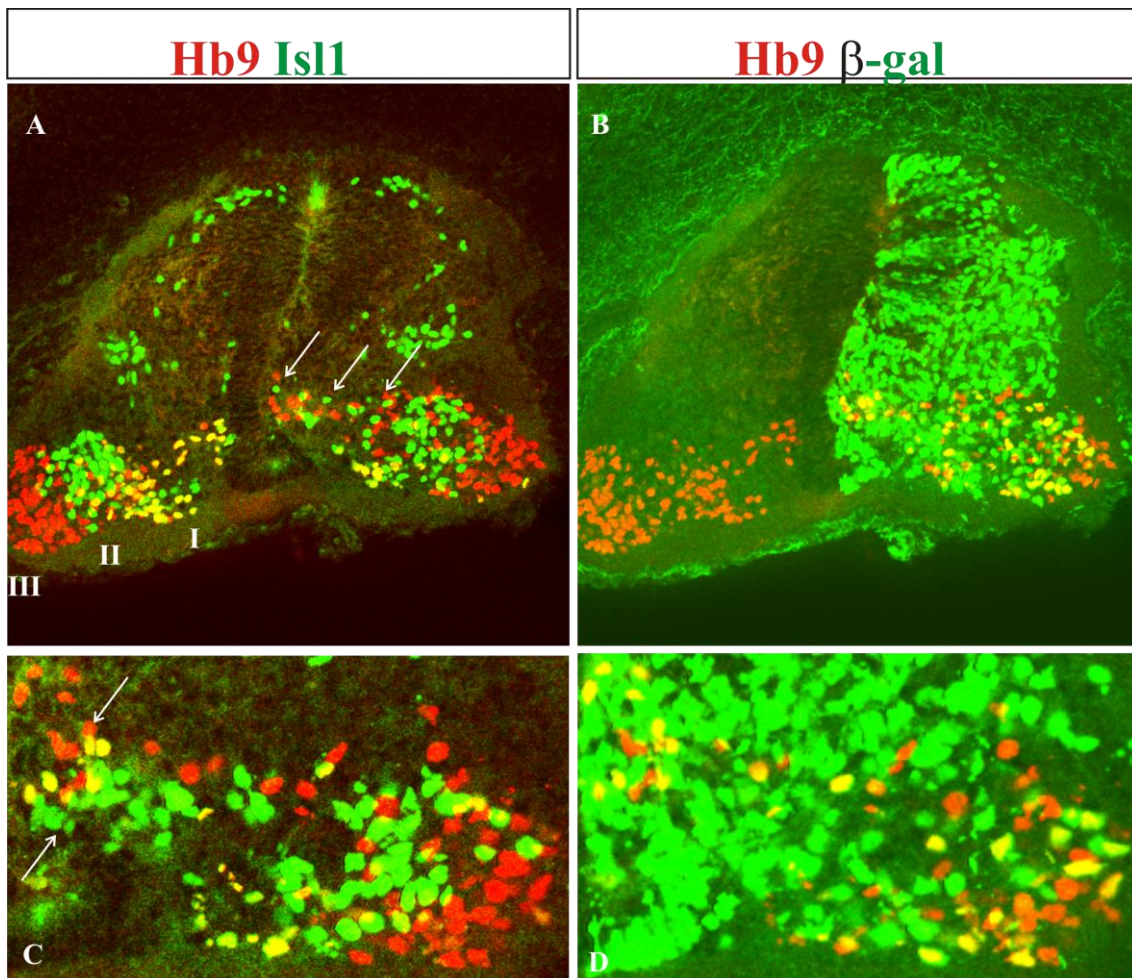
Figure 7.3 Perturbations of divisional segregation of the LMC following γ-catenin (L127A) expression.

A, effects of expression of γ-catenin (L127A) on the LMC segregation and migration in the ventral lumbar spinal cord at stage 29. Hb9 Islet-1 immunoreactivity following expression of the construct visualized by immunofluorescence for β-gal in **B**. LMCm and LMCl segregation (viewed by Hb9 and Islet-1 immunoreactivity) is normal on the left side of the spinal cord compared to the experimental side. The LMC spread over the entire extent of the ventral spinal cord from the area adjacent to the ventricular zone to the most lateral extent of the ventral horn, indicating disruption in the LMC organization compared to the normal on the control side (areas I, II, and III are the bins quantitated). **C** and **D** shows ventral horns of different embryos following the expression of the construct showing the disruption of normal organization of both LMCl and LMCm, the middle line is to the left of the panel showing some LMCl cells close to the ventricular zone.

124
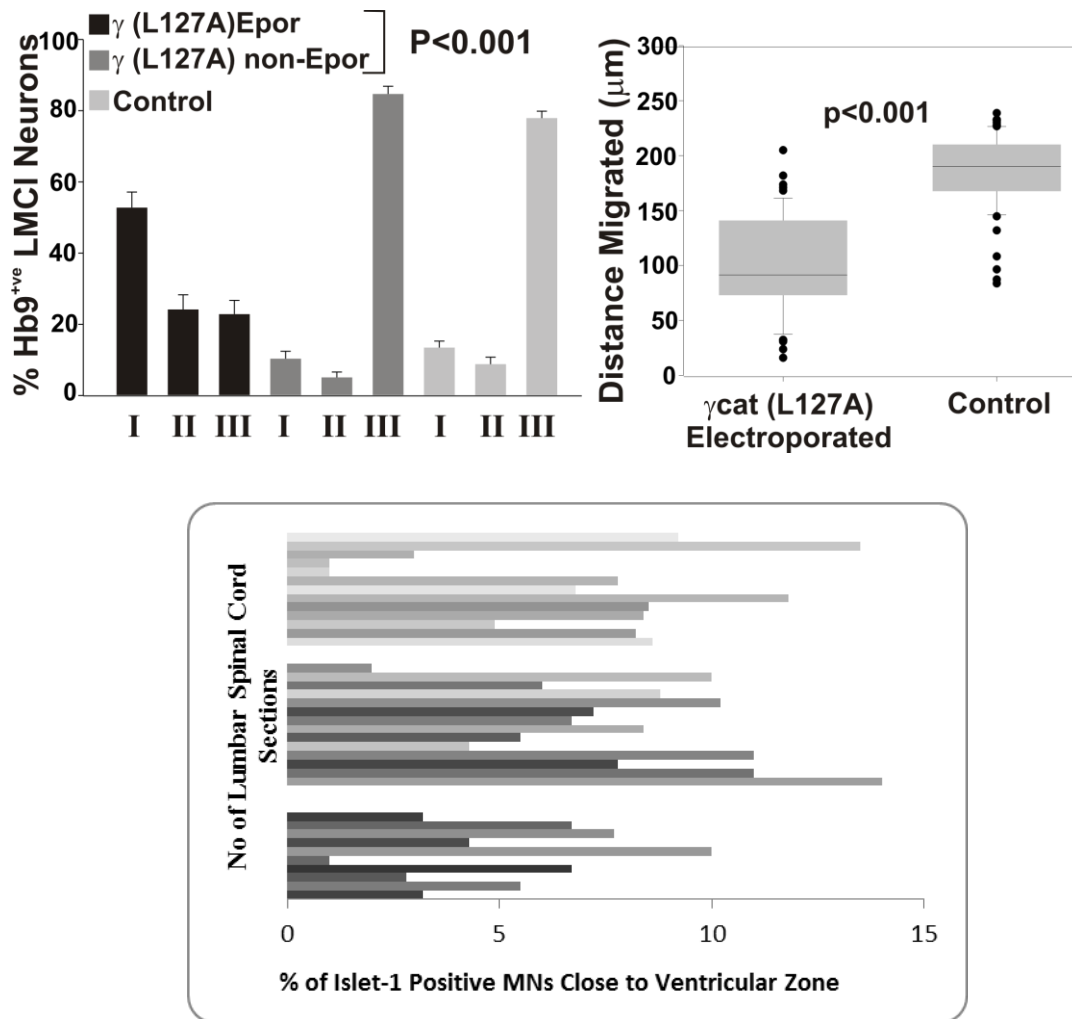
Figure 7.4 Quantitation of the % of LMC neurons found close to ventricular zone following γ-(L127A) expression in the ventral lumbar spinal cord.

Above left: Quantitation of LMCl neuron position in bins I γ-(L127A) electroporation, II γ-(L127A) non electroporated and III control. Migration deficit is more in the electroporated LMCl with majority found close to ventricular zone compared to control and non electroporated neurons. *Above right*: significant difference in the distance of migration between electroporated and control following γ-(L127A) expression.

Below the two upper panels: Quantitation of the number of LMC neurons located close to the ventricle zone at late stage of development following electroporation with γ-catenin and the disruption of the LMC organization observed in 41 sections from various embryos electroporated with the construct. The highest number cells found in area close to the ventricle zone was 13 LMC neurons positive for Islet-1 and Hb9 and the overall percentage of LMC cells is approximately 5% of the total motor neurons.
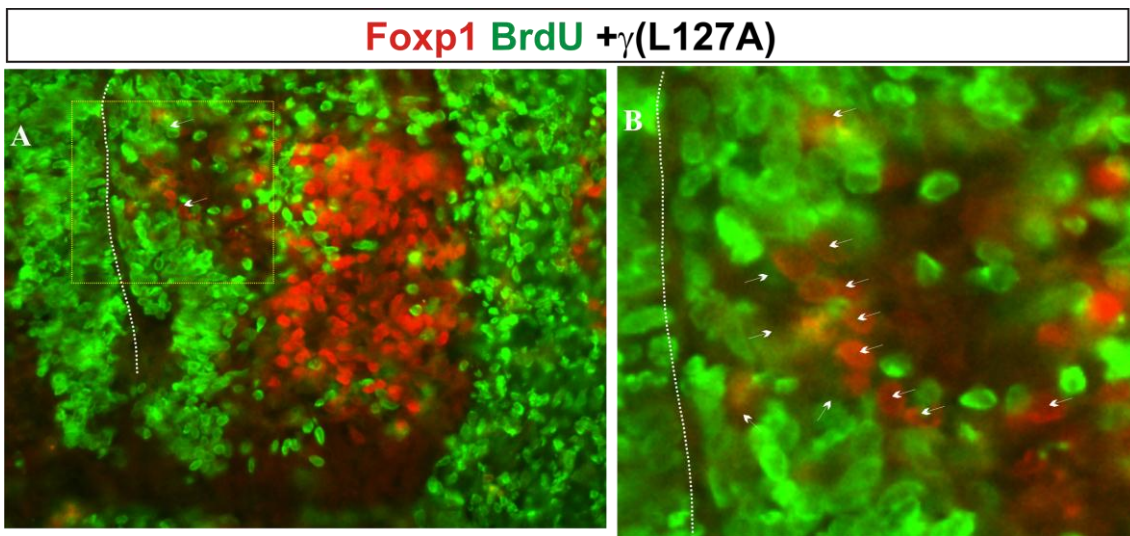
Foxp1 BrdU +γ(L127A)

Figure 7.5 γ-catenin (L127A) expression shows no localization of motor nuclei with BrdU.

A-Electroporation of the ventral lumbar spinal cord with γ-catenin (L127A) at stage 18 and, foxp1 BrdU expression following BrdU application between stage 23-28. There was no observable co-localization of motor neuron nuclei with BrdU (arrows in A-B) indicating the motor neurons were born before the application of the BrdU. *B* is the magnification of the boxed area in *A,* and the dotted lines in *A* and *B* indicated the midline. Also migrating foxp1 positive cells are not labelled with BrdU (arrows in B).
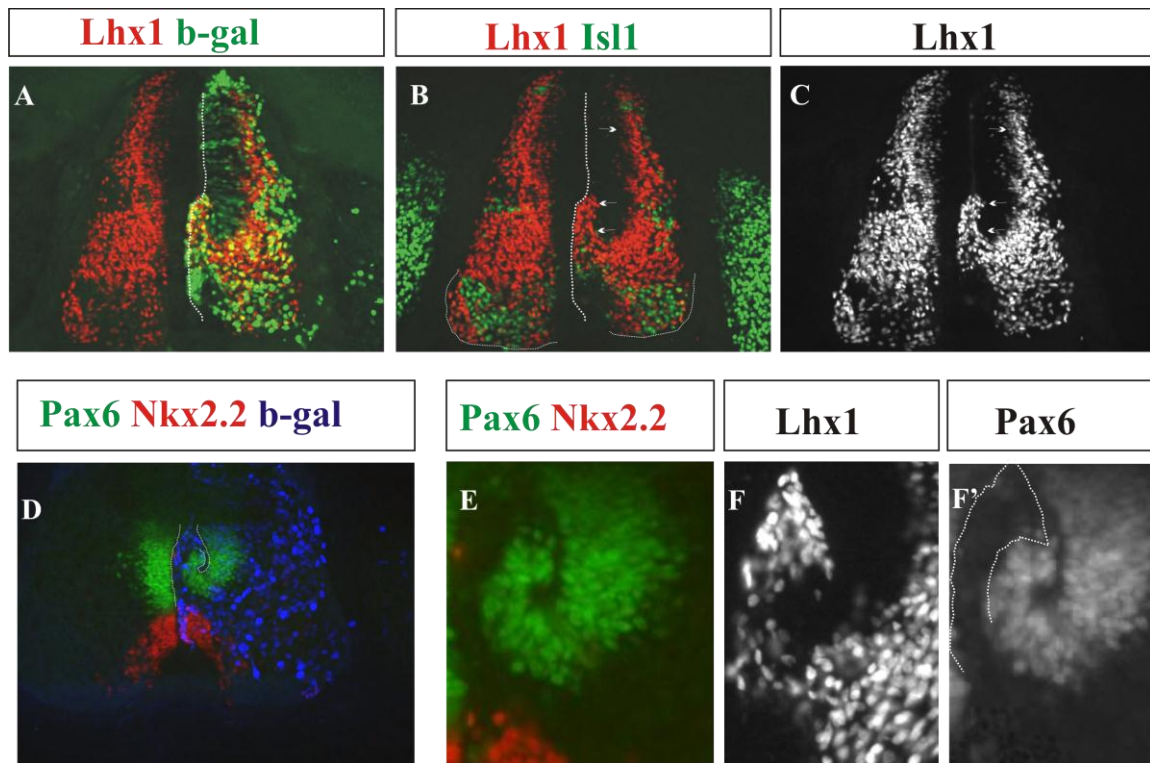
Figure 7.6 Arrested migration of spinal motor neurons following expression of γ (L127A) caused buckling of the pax6 domain.

A-C, Lhx-1 expressing ventral interneurons and LMCl neurons (**B**, **C**, left pointing arrows) are located close to the ventricular zone (dotted lines in A, and B) expression of the construct is marked by immunoreactivity for β-gal (in green in A). **B**, **C**, Right pointing arrow heads shows no effects on dorsal interneurons.

D-E, ventral pax6 (in green) progenitor domain is buckled in a dorso-medial direction after expression of γ-(L127A) while the Nkx2.2 (in red) progenitor domain remained unperturbed. Expression of the construct is marked by β-gal immunofluorescence (**D**, in blue) dotted lines indicate the ventricle surface. **E** shows the magnification of only the ventral progenitor domains (Pax6 and Nkx2.2) on the right side of the spinal cord in D.

The electroporated cells (stalled LMC neurons) are close to the ventricle in contrast to the majority of unelectroporated Pax6 positive cells. F, Lim-1/Lhx-1 immunofluorescence of the ventricular zone of the adjacent section to that shown in D and E. **F'**, position of the Lim-1/Lhx-1 cells indicated by the dotted lines in relation to the Pax6 domain of **E.**
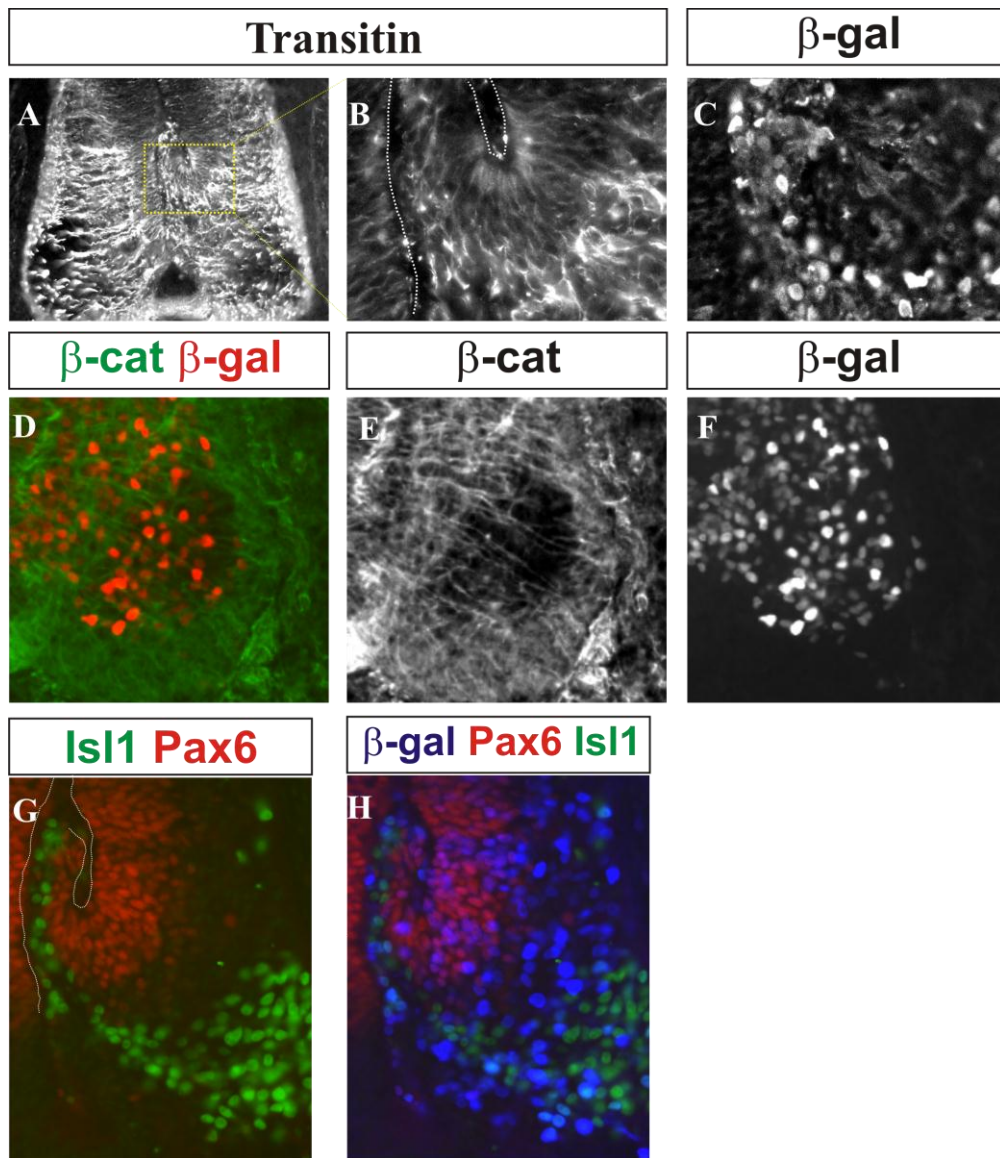
Figure 7.7 effects of γ-(L127A) catenin expression on the ventral progenitor domain Pax6.

A-C, Transitin immunofluorescence following expression of γ-catenin (L127A). A, right side of the spinal cord was electroporated evidenced by the buckling of the ventral pax6 domain. B, C, magnification of the boxed area in *A* with dotted lines in *B* representing the ventricle surface. *C*, magnified area in **A** showing β-gal immunoreactivity showing the electroporated cells. D-F β-catenin immunofluorescence (green) in radial glia in the ventral lumbar spinal cord at stage 25 following γ-catenin (L127A) expression marked by β-gal immunoreactivity (red). *E*, β-catenin immunoreactivity, *F*, β-gal immunofluorescence showing the electroporated cells. G, Islet-1(green) and Pax6 (red) immunofluorescence following expression of γ-catenin (L127A) visualized by β-gal immunofluorescence in *H*, Iset-1 cells ate arrested along their migratory route as a result of expression of the construct, and are adjacent to the buckled pax6 domain. *H*, β-gal immunoreactivity shows electroporated cells stalled in the buckled pax6 domain following expression of the construct at stage 26.

128

7.1 Expression of a point mutation in γ-catenin designed to uncouple with cadherins lacks effect on LMC organization.

With the results of effects of point mutants construct of γ-catenin (L127A) all showing the disruption of the organisation of the LMC divisional segregation in addition to abnormal migration of LMC neurons, I asked if expression of a mutated version of gamma catenin that does not bind to cadherins can produce effects similar to the point mutant constructs used previously (Momose et al., 1999; Nakamura et al., 2004; Price, 2004). To address this question, I expressed a version of γ-catenin, γ-catenin K450E generated in the price lab, at different stages of development.

First, I expressed γ-catenin (K450E) in to the ventral lumbar spinal cord at earlier stages of development and allow development to late stages of development to observe whether expression of the construct at an early stage can produce a similar phenotype with the previously used γ-catenin point mutant construct. Analysis of the early expression shows no observable difference in the divisional segregation of the LMC between the electroporated side and the control. Thus, expression of the dominant negative construct early in development seems to lack effect on the LMC organization (Fig.7.8A-C). I next analysed if there is any effects on the migration programme of the LMC, here I found almost all the cells that acquired the construct visualized by β-galactosidase fluorescence following expression of the construct appear to migrate normally to their definitive position in the LMCm or the LMCl. I asked if the lack of effect was due to early expression. Thus, I expressed the construct in the ventral lumbar spinal cord at a relatively advanced stage than the first group and followed their development. Consistent with the expression of γ-catenin (K450E) early in development, late stage expression also lacks effect on the total number of motor neurons of the experimental side compared to the control, as well as failure to perturb

129

the migration of the LMC neurons (Fig. 7.8D-F). Taken together, the results suggest that γ-catenin dominant negative has no influence on the segregation and migration of spinal motor neurons.

The expression of the γ-catenin point mutant construct (L127A) was associated with abrogation of apical localization of β-catenin in the dorsal spinal cord and in the radial glia fibres in the ventral spinal cord. I asked if the expression of the dominant negative construct could produce same result. I therefore expressed γ-catenin (K450E) at different stages of development and used β-gal immuno reactivity to follow the cells that acquired the construct. Following immunohistochemistry for β-gal and β-catenin, majority of the ventral spinal cord neurons acquired the construct with β-gal immunoreactivity extending across the whole ventral lumbar spinal cord. Immunohistochemistry for Islet-1 and Lhx-1 also revealed normal organization of the LMC and the LMC neurons migrate normally as well the normal localization of β-catenin. Thus, there is no effect on the localization of β-catenin on the electroporated side compared to the control as opposed to the abrogation of β-catenin when γ-catenin (L127A) was expressed.

The ventral progenitor domains of Pax6 and Nkx2.2 were affected when γ-catenin (L127A) was expressed. This involve the buckling of the pax6 ventral progenitor domain on itself along a dorso medial direction on the electroporated side compared to the control, other effects include the stalling of migration of LMC neurons and the abrogation of the localization of the adherence junction marker z01 on the experimental side compared to the control. Therefore I asked if the K450E construct have any influence on the ventral progenitor domains as well as adherence junction markers. Thus I conducted immunohistochemistry for Pax6 and Nkx2.2 and z01. There were no observable effects in terms of abrogation of β-catenin localization on the electroporated

side compared to the control side (Fig.7.8 G-I). There was also no observable difference in the ventral progenitor domains of pax6 and Nkx2.2 and no motor neurons were stalled along their migratory route (Fig.7.8J-L). Taken together, these results show that γ-catenin (K450E) lacks effects on virtually all developmental programmes of LMC neurons. These results suggest that the action of γ(L127A) may well be due to an uncoupling of the cadherin catenin complex from alpha catenin and not a more general perturbation of catenin function by titrating out alpha catenin levels (which might be predicted to occur with the K450E construct.
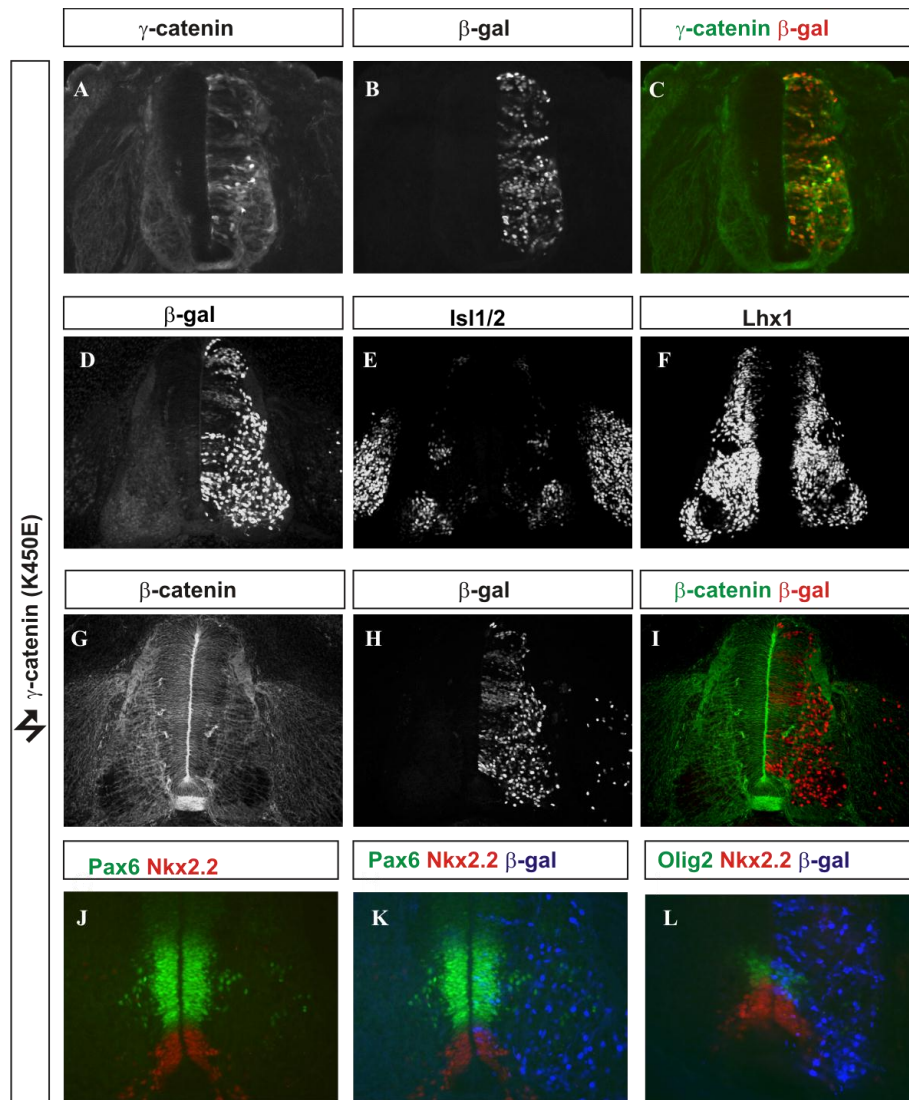
Figure 7.8 Lack of effects on LMC divisional segregation and migration following expression of a dominant negative γ-catenin (K450E).

A, immunofluorescence for γ-catenin (K450E). *B* immunoreactivity for β-gal following expression of the construct. *C*, merged immunofluorescence for γ-catenin and β-gal following electroporation with γ-catenin (K450E). *D*, β-gal immunofluorescence in the ventral lumbar spinal cord following electroporation with γ-catenin (K450E) shows the entire LMC positive for the construct. *E*, Islet-1(2) immunoreactivity following expression of γ-catenin (K450E) shows no observable difference in LMC divisional segregation between the electroporated side and the control. *F*, Lim-1/Lhx-1 immunofluorescence shows normal divisional segregation on both the experimental side and the control side. *G,* β-catenin immunofluorescence in radial glia in the ventral lumbar spinal cord following electroporation. *H, I*, merged immunofluorescence for β-catenin and γ-catenin (K450E) marked by β-gal immunofluorescence showing cells expressing the construct and normal. *J,K,L,* lack of effects on the ventral progenitor domains of Pax6 (green) and Nkx2.2 (red) following expression of γ-catenin (K450E) marked by β-gal immunoreactivity(blue) in *K, L*.
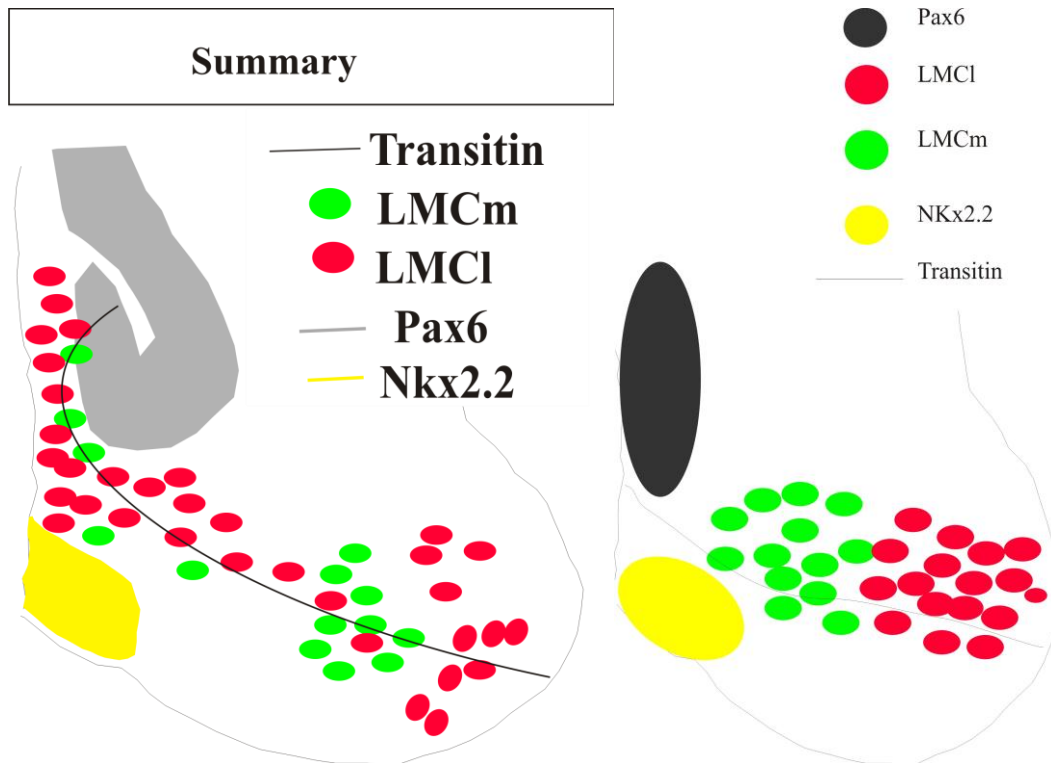
Figure 7.9 Summaries of effects of γ-(L127A) on the segregation and migration of LMC neurons and the ventral progenitor domains Pax6 and Nkx2.2.

Left: Summary of the results of manipulation of catenin function following expression of γ-catenin (L127A) construct shows the stalled motor neurons along migratory path, the relative position of transitin radial glia, mixing of the LMC neurons and the buckling of ventral progenitor domains of Pax6 compared to control on the right. Nkx2.2 domain appears unaffected following electroporation with the construct at different stages of development.

Right: Schematic representation of normal segregation and migration of spinal LMC neurons shows normal Pax6 domain and NKx2.2 as well as transitin radial glia in the ventral horn. Note that the LMCl and LMCm segregate and migrate along path delineated by transitin radial glia.

8 Manipulations of Cadherin Functions and its effects on LMC Neurons Segregation and Migration

8.1 Cadherin dominant-negative (CDN) Expression Results in Altered LMC Neurons Segregation and Migration.

The cadherin catenin interaction is critical to the strong intracellular action of cadherin adhesive action. In the previous chapter, I reported the effect of γ-catenin point mutant expression on the LMC migration as well as divisional segregation during development. (Bello et al., 2012). I thus sought another way of uncoupling cadherin-catenin interaction and its intracellular function to assess any effect on LMC neuronal migration and divisional segregation. Thus, I generated a cadherin dominant negative construct from the cDNAs of the type II cadherin-20 which lacked the extra cellular domain necessary for interaction with cadherins and is believed to act as a dominant negative by sequestering endogenous β- or γ-catenin required for cell adhesive function (Fujimori and Takeichi, 1993).

This cadherin dominant negative construct was electroporated first in the lower thoracic and then the upper lumbar segments of the developing spinal cord between HH stages 16-18 (Hamburger and Hamilton 1992) and dissected at HH stage 28-30 for analysis. Following in ovo electroporation, sections were immunostained for Islet-1 and Lim-1/Lhx-1 expression respectively. The level of the lower thoracic segments anatomically identified by the presence of the preganglionic motor column referred to as the column of Terni in chickens. I observed the presence of Islet-1 positive motor neurons along the progenitor rich ventricular zone, a location not expected to be normal for the developing spinal motor neurons at this stage of development. There were also few motor neurons arrested along their medio-lateral extent as well as a disorganization of the column of

Terni on the experimental side compared to the control (Fig 8.2). Taken together these results suggest that the effects of cadherin dominant negative construct are associated with neuronal nuclei disorganization in the thoracic segment of the developing chick spinal cord.

next the analysis was focused on the effects of the constructs on the columnar segregation as well as migration of LMC neurons at the lumbar levels of the developing spinal cord. In the same way as in the thoracic segments, β-gal fluorescence was used to follow the cells that acquire the construct as in the thoracic levels. Following expression of the cadherin dominant negative construct, the β-gal fluorescence on the electroporated side of the ventral spinal cord extends along the medio-lateral extent of the ventral lumbar spinal cord as with other constructs used previously in this study. Interestingly, the LMC neuronal segregation and migration were observed to be compromised in a manner reminiscent of what resulted from misexpression of the construct at the thoracic levels and lumbar levels with the catenin point mutations experiments of the developing spinal cord. However, compared to the results obtained in the previous experiments, the extents of the effects are less pronounced compared to the thoracic levels. In addition to β-galactosidase expression that was observed along the medio-lateral extent of the ventral lumbar spinal cord, there was very strong β-gal fluorescence in the dorsal spinal cord (Fig. 8.3). In strongly electroporated embryos, the experimental side showed a proportion of Islet-1 positive motor neurons in close apposition to the ventricular zone compared to the control side, a location not normally observed for motor neurons at these stages of development. The cadherin dominant negative expression was then conducted in the lumbar region of the developing spinal cord at various stages of development in order to observe stage specific effects of the construct on the organization of LMC. In all the stages observed the result was a

phenotype that is constantly weak in terms of LMC neuron migratory deficit and divisional segregation of the LMC respectively. Similarly, substantial number Islet positive motor neurons were observed to be located in positions midway between the progenitor rich ventricular zone and the ventral horn indicative of migratory route arrest of the LMC neurons (Fig.8.2A). However, the phenotype of this cadherin dominant negative was much weaker than that found using the γ-catenin point mutant misexpression. Next the results of cadherin dominant negative expression was analysed with respect to the total number of motor neurons on both the electroporated side and the control so as to rule out any underlying effect of the construct with respect to the generation of the LMC neurons. The analysis of the total number of LMC motor neurons on the experiment side compared to the control side all stages of development observed was found to be statistically not significant. Similarly, the LMC organization was analysed using the area of the LMC on both the electroporated and the control side as a major of dispersion of the LMC neurons, again there was no significant difference between the experiment side and the control side. Taken together, these results suggest that although cadherin dominant negative can cause nuclear disorganization in the developing spinal cord, its effects are less pronounced when compared to the effects of γ-catenin point mutant expression to the organization of the LMC.
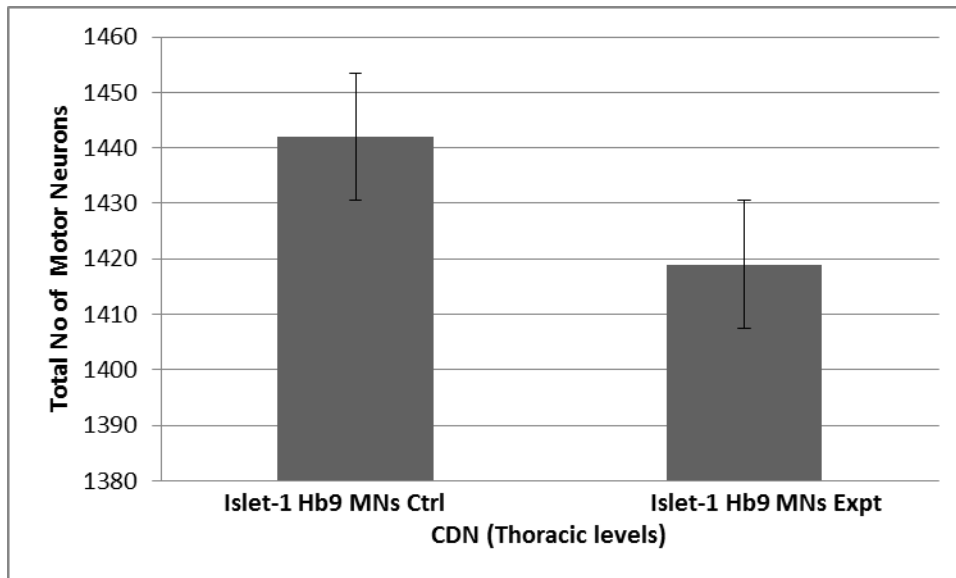
Figure 8.1 Quantitation of the number of thoracic motor neurons (HB9 and Islet-1) following CDN expression.

Student t-test measurement of number of motor neurons on the electroporated side compared to the control following in-ovo electroporation with cadherin dominant negative at the lower thoracic levels of the developing chick spinal cord to HH stage 29.
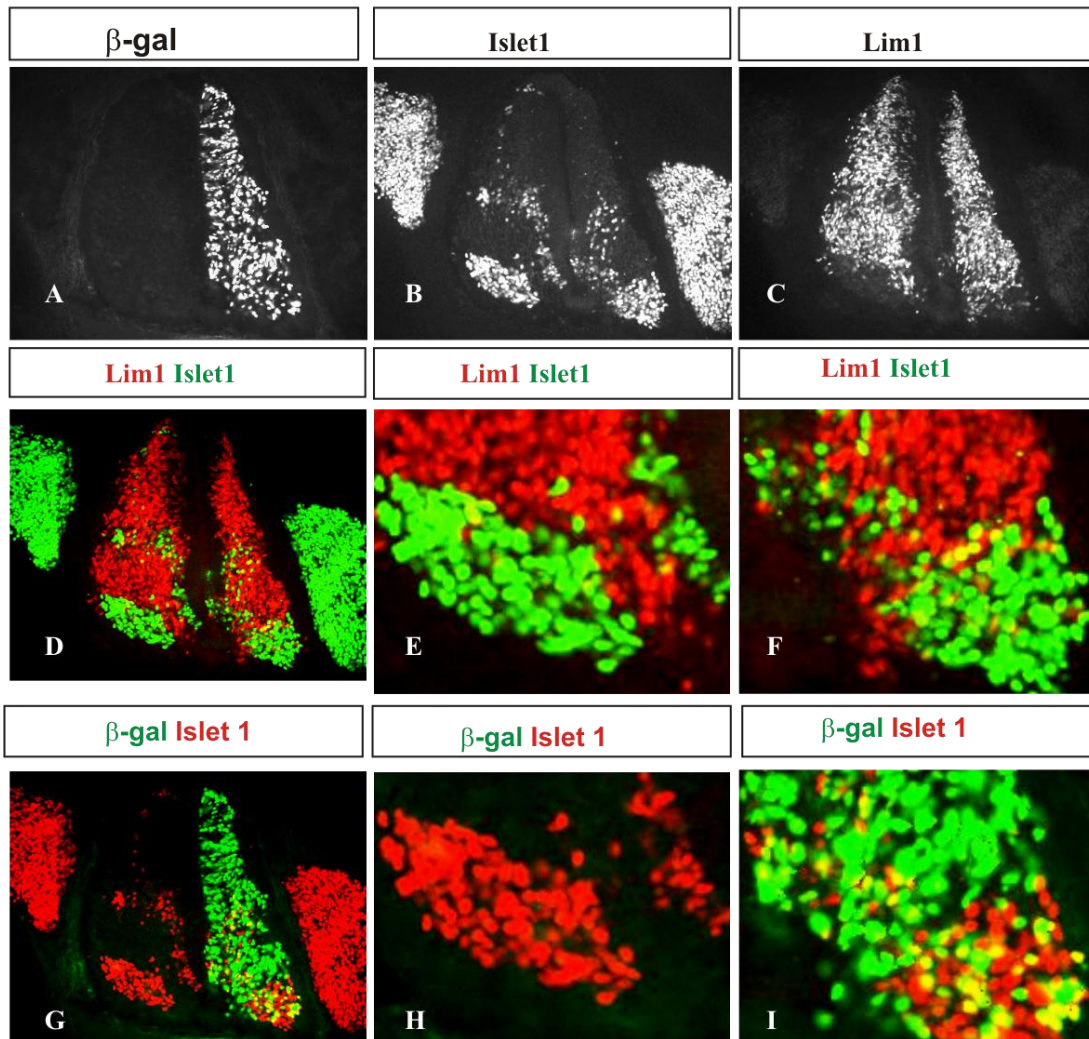
Figure 8.2 CDN misexpression at thoracic level shows little effects of desegregation of motor neurons.

(**A**), Beta-galactosidase on the electroporated side of the thoracic spinal cord. (**B**) Immunohistochemistry staining of Islet-1 showing some motor neurons in close proximity to the ventricular zone as well as mixing of cells along the medio-lateral path to the definitive LMC position. (**C**) Immunohistochemistry staining of Lim-1. (**D**) Immunofluorescence staining showing co-labelling of Islet-1 and Lim-1 with Islet-1 positive cells stacking in the ventricular zone and arrest of migration along their migratory path on the experiment side compared to control side. (**E-F**) Lim-1 and Islet-1, ventral thoracic spinal cord of the experiment side and the control showing desegregation and some mixing of cells. (**G-I**) Immunofluorescence for Beta-gal and Islet-1, showing the substantial number of cells in the ventricular zone and the ventro-lateral region of the spinal cord.
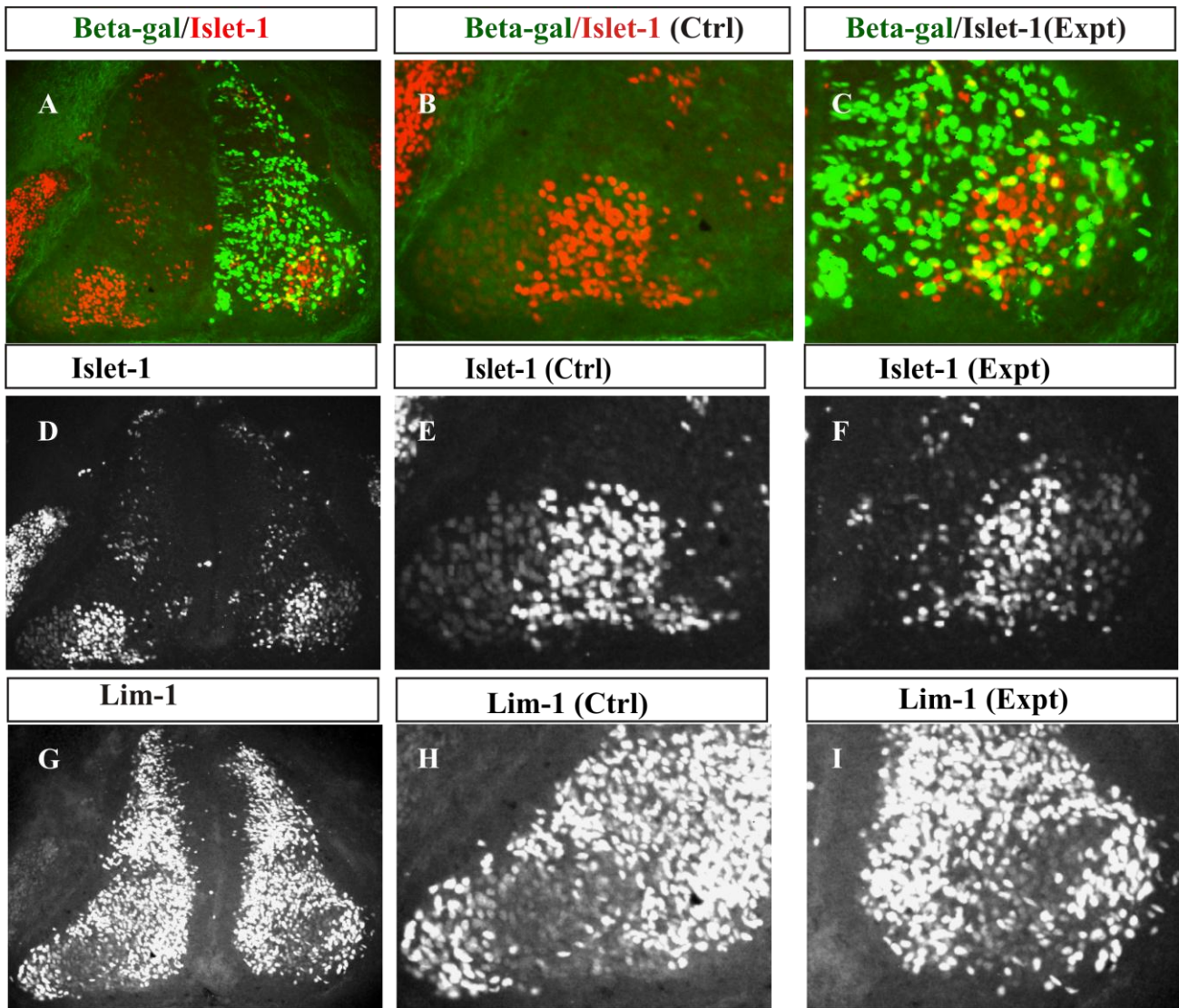
Figure 8.3 CDN expression at lumbar spinal cord region shows desegregation of LMC neurons

(**A**), Beta-galactosidae and Islet-1 immunoreactivity on the electroporated and control sides of the lumbar spinal cord covering the entire medio-lateral extent of ventral spinal cord. (**B**) Magnified control side in **a**, following immunohistochemistry for Islet-1 showing some motor neurons along the medio-lateral path to their definitive LMC position. (**C**), Magnified immunoreactivity for beta-gal and Islet-1(merged) on the experimental area of the lumbar spinal cord in A, showing desegregation of cells positive for Islet-1 along the medio-lateral extent of the lumbar spinal cord. (**D**) Immunofluorescence staining showing Islet-1 on the experimental side right and control left, with very few (low fluorescence) Islet-1 positive cells stacking in the ventricular zone and arrest of migration with relatively weak desegregation along their migratory path on the experiment side compared to control side. (**E-F**), Magnification of the areas (experiment and control sides) in **D** showing the effects of CDN on migration and segregation of LMC neurons. (**G-I**) Immunofluorescence for Lim-1, showing the substantial disruption of the area in between the most medial extent and the lateral extent of the ventral horn on the experimental side (I) compared to the control (**H**) suggestive of desegregation of the LMC **H,I** are magnification of the area in **G**.

8.2 Misexpression of cadherin N-Δ390 Experiments.

As a result of the weak phenotype found with the dominant negative form generated from cadherin-20 cDNAs, I sought other dominant negative isoforms that might more closely phenocopy the gamma catenin point mutation described earlier. Expression of a truncation of the extracellular domain of N-cadherin, NΔ390, has been shown to act in a cadherin dominant-negative fashion (Fujimori and Takeichi 1993). The construct I used to express N-Δ390 works under a doxycycline inducible system transposon mediated conditional expression of exogenous genes (Sato et al., 2007; Watanabe et al., 2007; Kawakami and Noda, 2004; Tanabe et al., 2006). Thus, I electroporated N-Δ390 comprising three plasmids namely: CAGGS-T2P, T2K-Cags-M2, and T2k-Cags-N-Δ390 cadherin in a ratio of 1:1:1 early in development between HH stage 13-18 and induced N-Δ390 expression through application of 400µl of 0.25µg/ml in filtered HBSS doxycycline in filtered HBSS solution in to the amnion of the developing embryos at HH stage 18. Following N-Δ390 cadherin expression, there was no significant difference in the total number of spinal LMC neurons on the experimental side compared to the control side following the expression of the construct. Expression of N-Δ390 at HH stage 18 caused a phenotype similar to γ-(L127A) expression, however at a slightly reduced level.   Approximately 5% of both LMCl and LMCm cells are found in an area adjacent the progenitor rich ventricular region (Fig.8.4A-F). These cells are believed to be stuck in the ventricular zone along their migratory route. Quantitation of divisional segregation using the neuronal mixing index shows a significant difference between the control side and the experimental (electroporated) side (student t –test p value =0.0006) *n=7*. I also observed a difference in the spinal motor columns morphology on the electroporated side compared to the control side. These result in a dramatic increase in the area occupied by the LMC neurons approximately twice the

control compared to the experimental side. Also a similar phenotype was observed when N-Δ390 cadherin was expressed at stage 20. Therefore, this raised the question whether this construct exerts it effects when expressed at advanced stage of LMC neurons divisional segregation? To address this question, the position of LMC neurons with respect to the columnar segregation at stage 24 to 28 was analyzed. There was no mixing of LMC neurons after addition of doxycycline from stage 24 onwards indicating that dramatic effects on LMC divisional segregation is restricted to the early phase of spinal LMC development with an abnormal columnar neuronal mixing index (Figure 8.4) (Bello et al., 2012).

I next asked whether N-Δ390 expression also caused a similar buckling of the ventricular zone to that found with gamma catenin point mutant expression. Folding of the ventricular zone following N-Δ390 cadherin expression was indeed found, albeit at a reduced level to gamma catenin manipulations. Additionally, the pathway of transitin positive radial glia follows the perturbed LMC neuron position but was still closely associated with the ventricle surface. Following N-Δ390 cadherin expression, I also observed deregulation in the localisation of β-catenin (Fig.8.6C), similar to that found with γ-(L127) catenin expression.

Strong columns mixing were observed in the embryos injected with Doxycycline only early in development. Mixing and stacking of cells being prominent between stages HH18-20 and very weak to normal segregation at HH 24 and beyond. Therefore, the essential features of the phenotype of γ-(L127A) expression on divisional segregation of the LMC and migration were replicated by the expression of cadherin dominant negative. Taken together, these results suggest that catenin-dependent cadherin function is necessary for the correct divisional segregation as well as radial migration of spinal LMC motor neurons.
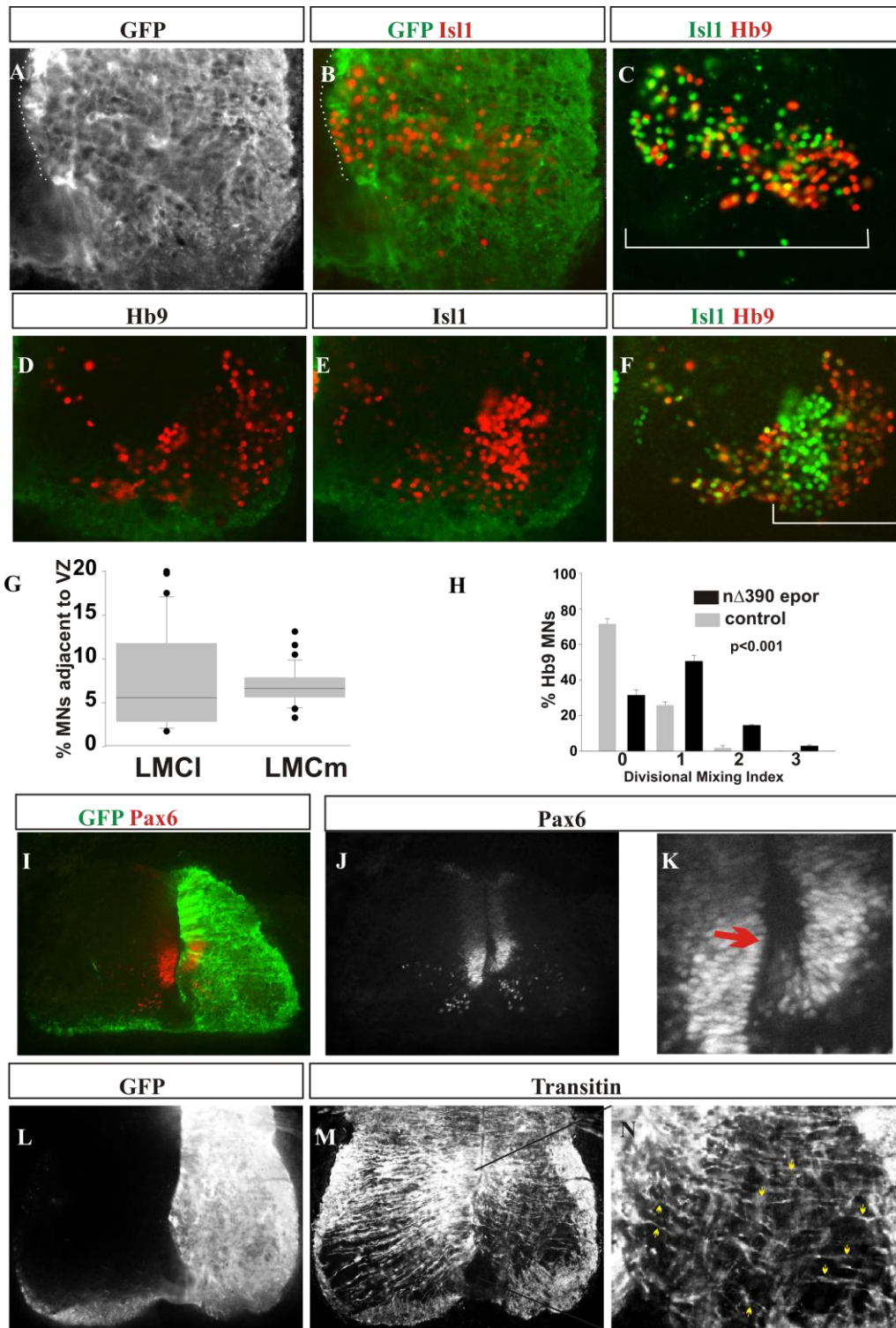
Figure 8.4 N-Δ390 dominant negative cadherin expression results disruption of spinal LMC divisional segregation.

A-C, GFP, Islet-1, and HB9 immunoreactivity following N-Δ390 cadherin expression shows stalled MNs and perturbation of divisional segregation of the LMC neurons. *D-F*, HB9 and Islet-1 immunoreactivity on the contralateral LMC. *A-B*, Dotted lines, ventricular surface. *C, F,* Solid lines shows the medio-lateral extent of the LMC. Note the medio-lateral extent of LMC on the experimental side approximately span twice the control side. *G-*H Quantification of the effect of the construct on LMC neuron position and **H,** neuronal mixing index. **I-K** buckling of Pax6 domain, Pax6 expression following N-Δ390 cadherin expression, marked by GFP in **G. I**, magnification of the buckled pax6 domain in **J,K**. **L**, immunoreactivity of transitin (*I-K*) following N-Δ390 cadherin expression marked by GFP in *L*. *M*,. *L*, transitin fibres course from the ventricle surface to the pial surface of the spinal cord. **N**, magnification of the area indicated by the black line in **M**

142

Hb9	Hb9(Ctrl)	Hb9(Expt)
Islet-1	Islet-1(Ctrl)	Islet-1(Expt)
Hb9/Islet-1	Hb9/Islet-1(Ctrl)	Hb9/Islet-1(Expt)
Gfp/Islet-1	Gfp/Islet-1(Ctrl)	Gfp/Islet-1(Expt)
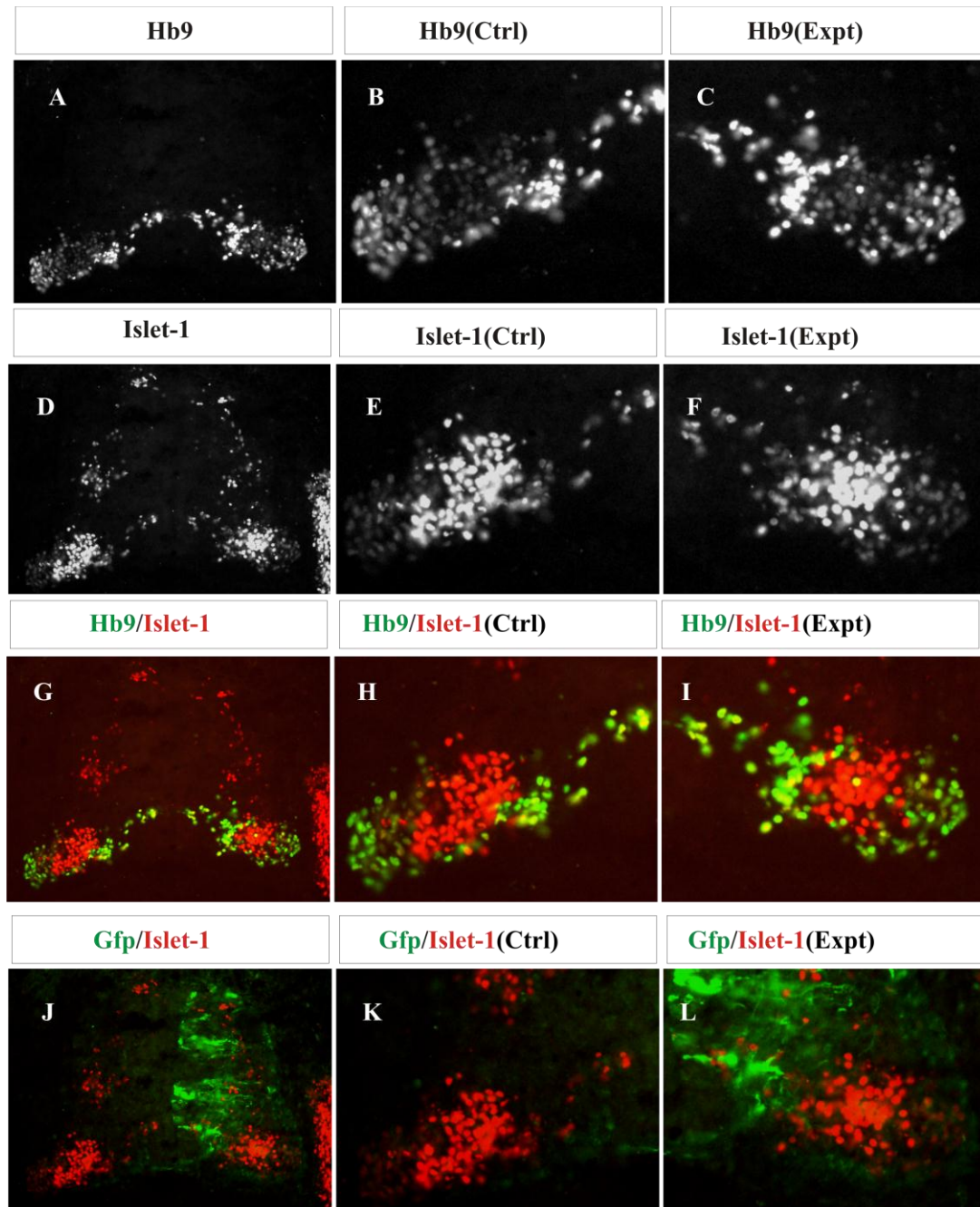
Figure 8.5 Application of doxycycline at stage 24 in NΔ390 cadherin expression does not affect LMC organization.

A-C, HB9 immunoreactivity following N-Δ390 cadherin expression with doxycline application at stage 24 shows normal divisional segregation of the LMC neurons in the control and experimental side. **D-F**, Islet-1 immunoreactivity on the both the control and the experimental side show normal LMC segregation with no migration deficit. **G-I**, merged immunoreactivity for Hb9 and Islet-1 on the control and experimental side shows normal development of the medio-lateral extent of the LMC. Note the medio-lateral extent of LMC on both sides is approximately the same. **J-L**, Immunoreactivity for gfp and Islet-1 following application of doxycline at stage 24 in N-Δ390 cadherin expression, marked by GFP in J shows no stalled MNs along the ventricular zone despite the medial aspect of the experimental side being acquired the construct than the lateral extent.

| Transitin | Betacatenin | B-cat/Transitin |
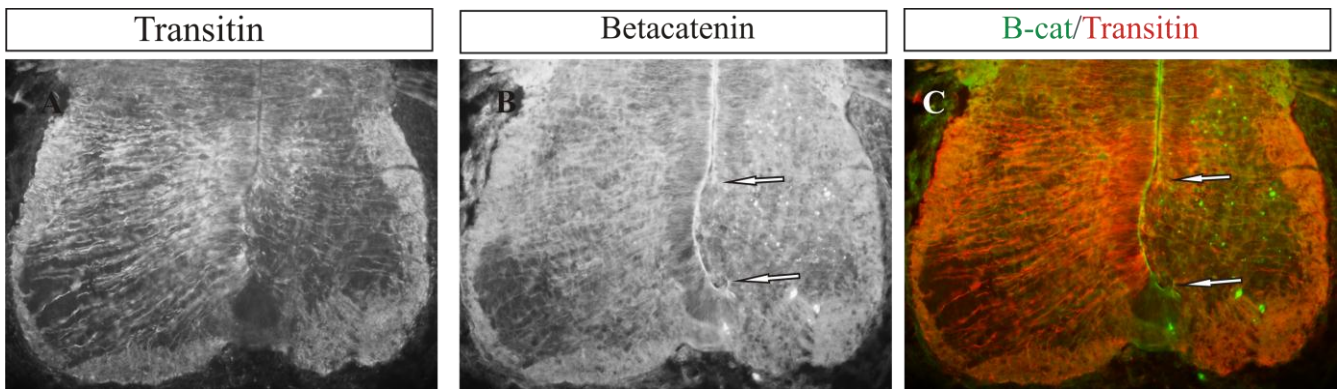
Figure 8.6 N-Δ390 dominant negative cadherin expression results in abrogation of β-catenin from the ventricular zone.

A, transitin immunoreactivity in the ventral lumbar spinal cord. Note the transitin fibres course in a medio-lateral direction from the ventricular zone to the ventral horn of the developing spinal cord on both experimental side and control side. B, β-catenin immunoreactivity following expression of N-Δ390 cadherin shows loss of β-catenin immunoreactivity in the experimental side (right side of the spinal cord) compared to the control side. Arrows indicate the extent of the loss of β-catenin immunoreactivity. C, Double immunoreactivity for β-catenin and transitin shows the loss of β-catenin staining on the right (experimental side) but preserved the fewer transitin fibres coursing from the ventricular zone o the ventral horn of the developing spinal cord on the electroporated side.

8.3 N-cadherin Expression Results in Normal Columnar Segregation of LMC Neurons.

I next asked whether misexpression of a cadherin not normally found in motor neurons caused any effects on LMC motor neuron migration and divisional segregation. I was concerned to try to control for possible extra adhesive effects of my manipulations of dominant negative cadherin and γ-catenin point mutant expression. During normal development the type I cadherin, N-cadherin, is excluded from LMC neurons both early at the beginning of the LMC neuronal divisional segregation and through till late in development. I thus asked whether N-cadherin expression had an effect on the LMC divisional segregation and migration. I over-expressed the chick N-cadherin, from which the dominant negative N-Δ390 cadherin construct was developed, using a transposon conditional expression of exogenous genes technique as in the N-Δ390 cadherin construct. Using this technique, three different plasmids were co-electroporated in a ratio of 1:1:1 as in (Tanabe et al., 2006).

The three plasmids used in a ratio of 1:1:1 are Cags-T2P, T2K-Cags-M2, and T2K-Cags-N-cadherin (described, tested and characterized in Tanabe et al., 2006) respectively. The conditional expression was induced by injecting 400μl of doxycycline (0.25μg/ml in filtered HBSS solution) in to the amnion of each embryo immediately after electroporation and at various stages of development following electroporation namely HH stage 18, 20 and 24 respectively.

Embryos were dissected at various stages of development for immunohistochemistry and further analysis of divisional segregation of LMC neurons as well as migration profile following the exogenous genes expression. Gfp fluorescence was used to follow the LMC neurons that express the exogenous N-cadherin in the ventral lumbar spinal cord and the immunoreactivity for Islet-1 and Hb9 was used to analyse the effects of

over expression of N-cadherin on the segregation of LMC neurons as well as migration. This analysis revealed a preservation of normal columnar organization of LMC neurons in the ventral spinal cord. The migration programme of LMC neurons was also preserved as there was no mixing of the LMC neurons in the experimental side compared to the control side in the developing ventral lumbar spinal cord. The results using the N-Δ390 cadherin construct shows compromised LMC neuronal migration as well as segregation with failure of some few percentages of LMC neurons to migrate leading to their localization in close proximity to the progenitor rich ventricular zone. I thus asked if the same phenotype pattern of arrested migration can be replicated following over expression of the transposon mediated conditional expression of N-cadherin with doxycycline application at stage 20, which in other construct produce the desegregation phenotype. My results shows normal migration and segregation of LMC neurons with the ventricular zone that is normal for the developmental stage and devoid of LMC neurons contrary to the N-Δ390 cadherin construct results. Taking together, these results suggest that over expression of N-cadherin has no effect on the LMC neuronal segregation and migration programme throughout development.

I next asked if there is any effect on the number of the motor neurons following the conditional over expression of N-cadherin. I analysed the total number of motor neurons in the LMCm and LMCl of the control side and electroporated side and found that there is no statistically significant difference between the experimental side and the control. I next analysed the total number of all motor neurons at different stages of development and found there was no statistically significant differences (*student-t test p value* =0.2511, n=5) between the experiment and control side. This preservation of LMC neurons segregation and migration programme is constant irrespective of the stage at which the conditional expression was induced or the stage of electroporation, thus, neuronal mixing index for this construct was not indicated.
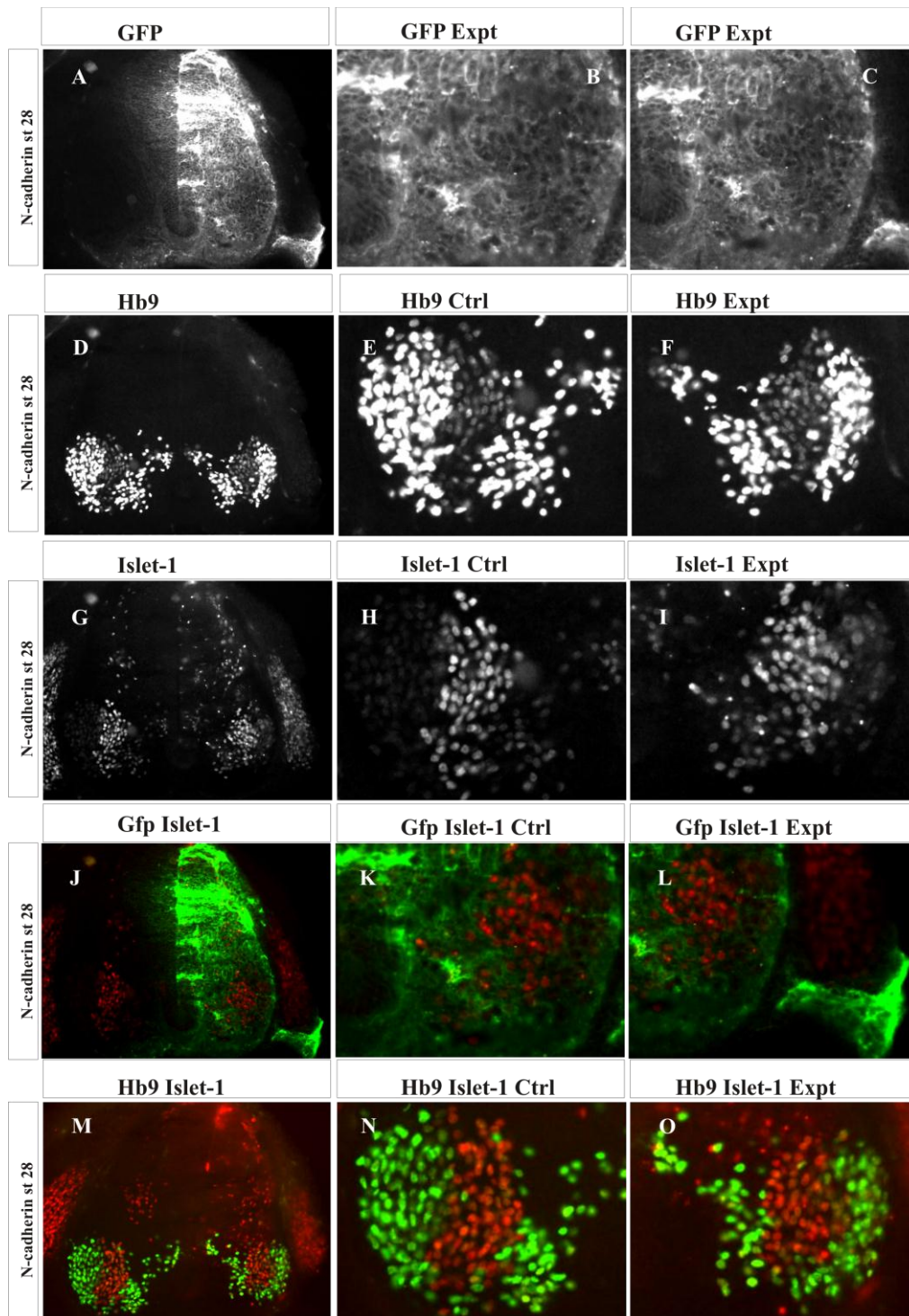
Figure 8.7 N-cadherin expression following electroporation and doxycycline injection at stage 20.

(A-C) gfp fluorescence showing labelling of ventral motor axons. (B) Hb9 immunohistochemistry staining shows normal segregation pattern of spinal motor neurons. (C) Islet-1 staining shows normal segregation and migration pattern (J-L) merged fluorescence image for gfp/islet-1 and Hb9/Islet-1(M-O) with normal column segregation.
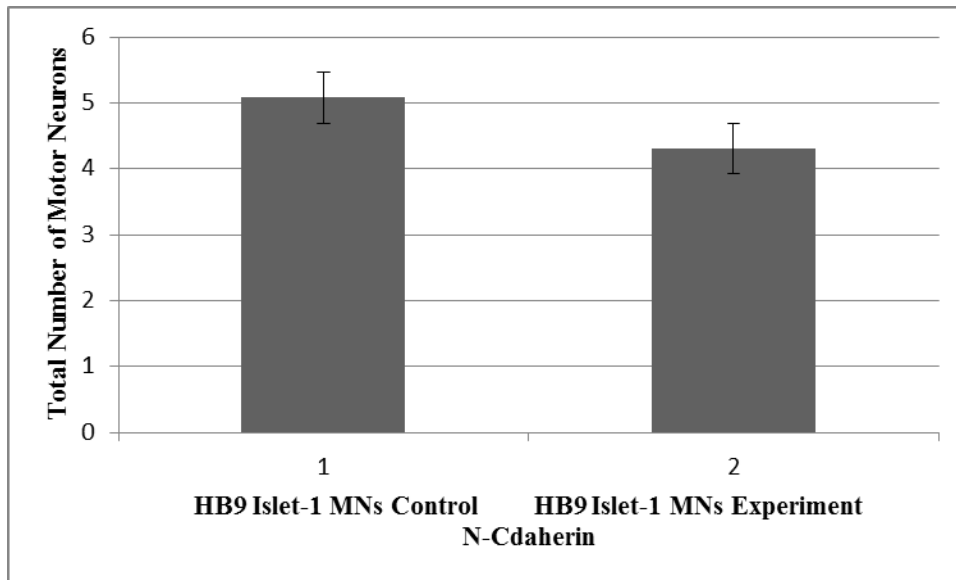
Figure 8.8 Quantitation of total number of MNs in the control and experimental side following expression of N-cadherin in the ventral lumbar spinal cord.

to HH stage 28 of development. There is no statistically significant difference between the control and experimental side, *student t-test p value*=0.2511. Error bars are standard error of means SEM

8.4 Cadherin-7 Control SiRNA Construct Does Not Perturb LMC Neuron Segregation and Migration.

Cadherin-7 (Cad7) is a classical type II cadherin superfamily member that is expressed in a distinct dorsal domain of the CNS (Nakagwa and Takeichi 1998). It is also expressed by some subsets of radial glia, developing gray matter, fibre tracts and various synapses of the developing CNS (Arndt and Redies, 1998). Previous studies shows cadherin-7 to be actively involved in the neuronal migration (Luo et al., 2004) and axon path finding (Treubert-Zimmermann et al., 2002) and generally plays a very important role in functional differentiation of specific regions of the CNS. Its expression in the developing spinal cord is regulated by the graded sonic hedgehog signalling (Ju et al 2004).

The expression pattern of cadherin-7 within motor neurons, contrary to the expression pattern of other type II cadherins, was found to be predominantly strong in the early stages of LMC divisional segregation. The expression of cadherin-7 is found to be down regulated in late stages following LMC segregation and by about stage 28 of development the expression of cadherin-7 is restricted to only few LMCl neurons in the ventral lumbar spinal cord (Fig.5.2A-D) (Price et al., 2002). I therefore asked whether the predominant effect of my cadherin manipulations on motor neuron migration and divisional segregation acted through cadherin-7 function. To establish the role for cadherin-7 expression in spinal motor neurons migration and segregation, I sought to down regulate its expression by spinal LMC neurons using a previously and successfully well characterized short interference RNA (SiRNA) approach (Barnes et al., 2010). Prior to this approach, I expressed a control shRNA construct of cadherin-7. Following successful in-ovo electroporation of control cadherin-7 SiRNA construct at various stages of development visualized by the Ds Red fluorescence, I observed that

the LMC neuronal migration from the progenitor rich ventricular region to their final settling position in the ventral lumbar spinal cord was normal and there was no arrest of migration along their migratory route or stacking of cells in the ventricular zone as observed with other cadherin/catenin constructs in this study. Similarly the LMC neuronal segregation process was also normal with the clear divisional segregation both on the electroporated side compared to the control side.

Electroporation of the control cadherin-7 SiRNA in the developing spinal cord was done between HH stages 16-18 followed by immunohistochemistry for Ds Red, Hb9 and Islet-1 respectively. Analysis of its effects was conducted between HH stages 28-30 when motor column segregation would have been completed. Ds Red fluorescence was used to follow good electroporation of motor neurons and was observed both in the ventral as well as the dorsal spinal cord with the ventral fluorescence extend from medial to lateral (Fig. 8.9 J-L). Analysis of column segregation shows no cells mixing on the electroporated side compared to control (Fig.8.9G-I). In the absence of any gross effects on LMC columnar segregation, we thus asked whether the electroporation may have some subtle effects on the total number of developing LMC neurons. Therefore, we quantitated the total number of both Islet-1 and Hb9 positive LMC neurons at various stages of development following electroporation using Ds Red fluorescence. There was no statistically significant difference (student t test p value = 0.0864) in the number of HB9 and Islet-1 positive motor neurons between the control and electroporated sides (Fig. 8.10). Thus control cadherin-7 SiRNA construct has no effect on the LMC divisional segregation and migration during development.
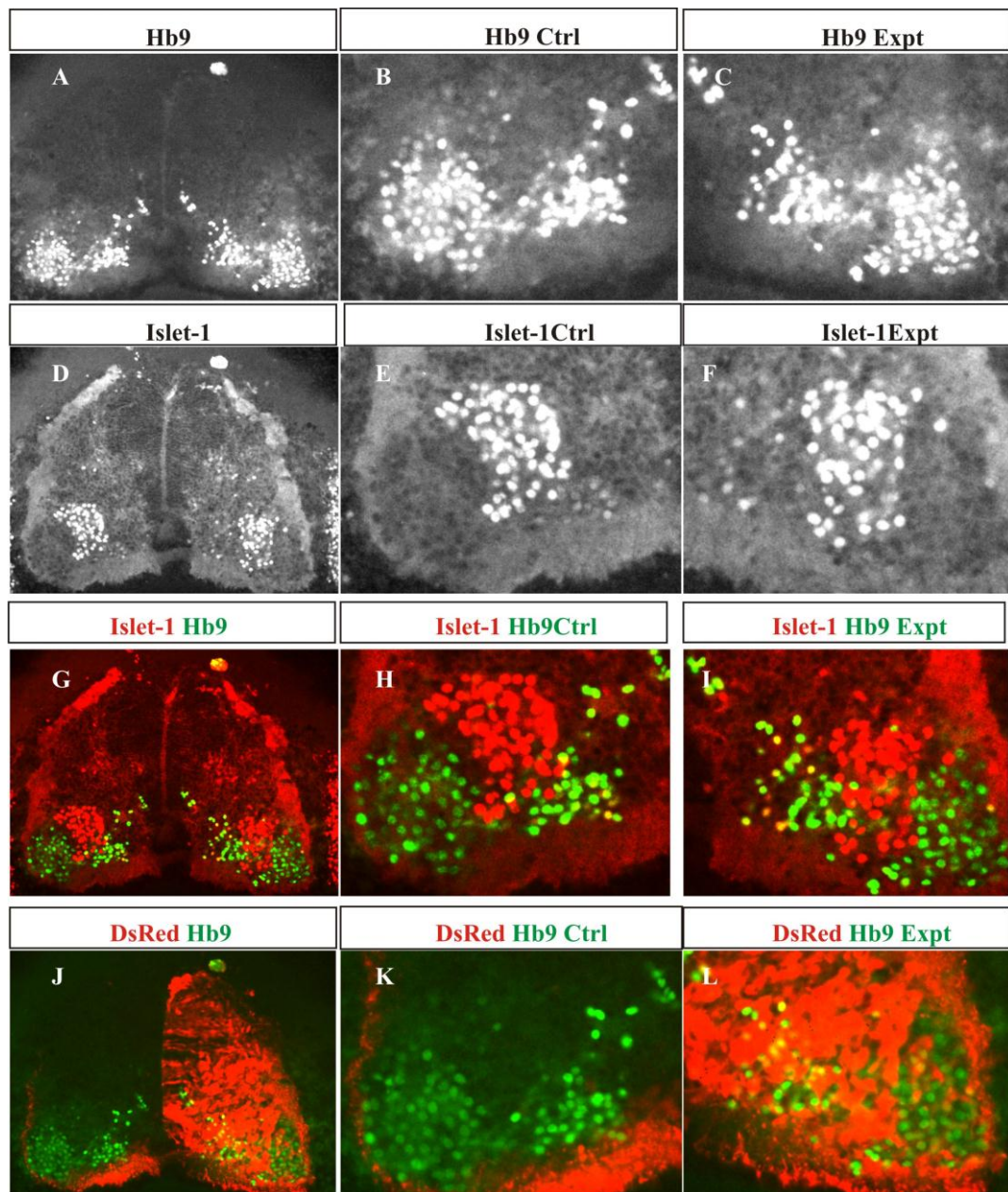
Figure 8.9 Expression of the control cadherin7 SiRNA in the ventral lumbar spinal cord

lacks effects on LMC neurons segregation.

A-B Hb9 immunohistochemistry stain of the experimental side (right side of the spinal cord) compared to the whole section. C-D Islet-1 immunohistochemistry staining showing no altered LMC segregation on the experimental side compared to the control side. E-F Ds Red and Hb9 immunofluorescence showing Ds Red labelled motor neuron along the medio-lateral migratory route to the definitive LMC position. G-H merged Islet-1 and Hb9 immunostaining shows a normal columnar segregation of LMC neurons on the control side H compared to the control side in G.
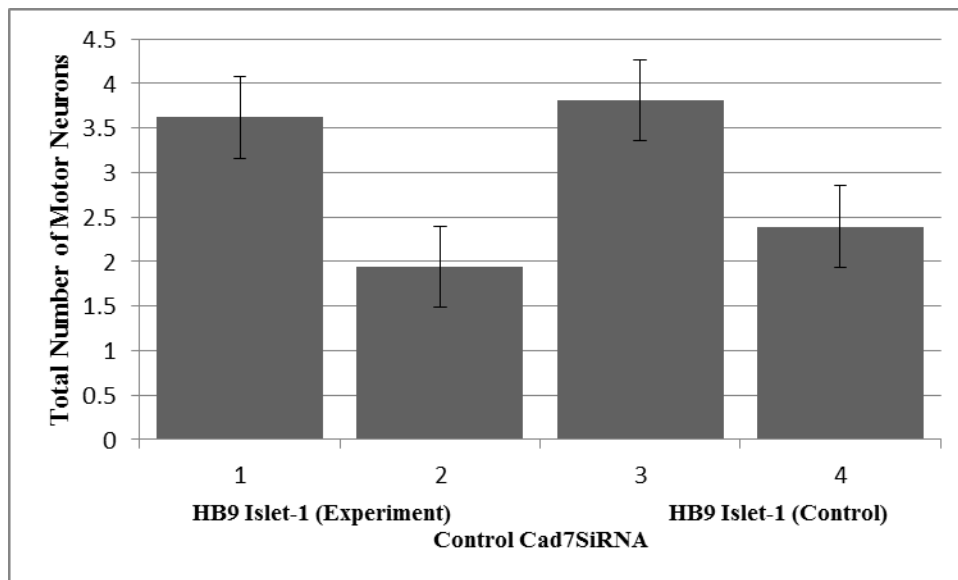
Figure 8.10 Quantification of the number of motor neurons   following electroporation with control cadherin 7 SiRNA.

Measurement following expression of construct to stage 30 in ventral lumbar spinal cord, paired student *t-test p* value= 0.0864 and error bars are Standard Error of Means SEM. Column 1 is the total number of HB9 positive cells   on the experiment side, column 2 is the total number of Islet-1 positive cells on the experiment side. Column 3 is the total number of HB9 positive cells on the control side, column 4 is the total number of Islet-1 positive cells on the control side

8.5 Cadherin-7 Expressions Is Important For LMC Neurons Migration and Segregation during Development

In contrast to the control cadherin-7 SiRNA construct experiments, following expression of the cadherin-7 SiRNA construct I observed an alteration in the LMC neuronal segregation programme. As with the control cadherin-7 construct, electroporation was conducted at early stages of LMC development and analysed later in development following immunohistochemistry for Ds Red, Hb9 and Islet-1. Ds Red fluorescence was used to follow cells that are well electroporated and cells that had acquired the SiRNA construct were observed to be located in the more medial location close to the progenitor rich ventricular zone on the electroporated side compared to the control side where the LMC neurons segregate normally to their final settling position (Fig. 8.11).

Similarly, the position of the LMCm and LMCl neurons following cadherin-7 expression was characterized and at HH stage 25 we observed the increased number of Islet-1 positive neurons in an area close to the progenitor rich ventricular zone. Also at HH stage 27 it was found that the Hb9 positive Islet-1 negative LMCl neurons are located medial to LMCm neurons, a position that shows abnormal sorting or segregation of the LMCl neurons. Quantitation of the effects of cadherin-7 SiRNA construct on the number and position of the LMC neurons in development revealed that the LMCm and the LMCl divisional segregation was compromised following acquisition of the construct on the electroporated side compared to the control. These data suggest that cells expressing cadherin-7 SiRNA were perturbed along their migratory route within the lateral motor column. Analysis of the neuronal mixing index between the control and experimental side of cadherin-7 SiRNA and control cadherin-7 SiRNA constructs shows statistically significant difference between the control construct and the

cadherin-7 SiRNA construct (Fig. 8.13). Taken together, these data suggest that down regulation of cadherin-7 expression stalls the migration of LMC neurons and perturbed the divisional segregation of spinal LMC neurons.
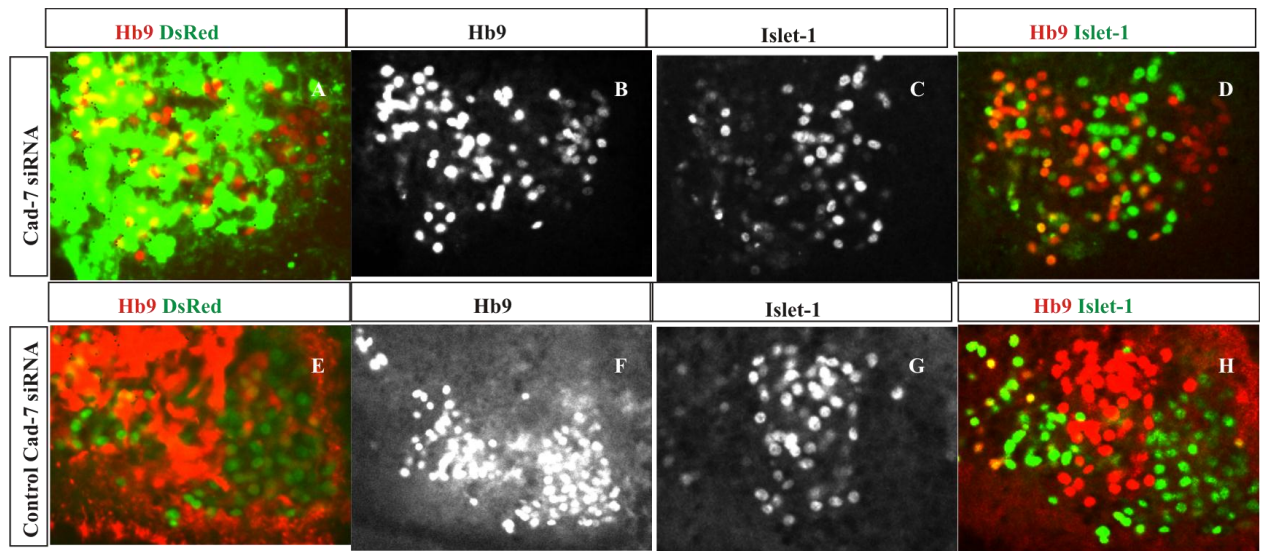
Figure 8.11 Comparisons of effects of cad7SiRNA and the control Cad7 SiRNA on segregation of spinal motor neurons.

A, Immunoreactivity for HB9 Ds Red following Cad-7 SiRNA to HH stage 28 electroporation in the ventral lumbar spinal cord. *B*, HB9 immunoreactivity shows desegregation with the vast area occupied by the Hb9 positive MNs. *C*, Islet-1 dispersed over an extended area along the medio-lateral extent of the ventral spinal cord. *D,* merged HB9 Islet-1immunofluorescence shows clear LMC columnar desegregation compared to the control cadherin-7 construct pattern in H. *E-H* shows uncompromised columnar segregation of LMC following electroporation with control cadherin-7 construct.
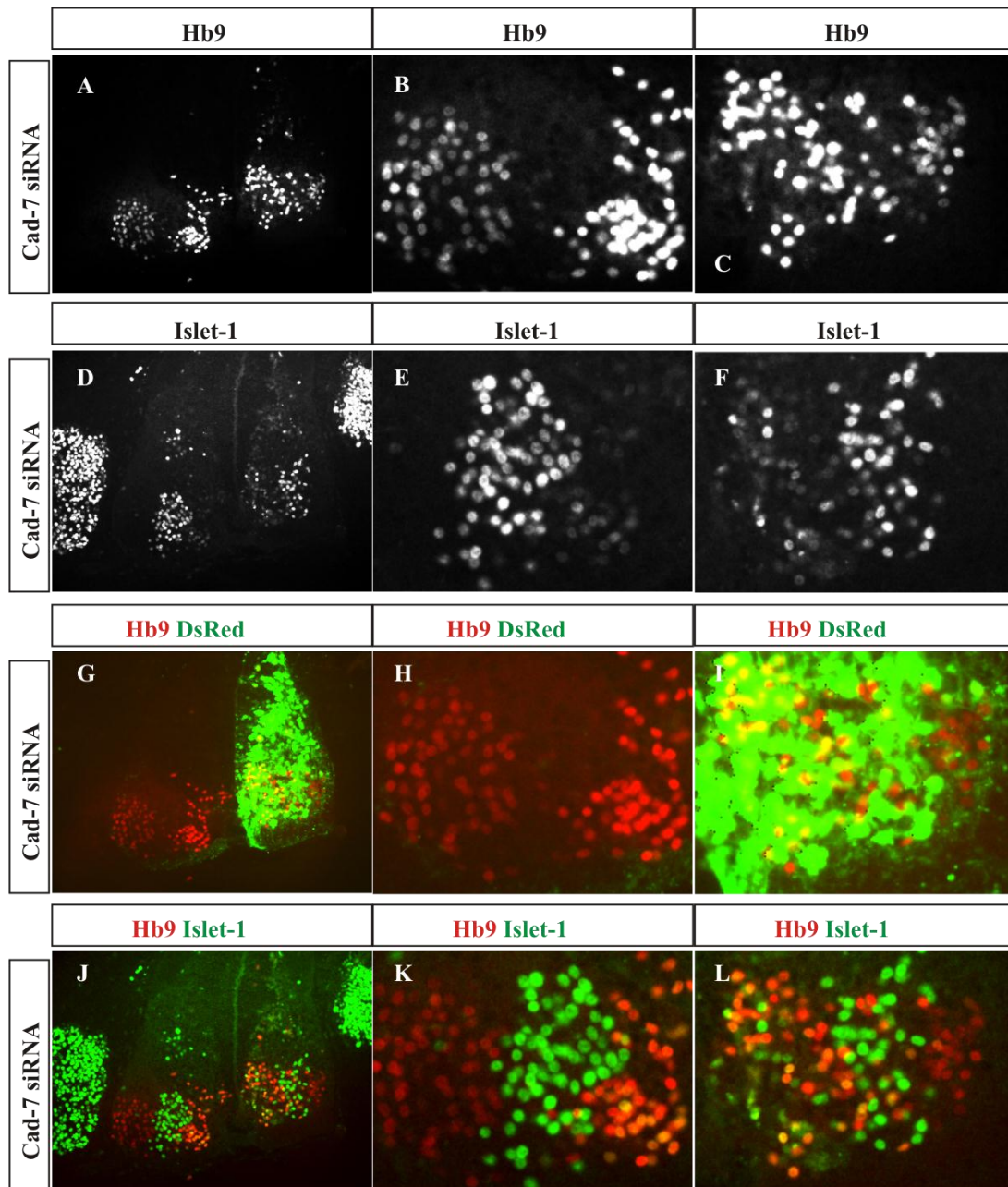
Figure 8.12 Cadherin 7 SiRNA misexpression in the ventral lumbar spinal cord affects segregation of spinal motor neurons.

(*A-C*) Hb9 immuno staining with altered segregation on the experimental side *(C)* compared to the control side *(B)*. *D-F* Islet-1 stains showing abnormal segregation of the experimental side F compared to the control side E. *G-I*, immunoreactivity for HB9 and Ds Red with acquisition of Cadherin-7 SiRNA by MNs as evidenced by Ds Red fluorescence on the experimental side I compared to the control side H. *J-L* cadherin-7 SiRNA construct result desegregation of the LMC *L* shows intermingling of both LMCl and LMCm over a wide are as well as LMCl cells close to ventricular zone on the experimental side **L** compared to the control side *K*.

9   Wnt signalling pathway control expressions and LMC neurons segregation and migration.

The canonical Wnt pathway comprises a series of events that occurs as a consequence of binding of Wnt proteins to cell-surface receptors of the frizzled family, leading the receptors to activate dishevelled family proteins and ultimately resulting in change in the amount of β-catenin reaching the nucleus. In addition to the effects on β-catenin, Wnt binding also inhibit other complex proteins that include axin, APC and glycogen synthase kinase 3β (GSK3β). The Wnt pathway is involved in almost all developmental process such as patterning of the neural tube, planar cell polarity, axon guidance, stem cell differentiation and self-renewal, and even non-canonical signalling. The perturbations of cadherin function have the potential to alter Wnt signalling as they all offer the possibility of sequestering or altering β-catenin function (Nelson and Nusse, 2004). Thus, I asked if the canonical pathway, which is β-catenin dependent, is involved in the segregation and migration of the LMC neurons.

To address this question, the components of the Wnt signalling pathway were examined with a view to being able to result in the up regulation and down regulation of the canonical Wnt pathway (Roose et al., 1999, Zhurinsky et al., 2000b).

9.1 Canonical Wnt Signaling Down Regulation Does Not Influence Spinal LMC Neuron Segregation and Migration.

To determine whether perturbation of the canonical Wnt signalling pathway through down regulation can have any consequences on the divisional segregation of the LMC and migration of the spinal motor neurons, I expressed in ovo HA tagged constructs at various stages of development in the ventral lumbar spinal cord and observed their effects.

9.1.1 Constitutively Active Glycogen Synthase Kinase Expression Does not affects LMC Neurons Segregation.

Glycogen synthase kinase (GSK3β) is involved in many cellular signaling pathways. The constitutively active glycogen synthase kinase 3β has its glycogen synthase kinase (GSK-S9A: where the 9th serine is switched to alanine) construct was electroporated in to the ventral lumbar spinal cord at various stages of development to correlate onset of effects, if any, with a stage of development as was done in the expression of cadherins and catenins.

Electroporation was conducted as early as stage 14-18 and following immuno histochemistry, analysis was done at late stages (28-30) of development when the motor neuron migration and segregation programme would have been completed. Haemaglutinin (HA) immunofluorescence was used to follow cells that take up the construct and this fluorescence extend from the medial to lateral aspect of the lumbar spinal cord indicating adequate coverage of the ventral lumbar spinal cord. In all stages analysed, there was no observable differences in terms of the divisional LMC neurons segregation on both the experiment and control side. Also there was no evidence of arrested migration of LMC neurons or abnormal positioning of LMC neurons close to the progenitor rich ventricular zone at advance stages of development as was observed

with the perturbation of the cadherin and catenins in the previous experiments. Similarly, there were no differences in either migration or segregation with respect to stage of electroporation and no statistically significant difference was observed in terms of total number of motor neurons following the down regulation. Thus, the stage of development at which the forced down regulations of the Wnt pathway take place does not have any consequences on the number, segregation and migration of the LMC neurons (Fig 9.1A-D).
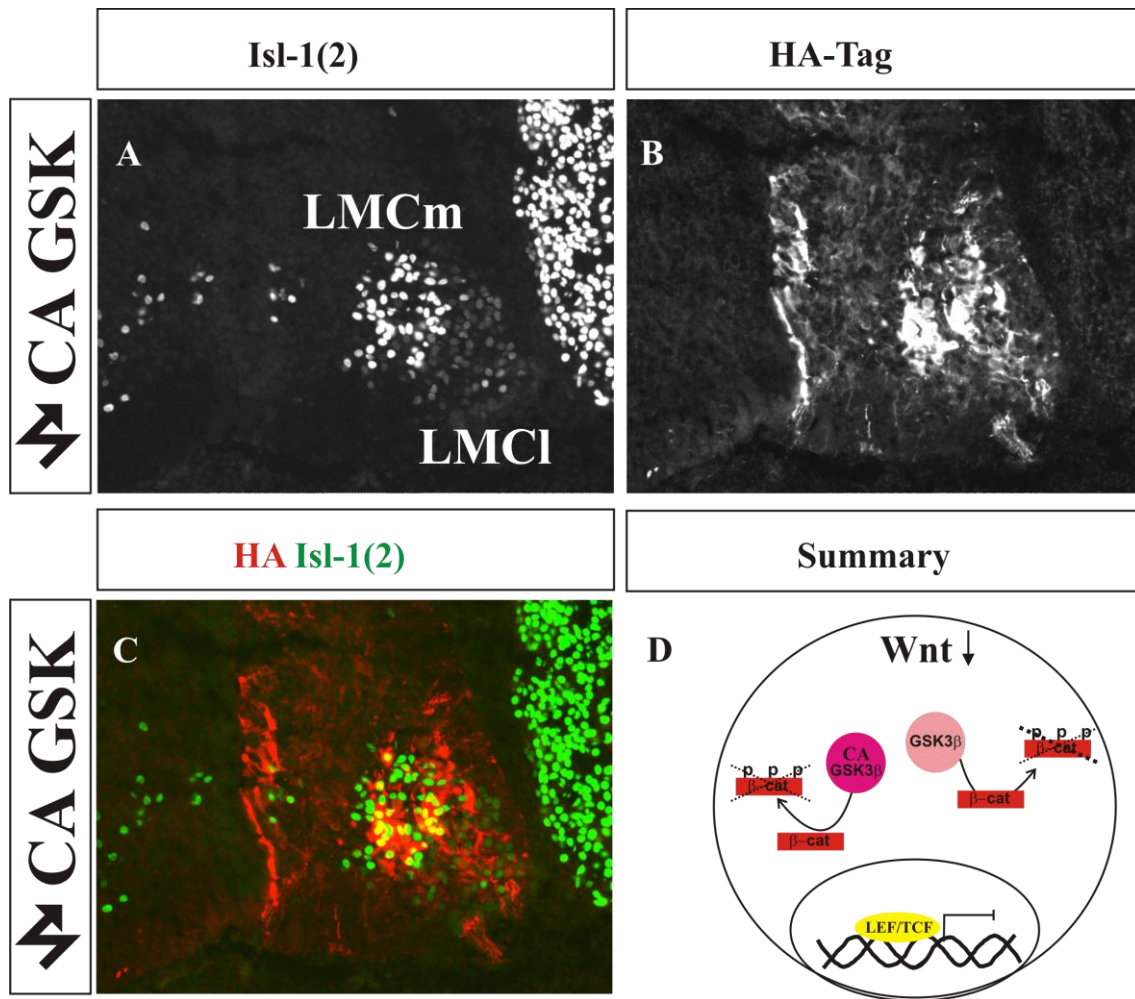
Figure 9.1 Down regulation of Wnt signalling pathway by expression of Constitutively active glycogen synthase kinase (CA-GSK3β) lacks effects of LMC neurons segregation and migration.

A, Immuoreactivity for Islet-1(2) clearly shows normal segregation of LMCm and LMCl neurons following expression of the construct marked by HA immunoreactivity, immunofluorescence of Islet-2 lower in LMCl than in LMCm. *B*, HA tag immunoreactivity in the ventral lumbar spinal cord following expression of the construct. *C*, merged immunoreactivity for both HA tag and Islet-1(2) shows most of the ventral lumbar spinal cord positive for Ha tag indicating the construct acquisition by the migrating LMC neurons results in normal migration and segregation following expression of the construct. *D*, Summary of action of the construct.

9.1.2 Wild Type Glycogen Synthase Kinase Expression Lacks effects on LMC segregation.

I next asked whether further down regulation of the canonical Wnt pathway by way expression of a different form of Glycogen Synthase kinase 3β will have effects on the segregation and migration of the LMC neurons during development. To address this, I down regulate the Wnt pathway by expression of wild type glycogen synthase kinase 3β in to the developing lumbar spinal cord at various stages of development and analysed the results at later stages of development as with the constitutively active glycogen synthase kinase 3β previously.

As with other constructs, haemaglutinin was used as tag to aid identification of cells that acquire the construct. Following immunohistochemistry for Islet-1, Lhx-1/Lim-1 and HA respectively, I observed that majority of the LMC neurons have acquired the construct evidenced by positive fluorescence for HA covering the entire medio-lateral extent of the ventral lumbar spinal cord more concentrated in the LMCl domain (Fig 9.2A-B). The results for this down regulation were t identical with the results of previous construct with respect to migration and segregation of LMC neurons. There was no observable difference in terms of segregation of the LMCm and LMCl neurons on the experimental side compared to the control side in all the embryos analysed. The remarkably normal segregation was observed throughout the different stages of development analysed. Similarly, there was no evidence of altered migration on the experimental side compared to control and there was no difference in the number of motor neurons in the experimental side compared to the control side throughout the various stages of development analysed (Fig.9.2C), similar to that obtained when down regulation was forced using the constitutively active glycogen synthase kinase 3β.
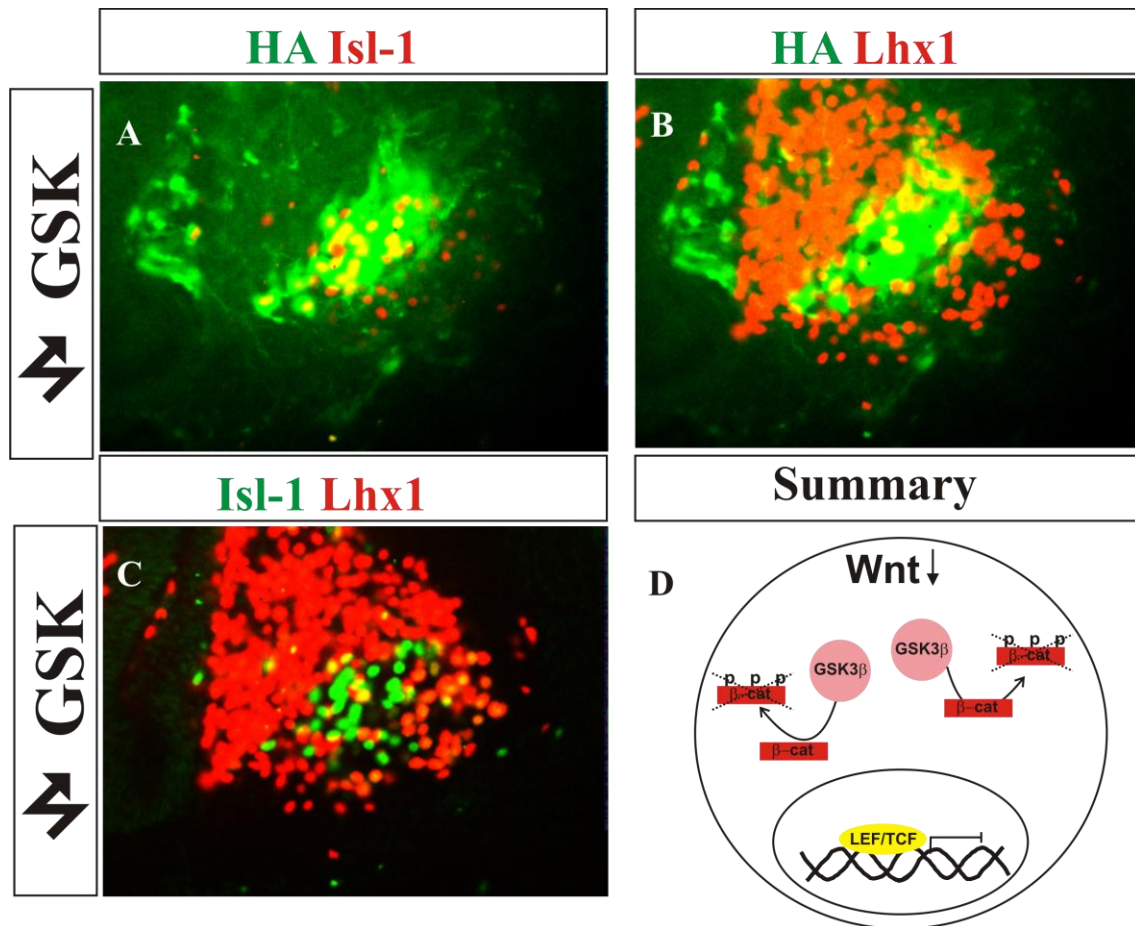
Figure 9.2 Lack of effect on LMC organization following expression of wild-type GSK3β.

A, HA-tag (green) and Islet-1(red) immunoreactivity following expression of the construct. *B*, merged HA-tag (green) and Lhx-1(red) immunoreativity following electroporation of the construct. *C*, merged immunoreactivity for Islet-1(green) and Lhx-1 (red) following expression of the construct revealed normal LMC neurons segregation. *D*, Summary of the action of the construct.

9.1.3 Dominant Negative TCF Transcription Factor Expression Does not influence LMC Neurons Segregation.

Due to the strategic role of the T-Cell factor in the Wnt signalling cascade and its interaction with β-catenin as part of the Dishevelled-GSK3β-APC-β-catenin complex in the Wnt pathway, I asked if it has any influence on the LMC neurons segregation and migration programme. Therefore, I further sought to down regulate the canonical Wnt signalling pathway through the expression of a dominant negative TCF construct (Fig. 9.3A-D) (Ciani et al., 2004). I electroporated the ventral lumbar spinal cord with dominant negative TCF at various stages of development (HH 16-18) and analysed the results at later stages when the migration and segregation of LMC neurons would have been completed (HH 28-30).

Here as with previous two forced down regulation of activity of the GSK3β and wild-type GSK3β, there was no observable difference in the nature of segregation and migration of the LMC neurons at different stages of development analysed. Interestingly, there was no observed deficit in migration of LMC and no difference was observed in the total number of LMCl and LMCm on the experiment side compared to the control side throughout the stages analysed. Thus consistent with previous constructs used in down regulation, dominant negative TCF lack any effects on the LMC neuronal segregation and migration programme. Taken together, down regulation of the canonical pathway of Wnt signalling does not affect the segregation of spinal LMC neurons segregation and migration.
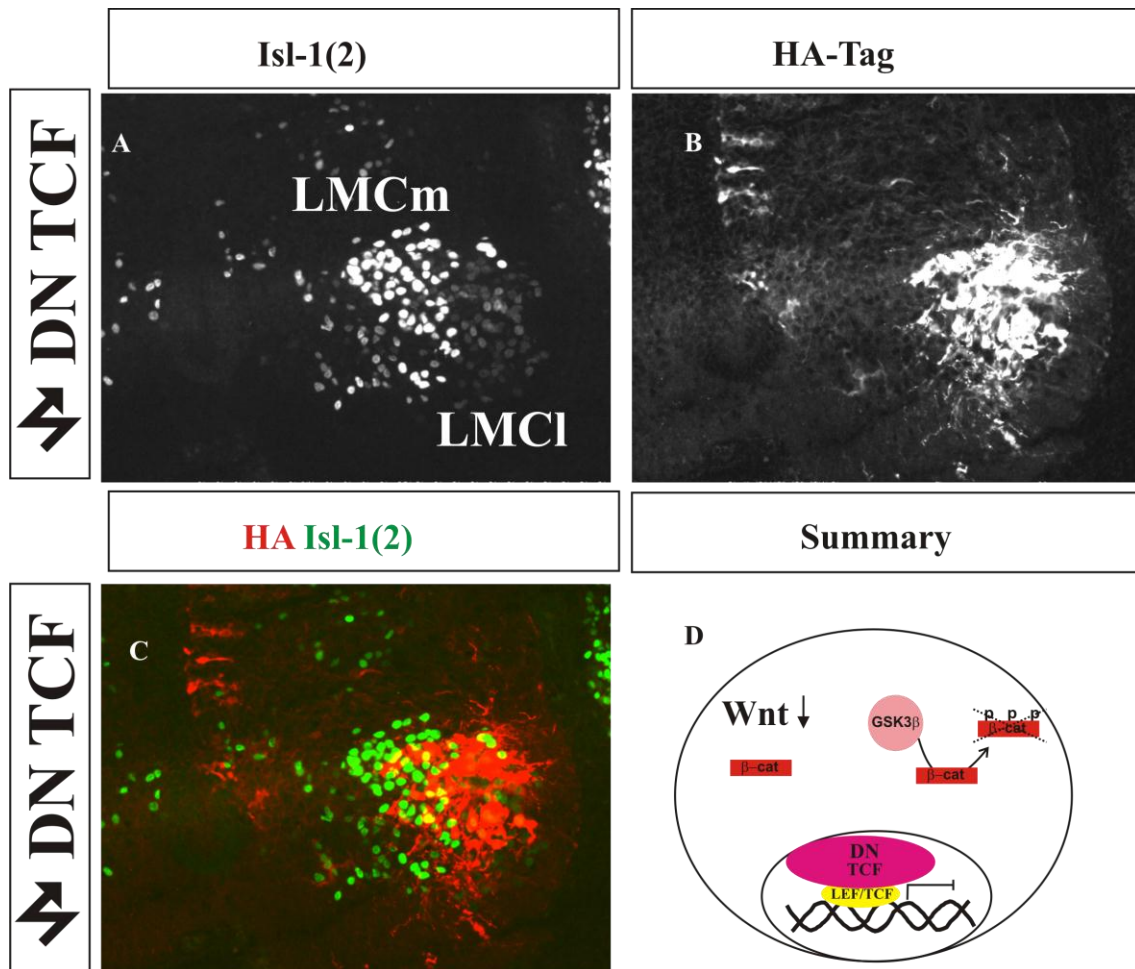
Figure 9.3 Down regulation following DN TCF trancription factor lacks effect on the LMC neurons segregation and migration.

A, Immunoreactivity for Islet-1(2) following expression of DN TCF evidence by HA-tag fluorescence (in B) immunofluorescence for Islet-(2) is lower in LMCl than in LMCm. *B*, HA-tag fluorescence in the ventral lumbar spinal cord shows acquisition of the construct by the majority of LMCm and LMCl neurons. *C*, Merged HA-tag and Islet-1(2) immunoreactivity following expression of the construct shows normal segregation of LMC neurons. *D*, Summary of action of the construct.

9.2 Canonical Wnt Signaling Up Regulation Does Not Influence Spinal LMC Neuron Migration and Segregation.

Following the direct perturbation of the canonical Wnt signalling pathway through the expression of construct known to down regulate the Wnt signalling pathway, the results showed no effects on the LMC neurons segregation and migration programme. I therefore asked if direct perturbation of the canonical Wnt signalling pathway through up regulation by way of expression of constructs in vivo that are known to up regulate the pathway could have any effects on the LMC neurons programme of segregation and migration (Roose et al., 1999, Krylova et al., 2000 Zhurinsky et al., 2000b) .

To address this, I expressed HA-tagged wild-type β-catenin construct, a truncated form of β-catenin (β-catenin-1-ins), and a dominant negative Glycogen Synthase Kinase 3β (DN GSK3β) known to up regulate the pathway and analysed their effects on the LMC neuronal segregation and migration.

9.2.1 Wild type Beta catenin expression does not affects normal LMC Neurons Segregation.

I electroporated Ha-tagged wild-type β-catenin construct in to the developing lumbar spinal cord at various stages of development (stages 16-18) and allowed to developed till late stages (28-30) when the LMC neurons migration and segregation would have been completed. Following immunohistochemistry for Islet-1, Hb9 and HA-tag, serial spinal cord sections were analysed. The HA-tag immunoreactivity was used to follow the cells that acquired the construct in the ventral lumbar spinal cord, and majority of LMCl and LMCm neurons acquired the construct evidenced by the HA-tag immunoreactivity extending across the medio-lateral extent of the ventral lumbar spinal cord.

Here, as with other constructs in the down regulation experiments, there was no observed difference on the electroporated side compared to the control sides in terms of LMC neuronal segregation as well as migration. Similarly, the number of motor neurons on the experimental side compared the control shows no differences throughout the various stages of development analysed. There was no difference in the nature of phenotype resulting from the expression of the constructs between earlier stages of development and late stages of development (Fig.9.3A-C). Additionally, expression of wild type β catenin using a pCS2 vector to enhance expression does not result in any observable effects on the LMC organization (Fig.9.5). Taking together, these results show the potential for up regulation of the canonical Wnt signalling pathway to follow the same pattern of lack of effects on the LMC neurons segregation and migration programme.
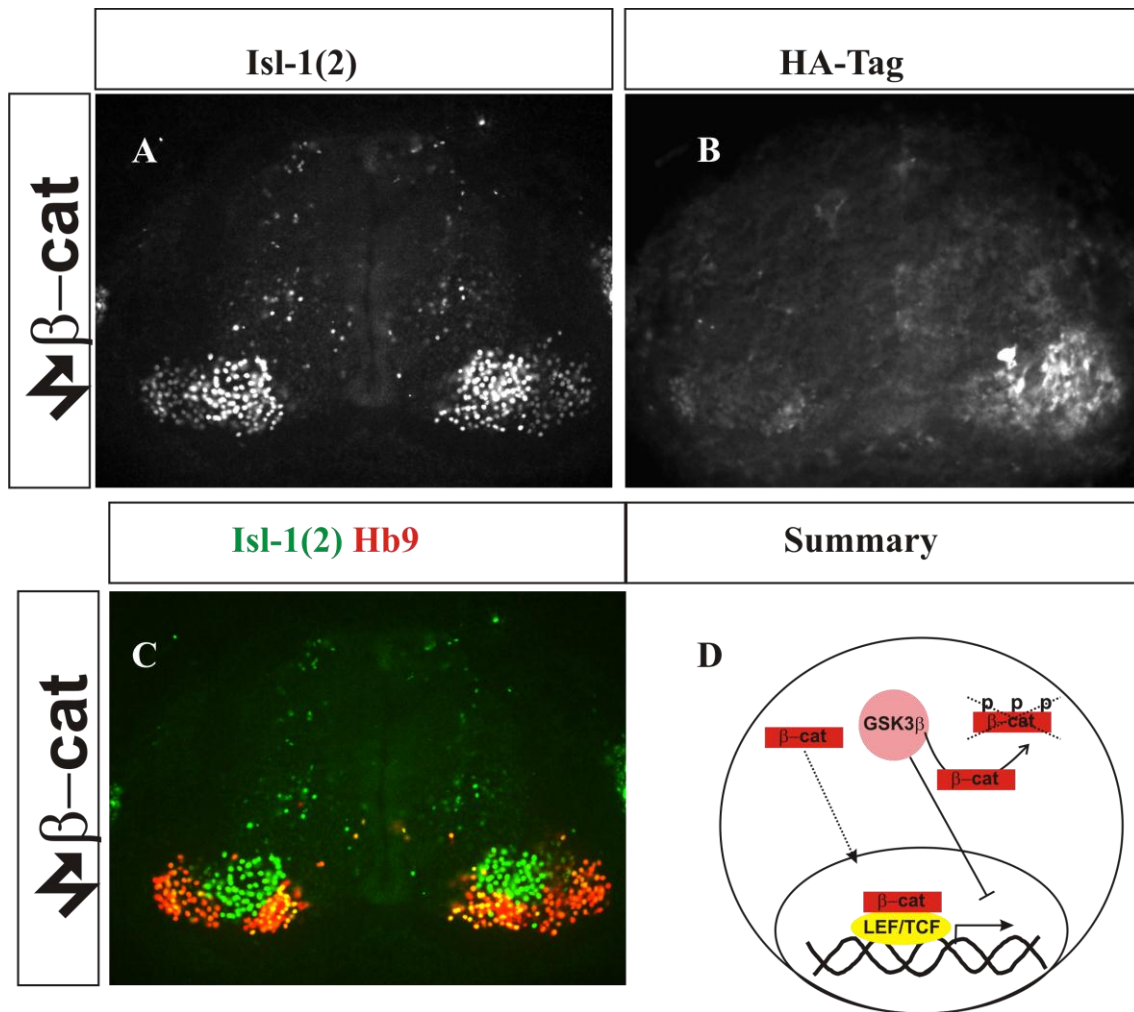
Figure 9.4 Over expression of wild-type βcatenin does not disrupt LMC neuron organization.

A, Islet-1(2) immunohistochemistry after β-catenin expression marked by HA-tag immunoreactivity (in **B**) with Islet-1(2) immunoreactivity more in the LMCm than in the LMCl. *B*, HA-tag immunoreactivity covering the entire LMCm and LMCl in the experimental side of ventral lumbar spinal cord compared to control. *C*, Merged Islet-1(2) and Hb9 immunohistochemistry following expression of wild-type β-catenin shows normal LMC divisional segregation on the experimental side as well as the control side. *D*, Summary of action of the wild-type β-catenin constructs.
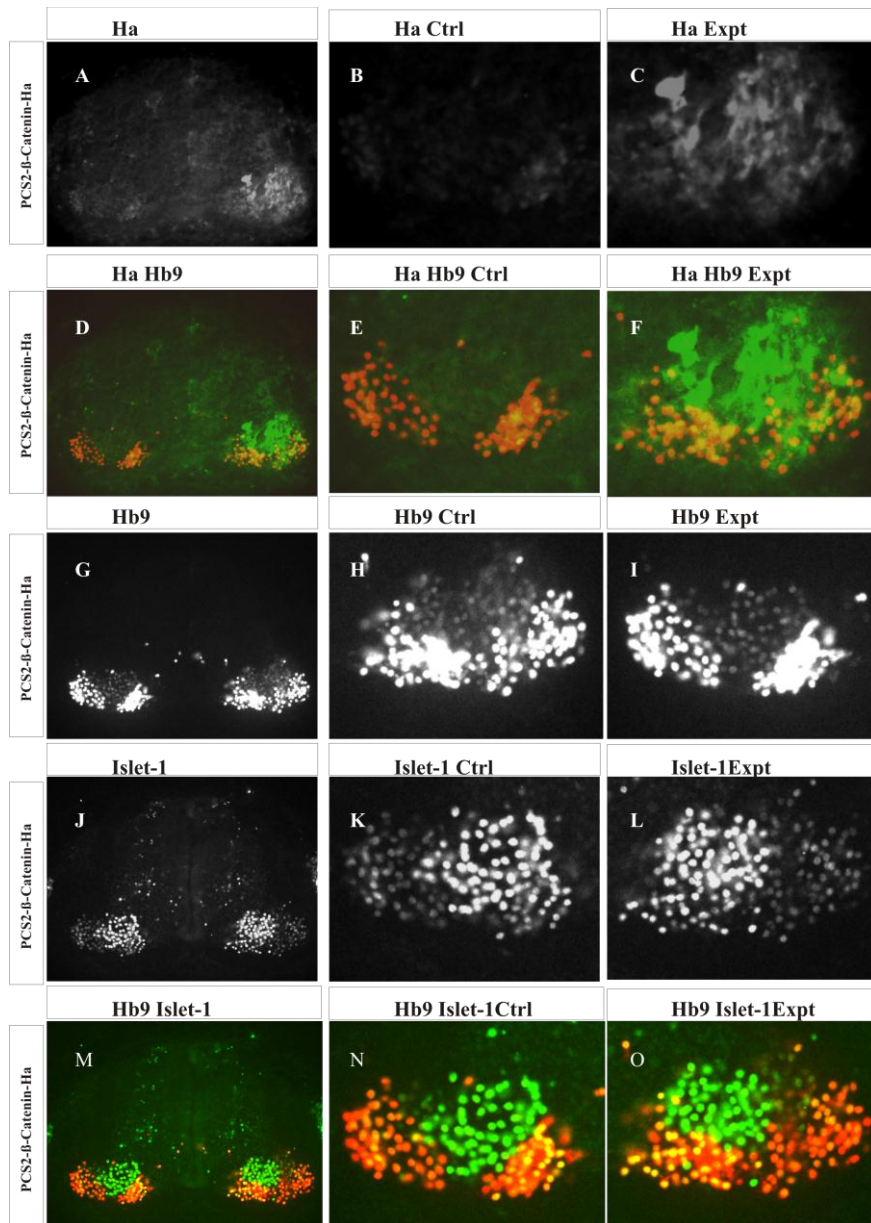
Figure 9.5 pCS2-β-cat-HA construct lack effects on the segregation of LMC neurons.

A-C, HA immunoreactivity following HA tagged pCS2β-catenin expression in the ventral lumbar spinal cord. **D-F**, HA, and Hb9 shows normal divisional segregation of HA positive Hb9 MNs on the electroporated side compared to control. **G-I**, Hb9 immunoreactivity shows normal divisional segregation on the experimental and control sides. **J-L**, Islet-1 immunoreactivity shows normal segregation of the Islet-1 positive LMC neurons. **M-O** merged Hb9 Islet- immunoreactivity showing normal divisional segregation of LMC neurons on the electroporated side as well as the control side.

9.2.2 **Expression of truncated version of β-catenin does not disrupt LMC Neurons segregation.**

Following the up regulation of the Wnt pathway by over expression of wild-type HA-tagged β-catenin construct and the similarity of results of this type of up regulation with the results of down regulation of the Wnt pathway, I asked if misexpression of a truncated form of β-catenin could result in altered migration or divisional segregation of LMC neurons.

Thus, I electroporated a truncated form of β-catenin-1-ins construct in to the developing ventral spinal cord at early stages and late stages of development and analysed the results as in the previous experiments. Again the HA-tag immuno fluorescence was used to track the cells that acquired the truncated β-catenin-1-ins construct. As with previous results, majority of the ventral LMC neurons both LMCm and LMCl acquired the construct evidenced by the medio-lateral extent of the HA-tag immuno reactivity in the ventral lumbar spinal cord which is a constant phenotype observed at different stages of development (Fig. 9.5B, E-F, and I-J).

Next, I analysed the nature of the organization of the LMC following immunohistochemistry for Islet-1(2) and Lim-1/Lhx-1. Here I observed no alteration of the integrity of the LMC columns despite acquiring the construct. This observation is constant irrespective of the stage of electroporation. Thus, there is no observable difference between the control and experimental side (Fig.9.6C-D, G-H, and K-L). I therefore asked if the electroporation of this truncated form of construct could have any effects on the number of the ventral spinal motor neuron and I analysed the total number of both Islet-1(2) positive neurons with no significant difference between the control and experimental side. Similar results were observed when Lim-1 positive cells of the ventral lumbar spinal cord of the experimental side compared to the control sides were

analysed throughout the various stages of development. Therefore, the expression of a truncated version of β-catenins-1-ins construct appears not to disrupt the LMC organization or alter the migration programme of the LMC neurons.
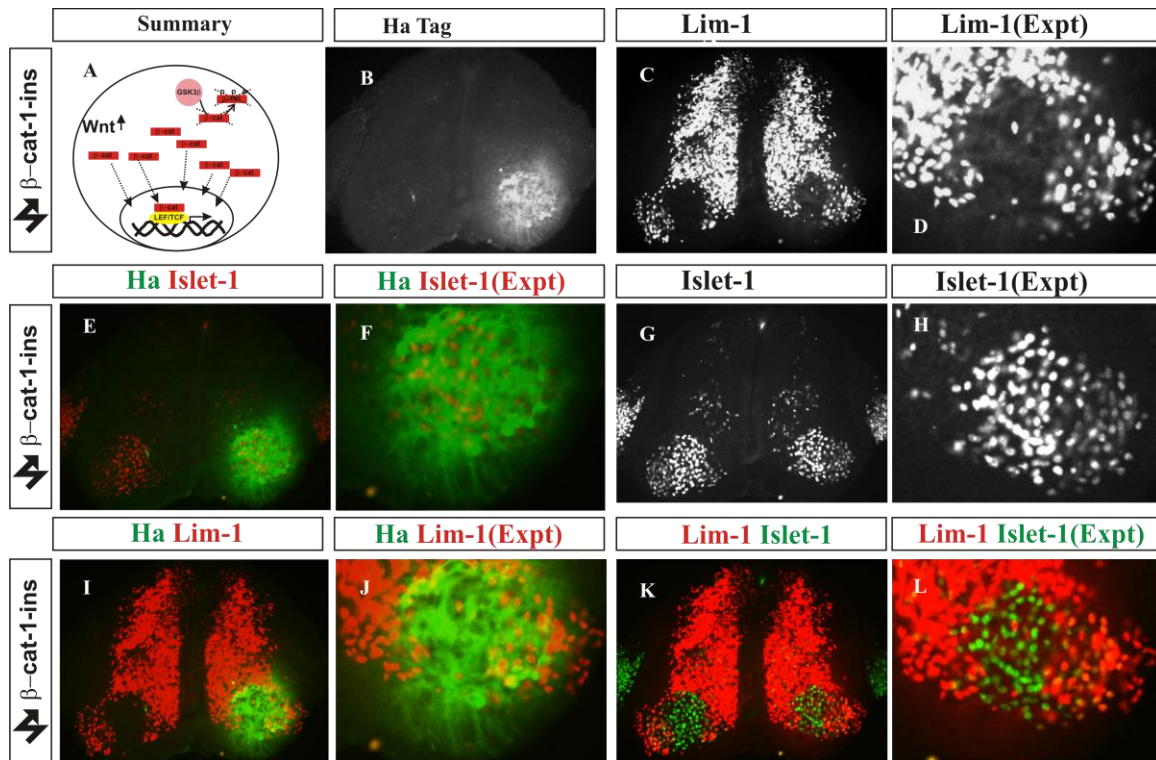
Figure 9.6 Upregulation of canonical Wnt signalling by epression of truncated version of β-catenin-1-ins construct does not disrupt LMC organization.

A, Summary of effects to increase Wnt signalling. *B*, HA-tag immuno fluorescence after expression of the construct. *C*, Lim-1immunoreactivity after expression of the construct marked by HA-tag immunoreactivity in B. *D*, Lim-1 immunoreactivity of the experimental side in C. *E*, Merged HA-tag and Islet-1(2) immunoreactivity following expression of the construct. *F*, experimental side in E. *G*, Islet-1(2) immunoreactivity. *H*, Experimental side in H, shows immunoreactivity of Islet-1(2) more in LMCm than in LMCl. *I-J*, Merged HA and Lim-1 immunoreactivity shows LMC domain acquired the construct and normal experimental side (J). And *K-L* shows normal merged Lim-1 and Islet-1(2) immunoreactivity following expression of β-catenin-1-ins construct shown normal LMC organization.

9.2.3 Expression of a Dominant Negative Glycogen Synthase Kinase 3β Lacks effects on LMC Neurons Organization.

GSK3β is known to phosphorylate and thus importantly inactivate β-catenin and glycogen synthase; it is involved in control of cellular responses. In the Wnt signalling pathway, it works to phosphorylate β-catenin, leading to ubiquitination and degradation by cellular proteases. In addition to its important role in the Wnt signalling pathway, which is required for establishing tissue patterning during development, glycogen synthase kinase is also critical for the protein synthesis that is induced in settings such as skeletal muscle hypertrophy. It's also a key regulator of both differentiation and cellular proliferation. Thus, I further expressed a dominant-negative form of glycogen synthase kinase 3β known to up regulate the canonical Wnt signalling pathway to see if it has any effect on the LMC neurons segregation during development.

I electroporated HA-tagged GSK3β dominant-negative at various stages of development and analysed the outcome of its inhibition and its effects on spinal motor neurons segregation. Embryos were electroporated at early stage of developing spinal cord HH16-18 and analysed at stages HH28-30. As with all regulators of the canonical Wnt pathway, this construct was HA-tagged and HA immunoreactivity was used to track the cells of the LMC domain that acquired the construct (Fig.9.7A-C). Following expression of the construct, immunohistochemistry for HA tag, Lhx-1 and Islet-1 was conducted on serial section of the ventral lumbar spinal cord. HA-tagged immunofluorescence was observed along the entire medio-lateral extent of the ventral spinal cord with both LMCl and LMCm immunoreactive for the construct. Analysis of the sections revealed no observable difference between the control and experimental side of in terms of the organization of the LMCl and LMCm.

Similarly, as with other previous up regulators used before there was no significant difference between the total number of motor neurons on the control side and the experimental side (Student t-test measurement P value= 0.5329, n=3) Fig.9.8. There was no desegregation of motor columns in the ventral spinal cord and no perturbation of motor neuron migration was observed compared to perturbations of cadherins and catenins previously. Thus the up regulation of the canonical Wnt signalling by expression of a dominant negative GSK3β does not disrupt the organization of the LMC neither it caused altered migration of neurons. Thus essentially the canonical Wnt pathway appears not to influence the LMC migration as observed in the NΔ390 experiment.
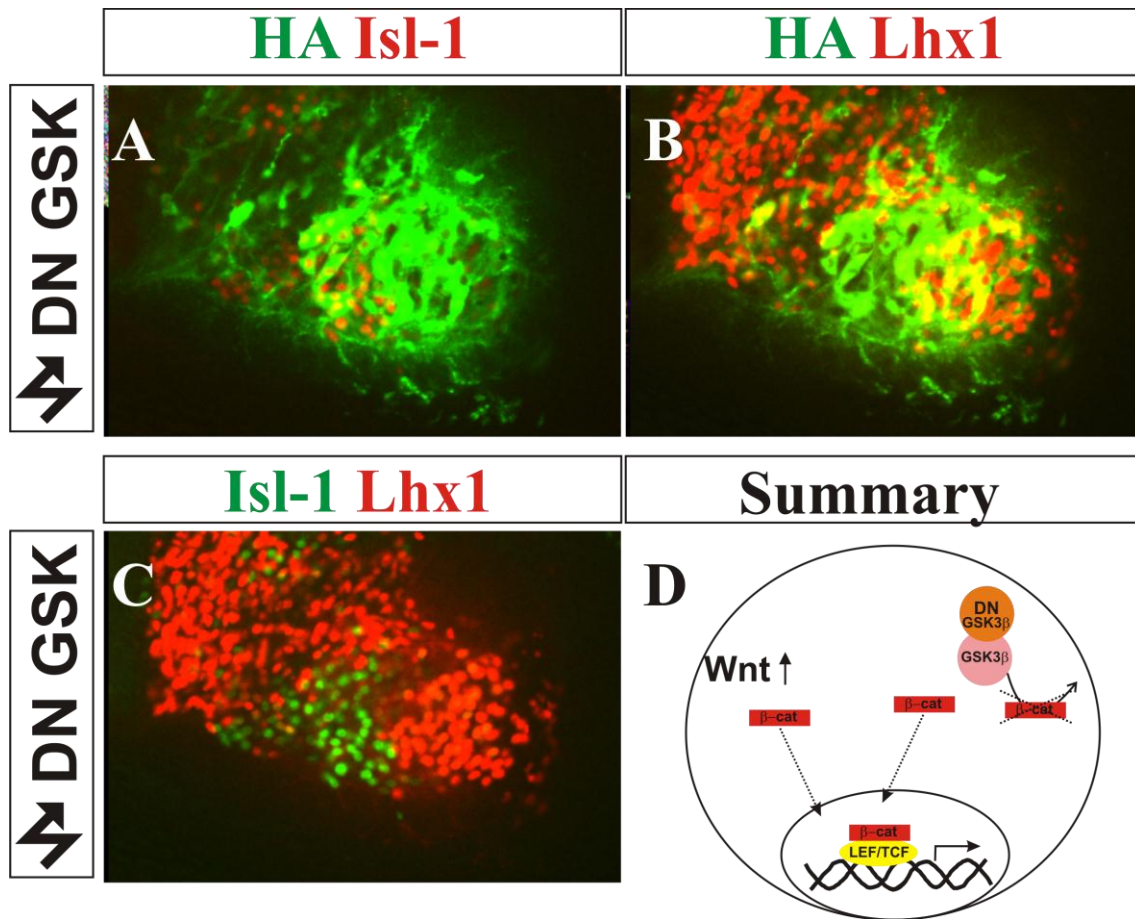
Figure 9.7 Expression of dominant negative GSK3β does not affect LMC organization. *A*, Immunoreactivity for Islet-1 and HA-tag following expression of dominant negative GSK3β construct visualized by HA-tag fluorescence in the ventral lumbar spinal cord shows normal LMC organization. HA-tag fluorescence extends along the entire medio-lateral extent of the ventral spinal cord. *B*, Merged immunoreactivity for HA-tag and Lhx-1 following expression of the construct shows normal LMC domain organization with the entire LMCl positive for the construct. *C*, Immunoreactivity for Islet-1 and Lhx-1 following expression of the construct shows normal Islet-1 and Lhx domain organization. *D*, Schematic of action of the construct.
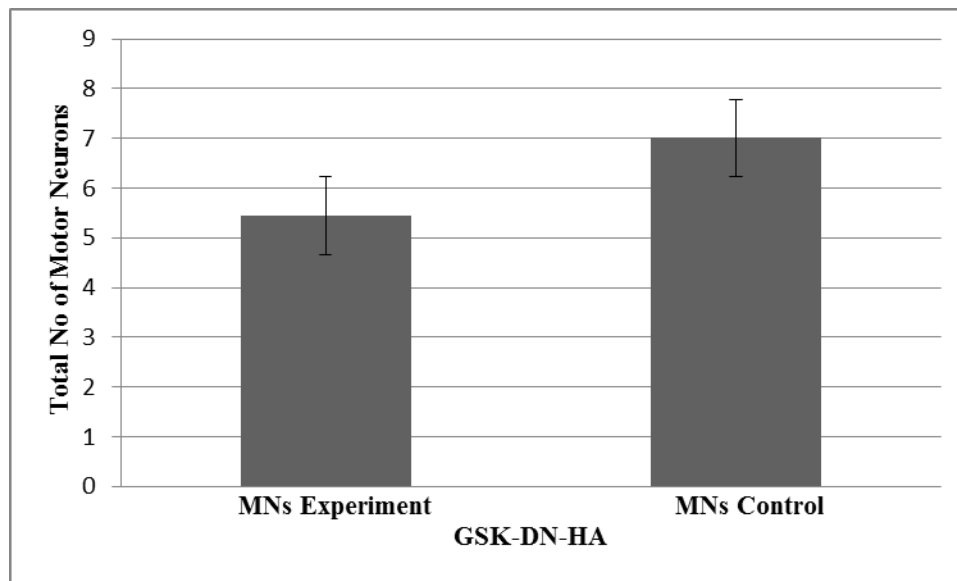
Figure 9.8 Quantitation of total number of Motor neurons following electroporation with dominant negative GSK3β.

Ha tagged dominant negative GSK3β experiment to HH stage 28.   Student t-test measurement P value= 0.5329 statistically no significant difference between the experiments (1) and control (2). Error bars are standard error of means SEM.

10 Discussion

Neuronal organization in the vertebrate central nervous system occurs along two main schemes, namely the laminae (stratified) and nuclei organization. While the laminae organization is the predominant mode of organization of neurons in the cortex, in the spinal cord it is the nuclei organization that is the predominant mode of neuronal organization (Ramoney Cajal). The molecular factors and mechanism governing the neural laminations in the cortex are beginning to be elucidated (Rakic, 2006). In contrast to lamination, it is not clear whether neuronal nuclei formation termed nucleogenesis is also governed by similar process (Agarwala et al., 2002).

Spinal motor neurons generated from a distinct progenitor domain in the medial-ventral spinal cord are organized as neuronal nuclei and are known to undergo highly stereotypical patterns of generation and migration to the ventral horn (Jessell et al., 2011. Jessell et al., 2000). Motor neurons that project to ventral limb muscles are generated first followed by those that project axons to dorsal limb muscles. However, the majority, approximately above 95%, of motor neurons are generated within a period of 24 hours. Although the generation of spinal motor neurons occur within a short period, the migration of motor neurons occurs over a relatively longer time course, an additional 48 hours (Hollyday, 1997; Whitelaw and Hollyday, 1983; Lin et al., 1998; William et al., 2003). Therefore, a backlog of motor neurons waiting to migrate is formed as a result of their rapid generation. Subsequent to their generation, column, division and pool identities arise through their expression of transcription factors. Hox proteins control column identity and initial motor neuron axon pathfinding, they also influence later motor pool specificity through instructing the expression of intermediate

transcription factors in pool restricted patterns (Dasen et al., 2008, Rousso et al., 2008, Dasen et al., 2005). Motor pool identity is defined early on in motor neuron development and different motor pools have distinct time of generation. Other aspects of motor neuron pool identity require additional extrinsic signals from the limb (Haase et al., 2002).

This work investigated the role of cadherins and catenins in the migration and segregation of the chick spinal motor neurons in the ventral lumbar spinal cord during development. Firstly, through perturbation of pan motor neuron cadherin function using both dominant negative cadherin and dominant negative catenin approaches. Secondly, through manipulation of single cadherin, cadherin-7 that is express during the developing motor neurons migration and results in less pronounced phenotype following perturbation of columnar segregation and migration compared to the phenotypes of the perturbations of pan cadherin and catenin function using the dominant negative approaches. Similarly, the work also demonstrated the possibility of spinal motor neurons migration occurring via radial glia. It also provided evidence that the machinery of the LMC segregation and migration is a function of cadherin and catenins and not the Wnt signalling pathway. The results of this work suggest an important and prolonged role for cadherin expression in the generation, migration and segregation of spinal motor neurons in the ventral horn of the developing spinal cord. Here, I discuss these findings in the context of a model for spinal motor neuron migration through the anchoring of the migration machinery in motor neurons via gamma-catenin and type II cadherins to transitin radial glia.

10.1 Regulated cadherin function and LMC neuronal nuclei formation

In the developing spinal cord, the LMC is organized as cluster of functionally related neurons called neuronal nucleus a feature that is generally characteristic of evolutionary older regions of the CNS. It is possible for the mechanism of LMC formation to point to similarities as well as differences with neuronal organization mechanism in newer regions of the CNS, such as the lamination of the cortex (Rakic, 2006; Lui et al., 2011). In the cortex, radial glia acts a scaffold for cortical neuronal migration and constitutes the majority of progenitor cell type of the ventricular zone with other subtypes generated from radial glia located in the sub-ventricular zone (Noctor et al., 2004). In the developing ventral spinal cord, spinal transitin labelled radial glia represents a smaller proportion of ventral progenitor cells compared to the compared to the cortex. Despite the disproportionality between the cortical radial glia and the spinal transitin radial glia, in the spinal cord the transitin radial glia delineate pathways for the migration of spinal motor neuron. In addition to this, spinal transitin radial glia are basal to the ventricular progenitor cells.

The fundamental difference in the of generation of motor neurons in the spinal cord compared to that of generation of motor neurons is the rate of LMC neurogenesis which is higher in spinal cord. This results in the backlog of neurons waiting to migrate to their final settling positions in the ventral horn. In contrast, neurons in the cortex that will eventually populate the superficial layers of the cortex are generated are born sequentially and migrate in a highly ordered process to generated the stratified or laminated cortex (Noctor et al., 2004). Therefore, it is possible that spinal radial glia represents a critical rate limiting step for motor neuron migration.

These results demonstrated that early pan-motor neuron cadherin function is required for LMC divisional segregation through neuronal migration. Subsequently, differential type II cadherin function is required for motor pool formation (price et al., 2002; Patel et al., 2006). Therefore, the results of this work suggest a prolonged role for cadherin in all phases of motor neuron organization.

10.2 Cadherin function in LMC neurons segregation and migration is a highly ordered process.

Spinal motor neurons are generated from a spatially distinct progenitor domain in the medial-ventral spinal cord (Jessell, 2000). After their generation, subsequent column, division and pool identities arise through their expression of distinct transcription factors. Recent studies suggest that Hox proteins control early columnar identity and influence the initial trajectory of motor axon pathfinding (Dassen et al, 2008; Rousso et al., 2008).

Hox genes also influence later motor pool specificity by instructing the expression of intermediate transcription factors in pool restricted patterns. The identity of spinal motor neuron pool appears to be defined early on in motor neuron development and different motor pools have slightly different time of generation from However, some aspects of motor neuron pool identity require additional, extrinsic signals from the limb. For example, the expression of a receptor for Glial-derived neurotrophic factor, GFRα-1, in a subset of motor pools allows those motor neurons to respond to mesenchymal expression of GDNF. The result of this neurotrophic signalling directs the expression of a transcription factor of the ETS family, namely PEA3, in a motor pool specific manner.

PEA3 expression controls late motor axon branching within the limb and, crucially, refinement of motor neuron cell body position. It is possible for similar mechanisms to be involved in the pool specific expression of other ETS domain proteins such as Er81 but is currently undefined. Therefore, motor neuron columns, divisions and pools are transcriptionally defined early in motor neuron development, suggesting that the positioning of motor neuron pools during development must have been facilitated by a highly complex process.

The majority of LMC motor neurons are generated in a relatively short period of time, approximately about 24 hours in the chicken and mouse. LMC neurons in chicken are generated within a 24 hour window period before stage 23, and so this rapid generation process creates a backlog of motor neurons waiting to migrate to their final settling position in the ventral lumbar spinal cord with peak generation of LMCl occurring between stages 20 to 21(Hollyday and Hamburger, 1977; whitelaw and Hollyday, 1983).

Early in development, LMCm dominated the ventral horn with LMCl medial to them. This topographic representation herald the beginning of the migration of LMCl through the LMCm to reach their final settling position. As the two LMC divisions are generated at different times during development, the medial division prior to the lateral division, this requires that the lateral division neurons migrate through the earlier born medial division neurons to achieve their final position within the ventral horn in a process reminiscent of the "inside-out" segregation of neurons in the cortex.

The LMC neurons segregation process is complete by stage 27 with majority of LMCl taking their definitive lateral position in the ventral horn of the developing spinal cord. Thus, motor neuron migration is essential to the segregation of divisions within the

LMC. Superimposed on the divisional segregation, is intra-divisional coalescence of motor pools on the motor neurons to generate the mature pattern of motor pool topographic positioning. What then control this motor neuron organisation at a cellular level? Work over the past decade has suggested an important role for the differential expression of members of the type II cadherin family of cell adhesion molecules (Price et al., 2002; Patel et al., 2006).

Cadherins have been implicated in the segregation of motor neurons in the spinal cord (Price et al 2002). In other regions of the CNS, cadherins regulate compartmentalization of neural populations evident by their pattern of expression (Suzuki et al, 1997) and misexpression of cadherin disrupts partitioning of the cortex and striatum (Inuoe et al, 2001).

During development spinal motor neurons expressed different classes of cadherin at various stages of development. While Type I cadherin including N-cadherin are excluded from motor neuron but instead are expressed in the radial fibres traversing the ventral spinal cord. Other types of cadherins including cadherin 7, cadherin 12 and cadherin 20 were expressed in the early stages of development, with refinement of their expression towards the end of the migration process (Price et al., 2002; Luo et al., 2006). These early pan-motor neuron expressions of cadherin in the ventral spinal cord suggest a role for these molecules in the segregation and migration process. I therefore addressed their specific role with respect to migration and divisional segregation of LMC neurons.

10.3 **Migration of spinal motor neuron require γ-catenin function**

The cytoplasmic binding of cadherins to β- or γ-catenin is an obligate requirement for robust cell adhesion activity. This catenin binding to cadherins promotes the formation of localised high densities of cadherin via anchoring to the actin cytoskeleton through an additional catenin, α-catenin, which provides a bridge for cadherin function to the actin cytoskeleton (Abe and Takeichi, 2008). It is believe that β-catenin is the major transducer of cadherin intracellularly. Surprisingly, β-catenin is absent from spinal motor neurons. Instead, α-catenin and β-catenin are the predominant catenins expressed in the LMC. Therefore within the chick LMC, γ-catenin is the major transducer of cadherin function. Expression of either γ-catenin or γ (L127A) leaves the total number of LMCm and LMCl unaffected. The timing of generation of spinal LMC was also unaffected. Additionally, motor neurons were labelling by retrograde labelling from the limbs following γ (L127A) expression, suggesting that the time required(>48 hours) for motor axon growth to the limb, (Tosney and Landmesser, 1985) had occurred despite motor neuron migration being retarded (Bello et al., 2012). Therefore, generation of LMC neurons is not perturbed by the expression of γ (L127A). Expression of γ (L127A) resulted in the perturbation of LMC motor neuron position cell autonomously; with about 60% of γ (L127A) positive LMCl motor neurons located close to the ventricular zone with additional 25% located within the LMCm domain an abnormal position for the LMCl neurons. Further analysis revealed the distances migrated were less than half compared with control neurons, suggesting that γ (L127A) severely compromised the migration of LMC neurons. Interestingly, LMC neuron on the experimental side that are not γ (L127A) positive appear to migrate normally similar to the control side of the spinal cord. There is the possibility of additional role of perturbed β-catenin expression in spinal transitin radial glia that may contribute to the perturbation of migration, but the

cell autonomous nature of the effect of γ (L127A) suggests that the predominant role for γ (L127A) is within spinal LMC neurons.

In a similar study on the nature of cadherin function using the armadillo family proteins, Demireva et al (2011) found both β- and γ-catenin to be expressed in all spinal motor neurons in mice. Conditional genetic ablation of both catenins in motor neurons resulted in a perturbation of motor column organisation, a mixing of LMC motor neuron divisions, and all motor neuron pools of the LMC that were assayed were desegregated with a concomitant expansion of the experimental area of the LMC compared to the control. The general rostrocaudal position of motor pools was essentially preserved; however, looking at the fact that spinal motor neuron position generally arises from a medio-lateral movement of the cells rather than a rostro-caudal movement. Thus, motor neurons of LMC divisions and pools at a given rostrocaudal level of the spinal cord fail to segregate following removal of the two catenins.

 Taken together, my results suggest a dual role for catenin in controlling spinal motor neuron migration and segregation, but raise some important issues. First, is this role for catenin restricted to the point mutations manipulation of γ-catenin (L127A) alone? Could perturbation of β-catenin expression in transitin radial glia have additional role in leading to a similar migration phenotype? Recently it has been reported that β-catenin is involved in the morphogenesis of the cerebellum (Schüller and Rowitch, 2007). Exploring other ways of manipulating catenin functions and observing its effects on neuronal nuclear formation in other regions of the CNS can shade more light in our understanding of the varied functions of catenins. Therefore, migration of spinal LMC neuron requires catenin function.

10.4 Cadherin function in motor neuron migration.

Experiments to manipulate cadherin expressions via the dominant negative approach and single cadherin manipulations not only showed cadherins are involved in segregation of motor neurons but also the migration of spinal motor neurons. Expression of a dominant negative cadherin which lacks the extracellular domain and thus caused the sequestration of the intracellular cadherin binding partners results in the divisional LMC desegregation and migration deficits (Fujimori and Takeichi, 1993), a phenotype similar to that of γ (L127A).

Expression profile of cadherins showed that type I cadherins were not expressed in LMC motor neurons. Amongst the classical type II cadherins, cadherin-7 was expressed in most of the LMC neurons during divisional segregation, but this expression is down regulated in the majority of LMC neurons thereafter. Downregulation of cadherin-7 by shRNA resulted in a similar migration and segregation phenotype to that observed in the dominant negative approach (NΔ390 expression). These include: localization of motor neurons in close proximity to the ventricular zone, and mixing of LMCl and LMCm divisions on the experimental side compared to the control as well as the migration deficit and increase in the area occupied by the LMCl and LMCm compared to the control side of the spinal cord. Because cadherin-7 expression is excluded in the ventral transitin radial glia, it is possible that the predominant role for cadherins in motor neuron migration is within the motor neurons themselves. Perturbations of LMC organization following ablation of β-catenin and γ-catenin from mouse motor neurons was reported (Damireva et al., 2011). These results are consistent with those presented in this work and Bello et al., 2012. The only significant difference with the results of the mouse conditional ablation is a milder form of migration phenotype than that obtained in our experiment using the chicken. The differences in gene expression, the rate of

generation of spinal motor neurons and migration between the chicken and mouse may be the underline caused of differences in severity of catenin and cadherin manipulations in these species.

It is complex to imagine how cadherin and catenin function facilitate spinal motor neuron migration and segregation. Recently, a model has been proposed where α-catenin acts a molecular clutch that links substrate adhesion to retrograde actin flow during cell migration (Bard et al., 2008). The results from catenin and cadherin manipulations are consistent with a model where both γ (L127A) and NΔ390 constructs perturb intracellular γ-catenin function within motor neurons, disrupting cell migration, possibly mediated in part through cadherin-7 based linkage to the migration machinery. It is not clear whether the proposed retrograde actin flow is the dominant factor in motor neuron migration as observed in other cell type, therefore this require further investigations and possible characterization of the molecular dynamics of cadherin and catenin linkages (Drees et al., 2005; Yamada et al., 2005) to the actin cytoskeleton during spinal motor neuron migration.

10.5 Transitin labelled radial glia acts as a scaffold for migrating LMC neurons.

Within the ventral spinal cord, there exists coexpression of transitin and β-catenin which identifies a subset of progenitor cells with characteristic of radial glia. Expression of β-catenin within the radial glia delineates two domains of ventral progenitor cells: apical cells that do not express β-catenin and more basal cells that express β-catenin.

Radial glia have previously been identified within the spinal cord (Liuzzi et al., 1985) and radial migration of spinal motor neurons has previously been inferred (Baron, 1946; Wentworth, 1984; Leber et al., 1990; Leber and Sanes, 1995; Edie and Glover, 1996). This work suggests that spinal motor neuron migration occur on transitin radial glia for

two reasons. First, retrograde labelling of migrating lumbar spinal motor neurons showed that their migration paths follow transitin radial glia. Secondly, there are relatively few transitin radial glia (approximately 14) in the ventral horn of lumbar spinal cord compared to the dorsal horn at various stages of development. Majority of these are juxtaposed to migrating neurons and it is very unlikely that this result from chance alone. More interestingly, stalled spinal motor neurons were still found along pathways defined by transitin radial glia following γ (L127A) and NΔ390 cadherin expression. It is not possible that spinal motor neuron decide the most direct route in their migration to their final settling position in the ventral horn, and these observation strongly suggest that spinal motor neurons follow migratory routes labelled by transitin radial glia.

The concept of radial migration available is largely assumed on the basis of little direct experimental evidence. However, there is no adequate direct evidence that spinal motor neurons use radial glia as a scaffold for their migration. This work suggests that in the ventral spinal cord, transitin radial glia act as a scaffold for spinal motor neuron migration. The concentration of these fibres seems to be more in the dorsal half of the spinal cord than the ventral lumbar spinal cord, a feature found to be constant in all stages of development. Whether this variation in concentration has any direct relation to the process of migration in the ventral spinal cord remains a subject for further study.

10.6 Disruption of LMC migration causes buckling of ventral pax6 progenitor domain

Both γ-catenin and β-catenin are not expressed by the majority of ventral Pax 6 cells. However, transitin radial glia representing approximately 30% of these progenitor cells express β-catenin at detectable levels. Following manipulations with γ (L127A) and

NΔ390 cadherin, the generation of motor neuron from this domain and its general integrity appears unaffected. Buckling of the ventral Pax6 domain was never observed in un electroporated motor neurons, but seen often few embryos where Pax6 cells were not electroporated. Additionally, motor neurons that had not acquired the γ (L127A) or NΔ390 constructs reached their normal final settling position. Therefore, it is probable that the motor neurons stalled in their migration contribute to the buckling of the ventral Pax6 domain. Continued mitotic activity of the ventral Pax6 domain cells was suggested to give rise to the force required for the buckling of the progenitor domain (Bello et al., 2012). BrdU labelling following γ (L127A) expression revealed that cell division is not disrupted. Interestingly, the number of Lhx-1 cells arrested close to the ventricular zone was greater than the LMCl neurons. Therefore, the ventral Pax6 domain continues to generate post mitotic Lhx-1 interneurons and this cell division is thought to exert force backward from the stalled LMC and result in the ventral progenitor domain buckling (Bello et al., 2012).

10.7 Control experiment results in no effects on the LMC segregation and migration.

Throughout the course of this work, the constructs used in the perturbation experiments for cadherins and catenin as well as the Wnt signalling pathway were tagged with fluorescence protein with green fluorescence protein (gfp) being the most widely used. Other proteins used to follow construct acquisition by developing LMC neurons include the enzyme β-galactosidae for cadherin dominant negative perturbation and γ-catenin perturbations respectively. Haemaglutinin (HA) for direct perturbation of the up regulators and down regulators of the canonical Wnt signalling pathway and Ds Red for the type II cadherin perturbation experiment of cadherin 7 via the shRNA approach and control cadherin 7shRNA. Could these proteins have influence in addition to that of the construct being investigated? To address this question I conducted control experiments using these proteins alone first and then in combination with the construct so that involvement of the tagged proteins is rule out.

In the cadherin perturbations experiments gfp fluorescence was used to follow the LMC neurons that acquire the construct and this fluorescence covers the experimental side of the spinal cord including the dorsal spinal cord it also extends from the medical to the most lateral extent of the ventral horn of the developing spinal cord. The expression of the tagged proteins follows the same pattern as with the construct under investigations with the expression at different stages of development. Following immunohistochemistry for islet-1(2) Lim-1/Lhx-1 and Hb9 the organization of the LMC was observed to be essentially the same on both the experimental side and the control. Thus gfp has no influence on the organization of the LMC.

Similar experiment with β-galactosidae revealed no observable defects in migration and segregation of the LMC neurons. The results of other tags used are essentially same as the gfp and β-gal. Experimental and control side were analysed for total number of islet-1(2) cells and HB9 positive cells with no observable or significant difference in the number of spinal motor neuron between the control and experimental side.

10.8   Wnt signaling and its regulators are not critical for spinal LMC neurons segregation and Migration.

The Wnt pathway is involved in many developmental processes and in the nervous system Wnt is thought to be involved in virtually most of the developmental processes from the patterning of the CNS to compartmentalization, neurogenesis, synapse formation(Feigenson et al., 2011; Hu et al., 2011), dorso ventral specification in the mouse telencephalon (Backman et al., 2005) and recently it is thought to be involved in the regulation of proliferation and differentiation of neuro epithelial cells in the dorsal spinal cord (Ille et al 2007). Additionally, Wnt is involved in the pathogenesis of many developmental disorders of the nervous system, and it has been implicated in many cases of neoplasms (Yuan et al., 2012).

Among the key component of the cadherin catenin complex is β- catenin known to act in Wnt signalling pathway activating the transcription of crucial target genes responsible for cellular proliferation and differentiation. It controls E-cadherin mediated cell adhesion at plasma membrane and mediates the interplay of adherens junction molecules with the actin cytoskeleton (Brembeck et al 2006). In the development of spinal motor neurons, Wnt is thought to have influence due to the involvement of the β-catenin in the control of spinal motor neuron migration and the strategic place of β-catenin in the canonical pathway.

Also, the perturbation experiments for both cadherin and catenins so far described here have the potential to alter the Wnt signalling particularly the canonical Wnt signalling pathway (Nelson and Nusse, 2004). Thus, I asked whether direct perturbation of canonical Wnt signalling can affect the divisional segregation and migration of LMC neurons in a similar way to that observed when cadherin and catenin functions were perturbed. So, I sought to explore the canonical Wnt signalling pathway to find out the specific contribution if any of the Wnt pathway in the spinal motor neuron migration. Thus, I expressed via in-ovo electroporation constructs that are known to up regulate or down regulate the canonical Wnt signalling pathway (Roose et al., 1999; Krylova et al., 2000; Zhurinsky et al., 2000).

Expression of haemaglutinin tagged wild-type β-catenin and a truncated version of β-catenin-1-ins construct as well as a dominant negative version of glycogen synthase kinase (GSK3β) result in no observable effects on spinal LMC neurons segregation and migration between the electroporated and un electroporated side of the spinal cord. Thus up regulation of the Wnt pathway does not influence the segregation and migration of LMC neurons. Can down regulation cause any effect on the LMC neurons programme of segregation or migration? To address this question I next expressed the constructs that are known to down regulate the canonical Wnt signalling pathway. Thus, I expressed haemaglutinin tagged wild-type glycogen synthase kinase (wt gsk3β), a constitutively active glycogen synthase kinase (ca-gsk3β) and a dominant negative TCF (Giani et al., 2004). Interestingly, the phenotype from these misexpressed Wnt proteins result in no observable defects in the divisional segregation of the LMC as well as normal migration. Therefore, the results of Wnt perturbation suggest that the observed phenotype from the perturbation of cadherin (NΔ390) and catenin (γ-catenin L127A) are not consistent with the perturbations of the canonical Wnt signalling pathway.

Could this up regulation and down regulation be exhaustive for a potential Wnt involvement in the control of the migration and segregation process of spinal motor neurons? Could enhancing the expression of β-catenin yield any positive clue of involvement of the Wnt signalling? To address this question, I further expressed a construct of β-catenin cloned in pcs2 vector in the ventral spinal cord early in development and observed its effect later in development. Consistent with other Wnt perturbation experiments there was no difference in the organization of the LMC neurons and their migration in the ventral horn of developing spinal cord. Thus the cadherin-catenin complex remains a focal point for further exploration with respect to neuronal migration and segregation as neurogenesis of spinal motor neuron in the ventral spinal cord.

10.9 **A prolonged role for cadherin functions in motor neuron organisation.**

The developmental time course of cadherin expression in the chick has two phases and normal progression from one phase to the other depends on the signals from the limb inducing ETS protein expression. During divisional segregation, most motor neurons display a similar cadherin expression profile, either all expressing or all not expressing a given cadherin. Following this phase, some cadherins are up regulated in a subset of motor neurons and others are down regulated to reveal the mature, differential cadherin expression profile required for motor pool clustering. For example, cadherin-7 is largely expressed only during the migratory phase of the LMC and is down regulated in the majority of LMC neurons subsequently. Our recent work revealed that early down regulation of cadherin-7 results in LMC divisions' segregation defects, most likely through a similar, albeit reduced migration deficiency to that of catenin manipulations. Cadherin-7 is also weakly expressed in ventral radial glia raising the possibility that cadherin-7 homophilic interactions between motor neurons and the radial glia could act to couple the migration machinery between these cell types, whilst the glia direct motor neuron migration.

Interestingly, type I cadherins, including N-cadherin, are absent from chick motor neurons. Cadherin-7 in chick LMC neurons, therefore, seems to be playing a role that may be undertaken by pan-LMC neuron N-cadherin expression in the mouse. Further investigation can potentially enable us to draw direct parallels between the mechanisms that drive motor neuron organisation in the chick with those of the mouse.

Can there be other extracellular molecules of equal or potential importance in driving the segregation and migration of spinal motor neurons? Of course, cadherins are not the only extracellular proteins with a direct role in motor neuron organisation. Other molecules including Reelin signalling has also been shown to be important.

192

However, cadherins coordinate multiple aspects of motor positioning. First, a pan-motor neuron cadherin function drives motor neuron divisional segregation and then differential cadherin expression drives motor pool clustering and next LMC neuronal migration is now established to be influenced by cadherin. This steady move from controlling one important biological role to the next depends on ETS protein induction through limb-derived signals. Thus, the coordination of cadherin expression in motor neurons is crucial to both the early pan-motor neuron and then pool specific phases of LMC organisation.

Why are motor neurons organised as pools? Primary sensory afferent input to motor neurons requires that motor neuron pools are located in the correct dorsal-ventral position in the ventral horn. Thus, the anatomical logic of motor pool organisation probably reflects on the mechanisms of specificity of synapse formation. It will be interesting to further explore whether differential cadherin expression also instructs the relative positioning of motor neuron pools within the ventral horn.

How closely related are the mechanisms of neural lamination in the cortex to nucleogenesis? Both Reelin signalling related to radial glia-directed migration and a role for cadherin expression in neuronal migration appear to be shared by the mechanisms of cortical lamination and nucleogenesis of spinal motor neurons, suggesting that both processes might utilise similar molecular machinery.

However, the topographic organisation of spinal motor neurons into motor pools involves a second dimension of neuronal movement superimposed on the initial radial migration and divisional segregation; here motor neurons within both LMCl and LMCm segregate to form discreet pools of functionally related neurons.

This secondary phase depends on regulation of cadherin expression via extrinsic signalling. In general, cortical neuronal lamination is understood in terms of a one-dimensional, radial movement of neurons, although intra-lamina movement of neurons does appear to occur. Further work is needed to test whether extrinsically-regulated, cadherin-based; mechanisms drive reorganisation of cortical neurons within a lamina, similar to that seen in nucleogenesis of spinal motor neurons. If it turns out that many of the processes that drive lamination are shared with those of nucleogenesis, raising the question of what constraints are put in place to maintain the differences in structure of laminae in the cortex and that of nuclei in other regions of the CNS.

This work investigated pan-motor neuron cadherin expression in spinal LMC organization through manipulations of catenin-cadherin binding and reduction of cadherin that's predominantly expressed during divisional segregation. Manipulation of catenin function through expression of a single amino acid mutant of γ-catenin, results in a cell autonomous disruption of spinal motor neuron migration as well as disruption of divisional segregation.

Manipulation of cadherin-catenin binding through uncoupling of cadherin from γ-catenin via dominant negative cadherin approach also stalls motor neuron migration and divisional segregation. The stalled migration of spinal motor neuron following catenin and catenin manipulations results in buckling of the ventral Pax6 progenitor domain, and knockdown of single cadherin, cadherin-7 perturbs divisional segregation. These results are consistent with a model whereby early pan-motor neuron cadherin function drives divisional segregation and migration of spinal LMC neuron in the ventral horn and suggest a prolonged role for cadherin function throughout the process of spinal motor neurons nucleogenesis.

Reference List:

1. Aberle, H., Schwartz, H. and Kemler, R., 1996. Cadherin-catenin complex: Protein interactions and their implications for cadherin function. *Journal of cellular biochemistry,* **61**(4), pp. 514-523.

2. Anton, E.S., Kreidberg, J.A. and Rakic, P., 1999. Distinct Functions of α3 and αV Integrin Receptors in Neuronal Migration and Laminar Organization of the Cerebral Cortex. *Neuron,* **22**(2), pp. 277-289.

3. Anton, E.S., Marchionni, M.A., Lee, K.F. and Rakic, P., 1997. Role of GGF/Neuregulin signaling in interactions between migrating neurons and radial glia in the developing cerebral cortex. *Development,* **124**(18), pp. 3501-3510.

4. Anton, E., Cameron, R. and Rakic, P., 1996. Role of neuron-glial junctional domain proteins in the maintenance and termination of neuronal migration across the embryonic cerebral wall. *The Journal of Neuroscience,* **16**(7), pp. 2283-2293.

5. Arber, S., Ladle, D.R., Lin, J.H., Frank, E. and Jessell, T.M., 2000. ETS Gene Er81 Controls the Formation of Functional Connections between Group IA Sensory Afferents and Motor Neurons. *Cell,* **101**(5), pp. 485-498.

6. Arber, S., Ladle, D.R., Lin, J.H., Frank, E. and Jessell, T.M., 2000. ETS Gene Er81 Controls the Formation of Functional Connections between Group Ia Sensory Afferents and Motor Neurons. *Cell,* **101**(5), pp. 485-498.

7. Arndt, K., Nakagawa, S., Takeichi, M. and Redies, C., 1998. Cadherin-Defined Segments and Parasagittal Cell Ribbons in the Developing Chicken Cerebellum. *Molecular and Cellular Neuroscience,* **10**(5–6), pp. 211-228.

8. Aumais, J.P., Tunstead, J.R., McNeil, R.S., Schaar, B.T., McConnell, S.K., Lin, S., Clark, G.D. and Yu-Lee, L., 2001. NudC Associates with Lis1 and the

Dynein Motor at the Leading Pole of Neurons. The Journal of Neuroscience, 21(24), pp. RC187-RC187.

9. Backman, M., Machon, O., Mygland, L., Van Den Bout, C.J., Zhong, W., Taketo, M.M. and Krauss, S., 2005. Effects of canonical Wnt signaling on dorso-ventral specification of the mouse telencephalon. *Developmental biology,* **279**(1), pp. 155-168.

10. Balsamo, J., Leung, T., Ernst, H., Zanin, M.K., Hoffman, S. And Lilien, J., 1996. Regulated binding of PTP1B-like phosphatase to N-cadherin: control of cadherin-mediated adhesion by dephosphorylation of beta-catenin. *The Journal of cell biology,* **134**(3), pp. 801-813.

11. Bang, A.G. and Goulding, M.D., 1996. Regulation of vertebrate neural cell fate by transcription factors. Current opinion in neurobiology, 6(1), pp. 25-32.

12. Barnes, S.H., Price, S.R., Wentzel, C. and Guthrie, S.C., 2010. Cadherin-7 and cadherin-6B differentially regulate the growth, branching and guidance of cranial motor axons. *Development,* **137**(5), pp. 805-814.

13. Barth, A.I., Näthke, I.S. and Nelson, W.J., 1997. Cadherins, catenins and APC protein: interplay between cytoskeletal complexes and signaling pathways. *Current opinion in cell biology,* **9**(5), pp. 683-690.

14. Barth, S.W., Bathgate, R.A.D., Mess, A., Parry, L.J., Ivell, R. and Grossmann, R., 1997. Mesotocin Gene Expression in the Diencephalon of Domestic Fowl: Cloning and Sequencing of the MT cDNA and Distribution of MT Gene Expressing Neurons in the Chicken Hypothalamus. *Journal of neuroendocrinology,* **9**(10), pp. 777-787.

15. Bayarsaikhan, M., Takino, T., Gantulga, D., Sato, H., Ito, T. and Yoshioka, K., 2007. Regulation of N-cadherin-based cell–cell interaction by JSAP1 scaffold in

PC12h cells. *Biochemical and biophysical research communications,* **353**(2), pp. 357-362.

16. Bello, S.M., Millo, H., Rajebhosale, M. and Price, S.R., 2012. Catenin-Dependent Cadherin Function Drives Divisional Segregation of Spinal Motor Neurons. *The Journal of Neuroscience,* **32**(2), pp. 490-505.

17. Ben-Ze'ev, A., Shtutman, M. and Zhurinsky, J., 2000. The Integration of Cell Adhesion with Gene Expression: The Role of β-Catenin. *Experimental cell research,* **261**(1), pp. 75-82.

18. Bienz, M. and Clevers, H., 2000. Linking Colorectal Cancer to Wnt Signaling. *Cell,* **103**(2), pp. 311-320.

19. Bixby, J.L. and Zhang, R., 1990. Purified N-cadherin is a potent substrate for the rapid induction of neurite outgrowth. *The Journal of cell biology,* **110**(4), pp. 1253-1260.

20. Bradley, R.S., Espeseth, A. and Kintner, C., 1998. NF-protocadherin, a novel member of the cadherin superfamily, is required for Xenopus ectodermal differentiation. *Current Biology,* **8**(6), pp. 325-334.

21. Brady-Kalnay, S.M., Mourton, T., Nixon, J.P., Pietz, G.E., Kinch, M., Chen, H., Brackenbury, R., Rimm, D.L., Del Vecchio, R.L. and Tonks, N.K., 1998. Dynamic Interaction of PTPμ with Multiple Cadherins in Vivo. *The Journal of cell biology,* **141**(1), pp. 287-296.

22. Brakeman, J.S.F., Gu, S.H., Wang, X.B., Dolin, G. and Baraban, J.M., 1999. Neuronal localization of the adenomatous polyposis coli tumor suppressor protein. *Neuroscience,* **91**(2), pp. 661-672.

23. Brembeck, F.H., Rosário, M. and Birch Meier, W., 2006. Balancing cell adhesion and Wnt signaling, the key role of β-catenin. *Current opinion in genetics & development,* **16**(1), pp. 51-59.

24. Brenowitz, G.L., Collins Iii, W.F. and Erulkar, S.D., 1983. Dye and electrical coupling between frog motoneurons. *Brain research,* **274**(2), pp. 371-375.

25. Breviario, F., Caveda, L., Corada, M., Martin-Padura, I., Navarro, P., Golay, J., Introna, M., Gulino, D., Lampugnani, M.G. and Dejana, E., 1995. Functional Properties of Human Vascular Endothelial Cadherin (7B4/Cadherin-5), an Endothelium-Specific Cadherin. *Arteriosclerosis, Thrombosis, and Vascular Biology,* **15**(8), pp. 1229-1239.

26. Brieher, W.M., Yap, A.S. and Gumbiner, B.M., 1996. Lateral dimerization is required for the homophilic binding activity of C-cadherin. *The Journal of cell biology,* **135**(2), pp. 487-496.

27. Briscoe, J. and Novitch, B.G., 2008. Regulatory Pathways Linking Progenitor Patterning, Cell Fates and Neurogenesis in the Ventral Neural Tube. *Philosophical Transactions: Biological Sciences,* **363**(1489, Stem Cells and Brain Repair), pp. pp. 57-70.

28. Briscoe, J., Pierani, A., Jessell, T.M. and Ericson, J., 2000. A Homeodomain Protein Code Specifies Progenitor Cell Identity and Neuronal Fate in the Ventral Neural Tube. *Cell,* **101**(4), pp. 435-445.

29. Burden-Gulley, S.M. and Brady-Kalnay, S.M., 1999. PTPμ Regulates N-Cadherin–dependent Neurite Outgrowth. *The Journal of cell biology,* **144**(6), pp. 1323-1336.

30. Burden-Gulley, S.M., Ensslen, S.E. and Brady-Kalnay, S.M., 2002. Protein Tyrosine Phosphatase-μ Differentially Regulates Neurite Outgrowth of Nasal

and Temporal Neurons in the Retina. *The Journal of Neuroscience,* **22**(9), pp. 3615-3627.

31. Butz, S., Stappert, J., Weissig, H., Kemler, R., Mccrea, P.D., Turck, C.W. and Gumbiner, B., 1992. Plakoglobin and β-Catenin: Distinct But Closely Related. *Science,* **257**(5073), pp. pp. 1142-1144.

32. Cajal SRY. Histology of the nervous system of man and vertebrates. New York: Oxford University Press. 1995: 1v 14p.

33. Cameron, R. and Rakic, P., 1994. Identification of membrane proteins that comprise the plasmalemmal junction between migrating neurons and radial glial cells. *The Journal of Neuroscience,* **14**(5), pp. 3139-3155.

34. Carpenter, R.H.S., 1997. Sensorimotor processing: Charting the frontier. *Current Biology,* **7**(6), pp. R348-R351.

35. Ciani, L., Krylova, O., Smalley, M.J., Dale, T.C. and Salinas, P.C., 2004. A divergent canonical Wnt-signaling pathway regulates microtubule dynamics. *The Journal of cell biology,* **164**(2), pp. 243-253.

36. Cole, G.J. and Lee, J., 1997. Immunocytochemical localization of a novel radial glial intermediate filament protein. *Developmental Brain Research,* **101**(1–2), pp. 225-238.

37. Copp, A.J., Carvalho, R., Wallace, A., Sorokin, L., Sasaki, T., Greene, N.D.E. and Ybot-Gonzalez, P., 2011. Regional differences in the expression of laminin isoforms during mouse neural tube development. *Matrix Biology,* **30**(4), pp. 301-309.

38. Copp, A.J., Carvalho, R., Wallace, A., Sorokin, L., Sasaki, T., Greene, N.D.E. And Ybot-Gonzalez, P., 2011. Regional differences in the expression of laminin

isoforms during mouse neural tube development. *Matrix Biology,* **30**(4), pp. 301-309.

39. Daniel, J.M. and Reynolds, A.B., 1997. Tyrosine phosphorylation and cadherin/catenin function. *BioEssays,* **19**(10), pp. 883-891.

40. Dasen, J.S., De Camilli, A., Wang, B., Tucker, P.W. and Jessell, T.M., 2008. Hox Repertoires for Motor Neuron Diversity and Connectivity Gated by a Single Accessory Factor, FoxP1. *Cell,* **134**(2), pp. 304-316.

41. Dasen, J.S., Tice, B.C., Brenner-Morton, S. and Jessell, T.M., 2005. A Hox Regulatory Network Establishes Motor Neuron Pool Identity and Target-Muscle Connectivity. *Cell,* **123**(3), pp. 477-491.

42. De Castro, S.C.P., Leung, K., Savery, D., Burren, K., Rozen, R., Copp, A.J. and Greene, N.D.E., 2010. Neural tube defects induced by folate deficiency in mutant curly tail (Grhl3) embryos are associated with alteration in folate one-carbon metabolism but are unlikely to result from diminished methylation. *Birth Defects Research Part A: Clinical and Molecular Teratology,* **88**(8), pp. 612-618.

43. Deazevedo, L.C., Fallet, C., Moura-Neto, V., Daumas-Duport, C., Hedin-Pereira, C. and Lent, R., 2003. Cortical radial glial cells in human fetuses: Depth-correlated transformation into astrocytes. *Journal of neurobiology,* **55**(3), pp. 288-298.

44. Demireva, E., Shapiro, L., Jessell, T. and Zampieri, N., 2011. Motor Neuron Position and Topographic Order Imposed by β- and γ-Catenin Activities. *Cell,* **147**(3), pp. 641-652.

45. Doherty, P. and Walsh, F.S., 1996. CAM-FGF Receptor Interactions: A Model for Axonal Growth. *Molecular and Cellular Neuroscience,* **8**(2–3), pp. 99-111.

46. Dong, G., Loukinova, E., Chen, Z., Gangi, L., Chanturita, T.I., Liu, E.T. and Van Waes, C., 2001. Molecular Profiling of Transformed and Metastatic Murine Squamous Carcinoma Cells by Differential Display and cDNA Microarray Reveals Altered Expression of Multiple Genes Related to Growth, Apoptosis, Angiogenesis, and the NF-κB Signal Pathway. *Cancer research,* **61**(12), pp. 4797-4808.

47. Edlund, T. and Jessell, T.M., 1999. Progression from Extrinsic to Intrinsic Signaling in Cell Fate Specification: A View from the Nervous System. Cell, 96(2), pp. 211-224.

48. Ekonomu A, Kazanis I, Malas S, Wood H, Alifragis P, et al., 2005. Neuronal Migration and Ventral Subtype Identity in the Telencephalon Depend on SOX1. PLoS Biol 3 (6): e186. Doi:10.1371/journal.pbio.0030186

49. Ericson, J., Rashbass, P., Schedl, A., Brenner-Morton, S., Kawakami, A., Van Heyningen, V., Jessell, T.M. and Briscoe, J., 1997. Pax6 Controls Progenitor Cell Identity and Neuronal Fate in Response to Graded Shh Signaling. *Cell,* **90**(1), pp. 169-180.

50. Ericson, J., Morton, S., Kawakami, A., Roelink, H. and Jessell, T.M., 1996. Two Critical Periods of Sonic Hedgehog Signaling Required for the Specification of Motor Neuron Identity. *Cell,* **87**(4), pp. 661-673.

51. Fannon, A.M. and Colman, D.R., 1996. A Model for Central Synaptic Junctional Complex Formation Based on the Differential Adhesive Specificities of the Cadherins. *Neuron,* **17**(3), pp. 423-434.

52. Fischer, A.J. and Omar, G., 2005. Transitin, a nestin-related intermediate filament is expressed by neural progenitors and can be induced in Müller glia in the chicken retina. *The Journal of comparative neurology,* **484**(1), pp. 1-14.

53. Fishell, G. and Hatten, M.E., 1991. Astrotactin provides a receptor system for CNS neuronal migration. *Development,* **113**(3), pp. 755-765.

54. Fujimori, T. and Takeichi, M., 1993. Disruption of epithelial cell-cell adhesion by exogenous expression of a mutated nonfunctional N-cadherin. *Molecular biology of the cell,* **4**(1), pp. 37-47.

55. Gallin, W.J., 1998. Evolution of the "classical" cadherin family of cell adhesion molecules in vertebrates. *Molecular biology and evolution,* **15**(9), pp. 1099-1107.

56. Gongidi, V., Ring, C., Moody, M., Brekken, R., Sage, E.H., Rakic, P. and Anton, E.S., 2004. SPARC-like 1 regulates the Terminal Phase of Radial Glia-Guided Migration in the Cerebral Cortex. *Neuron,* **41**(1), pp. 57-69.

57. Gonzalez-Reyes, A. and St Johnston, D., 1998. The Drosophila AP axis is polarised by the cadherin-mediated positioning of the oocyte. *Development,* **125**(18), pp. 3635-3644.

58. Goulding, M., 1998. Specifying Motor Neurons and their Connections. *Neuron,* **21**(5), pp. 943-946.

59. Gumbiner, B.M., 2005. Coordinate Gene Regulation by Two Different Catenins. *Developmental Cell,* **8**(6), pp. 795-796.

60. Gumbiner, B.M., 1996. Cell Adhesion: The Molecular Basis of Tissue Architecture and Morphogenesis. *Cell,* **84**(3), pp. 345-357.

61. Haase, G., Dessaud, E., Garcès, A., De Bovis, B., Birling, M., Filippi, P., Schmalbruch, H., Arber, S. and Delapeyrière, O., 2002. GDNF Acts through PEA3 to Regulate Cell Body Positioning and Muscle Innervation of Specific Motor Neuron Pools. *Neuron,* **35**(5), pp. 893-905.

62. Hamburger, V. and Hamilton, H.L., 1992. A series of normal stages in the development of the chick embryo. *Developmental Dynamics,* **195**(4), pp. 231-272.

63. Hamaguchi, M., Matsuyoshi, N., Ohnishi, Y., Gotoh, B., Takeichi, M., and Nagai, Y., 1993. P60v-src causes tyrosine phosphorylation and inactivation of N-cadherin-catenin cell adhesion system. Embo J, 12(1), 307-314.

64. Hatten, M.E., Liem, R.K.H., Shelanski, M.L. and Mason, C.A., 1991. Astroglia in CNS injury. *Glia,* **4**(2), pp. 233-243.

65. Hirano, S., Kimoto, N., Shimoyama, Y., Hirohashi, S. and Takeichi, M., 1992. Identification of a neural α-catenin as a key regulator of cadherin function and multicellular organization. *Cell,* **70**(2), pp. 293-301.

66. Hirano, S., Ono, T., Yan, Q., Wang, X., Sonta, S. and Suzuki, S.T., 1999. Protocadherin 2C: A New Member of the Protocadherin 2 Subfamily Expressed in a Redundant Manner with OL-Protocadherin in the Developing Brain. *Biochemical and biophysical research communications,* **260**(3), pp. 641-645.

67. Hirano, S., Yan, Q. and Suzuki, S.T., 1999. Expression of a Novel Protocadherin, OL-Protocadherin, in a Subset of Functional Systems of the Developing Mouse Brain. *The Journal of Neuroscience,* **19**(3), pp. 995-1005.

68. Hobmayer, E., Hatta, M., Fischer, R., Fujisawa, T., Holstein, T.W. and Sugiyama, T., 1996. Identification of a Hydra homologue of the β-catenin/plakoglobin/armadillo gene family. *Gene,* **172**(1), pp. 155-159.

69. Hollyday, M., 1980. Organization of motor pools in the chick lumbar lateral motor column. *The Journal of comparative neurology,* **194**(1), pp. 143-170.

70. Hollyday, M. and Hamburger, V., 1977. An autoradiographic study of the formation of the lateral motor column in the chick embryo. *Brain research,* **132**(2), pp. 197-208.

71. Huber, O., Bierkamp, C. and Kemler, R., 1996. Cadherins and catenins in development. *Current opinion in cell biology,* **8**(5), pp. 685-691.

72. Huber, O., Korn, R., McLaughlin, J., Ohsugi, M., Herrmann, B.G. And Kemler, R., 1996. Nuclear localization of β-catenin by interaction with transcription factor LEF-1. *Mechanisms of development,* **59**(1), pp. 3-10.

73. Huber, P., Dalmon, J., Engiles, J., Breviario, F., Gory, S., Siracusa, L.D., Buchberg, A.M. and Dejana, E., 1996. Genomic Structure and Chromosomal Mapping of the Mouse VE-Cadherin Gene (Cdh5). *Genomics,* **32**(1), pp. 21-28.

74. Ille, F., Atanasoski, S., Falk, S., Ittner, L.M., Märki, D., Büchmann-Møller, S., Wurdak, H., Suter, U., Taketo, M.M. and Sommer, L., 2007. Wnt/BMP signal integration regulates the balance between proliferation and differentiation of neuroepithelial cells in the dorsal spinal cord. *Developmental biology,* **304**(1), pp. 394-408.

75. Inoue, A. and Sanes, J.R., 1997. Lamina-Specific Connectivity in the Brain: Regulation by N-Cadherin, Neurotrophins, and Glycoconjugates. *Science,* **276**(5317), pp. 1428-1431.

76. Inuzuka, H., Redies, C. and Takeichi, M., 1991. Differential expression of R- and N-cadherin in neural and mesodermal tissues during early chicken development. *Development,* **113**(3), pp. 959-967.

77. Inuzuka, H., Miyatani, S. and Takeichi, M., 1991. R-cadherin: A novel Ca2+- dependent cell-cell adhesion molecule expressed in the retina. *Neuron,* **7**(1), pp. 69-79.

78. Iwai, Y., Usui, T., Hirano, S., Steward, R., Takeichi, M. and Uemura, T., 1997. Axon Patterning Requires D N-cadherin, a Novel Neuronal Adhesion Receptor, in the Drosophila Embryonic CNS. *Neuron,* **19**(1), pp. 77-89.

79. Ju, M.J., Aroca, P., Luo, J., Puelles, L. and Redies, C., 2004. Molecular profiling indicates avian branchiomotor nuclei invade the hindbrain alar plate. *Neuroscience,* **128**(4), pp. 785-796.

80. Kania, A. and Jessell, T.M., 2003. Topographic Motor Projections in the Limb Imposed by LIM Homeodomain Protein Regulation of Ephrin-A:EphA Interactions. *Neuron,* **38**(4), pp. 581-596.

81. Kania, A., Johnson, R.L. and Jessell, T.M., 2000. Coordinate Roles for LIM Homeobox Genes in Directing the Dorsoventral Trajectory of Motor Axons in the Vertebrate Limb. *Cell,* **102**(2), pp. 161-173.

82. Kania, A., Johnson, R.L. and Jessell, T.M., 2000. Coordinate Roles for LIM Homeobox Genes in Directing the Dorsoventral Trajectory of Motor Axons in the Vertebrate Limb. *Cell,* **102**(2), pp. 161-173.

83. Kawaguchi, J., Takeshita, S., Kashima, T., Imai, T., Machinami, R. and Kudo, A., 1999. Expression and Function of the Splice Variant of the Human Cadherin-11 Gene in Subordination to Intact Cadherin-11. *Journal of Bone and Mineral Research,* **14**(5), pp. 764-775.

84. Kawakami, K. and Noda, T., 2004. Transposition of the Tol2 Element, an Ac-Like Element from the Japanese Medaka Fish Oryzias latipes, in Mouse Embryonic Stem Cells. *Genetics,* **166**(2), pp. 895-899.

85. Kido, M., Obata, S., Tanihara, H., Rochelle, J.M., Seldin, M.F., Taketani, S. and Suzuki, S.T., 1998. Molecular Properties and Chromosomal Location of Cadherin-8. *Genomics,* **48**(2), pp. 186-194.

86. Kimura, Y., Matsunami, H., Inoue, T., Shimamura, K., Uchida, N., Ueno, T., Miyazaki, T. and Takeichi, M., 1995. Cadherin-11 Expressed in Association with Mesenchymal Morphogenesis in the Head, Somite, and Limb Bud of Early Mouse Embryos. *Developmental biology,* **169**(1), pp. 347-358.

87. Kohmura, N., Senzaki, K., Hamada, S., Kai, N., Yasuda, R., Watanabe, M., Ishii, H., Yasuda, M., Mishina, M. and Yagi, T., 1998. Diversity Revealed by a Novel Family of Cadherins Expressed in Neurons at a Synaptic Complex. *Neuron,* **20**(6), pp. 1137-1151.

88. Köster, R.W. and Fraser, S.E., 2001. Direct imaging of in vivo neuronal migration in the developing cerebellum. Current Biology, 11(23), pp. 1858-1863.

89. Krylova, O., Messenger, M.J. and Salinas, P.C., 2000. Dishevelled-1 Regulates Microtubule Stability. *The Journal of cell biology,* **151**(1), pp. 83-94.

90. Kypta, R.M., Su, H. and Reichardt, L.F., 1996. Association between a transmembrane protein tyrosine phosphatase and the cadherin-catenin complex. *The Journal of cell biology,* **134**(6), pp. 1519-1529.

91. Landmesser, L., 1978. The development of motor projection patterns in the chick hind limb. *The Journal of physiology,* **284**(1), pp. 391-414.

92. Landmesser, L.T., 2001. The acquisition of Moto neuron subtype identity and motor circuit formation. *International Journal of Developmental Neuroscience,* **19**(2), pp. 175-182.

93. Larue, L., Antos, C., Butz, S., Huber, O., Delmas, V., Dominis, M. and Kemler, R., 1996. A role for cadherins in tissue formation. *Development,* **122**(10), pp. 3185-3194.

94. Letourneau, P.C., Shattuck, T.A., Roche, F.K., Takeichi, M. and Lemmon, V., 1990. Nerve growth cone migration onto Schwann cells involves the calcium-dependent adhesion molecule, N-cadherin. *Developmental biology,* **138**(2), pp. 430-442.

95. Lickert, H., Domon, C., Huls, G., Wehrle, C., Duluc, I., Clevers, H., Meyer, B.I., Freund, J.N. and Kemler, R., 2000. Wnt/(beta)-catenin signaling regulates the expression of the homeobox gene Cdx1 in embryonic intestine. *Development,* **127**(17), pp. 3805-3813.

96. Lickert, H., Bauer, A., Kemler, R. and Stappert, J., 2000. Casein Kinase II Phosphorylation of E-cadherin Increases E-cadherin/β-Catenin Interaction and Strengthens Cell-Cell Adhesion. *Journal of Biological Chemistry,* **275**(7), pp. 5090-5095.

97. Lin, A.W. and Carpenter, E.M., 2003. Hoxa10 and Hoxd10 coordinately regulate lumbar motor neuron patterning. *Journal of neurobiology,* **56**(4), pp. 328-337.

98. Lin, J.H., Saito, T., Anderson, D.J., Lance-Jones, C., Jessell, T.M. and Arber, S., 1998. Functionally Related Motor Neuron Pool and Muscle Sensory Afferent Subtypes Defined by Coordinate ETS Gene Expression. *Cell,* **95**(3), pp. 393-407.

99. Lin, J.H., Saito, T., Anderson, D.J., Lance-Jones, C., Jessell, T.M. and Arber, S., 1998. Functionally Related Motor Neuron Pool and Muscle Sensory Afferent Subtypes Defined by Coordinate ETS Gene Expression. *Cell,* **95**(3), pp. 393-407.

100. Lin, J., Wang, C. and Redies, C., 2012. Expression of delta-protocadherins in the spinal cord of the chicken embryo. *The Journal of comparative neurology,* **520**(7), pp. 1509-1531.

101. Liuzzi, F.J. and Lasek, R.J., 1985. Regeneration of lumbar dorsal root axons into the spinal cord of adult frogs (rana pipiens), an HRP study. *The Journal of comparative neurology,* **232**(4), pp. 456-465.

102. Livet, J., Sigrist, M., Stroebel, S., De Paola, V., Price, S.R., Henderson, C.E., Jessell, T.M. and Arber, S., 2002. ETS Gene Pea3 Controls the Central Position and Terminal Arborization of Specific Motor Neuron Pools. *Neuron,* **35**(5), pp. 877-892.

103. Lom, B., Höpker, V., Mcfarlane, S., Bixby, J.L. and Holt, C.E., 1998. Fibroblast growth factor receptor signaling in Xenopus retinal axon extension. *Journal of neurobiology,* **37**(4), pp. 633-641.

104. Loureiro, J. and Peifer, M., 1998. Roles of Armadillo, a Drosophila catenin, during central nervous system development. *Current Biology,* **8**(11), pp. 622-633.

105. Lumsden, A. and Krumlauf, R., 1996. Patterning the Vertebrate Neuraxis. *Science,* **274**(5290), pp. pp. 1109-1115.

106. Luo, J., Ju, M.J. And Redies, C., 2006. Regionalized cadherin-7 expression by radial glia is regulated by Shh and Pax7 during chicken spinal cord development. *Neuroscience,* **142**(4), pp. 1133-1143.

107. Luo, J., Ju, M.J. and Redies, C., 2006. Regionalized cadherin-7 expression by radial glia is regulated by Shh and Pax7 during chicken spinal cord development. *Neuroscience,* **142**(4), pp. 1133-1143.

108.   Luo, Y., High, F.A., Epstein, J.A. and Radice, G.L., 2006. N-cadherin is required for neural crest remodeling of the cardiac outflow tract. *Developmental biology,* **299**(2), pp. 517-528.

109.   Lyn, Levesque., Willem, Annaert., Katleen, Craessaerts., Paul M. Mathews., Mary Seeger., Ralph A. Nixon., Fred Van Leuven., Sam Gandy., David Westaway., Peter St George-Hyslop., Bart De Strooper., and Paul E. Fraser.. 1999. Developmental Expression of Wild-Type and Mutant Presenilin-1 in Hippocampal Neurons from Transgenic Mice: Evidence for Novel Species Specific Properties of Human Presenilin-1. Molecular Medicine, (5), pp. 542-554.

110.   Matsunami, H., Miyatani, S., Inoue, T., Copeland, N.G., Gilbert, D.J., Jenkins, N.A. And Takeichi, M., 1993. Cell binding specificity of mouse R-cadherin and chromosomal mapping of the gene. *Journal of cell science,* **106**(1), pp. 401-409.

111.   Mbalaviele, G., Nishimura, R., Myoi, A., Niewolna, M., Reddy, S.V., Chen, D., Feng, J., Roodman, D., Mundy, G.R. and Yoneda, T., 1998. Cadherin-6 Mediates the Heterotypic Interactions between the Hemopoietic Osteoclast Cell Lineage and Stromal Cells in a Murine Model of Osteoclast Differentiation. *The Journal of cell biology,* **141**(6), pp. 1467-1476.

112.   McMahon, A.P., 2000. Neural patterning: The role of Nkx genes in the ventral spinal cord. *Genes & development,* **14**(18), pp. 2261-2264.

113.   Mission, J., Austin, C.P., Takahashi, T., Cepko, C.L. And Caviness, V.S., 1991. The Alignment of Migrating Neural Cells in Relation to the Murine Neopallial Radial Glial Fiber System. *Cerebral Cortex,* **1**(3), pp. 221-229.

114.   Miyatani, S., Shimamura, K., Hatta, M., Nagafuchi, A., Nose, A., Matsunaga, M., Hatta, K. and Takeichi, M., 1989. Neural Cadherin: Role in Selective Cell-Cell Adhesion. *Science,* **245**(4918), pp. pp. 631-635.

115.   Miyatani, S., Shimamura, K., Hatta, M., Nagafuchi, A., Nose, A., Matsunaga, M., Hatta, K. and Takeichi, M., 1989. Neural Cadherin: Role in Selective Cell-Cell Adhesion. *Science,* **245**(4918), pp. pp. 631-635.

116.   Momose, T., Tonegawa, ?.A., Takeuchi, J., Ogawa, H., Umesono, K. And Yasuda, K., 1999. Efficient targeting of gene expression in chick embryos by microelectroporation. *Development, growth & differentiation,* **41**(3), pp. 335-344.

117.   Mukouyama, Y., Deneen, B., Lukaszewicz, A., Novitch, B.G., Wichterle, H., Jessell, T.M. and Anderson, D.J., 2006. Olig2 + neuroepithelial Moto neuron progenitors are not multipotent stem cells in vivo. *Proceedings of the National Academy of Sciences of the United States of America,* **103**(5), pp. 1551-1556.

118.   Mukouyama, Y., Deneen, B., Lukaszewicz, A., Novitch, B.G., Wichterle, H., Jessell, T.M. and Anderson, D.J., 2006. Olig2^{+} Neuroepithelial Motoneuron Progenitors Are Not Multipotent Stem cells in vivo. *Proceedings of the National Academy of Sciences of the United States of America,* **103**(5), pp. pp. 1551-1556.

119.   Murphy-Erdosh, C., Yoshida, C.K., Paradies, N. And Reichardt, L.F., 1995. The cadherin-binding specificities of B-cadherin and LCAM. *The Journal of cell biology,* **129**(5), pp. 1379-1390.

120.   Nadarajah, B., Alifragis, P., Wong, R.O.L. And Parnavelas, J.G., 2003. Neuronal Migration in the Developing Cerebral Cortex: Observations Based on Real-time Imaging. Cerebral Cortex, 13(6), pp. 607-611.

121.   Nagar, B., Overduin, M., Ikura, M., and Rinji, J.M., 1996. Structural basis of calcium-induced E-cadherin rigidification and dimerization. *Nature*, 28:380(6572): 360-4.

122.   Nakagawa, S. and Takeichi, M., 1998. Neural crest emigration from the neural tube depends on regulated cadherin expression. *Development,* **125**(15), pp. 2963-2971.

123.   Nakagawa, S. and Takeichi, M., 1995. Neural crest cell-cell adhesion controlled by sequential and subpopulation-specific expression of novel cadherins. *Development,* **121**(5), pp. 1321-1332.

124.   Nelson, W.J. and Nusse, R., 2004. Convergence of Wnt, β-Catenin, and Cadherin Pathways. *Science,* **303**(5663), pp. pp. 1483-1487.

125.   Noctor SC, Martínez-Cerdeño V, Ivic L, and Kriegstein AR (2004) Cortical neurons arise in symmetric and asymmetric division zones and migrate through specific phases. Nat Neurosci 7:136–144.

126.   Nollet F, Kools P, van Roy F. Phylogenetic analysis of the cadherin superfamily allows identification of six major subfamilies besides several solitary members. J Mol Biol 2000; 299: 551–572.

127.   Nose, A., Nagafuchi, A. and Takeichi, M., 1988. Expressed recombinant cadherins mediate cell sorting in model systems. *Cell,* **54**(7), pp. 993-1001.

128.   Nose, A., Tsuji, K. and Takeichi, M., 1990. Localization of specificity determining sites in cadherin cell adhesion molecules. *Cell,* **61**(1), pp. 147-155.

129.   Obata, S., Sago, H., Mori, N., Rochelle, J.M., Seldin, M.F., Davidson, M., St John, T., Taketani, S. and Suzuki, S.T., 1995. Protocadherin Pcdh2 shows properties similar to, but distinct from, those of classical cadherins. *Journal of cell science,* **108**(12), pp. 3765-3773.

130.   O'Rourke, N.A., Dailey, M.E., Smith, S.J. And McConnell, S.K., 1992. Diverse Migratory Pathways in the Developing Cerebral Cortex. *Science,* **258**(5080), pp. pp. 299-302.

131.   Overduin, M., Harvey, T.S., Bagby, S., Tong, K.I., Yau, P., Takeichi, M. And Ikura, M., 1995. Solution Structure of the Epithelial Cadherin Domain Responsible for Selective Cell Adhesion. *Science,* **267**(5196), pp. pp. 386-389.

132.   Park, K. And Gumbiner, B.M., 2010. Cadherin 6B induces BMP signaling and de-epithelialization during the epithelial mesenchymal transition of the neural crest. *Development,* **137**(16), pp. 2691-2701.

133.   Patapoutian, A. and Reichardt, L.F., 2000. Roles of Wnt proteins in neural development and maintenance. *Current opinion in neurobiology,* **10**(3), pp. 392-399.

134.   Patel, S.D., Ciatto, C., Chen, C.P., Bahna, F., Rajebhosale, M., Arkus, N., Schieren, I., Jessell, T.M., Honig, B., Price, S.R. and Shapiro, L., 2006. Type II Cadherin Ectodomain Structures: Implications for Classical Cadherin Specificity. *Cell,* **124**(6), pp. 1255-1268.

135.   Pokutta, S., Herrenknecht, K., Kemler, R. and Engel, J., 1994. Conformational changes of the recombinant extracellular domain of E-cadherin upon calcium binding. *European Journal of Biochemistry,* **223**(3), pp. 1019-1026.

136.   Polakis, P., 2000. Wnt signaling and cancer. *Genes & development,* **14**(15), pp. 1837-1851.

137.   Prasad, M.S. and Paulson, A.F., 2011. A combination of enhancer/silencer modules regulates spatially restricted expression of cadherin-7 in neural epithelium. *Developmental Dynamics,* **240**(7), pp. 1756-1768.

138.   Price, S.R. and Briscoe, J., 2004. The generation and diversification of spinal motor neurons: signals and responses. *Mechanisms of development,* **121**(9), pp. 1103-1115.

139.   Price, S.R., De Marco Garcia, N.V., Ranscht, B. and Jessell, T.M., 2002. Regulation of Motor Neuron Pool Sorting by Differential Expression of Type II Cadherins. *Cell,* **109**(2), pp. 205-216.

140.   Qin, Y., Capaldo, C., Gumbiner, B.M. and Macara, I.G., 2005. The mammalian Scribble polarity protein regulates epithelial cell adhesion and migration through E-cadherin. *The Journal of cell biology,* **171**(6), pp. 1061-1071.

141.   Rakic, P. and Nowakowski, R.S., 1981. The time of origin of neurons in the hippocampal region of the rhesus monkey. *The Journal of comparative neurology,* **196**(1), pp. 99-128.

142.   Rakic, P. and Sidman, R.L., 1973. Weaver Mutant Mouse Cerebellum: Defective Neuronal Migration Secondary to Abnormality of Bergmann Glia. *Proceedings of the National Academy of Sciences,* **70**(1), pp. 240-244.

143.   Rakic, P., 2003. Developmental and Evolutionary Adaptations of Cortical Radial Glia. *Cerebral Cortex,* **13**(6), pp. 541-549.

144.   Rakic, P., 1972. Mode of cell migration to the superficial layers of fetal monkey neocortex. *The Journal of comparative neurology,* **145**(1), pp. 61-83.

145.   Rakic, P., Cameron, R.S. And Komuro, H., 1994. Recognition, adhesion, transmembrane signaling and cell motility in guided neuronal migration. *Current opinion in neurobiology,* **4**(1), pp. 63-69.

146.   Redies, C. and Müller, H.-J., 1994. Similarities in Structure and Expression between Mouse P-Cadherin, Chicken B-Cadherin and Frog XB/U-Cadherin. *Cell Commun Adhes,* **2**(6), pp. 511-520.

147.   Rio, C., Rieff, H.I., Qi, P. and Corfas, G., 1997. Neuregulin and erbB Receptors Play a Critical Role in Neuronal Migration. *Neuron,* **19**(1), pp. 39-50.

148.   Robinson, A., Escuin, S., Doudney, K., Vekemans, M., Stevenson, R.E., Greene, N.D.E., Copp, A.J. and Stanier, P., 2012. Mutations in the planar cell polarity genes CELSR1 and SCRIB are associated with the severe neural tube defect craniorachischisis. *Human mutation,* **33**(2), pp. 440-447.

149.   Roelink, H., Porter, J.A., Chiang, C., Tanabe, Y., Chang, D.T., Beachy, P.A. And Jessell, T.M., 1995. Floor plate and motor neuron induction by different concentrations of the amino-terminal cleavage product of sonic hedgehog autoproteolysis. *Cell,* **81**(3), pp. 445-455.

150.   Romanes GJ. The Motor Pools of the Spinal Cord. Prog Brain Res 1964; 11: 93-119.

151.   Roose, J., Huls, G., Beest, M.V., Moerer, P., Horn, K.V.D., Goldschmeding, R., Ton Logtenberg and Clevers, H., 1999. Synergy between Tumor Suppressor APC and the β-Catenin-Tcf4 Target Tcf1. *Science,* **285**(5435), pp. pp. 1923-1926.

152.   Rousso, D.L., Gaber, Z.B., Wellik, D., Morrisey, E.E. and Novitch, B.G., 2008. Coordinated Actions of the Forkhead Protein Foxp1 and Hox Proteins in

the Columnar Organization of Spinal Motor Neurons. *Neuron,* **59**(2), pp. 226-240.

153.   Salinas, P.C. and Price, S.R., 2005. Cadherins and catenins in synapse development. *Current opinion in neurobiology,* **15**(1), pp. 73-80.

154.   Sato, Y., Kasai, T., Nakagawa, S., Tanabe, K., Watanabe, T., Kawakami, K. and Takahashi, Y., 2007. Stable integration and conditional expression of electroporated transgenes in chicken embryos. *Developmental biology,* **305**(2), pp. 616-624.

155.   Schmid, R.S. and Anton, E.S., 2003. Role of Integrins in the Development of the Cerebral Cortex. *Cerebral Cortex,* **13**(3), pp. 219-224.

156.   Schüller, U. and Rowitch, D.H., 2007. β-catenin function is required for cerebellar morphogenesis. Brain research, 1140(0), pp. 161-169.

157.   Serres, M., Filhol, O., Lickert, H., Grangeasse, C., Chambaz, E.M., Stappert, J., Vincent, C. and Schmitt, D., 2000. The Disruption of Adherens Junctions Is Associated with a Decrease of E-Cadherin Phosphorylation by Protein Kinase CK2. *Experimental cell research,* **257**(2), pp. 255-264.

158.   Shah, V., Drill, E. and Lance-Jones, C., 2004. Ectopic expression of Hoxd10 in thoracic spinal segments induces motoneurons with a lumbosacral molecular profile and axon projections to the limb. *Developmental Dynamics,* **231**(1), pp. 43-56.

159.   Shapiro, V.S., Lee, P. and Winoto, A., 1995. Identification and cloning of the G3B cDNA encoding a 3′ segment of a protein binding to GATA-3. *Gene,* **163**(2), pp. 329-330.

160.   Sharma, K., Sheng, H.Z., Lettieri, K., Li, H., Karavanov, A., Potter, S., Westphal, H. and Pfaff, S.L., 1998. LIM Homeodomain Factors Lhx3 and Lhx4 Assign Subtype Identities for Motor Neurons. *Cell,* **95**(6), pp. 817-828.

161.   Sharma, K., Leonard, A. E., Lettieri, K., and Pfaff, S. L., 2000. Genetic and epigenetic mechanisms contribute to motor neuron pathfinding. *Nature*, 406(6795): 515-9.

162.   Sheibani, N., Sorenson, C.M. and Frazier, W.A., 2000. Differential Modulation of Cadherin-mediated Cell–Cell Adhesion by Platelet Endothelial Cell Adhesion Molecule-1 Isoforms through Activation of Extracellular Regulated Kinases. *Molecular biology of the cell,* **11**(8), pp. 2793-2802.

163.   Shibuya, Y., Mizoguchi, A., Takeichi, M., Shimada, K. and Ide, C., 1995. Localization of N-cadherin in the normal and regenerating nerve fibers of the chicken peripheral nervous system. *Neuroscience,* **67**(1), pp. 253-261.

164.   Shimoyama, Y., Takeda, H., Yoshihara, S., Kitajima, M. and Hirohashi, S., 1999. Biochemical Characterization and Functional Analysis of Two Type II Classic Cadherins, Cadherin-6 and -14, and Comparison with E-cadherin. *Journal of Biological Chemistry,* **274**(17), pp. 11987-11994.

165.   Shum, A.S.W., Tang, L.S.C., Copp, A.J. and Roelink, H., 2010. Lack of motor neuron differentiation is an intrinsic property of the mouse secondary neural tube. *Developmental Dynamics,* **239**(12), pp. 3192-3203.

166.   Sidman, R.L. and Rakic, P., 1973. Neuronal migration, with special reference to developing human brain: a review. *Brain research,* **62**(1), pp. 1-35.

167.   Simcha, I., Shtutman, M., Salomon, D., Zhurinsky, J., Sadot, E., Geiger, B. and Ben-Ze'ev, A., 1998. Differential Nuclear Translocation and

Transactivation Potential of β-Catenin and Plakoglobin. *The Journal of cell biology,* **141**(6), pp. 1433-1448.

168.   Sockanathan, S. and Jessell, T.M., 1998. Motor Neuron–Derived Retinoid Signaling Specifies the Subtype Identity of Spinal Motor Neurons. *Cell,* **94**(4), pp. 503-514.

169.   Steinberg, M.S., 1963. "ECM": Its nature, origin and function in cell aggregation. *Experimental cell research,* **30**(2), pp. 257-279.

170.   Steinberg, M.S. And McNutt, P.M., 1999. Cadherins and their connections: adhesion junctions have broader functions. *Current opinion in cell biology,* **11**(5), pp. 554-560.

171.   Steinberg, M.S., and Takeichi, M., 1994. Experimental specification of cell sorting, tissue spreading and specific spatial patterning by quantitative differences in cadherin expression. *Proc Natl Acad Sci USA* v 91(1) 206-209.

172.   Sugimoto, K., Honda, S., Yamamoto, T., Ueki, T., Monden, M., Kaji, A., Matsumoto, K. and Nakamura, T., 1996. Molecular Cloning and Characterization of a Newly Identified Member of the Cadherin Family, PB-cadherin. *Journal of Biological Chemistry,* **271**(19), pp. 11548-11556.

173.   Sugimoto, K., Honda, S., Yamamoto, T., Ueki, T., Monden, M., Kaji, A., Matsumoto, K. and Nakamura, T., 1996. Molecular Cloning and Characterization of a Newly Identified Member of the Cadherin Family, PB-cadherin. *Journal of Biological Chemistry,* **271**(19), pp. 11548-11556.

174.   Suzuki, S.C., Inoue, T., Kimura, Y., Tanaka, T. and Takeichi, M., 1997. Neuronal Circuits Are Subdivided by Differential Expression of Type-II Classic Cadherins in Postnatal Mouse Brains. *Molecular and Cellular Neuroscience,* **9**(5–6), pp. 433-447.

175.   Takeichi, M., 1995. Morphogenetic roles of classic cadherins. *Current opinion in cell biology,* **7**(5), pp. 619-627.

176.   Takeichi, M., 1991. Cadherin Cell Adhesion Receptors as a Morphogenetic Regulator. *Science,* **251**(5000), pp. pp. 1451-1455.

177.   Takeichi, M., Atsumi, T., Yoshida, C., Uno, K. And Okada, T.S., 1981. Selective adhesion of embryonal carcinoma cells and differentiated cells by Ca2+-dependent sites. *Developmental biology,* **87**(2), pp. 340-350.

178.   Takeichi, M., Inuzuka, H., Shimamura, K., Matsunaga, M. and Nose, A., 1990. Cadherin-mediated cell-cell adhesion and neurogenesis. *Neuroscience Research Supplements,* **13**(0), pp. S92-S96.

179.   Tamura, K., Shan, W., Hendrickson, W.A., Colman, D.R. and Shapiro, L., 1998. Structure-Function Analysis of Cell Adhesion by Neural (N-) Cadherin. *Neuron,* **20**(6), pp. 1153-1163.

180.   Tamura, S., Morikawa, Y., Iwanishi, H., Hisaoka, T. and Senba, E., 2003. Expression pattern of the winged-helix/forkhead transcription factor Foxp1 in the developing central nervous system. *Gene Expression Patterns,* **3**(2), pp. 193-197.

181.   Tanabe, K., Kiryu-Seo, S., Nakamura, T., Mori, N., Tsujino, H., Ochi, T. and Kiyama, H., 1998. Alternative expression of Shc family members in nerve-injured motoneurons. *Molecular Brain Research,* **53**(1–2), pp. 291-296.

182.   Tanabe, K., Takahashi, Y., Sato, Y., Kawakami, K., Takeichi, M. and Nakagawa, S., 2006. Cadherin is required for dendritic morphogenesis and synaptic terminal organization of retinal horizontal cells. *Development,* **133**(20; required for dendrite morphogenesis of horizontal cells and subsequent synapse formation with photoreceptor cells in the vertebrate retina.), pp. 4085-4096.

183.   Tanabe, K., Takahashi, Y., Sato, Y., Kawakami, K., Takeichi, M. and Nakagawa, S., 2006. Cadherin is required for dendritic morphogenesis and synaptic terminal organization of retinal horizontal cells. *Development,* **133**(20), pp. 4085-4096.

184.   Tanabe, Y. and Jessell, T.M., 1996. Diversity and Pattern in the Developing Spinal Cord. *Science,* **274**(5290), pp. pp. 1115-1123.

185.   Tanabe, Y., Roelink, H. and Jessell, T.M., 1995. Induction of motor neurons by Sonic hedgehog is independent of floor plate differentiation. *Current Biology,* **5**(6), pp. 651-658.

186.   Tessier-Lavigne, M. and Goodman, C.S., 1996. The Molecular Biology of Axon Guidance. *Science,* **274**(5290), pp. pp. 1123-1133.

187.   Treubert-Zimmermann, U., Heyers, D. and Redies, C., 2002. Targeting Axons to Specific Fiber Tracts In Vivo by Altering Cadherin Expression. *The Journal of Neuroscience,* **22**(17), pp. 7617-7626.

188.   Tsuchida, T., Ensini, M., Morton, S.B., Baldassare, M., Edlund, T., Jessell, T.M. and Pfaff, S.L., 1994. Topographic organization of embryonic motor neurons defined by expression of LIM homeobox genes. *Cell,* **79**(6), pp. 957-970.

189.   Uchida, N., Honjo, Y., Johnson, K.R., Wheelock, M.J. and Takeichi, M., 1996. The catenin/cadherin adhesion system is localized in synaptic junctions bordering transmitter release zones. *The Journal of cell biology,* **135**(3), pp. 767-779.

190.   Uchida, N., Shimamura, K., Miyatani, S., Copeland, N.G., Gilbert, D.J., Jenkins, N.A. and Takeichi, M., 1994. Mouse αN-Catenin: Two Isoforms,

Specific Expression in the Nervous System, and Chromosomal Localization of the Gene. *Developmental biology,* **163**(1), pp. 75-85.

191.   Uemura, M. And Takeichi, M., 2006. αN-catenin deficiency causes defects in axon migration and nuclear organization in restricted regions of the mouse brain. *Developmental Dynamics,* **235**(9), pp. 2559-2566.

192.   Valdivia, R.H., Hromockyj, A.E., Monack, D., Ramakrishnan, L. and Falkow, S., 1996. Applications for green fluorescent protein (GFP) in the study of host pathogen interactions. *Gene,* **173**(1), pp. 47-52.

193.   Van Veelen, W., Le, N.H., Helvensteijn, W., Blonden, L., Theeuwes, M., Bakker, E.R.M., Franken, P.F., Van Gurp, L., Meijlink, F., Van Der Valk, M.A., Kuipers, E.J., Fodde, R. and Smits, R., 2011. β-catenin tyrosine 654 phosphorylation increases Wnt signalling and intestinal tumorigenesis. *Gut,* **60**(9), pp. 1204-1212.

194.   Varela-Echavarrä±´A, A., Pfaff, S.L. and Guthrie, S., 1996. Differential Expression of LIM Homeobox Genes among Motor Neuron Subpopulations in the Developing Chick Brain Stem. *Molecular and Cellular Neuroscience,* **8**(4), pp. 242-257.

195.   Watanabe, T., Saito, D., Tanabe, K., Suetsugu, R., Nakaya, Y., Nakagawa, S. and Takahashi, Y., 2007. Tet-on inducible system combined with in ovo electroporation dissects multiple roles of genes in somitogenesis of chicken embryos. *Developmental biology,* **305**(2), pp. 625-636.

196.   Whitelaw, V. and Hollyday, M., 1983. Neural pathway constraints in the motor innervation of the chick hind limb following dorsoventral rotations of distal limb segments. *The Journal of Neuroscience,* **3**(6), pp. 1226-1233.

197.   Whitelaw, V. and Hollyday, M., 1983. Position-dependent motor innervation of the chick hind limb following serial and parallel duplications of limb segments. *The Journal of Neuroscience,* **3**(6), pp. 1216-1225.

198.   Whitelaw, V. and Hollyday, M., 1983. Thigh and calf discrimination in the motor innervation of the chick hind limb following deletions of limb segments. *The Journal of Neuroscience,* **3**(6), pp. 1199-1215.

199.   William, C.M., Tanabe, Y. and Jessell, T.M., 2003. Regulation of motor neuron subtype identity by repressor activity of Mnx class homeodomain proteins. *Development,* **130**(8), pp. 1523-1536.

200.   Wu, Q. and Maniatis, T., 1999. A Striking Organization of a Large Family of Human Neural Cadherin-like Cell Adhesion Genes. *Cell,* **97**(6), pp. 779-790.

201.   Xie, F., Padival, M. and Siegel, R.E., 2007. Association of PSD-95 with ErbB4 facilitates neuregulin signaling in cerebellar granule neurons in culture. *Journal of neurochemistry,* **100**(1), pp. 62-72.

202.   Yamagata, K., Andreasson, K.I., Sugiura, H., Maru, E., Dominique, M., Irie, Y., Miki, N., Hayashi, Y., Yoshioka, M., Kaneko, K., Kato, H. and Worley, P.F., 1999. Arcadlin Is a Neural Activity-regulated Cadherin Involved in Long Term Potentiation. *Journal of Biological Chemistry,* **274**(27), pp. 19473-19479.

203.   Yap, A.S., Brieher, W.M., Pruschy, M. and Gumbiner, B.M., 1997. Lateral clustering of the adhesive ectodomain: a fundamental determinant of cadherin function. *Current Biology,* **7**(5), pp. 308-315.

204.   Yoshida, K., Yoshitomo-Nakagawa, K., Seki, N., Sasaki, M. and Sugano, S., 1998. Cloning, Expression Analysis, and Chromosomal Localization

of BH-Protocadherin (PCDH7), a Novel Member of the Cadherin Superfamily. *Genomics,* **49**(3), pp. 458-461.

205.   Yuan, L., Le Bras, A., Sacharidou, A., Itagaki, K., Zhan, Y., Kondo, M., Carman, C.V., Davis, G.E., Aird, W.C. and Oettgen, P., 2012. ETS-related Gene (ERG) Controls Endothelial Cell Permeability via Transcriptional Regulation of the Claudin 5 (CLDN5) Gene. *Journal of Biological Chemistry,* **287**(9), pp. 6582-6591.

206.   Yuan, Y., Lee, J., Napier, A. and Cole, G.J., 1997. Molecular Cloning of a New Intermediate Filament Protein Expressed by Radial Glia and Demonstration of Alternative Splicing in a Novel Heptad Repeat Region Located in the Carboxy-Terminal Tail Domain. *Molecular and Cellular Neuroscience,* **10**(1–2), pp. 71-86.

207.   Zecevic, N., 2004. Specific characteristic of radial glia in the human fetal telencephalon. *Glia,* **48**(1), pp. 27-35.

208.   Zhou, H., Welcher, A.A. and Shooter, E.M., 1997. BDNF/NT4-5 receptor TrkB and cadherin participate in cell-cell adhesion. *Journal of neuroscience research,* **49**(3), pp. 281-291.

209.   Zhurinsky, J., Shtutman, M. and Ben-Ze'ev, A., 2000. Plakoglobin and beta-catenin: protein interactions, regulation and biological roles. *Journal of cell science,* **113**(18), pp. 3127-3139.

210.   Zhurinsky, J., Shtutman, M. and Ben-Ze'ev, A., 2000(b). Differential Mechanisms of LEF/TCF Family-Dependent Transcriptional Activation by β-Catenin and Plakoglobin. *Molecular and cellular biology,* **20**(12), pp. 4238-4252.

Appendix A (Bello et al., 2012)

Cellular/Molecular

Catenin-Dependent Cadherin Function Drives Divisional Segregation of Spinal Motor Neurons

Sanusi M. Bello, Hadas Millo, Manisha Rajebhosale, and Stephen R. Price

Research Department of Cell and Developmental Biology, University College London, London, WC1E 6BT, United Kingdom

Motor neurons that control limb movements are organized as a neuronal nucleus in the developing ventral horn of the spinal cord called the lateral motor column. Neuronal migration segregates motor neurons into distinct lateral and medial divisions within the lateral motor column that project axons to dorsal or ventral limb targets, respectively. This migratory phase is followed by an aggregation phase whereby motor neurons within a division that project to the same muscle cluster together. These later phases of motor neuron organization depend on limb-regulated differential cadherin expression within motor neurons. Initially, all motor neurons display the same cadherin expression profile, which coincides with the migratory phase of motor neuron segregation. Here, we show that this early, pan-motor neuron cadherin function drives the divisional segregation of spinal motor neurons in the chicken embryo by controlling motor neuron migration. We manipulated pan-motor neuron cadherin function through dissociation of cadherin binding to their intracellular partners. We found that of the major intracellular transducers of cadherin signaling, γ-catenin and α-catenin predominate in the lateral motor column. *In vivo* manipulations that uncouple cadherin–catenin binding disrupt divisional segregation via deficits in motor neuron migration. Additionally, reduction of the expression of cadherin-7, a cadherin predominantly expressed in motor neurons only during their migration, also perturbs divisional segregation. Our results show that γ-catenin-dependent cadherin function is required for spinal motor neuron migration and divisional segregation and suggest a prolonged role for cadherin expression in all phases of motor neuron organization.

Introduction

Neuronal nuclei are a recurrent organizational scheme within the CNS that clusters functionally related neuronal soma as spatially distinct groups (Cajal, 1995). Despite the critical functions of neuronal nuclei, little is known of the molecular mechanisms that drive their clustering during development, a process termed nucleogenesis (Agarwala and Ragsdale, 2002).

The spinal motor neurons that control limb movement form a neuronal nucleus termed the lateral motor column (LMC) (Jessell, 2000). As with other neuronal nuclei, LMC internal structure is related to the axonal targets of the neurons in the nucleus (Landmesser, 1978). The LMC segregates into lateral (LMCl) and medial (LMCm) divisions related to the dorsal or ventral com-partments of the limb to which each division projects. Divisional segregation occurs by inside-out migration of LMCl neurons through the earlier-born LMCm (Hollyday and Hamburger, 1977).

Following motor neuron migration, clusters of motor neurons that project axons to an individual muscle emerge (Whitelaw and Hollyday, 1983). Clustering of these so-called motor neuron pools (Romanes, 1964) results from differential expression of members of the type II family of cadherin cell adhesion molecules (Price et al., 2002). Cadherin expression within the LMC is highly dynamic and encompasses a pan-motor neuron phase during divisional segregation with a later motor pool-specific phase. For example, expression of cadherin-20 is initiated in all motor neurons soon after their generation and is refined via limb-derived signals to a motor pool-specific pattern only after divisional segregation is well underway (Price et al., 2002). Absence of these limb-derived signals perturbs motor pool sorting while leaving divisional segregation intact (Haase et al., 2002; Livet et al., 2002). This suggests that divisional segregation and pool sorting are separable and raises the possibility that early, pan-motor neuron cadherin expression could drive divisional segregation before pool sorting.

The cytoplasmic domain of type II cadherins binds to members of the armadillo family of catenins: β-catenin or γ-catenin (plakoglobin) (Nollet et al., 2000). β-Catenin and γ-catenin bind to α-catenin, which anchors cadherin adhesion to the actin cytoskeleton via the linker protein EPLIN (Abe and Takeichi, 2008). Thus, function of all type II cadherins converges on their interaction with either β- or γ-catenin and absence of β- or γ-catenin

abrogates cadherin function (Kintner, 1992; Weis and Nelson, 2006).

We investigated pan-motor neuron cadherin expression in LMC organization through manipulations of catenin–cadherin binding and reduction of a cadherin predominantly expressed during divisional segregation. Expression of a single amino acid mutant of γ-catenin, predicted to uncouple interaction with α-catenin, results in a cell autonomous stalling of motor neuron migration with a concomitant disruption of divisional segregation. Dissociation of cadherin from γ-catenin via expression of an extracellular deleted dominant-negative cadherin also perturbs motor neuron migration and divisional segregation. Finally, knockdown of cadherin-7 perturbs divisional segregation. These data are consistent with a model whereby early pan-motor neuron cadherin function drives the migration of LMC neurons into the ventral horn and suggest a role for cadherin expression throughout nucleogenesis of spinal motor neurons.

Materials and Methods

Chick embryo preparation. Fertilized Brown Bovan Gold Hen's eggs (Henry Stewart Farms) were incubated in a forced draft incubator at 38°C and staged as in Hamburger and Hamilton (1992). All embryos were treated in accordance with the Animals (Scientific Procedures) Act of 1986, UK. Embryos of both sexes were used in our experiments.

Labeling of migrating neurons. Horse radish peroxidase (HRP; Roche) 50% solution in PBS with 1% lysolecithin (Sigma) was pressure injected into the dorsal limb essentially as described by Lin et al. (1998) to retrograde label neurons.

BrdU labeling. BrdU (200 μl, 1 mM; Sigma) was injected directly under the embryo and the eggs sealed and returned to the incubator for the desired length of time. Following cryosectioning, embryo sections were incubated for 5 min in 2 M HCl (Sigma) followed by five washes in PBS, each for 5 min. Primary antibodies to BrdU and subsequent secondary antibody detection was as described in Immunohistochemistry, below.

In situ hybridization histochemistry. Digoxigenin (DIG)-labeled antisense cRNA probes were used for *in situ* hybridization histochemistry on 15-μm-thick cryostat sections as in Price et al. (2002). Dual *in situ* hybridization histochemistry with BrdU labeling was performed by sequential *in situ* hybridization followed by a 2 M HCl treatment at 20°C for 5 min, three washes in PBS for 5 min, each followed by immunohistochemistry for BrdU with secondary antibodies conjugated to HRP followed by IMPACT DAB staining according to the manufacturers protocol (Vector Labs).

In ovo electroporation. Expression of cDNAs was achieved by *in ovo* electroporation using an ECM830 electro-squareporator (BTX). Approximately 0.1 μl of DNA constructs [1–10 μg/μl in H$_2$O with 0.1% Fast Green (Sigma)] was pressure injected into the lumen of the spinal cord. Five 30 volt electrical pulses of 50 ms duration equally spaced over a 5 s period were applied by placing electrodes adjacent to each side of the spinal cord of the embryo. Embryos were electroporated at Hamburger and Hamilton (HH) stages 12–18 and analyzed at HH stages 25–32.

Generation of constructs. A full-length cDNA for chick γ-catenin was cloned by screening an E3 chick cDNA library. The sequence of chick γ-catenin has been submitted to GenBank (accession number HM102357). Point mutation (L127A) was generated using the QuikChange kit (Stratagene) following the manufacturers protocol. γ-Catenin and γ-catenin (L127A) cDNAs were cloned into a pCAGGS vector containing an internal ribosome entry sequence followed by a cDNA encoding nuclear localization sequence tagged β-galactosidase (pCAGGS inlz). Other constructs used in this work included HA-tagged dominant-negative GSK, HA-tagged β-catenin ΔARM, HA-tagged β-catenin-1-ins, HA-tagged constitutively active GSK, HA-tagged dominant-negative TCF, transposase integrated doxycycline inducible N-cadherinΔ390 (Kawakami and Noda, 2004; Tanabe et al., 2006; Sato et al., 2007; Watanabe et al., 2007), cad-7 shRNA knock-down, control cad-7 shRNA [described, tested and characterized in Barnes et al. (2010), these constructs follow the method described by Das et al. (2006)], pCAGGS inlz, and CMV eGFP (Invitrogen).

In situ hybridization probes for cad-20 (MN-cad) and cad-12 were described by Price et al. (2002).

Immunohistochemistry. Antibodies used in this study were as follows: rabbit (R) anti-GFP (1/1000; Invitrogen), R anti-β-catenin (1/1000; Sigma), R anti-pan-cadherin (1/1000; Sigma), R anti-Hb9 (1/5000), R anti-N-cadherin (1/1000; AbCAM,), Dylight 488-conjugated R anti-HRP (The Jackson Laboratory), rat anti-HA (1/500; Roche), guinea pig (GP) anti-Islet-1(2) (1/20000), GP anti-FoxP1, goat (G) anti-HRP (1/2000; Jackson ImmunoResearch), G anti-β-galactosidase (1/1000), mouse (M) anti-α-E-catenin (1/100; Zymed), M anti-γ-catenin (1/100; BD Biosciences), M anti-GFP (1/100; Invitrogen), M anti-BrdU (1/50; Roche), M anti-HA (1/50; Covance). The following mouse monoclonal antibodies were purchased from the Developmental Studies Hybridoma Bank: 745A5 (anti-Nkx2.2) PAX6 (anti-Pax6), 4F2 (anti-Lim1/Lhx1), 2D6 and 4D5 (anti-Islet-1), 5C10 (anti-MNR2/Hb9), A2B11 and EAP3 (anti-transitin), CCD7–1 (anti-cadherin-7). Alkaline phosphatase-conjugated sheep anti-DIG Fab fragments (1/5000; Roche) immunocytochemistry was performed essentially as described previously (Price et al., 2002). Cryostat sections mounted on superfrost plus glass slides were incubated in PBS for 5 min followed by incubation in block solution (PBS with 1% goat serum; Sigma) for 30 min at 20°C. This solution was replaced by antibody diluted in block solution and incubated for 12–16 h at 4°C. Following three washes of 5 min each in PBS, fluorescent-conjugated secondary antibodies were incubated with the sections for 30 min at 20°C in block solution, washed, and mounted with vectashield fluorescent mounting medium (Vector Labs).

Image acquisition and data analysis. Images were acquired on a Nikon Eclipse E80i fluorescence microscope equipped with a Nikon DS5M and Hamammatsu ORCA ER digital camera or on a Leica SPE confocal microscope. Quantitation of migration lengths was performed using ImageJ software to trace the pathway from ventricular zone to identified motor neurons using knowledge of the curved nature of the pathway following γ-catenin (L127A) expression.

Divisional mixing index. The divisional mixing index was calculated by focusing on one LMCl cell at a time and counting the number of LMCm that were immediately adjacent to it. The control side of the spinal cord and control electroporations resulted in close to 100% of such cells having no LMCm cells surrounding them. These results were quantitated for at least five different embryos of each phenotype and presented as mean ± SEM percentages in each bin of the mixing index.

Results

LMC neurons migrate in an orderly series during divisional segregation

We first characterized the timing of LMC formation as a nucleus in the ventral horn through analysis of the expression of transcription factors that define divisions of the LMC. At lumbar spinal cord levels, expression of the forkhead transcription factor Foxp1 identifies the LMC (Dasen et al., 2008; Rousso et al., 2008). Further, expression of the LIM homeodomain factor Islet-1 identifies neurons of the LMCm (Tsuchida et al., 1994). Neurons of the LMCl express Hb9 (William et al., 2003). The expression of these transcription factors persists through the migratory phase of LMC formation (Tsuchida et al., 1994; William et al., 2003; Dasen et al., 2008; Rousso et al., 2008). Neurons of the medial motor column, which project axons to axial or body wall muscles, coexpress both Islet-1 and Hb9 but do not express Foxp1 (Dasen et al., 2008; Rousso et al., 2008).

More than 95% of LMC neurons are born within the 24 h period before HH (Hamburger and Hamilton, 1992) stage (st) 23, with the peak generation of LMCm in rostral lumbar regions from st18 to st20 and LMCl occurring at st20 and st21 (Hollyday and Hamburger, 1977; Whitelaw and Hollyday, 1983). We thus assessed the time course of motor neuron migration from st23 to st27. Consistent with previous studies, we found that at HH st23, LMCm neurons dominate in the ventral horn with the majority of LMCl neurons found medial to this group (Fig. 1 A–C) (Lin et

al., 1998; Sockanathan and Jessell, 1998; William et al., 2003). LMCl neurons were first detected in the lateral ventral horn at approximately st24 (data not shown) and divisional segregation continued until approximately st27 (Fig. 1 D–I, summarized in Fig. 1 J–L). Therefore, ~24 h appears to be required for the migration of a given LMCl neuron, with LMCl migration extending over a continuous 48 h period after they are generated. Thus, LMCl neurons initiate their migration in an ordered series during divisional segregation.

γ-Catenin and α-catenin are expressed by the LMC during divisional segregation

We next characterized the expression of classical cadherin signaling components during the stages of motor neuron migration and divisional segregation (Nollet et al., 2000; Zhurinsky et al., 2000a; Hirano et al., 2003; Yamada et al., 2005; Uemura and Takeichi, 2006). We focused our attention on the cytoplasmic binding partners for classical cadherins, which play roles critical to cadherin function, α-catenin, β-catenin, and γ-catenin. We found that α-catenin is expressed in most neurons in the spinal cord and appeared to be expressed in all spinal motor neurons, including the LMC, at all stages analyzed (st20–st32; Fig. 2 A,B; data not shown). γ-Catenin was also found in the majority of LMC neurons on both their soma and axons from the time of their first generation to at least HH st32 (Fig. 2 C–J; data not shown).

β-Catenin is expressed by transitin radial glia in the ventral spinal cord

In contrast to α- and γ-catenin, β-catenin expression was found in a radial pattern within the ventral horn (Fig. 3A). β-Catenin transcript was predominantly found in cells (~14 per section) in a line approximately parallel to the ventricle within the ventral part of the spinal cord, at the ventricular surface, and in the floor plate (Fig. 3B–E). This expression persisted from st21 to at least st29. Outside of this ventricular zone expression, only low levels of β-catenin could be found in only a small number of cells within the ventral horn; this became more apparent after st26. Within more dorsal regions of the spinal cord, β-catenin was detected in the majority of cells (Fig. 3C–E). Outside the spinal cord, β-catenin expression was also observed at the ventral root exit points (Fig. 3B, arrow).

We asked whether the ventral line of cells that express β-catenin progress through the cell cycle. A 1 h pulse of BrdU was applied to embryos at HH st22 and subsequent immunohistochemistry for BrdU and in situ hybridization for β-catenin was performed. We found that ~30% of BrdU^{+ve} cells were colabeled with β-catenin, suggesting that β-catenin-expressing cells synthesize DNA but that only a subset of progenitor cells express detectable levels of β-catenin (Fig. 3F). We also confirmed that γ-catenin is predominantly expressed within motor neurons while β-catenin is excluded from mo-
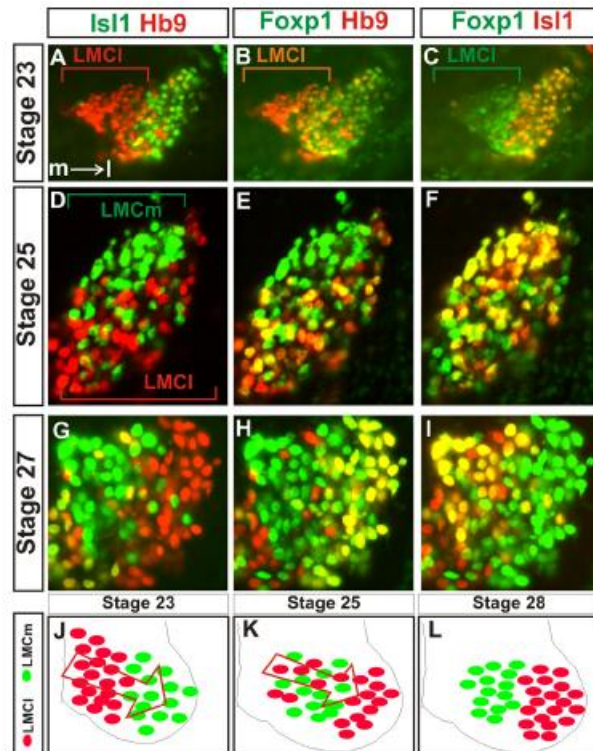

Figure 1. Time course of LMC divisional segregation. *A–C*, Expression in the ventral horn of a stage 23 embryo of Islet-1 and HB9 (*A*), Hb9 and Foxp1 (*B*), and FoxP1 and Islet-1 (*C*). Foxp1 marks the entire lateral motor column. Hb9 and Islet-1 are LMC divisional markers. LMCl cells are, at this stage, more medial to the LMCm cells. *D–F*, Ventral horn expression at stage 25 of the divisional markers Hb9 (*D, E*) and Islet-1 (*D, F*) and the LMC marker Foxp1 (*E, F*). Note that LMCl and LMCm cells are intermingled. *G–I*, Columnar segregation is largely complete by stage 27 as assessed by ventral horn expression of Foxp1 (*H, I*), Islet-1 (*G, I*), and Hb9 (*G, H*). *J–L*, Summary of the migration of LMCl cells through LMCm cells during motor neuron divisional segregation at st23 (*J*), st25 (*K*), and st28 (*L*).

tor neurons by double immunofluorescence of the two proteins (Fig. 3G–I).

The expression of β-catenin within a subset of progenitor cells suggested that the radial staining of β-catenin could be within radial glia. Within the chick spinal cord, radial glia express the intermediate filament protein transitin (Cole and Lee, 1997). Double immunofluorescence staining indicated a colocalization of transitin-expressing radial fibers and β-catenin within the ventral spinal cord (Fig. 3J–R). Within the ventral horn, transitin immunofluorescence at HH st26 showed an average of 14 (modal value; range 12–15) glial fibers (Fig. 3S), similar to the number of β-catenin cells observed in the ventral ventricular zone. Together, this suggests that β-catenin is predominantly expressed in transitin radial glia in the ventral spinal cord and that these radial glia represent a subset of ventral progenitor cells.

Transitin radial glia mark pathways of motor neuron migration

We further characterized the transitin/β-catenin radial glia by asking whether the pathways of migration of LMC neurons coincide with them. We identified subsets of migrating LMCl motor neurons through injection of the retrograde axonal tracer, HRP,
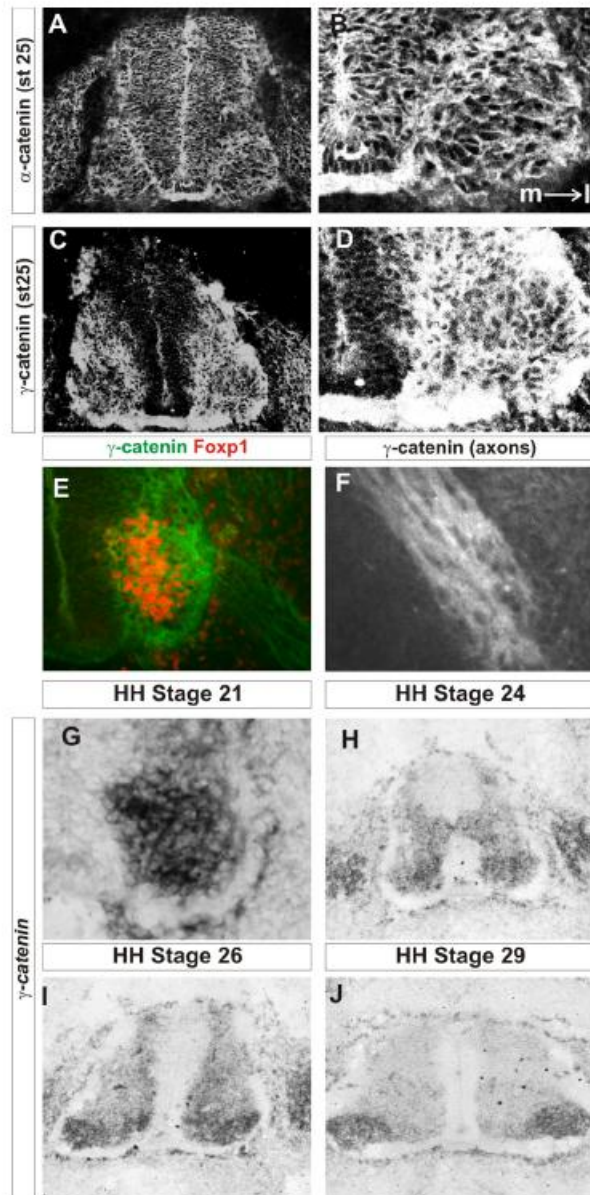
Figure 2. α-Catenin and γ-catenin are expressed in the lateral motor column during motor neuron migration. *A*, *B*, α-Catenin immunofluorescence in the lumbar spinal cord at st25. The whole spinal cord is shown in *A*. The ventral horn is shown in *B*. Medial is to the left, as shown in *B*. *C*, *D*, γ-Catenin immunofluorescence in the lumbar spinal cord at st25. The whole spinal cord is shown in *C*. The ventral horn is shown in *D*. Medial is to the left. *E*, γ-Catenin is expressed within the LMC, as marked by Foxp1 expression. *F*, γ-Catenin immunofluorescence in motor axons. *G*, γ-Catenin transcript expression in the ventral horn of stage 21 lumbar spinal cord. *H–J*, Lumbar spinal cord expression of γ-catenin transcript at st24 (*H*), st26 (*I*), and st29 (*J*).

lyzed within the LMCm), transitin fibers and migrating motor neurons were closely juxtaposed (Fig. 3*T*). Additionally, we found evidence of motor axons following the paths of transitin radial glia (Fig. 3*U*). This suggests that transitin/β-catenin radial glia mark the pathways of LMC migration during LMC divisional segregation.

Overexpression of γ-catenin leaves LMC organization unperturbed

We focused our attention on γ-catenin as motor neurons express it predominantly. We cloned a full-length cDNA of chick *γ-catenin* and found that the transcript was 86% identical to that of human *γ-catenin* and its amino acid sequence was 89% identical (94% similar) to that of human γ-catenin. Additionally, chick γ-catenin was 69% identical (89% similar) to chick β-catenin, illustrating the high level of conservation between these two armadillo family members (data not shown). We expressed wild-type γ-catenin by *in ovo* electroporation (Momose et al., 1999) and confirmed expression of the protein, noting in particular its presence at the apical surface of the ventricular zone (data not shown). Overexpression of γ-catenin (marked by nuclear β-galactosidase immunoreactivity in Fig. 4*A*) or the empty DNA vector had no observable effect on the total number of motor neurons or the position of those motor neurons in the ventral horn or the segregation of LMCl and LMCm divisions (Fig. 4*A*,*B*; data not shown). This suggests that the levels of γ-catenin are saturating with regard to a role in motor neuron migration.

Expression of a point mutation in γ-catenin

Previous work identified a 29 amino acid region of γ-catenin that is both necessary and sufficient for binding to α-catenin (Aberle et al., 1996). This region is highly conserved between different species with only one replacement (to a similar amino acid) between chicken and human γ-catenin. Additionally, single amino acid mutations in this region can reduce binding to α-catenin to background levels (Aberle et al., 1996). We reasoned that expression of γ-catenin containing such a mutation might uncouple cadherin–catenin interaction, thus abrogating cadherin function. We generated a single amino acid substitution of chick γ-catenin of L127-A, γ(L127A), which is located in the α-catenin binding domain of γ-catenin and reduces this binding to <2% of the wild-type γ-catenin for the human protein (Aberle et al., 1996). We expressed γ(L127A) by *in ovo* electroporation, confirming its misexpression by immunofluorescence (Fig. 4*C*,*D*; electroporated cells are marked by nuclear β-gal staining in

into the dorsal limb mesenchyme at st25. Migrating motor neurons were identified by their location within the LMCm domain at the time of analysis. Confocal analysis of 0.15-μm-thin optical sections revealed that in all cases (50/50 HRP^{+ve} neurons ana-

226

β-catenin (st 25) | **β-catenin (st 21)** | **HH Stage 24**
HH Stage 26 | **HH Stage 29** | **β-catenin BrdU**
γ-catenin | **β-catenin** | **β-catenin γ-catenin**
Transitin β-catenin | **β-catenin** | **Transitin**
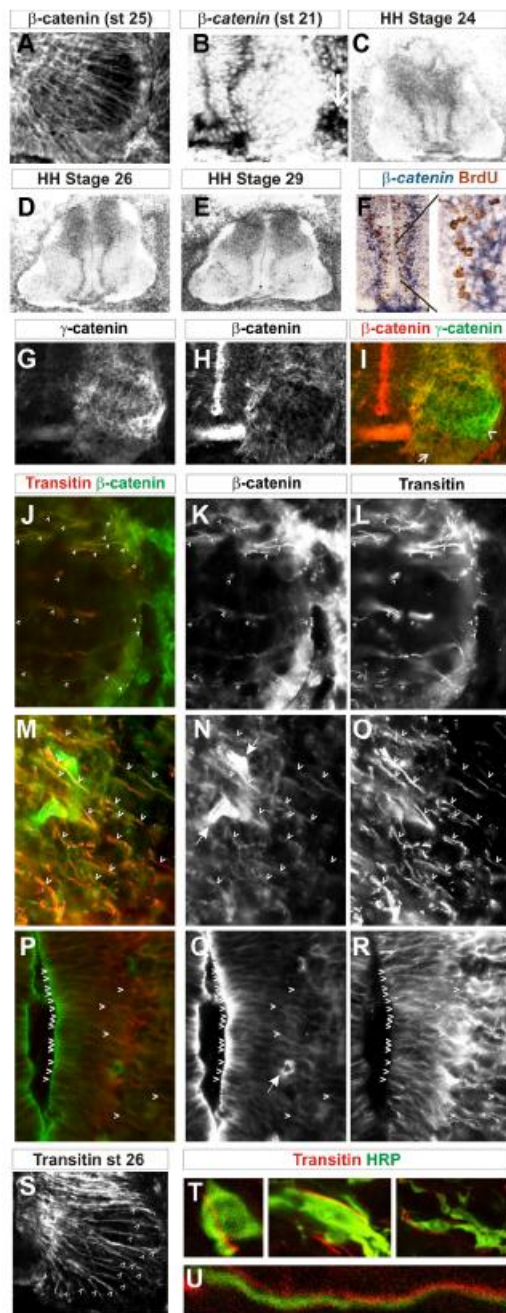**Transitin st 26** | **Transitin HRP**

Figure 3. β-Catenin is expressed in transitin radial glia. *A*, β-Catenin immunoreactivity in the ventral horn of a stage 25 embryo. *B–E*, β-Catenin transcript expression in stage 21 ventral spinal cord (*B*), stage 24 (*C*), stage 26 (*D*), and stage 29 (*E*) lumbar spinal cords. *F*, BrdU expression (brown) with β-catenin transcript (blue) following a 1 h pulse application of BrdU to a stage 23 embryo. Right, Magnification of the area shown by the black lines. *G–I*, Double immunofluorescence of γ-catenin (*G, I*) and β-catenin (*H, I*) at stage 25. *I*, Arrow, β-Catenin expression in radial glia; arrowhead, γ-catenin expression in motor neurons. *J–R*, β-Catenin (*J, K, M, N, P, Q*) and transitin (*J, L, M, O, P, R*) localization at stage 26 in the ventral horn (*J–L*), intermediate part of the ventral spinal cord (*M–O*), and ventral ventricular zone (*P–R*). Arrowheads, Regions of colocalization in radial glia. *N, Q*, Arrows, Blood vessel expression of β-catenin. *S*, Transitin immunofluorescence in the ventral spainal cord of a st26 embryo. Arrowheads, Individual transitin radial glia processes. *T, U*, Confocal sections (0.15 μm) showing HRP labelling of migrating motor neurons (green) and transitin (red) expression following retrograde tracing of LMCl cells. *T*, Cell bodies of five different motor neurons are shown. Note the close apposition of the motor neurons to the transitin fibers. *U*, Motor axons could also be observed in close apposition to transitin radial glial processes.

D). γ(L127A) expression should result in a delocalization of adherens junctional complexes, which depend on interaction with the actin cytoskeleton via α-catenin. We found that the apical expression of β-catenin in radial glia in the dorsal spinal cord was disrupted following γ(L127A) expression (Fig. 4*E,F*), consistent with its predicted mode of action. α-Catenin binds to the tight junction protein ZO1 and disruption of cadherin function follows disruption of ZO1 binding to the cadherin complex (Itoh et al., 1997; Imamura et al., 1999). We thus followed the localization of ZO1 protein expression following γ(L127A) expression and again found that its localization to the apical end-feet of radial glia was disrupted (Fig. 4*G,H*). Together, these data suggest that γ(L127A) disrupts cadherin function most likely through uncoupling the cadherin–catenin complex.

Following γ(L127A) expression, the total number of LMCm and LMCl motor neurons (56 ± 5 and 58 ± 3 motor neurons per section, respectively) was not significantly different to the control side of the spinal cord (62 ± 6 and 55 ± 5 per section, respectively; $p > 0.05$, Student's t test), indicating that the general differentiation of LMC divisions was not perturbed. We did, however, observe an ~50% decrease in the number of medial motor column neurons when γ(L127A) was expressed (25 ± 3 vs 15 ± 2; control vs experimental; $p < 0.05$, Student's t test). Application of BrdU to embryos from st23 to st27, following γ(L127A) expression, revealed that LMC neurons were born before stage 23, as is found in wild-type embryos (Fig. 4*I,J*). Thus, the major program of LMC differentiation in terms of neuron number within each division and the timing of motor neuron generation is not perturbed by γ(L127A) expression. This finding allowed us to investigate the role of γ(L127A) expression on LMC divisional segregation.

LMC neuron position and divisional segregation is perturbed by γ(L127A) cell autonomously

LMC divisional segregation is normally complete before st29, 4 d after the first generation of LMC neurons. We thus investigated the effect of γ(L127A) expression on divisional segregation at st29. Following γ(L127A) expression, we observed a striking perturbation of LMC neuron positioning. In contrast to the control, nonelectroporated side of the spinal cord (Fig. 4*K–N*), the area encompassing the LMC was greatly expanded (over twofold) with neurons of both LMCl and LMCm found close to the ventricle. Divisional segregation was also severely disrupted with many of the Hb9^{+ve}/Islet-1^{-ve} LMCl neurons located in a position medial to the Hb9^{-ve}/Islet-1^{+ve} LMCm neurons (Fig. 4*K*, arrows). We also observed mixing of LMCm and LMCl with LMCl neurons found within the domain normally occupied by LMCm neurons.

We quantitated LMCl cell body position by considering the percentage of neurons that were located in three defined mediolateral bins in the ventral spinal cord, bin 1 being most
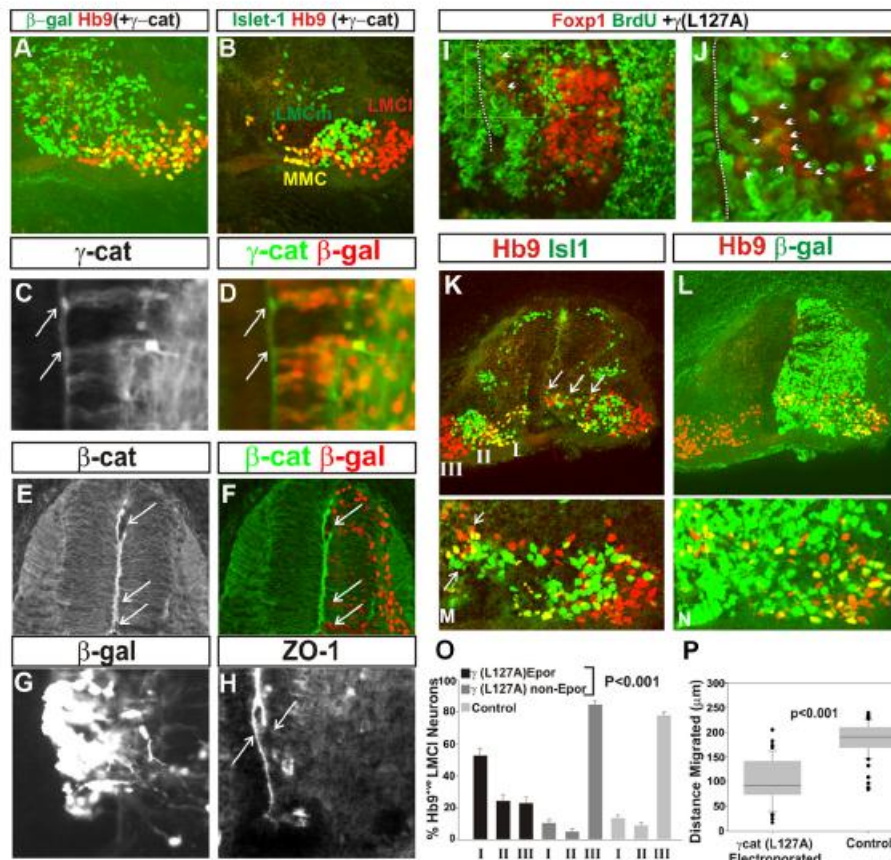
227

Figure 4. γ-Catenin (L127A) expression disrupts LMC migration and divisional segregation. *A, B,* Lack of effect of γ-catenin overexpression on divisional segregation at stage 29. Cells that had been electroporated are marked by β-gal immunoreactivity (*A,* green). Hb9 (*A, B*) and Islet-1 (*B*) mark the medial motor column (MMC), LMCl, and LMCm in the ventral horn. *C, D,* Expression of γ-catenin (L127A) viewed by γ-catenin immunoreactivity. Electroporated cells are marked by β-gal immunofluorescence (*D,* red). Arrows, Apical expression of γ-catenin at the ventricle surface. *E, F,* Disruption of β-catenin apical expression following γ-catenin(L127A) expression. Arrows, Regions of disruption. *G, H,* Disruption of ZO1 apical expression following γ-catenin(L127A) expression. *H,* Left arrow, ZO1 apical expression on the contralateral spinal cord; right arrow, disruption on the electroporated side of the spinal cord. *I, J,* The ventral spinal cord after electroporation with γ-catenin (L127A) at st18. Foxp1 (red) and BrdU (green) expression after BrdU application from st23 to st28. No colocalization of motor nuclei with BrdU was observed, indicating that all motor neurons had been born before st23 following γ-catenin(L127A) expression. *J,* Magnification of boxed area in *I. I, J,* Dotted lines, Midline; arrows, Foxp1 nuclei stalled in their migration and are unlabeled by BrdU. *K–N,* Effects of γ-catenin(L127A) expression on divisional segregation in st29 lumbar spinal cords. *K, L,* The left side of the spinal cord is unelectroporated (β-gal immunofluorescence is absent; *L*). *K,* LMCm and LMCl segregate normally on the left side, as viewed with Hb9 (red) and Islet-1 (green) immunofluorescence. Following γ-catenin(L127A) expression on the right side of the spinal cord, LMCl and LMCm segregation was perturbed. The LMC spread over a much larger area than the control, with LMC cells found close to the ventricle and LMCl and LMCm cells intermingled. *K,* Arrows, Some of the LMC cells that stalled in their migration. *M, N,* Ventral horn of a different embryo electroporated by γ-catenin(L127A) showing that both LMCm and LMCl were affected; the midline as at the left side of the panel. *M,* Arrows, Some of the LMCm and LMCl cells close to the ventricle surface. *K,* I, II, III, Regions quantitated in *O. O,* Quantitation of LMCl neuron position in bins illustrated in *K. P,* Quantitation of distance migrated by γ-catenin(L127A)-expressing LMCl neurons compared with those on the electroporated (Epor) side of the spinal cord that did not express γ-catenin(L127A). Error bars are SEM.

medial and bin III the most lateral (Fig. 4*K*). Expression of γ(L127A) results in a mosaic misexpression due to stochastic incorporation of the electroporated construct (indicated by nuclear-localized β-galactosidase). We could thus quantify the cell autonomy of mispositioning of LMC cells in relation to their expression of γ(L127A) (Fig. 4*O*). In bin I, 54 ± 3% of LMCl neurons and 20% of LMCm neurons that had acquired γ(L127A) were found, compared with 12% and 3% respectively on the control side of the spinal cord ($p < 0.001$, Student's *t* test). In contrast, 85 ± 4% of Hb9^{+ve}/Islet-1^{-ve}/β-gal^{-ve} LMCl neurons were located in bin III, similar to that found in the control ventral horn ($p > 0.1$, Student's *t* test; Fig.

2*K*). Additionally, ~25% of Hb9^{+ve}/Islet-1^{-ve}/β-gal^{+ve} LMCl neurons were found within the LMCm, indicating that divisional mixing also occurs following γ(L127A) expression. These data are consistent with a cell autonomous perturbation of LMC divisional segregation and motor neuron positioning in response to γ(L127A) expression.

We next quantitated the distance migrated by either Hb9^{+ve}/Islet-1^{-ve}/β-gal^{+ve} or Hb9^{+ve}/Islet-1^{-ve}/β-gal^{-ve} cells. We found that LMCl cells expressing γ(L127-A) had migrated approximately half the distance of controls (Fig. 4*P*). This suggests that LMC cell body positioning defects are due to a perturbation in the distance migrated by the cells.
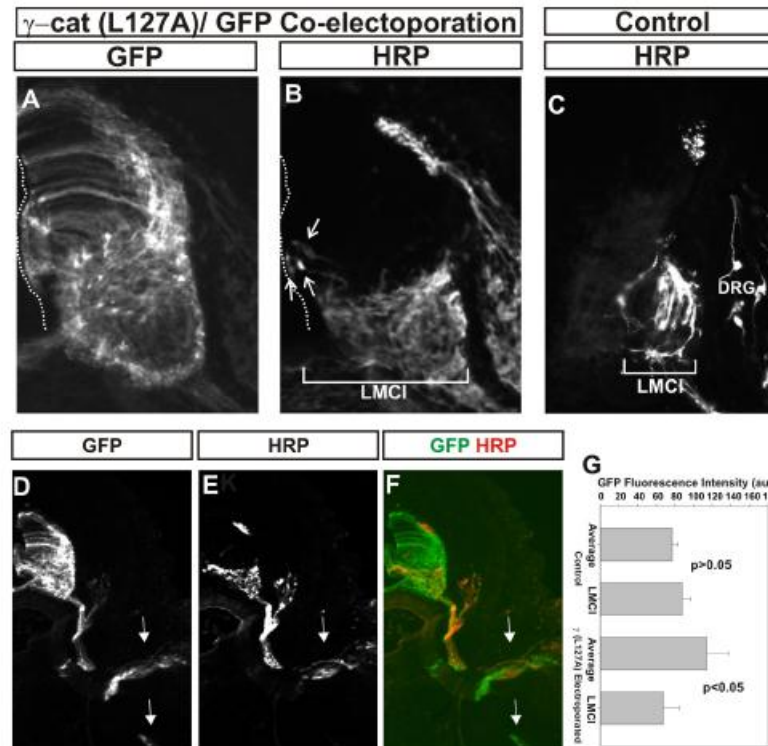
Figure 5. Motor neuron projections appear normal following γ-catenin (L127A) expression. GFP and γ-catenin(L127A) were coelectroporated at stage 18 and HRP was injected into the dorsal limb at stage 29. *A, B*, GFP (*A*) and HRP (*B*) immunofluorescence in one section. *B*, Arrows, Motor neurons close the ventricular surface that projected into the dorsal limb. *A, B*, Dotted lines, Ventricle surface. *C*, HRP retrograde labeling in control embryos. *B, C*, Bars, Mediolateral extent of retrogradely labeled motor neurons. Note that the bar in *B* is more than twice as long as the one in *C*. *D–G*, GFP immunofluorescence is more intense medially in the spinal cord than in controls following γ-catenin(L127A)/GFP coelectroporation. *D, F*, GFP immunofluorescence. *E, F*, HRP immunofluorescence. *G*, Quantitation of average GFP immunofluorescence in the spinal cord versus that found in the lateral LMC following GFP or γ-catenin(L127A)/GFP coelectroporation. GFP fluorescence is lower in the lateral ventral horn following γ-catenin(L127A) expression, consistent with a defect in motor neuron migration. *D–F*, Arrows, Motor axon tracks to dorsal and ventral limb. Note that GFP is present in both, whereas HRP immunofluorescence is exclusively in the dorsal limb tracks. Error bars are SEM.

Stalled LMCl neurons project axons into the limb normally

The perturbation of LMC neuron positioning prompted us to ask whether motor axon trajectory proceeded normally following γ(L127A) expression. To address this, we injected HRP into the dorsal limb mesenchyme at HH st28 to trace LMCl cell body position following coexpression of γ(L127A) and GFP, the latter to trace motor neuron cell body and axon position. We found that following γ(L127A)/GFP coexpression, the region of the spinal cord occupied by HRP [+ve] cells was increased compared with controls (Fig. 5A–C). Particularly notable was the presence of HRP labeling in neurons located close to the ventricle (Fig. 5B, arrows). This indicated that the mispositioned LMCl neurons still project axons to the dorsal limb. In contrast, axonal GFP was not restricted to the dorsal limb mesenchyme, suggesting normal axon trajectories of LMCm and LMCl cells following γ(L127-A) expression (Fig. 5D–F, arrows). Additionally, we noted that within the ventral spinal cord, GFP fluorescence was enhanced medially compared with control expression of GFP alone (Fig. 5G), consistent with the cell autonomous perturbation of LMCl position following γ(L127A) expression. This further suggests that the normal program of LMC differentiation occurs following expression of γ(L127A) despite aberrant motor neuron positioning.

γ-Catenin (L127A) expression does not perturb dorsal interneuron positioning

The predominant expression of γ-catenin is within the ventral horn. We thus asked whether the observed migration defect following γ(L127A) expression is specific to the ventral spinal cord. We investigated the effect of γ(L127A) expression on the positioning of both interneurons and motor neurons within the spinal cord at st29 through Lhx1 expression, a LIM homeodomain transcription factor expressed within the LMCl and also within the majority of interneurons within the spinal cord. We also assessed the positioning of the subset of dorsal commissural interneurons that express Islet-1. Consistent with previous results, following γ(L127A) expression, we detected a large number of Lhx1 [+ve] cells adjacent to the ventral ventricular surface with a concomitant reduction in the number of Lhx1 [+ve] cells in the lateral ventral horn (Fig. 6A–C). However, we saw no defect in positioning of either Lhx1 [+ve] or Islet-1 [+ve] dorsal interneurons following γ(L127A) expression (Fig. 6B,C, right arrows). These data suggest that the mispositioning of neurons following γ(L127A) expression is specific to the ventral region of the spinal cord and does not result in a general perturbation of cell body positioning in the spinal cord.

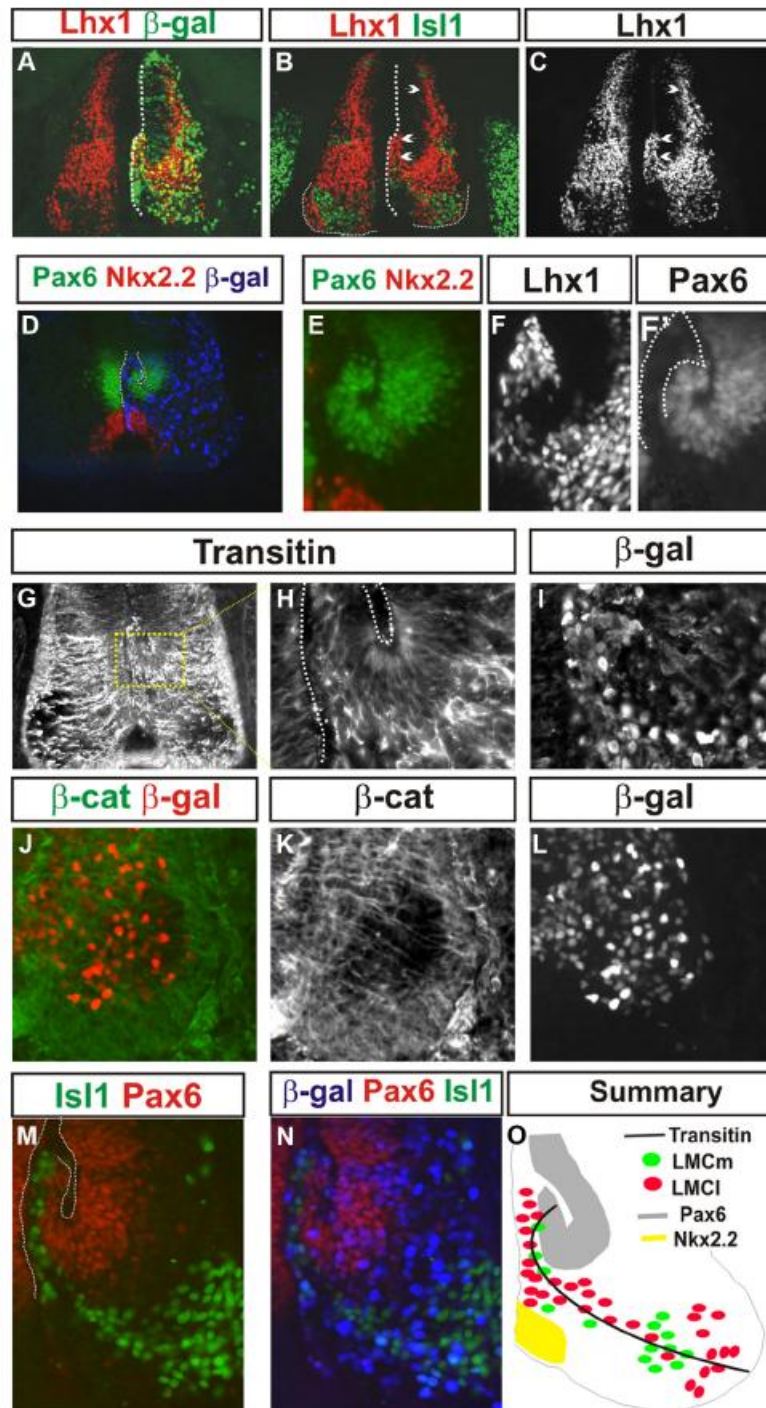**Figure 6.** Stalled motor neuron migration results in bucking of the ventral Pax6 domain following γ-catenin(L127A) expression. *A–C*, Lhx1-expressing ventral interneurons and LMCl neurons (*B*, *C*, left-pointing arrowheads) and islet-1 cells (*J*) are found close to the ventricle (*A*, *B*, dotted lines). Electroporated neurons are marked by β-gal immunofluorescence (*Figure legend continues.*)

Stalled LMC migration causes the motor neuron progenitor domain to buckle

The location of Lhx-1 $^{+ve}$, Islet-1 $^{+ve}$/Hb9 $^{-ve}$, and Islet-1 $^{-ve}$/Hb9 $^{+ve}$ cells close to the ventricle following γ(L127A) expression prompted us to investigate the integrity of the spinal progenitor cells within the ventricular zone at these later stages of spinal cord development. We analyzed the expression at st28 of homeodomain transcription factors expressed within ventral progenitor domains, specifically Pax6 and Nkx2.2, which label adjacent domains (Briscoe et al., 2000). On the γ(L127A) electroporated side of the spinal cord, the v3 (Nkx2.2) progenitor domain was found in a normal ventral position, adjacent to the floor plate. (Fig. 6 D,E). In contrast, the ventral part of the Pax6 domain folded medially and dorsally such that its more ventrolateral aspect was closer to the ventricle (Fig. 6 D,E). We noted that in many embryos it was only the stalled motor neurons and not the ventral Pax6 domain that was electroporated. This suggested that the buckling of the Pax6 domain is a noncellautonomous effect most likely mediated by γ(L127A) expression in motor neurons. The position of stalled ventral Lhx1 cells fits between the Pax6 domain and the ventricle surface (Fig. 6 F,F'). The length of the Pax6 domain as a coherent group of cells was, however, similar to the control side of the spinal cord (239.6 ± 8.4 μm vs 240.6 ± 7.8 μm; $p > 0.1$, Student's t test). Additionally, the dorsal part of the Pax6 domain resided in a normal position. At this stage, a small number of Pax6 cells were found in the mantle zone of the spinal cord, presumably having migrated from the ventricular zone. We observed that following γ(L127A) expression, the total number of these cells was not significantly different from the control side of the spinal cord (13 ± 1 vs 13 ± 3 cells per section; $p > 0.1$, χ^2 test). This suggests that the general integrity of the Pax6 progenitor domain is not affected by γ(L127A) expression.

Transitin/β-catenin radial glia still traverse to the ventral horn following γ(L127A) expression

Because of the bucking of the ventral Pax6 progenitor domain, we investigated the morphology of transitin radial glia fibers in the vicinity of stalled motor neurons. We found that in the ventral spinal cord, transitin/β-catenin fibers still course from the ventricular zone to the pial surface within the ventral horn (Fig. 6 G–L). However, the folded nature of the ventral Pax-6 domain resulted in these fibers first taking a ventral and then lateral route

←

(*Figure legend continued.*) (*A,* green). *B, C,* Right-pointing arrowheads, Absence of effect on dorsal interneuron populations. *D, E,* The ventral Pax 6 (green) progenitor domain buckles following γ-catenin(L127A) expression but the Nkx2.2 (red) domain is unperturbed. Electroporation is marked by β-gal immunofluorescence (*D,* blue). *D,* Dotted lines, Ventricle surfaces. *E,* Magnified image of the ventral progenitor domains of the right side of the spinal cord in *D.* Note that the electroporated cells (stalled LMC neurons) are close to the ventricle, whereas the majority of the buckled ventral Pax6 domain is not electroporated. *F,* Lhx1 immunofluorescence focusing on the ventricular zone of the adjacent section to that shown in *D* and *E. F',* Position of the Lhx1 cells (outlined by the dotted lines) in relation to the Pax6 domain of *E. G–I,* Transitin immunofluorescence (*G, H*) following electroporation of γ-catenin(L127A). The right side of the spinal cord in *G* was electroporated. *H, I,* Magnified images of the dotted box in *G. H,* Dotted lines, Ventricle surfaces. *I,* β-Gal immunoreactivity showing electroporated cells. *J–L,* β-Catenin (β-cat; *J, K*) immunofluorescence in radial glia in the ventral horn at stage 25 after γ(L127A) expression marked by β-gal immunoreactivity in *J* and *L. M, N,* Islet-1 (green) and Pax6 (red) immunofluorescence at stage 26 following γ-catenin(L127A) expression, showing that motor neurons stalled in their migration are found adjacent to the bucked Pax6 domain (as in *F, F'*). Motor neuron position relative to the Pax6 domain is therefore normal. β-gal immunoreactivity (*N,* blue) shows electroporated neurons. *O,* Summary of the data in this figure showing the relative positions of transitin radial glia, progenitor domains, and LMC neurons following γ-catenin(L127A) expression.

(Fig. 6 G,H). Related to the Pax6 domain, the position of stalled LMC neurons located close to the ventricle were, however, normal (Fig. 6 M,N). This indicates that motor neurons adjacent to the ventricular surface are not within the ventricular zone itself, as defined by the expression of Pax6. Thus, following γ(L127A) expression, the pathway of migration of spinal motor neurons still follows the course outlined by transitin $^{+ve}$ fibers (Summarized in Fig. 6 O).

Cadherin dominant-negative expression stalls migration of LMC neurons

The effects of γ(L127A) expression suggests a cadherin dependence of γ-catenin function in LMC neuron migration and divisional segregation. We therefore asked whether uncoupling cadherin function from intracellular binding to γ-catenin also perturbed motor neuron divisional segregation. Expression of a truncation of the extracellular domain of N-cadherin, NΔ390, has been shown to act in a cadherin dominant-negative fashion by sequestering endogenous β- or γ-catenin (Fujimori and Takeichi, 1993). Expression of NΔ390 from st18 caused a phenotype similar to γ(L127A) expression, albeit at a reduced level (Fig. 7 A–F). In contrast to γ(L127A) expression, we did, however, observe a small decrease (~20%) in the total number of motor neurons cells (64 ± 2 Hb9 cells vs 73 ± 2; $p < 0.05$, χ^2 test; 39 ± 2 vs 50 ± 2 Islet-1 cells per section; $p < 0.05$, χ^2 test). Similar to γ(L127A) expression, NΔ390 expression left the LMC spread over a greater area, approximately double that of controls. Additionally, we found ~5% of both LMCl and LMCm cells adjacent to the ventricular surface (Fig. 7 G). We quantitated divisional segregation of LMCl and LMCm and found that LMCl cells mingled throughout the LMCm division (Fig. 7 H), consistent with a perturbation of LMC migration.

Further, similar to γ(L127A) expression, we observed a dorsomedial folding of the ventral Pax6 progenitor domain. However, we noted that the extent of folding of the ventricular zone following NΔ390 expression was smaller than that following γ(L127A) expression, consistent with the reduced effect of NΔ390 compared with γ(L127A) expression (Fig. 7 I–K). Additionally, similar to γ(L127A) expression, the pathway of transitin $^{+ve}$ radial glia mirrored the perturbed LMC neuron position and were still associated with the ventricle surface (Fig. 7 L–N). Thus, the essential features of the phenotype of γ(L127A) expression on LMC migration were captured by expression of a cadherin dominant-negative. Together, these results suggest that catenin-dependent cadherin function is necessary for the correct radial migration of spinal motor neurons.

Canonical Wnt signaling does not influence LMC migration

The perturbations of cadherin and catenin function described here have the potential to alter canonical Wnt signaling (Nelson and Nusse, 2004). We thus asked whether direct perturbations of Wnt signaling alter motor neuron migration and LMC divisional segregation. We expressed constructs *in vivo* that have been shown to result in the upregulation or downregulation of canonical Wnt signaling (Roose et al., 1999; Krylova et al., 2000; Zhurinsky et al., 2000b). Expression of either wild-type β-catenin (Fig. 8 A–D) or a truncated version of β-catenin [β-cat-1-ins (Zhurinsky et al., 2000b); Fig. 8 E–H] or a dominant-negative GSK3β construct (Fig. 8 I–L) resulted in no observable difference in motor neuron migration compared with the control, unelectroporated side of the spinal cord. Thus, constructs that upregulate Wnt signaling have no effect on LMC divisional segregation.
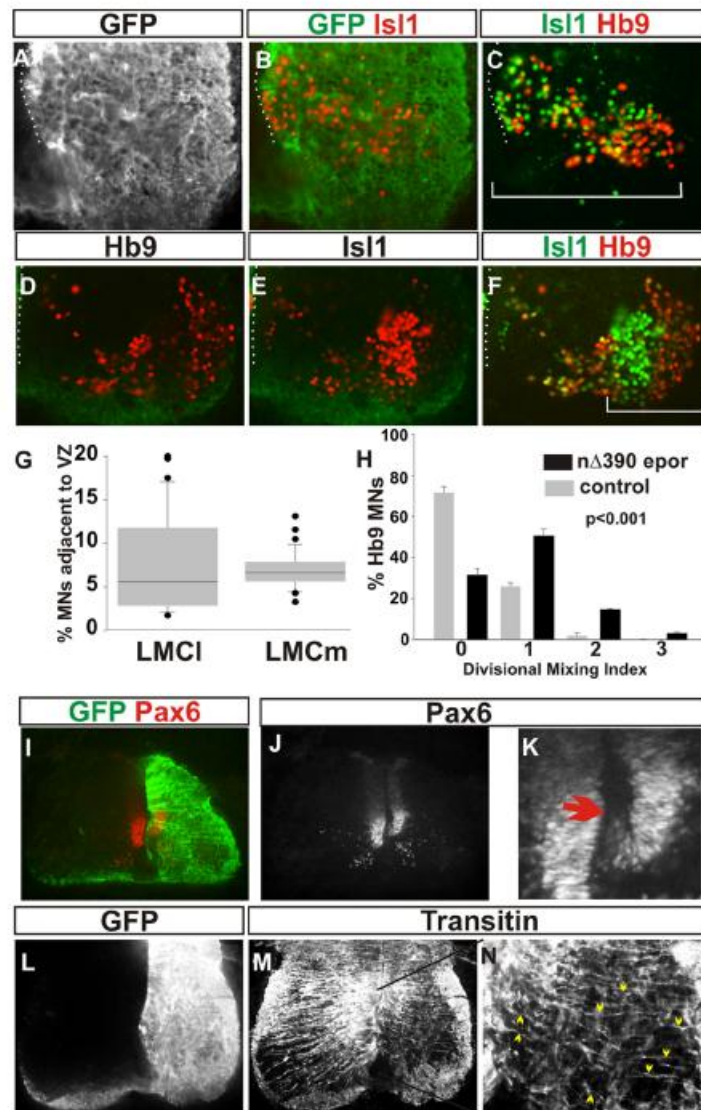
Figure 7. NΔ390 dominant-negative cadherin expression results in a similar phenotype to γ-catenin(L127A) expression in disruption of LMC divisional segregation. **A–C**, GFP, Islet-1, and HB9 immunoreactivity following NΔ390 cadherin expression shows stalled motor neurons (MNs) and perturbed divisional segregation of the LMC. **D–F**, Hb9 and Islet-1 immunoreactivity on the contralateral LMC. **A–F**, Dotted lines, Ventricular surface. **C**, **F**, Solid lines, Mediolateral extent of the LMC. Note that following NΔ390 cadherin expression, the LMC spans approximately twice the extent of the contralateral LMC. **G**, Percentage of Hb9 and Islet-1 cells adjacent to the ventricular zone (VZ) following NΔ390 cadherin expression. Contralateral spinal cords have no cells in similar positions. **H**, Divisional mixing index following NΔ390 cadherin expression compared with contralateral spinal cord (Student's t test of bins 0, 1, and 2, $p < 0.001$; χ^2 test, $p < 0.001$ of the entire distribution 2df). Error bars are SEM. **I–K**, Pax6 expression following NΔ390 cadherin expression, marked by GFP in **I**. **K**, Magnification of the buckled Pax 6 domain (arrow) in **J**. **L–N**, Transitin immunoreactivity (**M**, **N**) following NΔ390 cadherin expression marked by GFP in **L**. **N**, Magnification of area indicated by black line in **M**. **N**, Arrowheads, Transitin fibers coursing from the ventricle surface to the pial surface of the spinal cord.

observed no differences in spinal motor neuron migration following expression of these constructs. These data suggest that the observed migration and divisional segregation defects following γ(L127A) or NΔ390 expression are not consistent with a perturbation of canonical Wnt signaling.

Cadherin-7 is required for LMC migration and divisional segregation

We have shown that uncoupling general cadherin function intracellularly disrupts divisional segregation by neuronal migration. We sought to manipulate the expression of a single cadherin that was predominantly expressed during LMC migration with little or no expression later in development. To begin to address this, we screened expression of type I and type II cadherin family members for such an expression profile. We found that type I cadherins, including *N*-cadherin, appear excluded from LMC neurons, and instead were found in radial fibers in the ventral horn (Fig. 10*A–D*). In contrast, type II cadherins, including cad-7, cad-12, and cad-20, were expressed in the majority of the LMC at early stages of development (Fig. 10*E–L*) (Luo et al., 2006). Both cadherin-12 and cadherin-20 also have prominent expression within a number of motor neuron pools after divisional segregation (Fig. 10*F,H*) (Price et al., 2002). In contrast, cad-7 was predominantly expressed early during LMC divisional segregation and is downregulated in the vast majority of LMC neurons after divisional segregation is complete (st28; Fig. 10*I–L*) (Price et al., 2002). Therefore, cad-7 is expressed within the majority of the LMC neurons during their migration; we thus focused our attention on its function during LMC divisional segregation (Luo et al., 2006).

To address a role for cad-7 expression in spinal motor neuron migration, we reduced its expression using a previously characterized and successful shRNA approach (Barnes et al., 2010). Following expression of a control cad-7 shRNA construct, visualized by dsRed fluorescence, both migration of LMCm and LMCl cells and their segregation into divisions appeared normal (Fig. 10*M–P*). DsRed fluorescence was also observed laterally as well as medially in the ventral horn (Fig. 10*M*). In contrast, following expression of the cad-7 shRNA construct, cells that had acquired the shRNA were concentrated more medially (Fig. 10*Q*). These data suggest that the cells expressing cad-7 shRNA were perturbed in their migration within the lateral motor column. We next characterized the position of LMCm and LMCl cells following cad-7 shRNA expression. At

Additionally, we sought to downregulate canonical Wnt signaling pathway through the expression of wild-type GSK3β (Fig. 9*A–D*), constitutively active GSK3β (Fig. 9*E–H*), or a dominant-negative TCF construct (Fig. 9*I–L*) (Ciani et al., 2004). Again, we
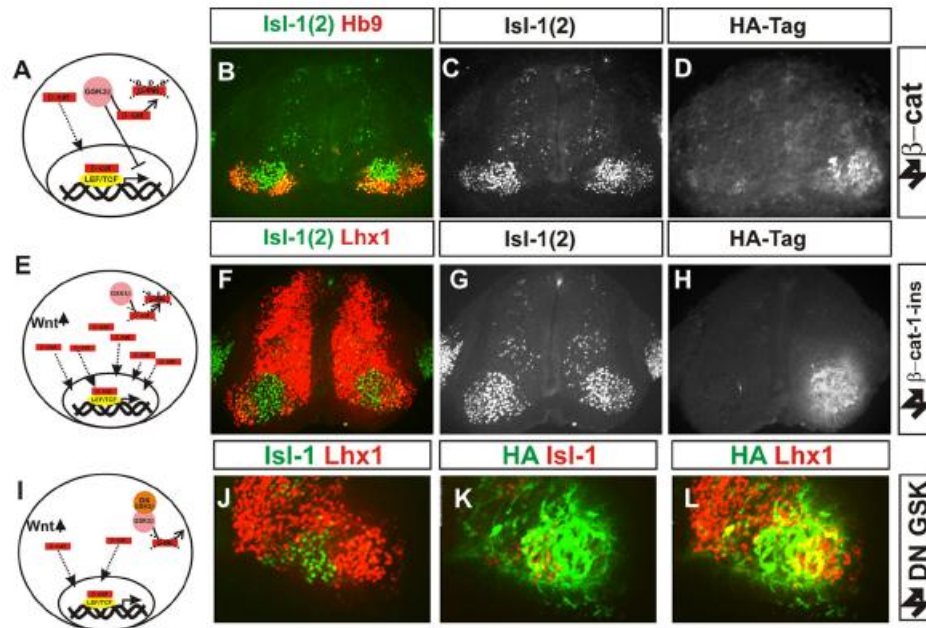
Figure 8. Upregulation of canonical Wnt signaling does not disrupt LMC neuron organization. *A–D*, Overexpression of β-catenin. *A*, Summary of Wnt signaling. *B–D*, Hb9 and Islet-1(2) (*B, C*) immunohistochemistry after β-catenin expression marked by HA immunoreactivity (*D*). *E–H*, Expression of β-catenin-1-ins construct. *E*, Summary of effect to increase Wnt signaling. *F–H*, Lhx1 and islet-1(2) (*F, G*) immunoreactivity after β-cat-1-ins expression marked by HA immunoreactivity (*H*). *I–L*, Lack of effect on LMC organization of expression of a dominant-negative GSK3β construct. *I*, Schematic of action of the construct. *J–L*, HA-tag (*K, L*, green), Islet-1 (*J*, green; *K*, red), and Lhx1 (*J, L*, red) immunoreactivity following electroporation of the construct.

st27, cad-7 shRNA expression resulted in HB9 [+ve] Islet-1 [−ve] LMCl cells located medial to the LMCm (Fig. 10*R–T*). Quantitation of the effect of cad-7 shRNA at st27 showed divisional segregation of LMCm and LMCl was compromised (Fig. 10*U*). Further, at earlier stages (st25), we observed an increase in the number of Islet-1 [+ve] LMCm cells located medially close to the ventricular zone (Fig. 10*V–X*). Together, these data suggest that knockdown of cad-7 stalls the migration of LMC motor neurons and perturbs LMC divisional segregation.

Discussion

Spinal motor neuron migration to the ventral horn is highly organized. More than 95% of motor neurons are born rapidly over ~24 h, whereas their migration occurs over a substantially longer time course (Hollyday and Hamburger, 1977; Whitelaw and Hollyday, 1983; Lin et al., 1998; Sockanathan and Jessell, 1998; William et al., 2003). Thus, because of their rapid generation, a backlog of motor neurons waiting to migrate is formed. Our data (schematized in Fig. 11) suggest that γ-catenin-dependent cadherin function is required for the migration of spinal motor neurons.

Transitin radial glia as a scaffold for motor neuron migration

Within the ventral spinal cord, coexpression of transitin and β-catenin identifies a subset of progenitor cells with characteristics of radial glia. Expression of β-catenin within radial glia demarcates two domains of ventral progenitor cells: apical cells that do not express β-catenin and more basal cells that do express it. Radial migration of spinal motor neurons has previously been inferred (Barron, 1946; Wentworth, 1984; Leber et al., 1990;

Leber and Sanes, 1995; Eide and Glover, 1996) and we suggest that this occurs on transitin radial glia for two reasons. First, retrograde labeling of migrating motor neurons indicated that their migration paths follow transitin radial glia. There are relatively few transitin glia (~14) in the ventral horn and their juxtaposition to migrating motor neurons seems unlikely to result from chance alone. More tellingly, stalled motor neurons were still found along pathways defined by transitin glia following γ(L127A) expression. This would not be predicted by motor neurons taking the most direct route in their migration and strongly suggests that spinal motor neuron migration follows routes labeled by transitin glia.

Motor neuron migration requires γ-catenin function

Both β- and γ-catenin bind to classical cadherins and link their extracellular interactions to intracellular signaling (Hirano et al., 2003), particularly via α-catenin, which provides a bridge for cadherin function to the actin cytoskeleton (Abe and Takeichi, 2008). Generally, it is believed that β-catenin is the major transducer of cadherin signaling intracellularly. We were thus surprised to find that β-catenin is absent from spinal motor neurons. Instead, α-catenin and γ-catenin are the predominant catenins expressed in the LMC. Thus, within the chick LMC, γ-catenin is the major transducer of cadherin function.

Expression of either γ-catenin or γ(L127A) leaves the total number and timing of generation of LMCm and LMCl cells unaffected. Additionally, motor neurons were labeled by retrograde tracing from the limb following γ(L127A) expression, suggesting that the time required for axon growth to the limb [>48 h (Tosney and Landmesser, 1985)] had occurred despite motor
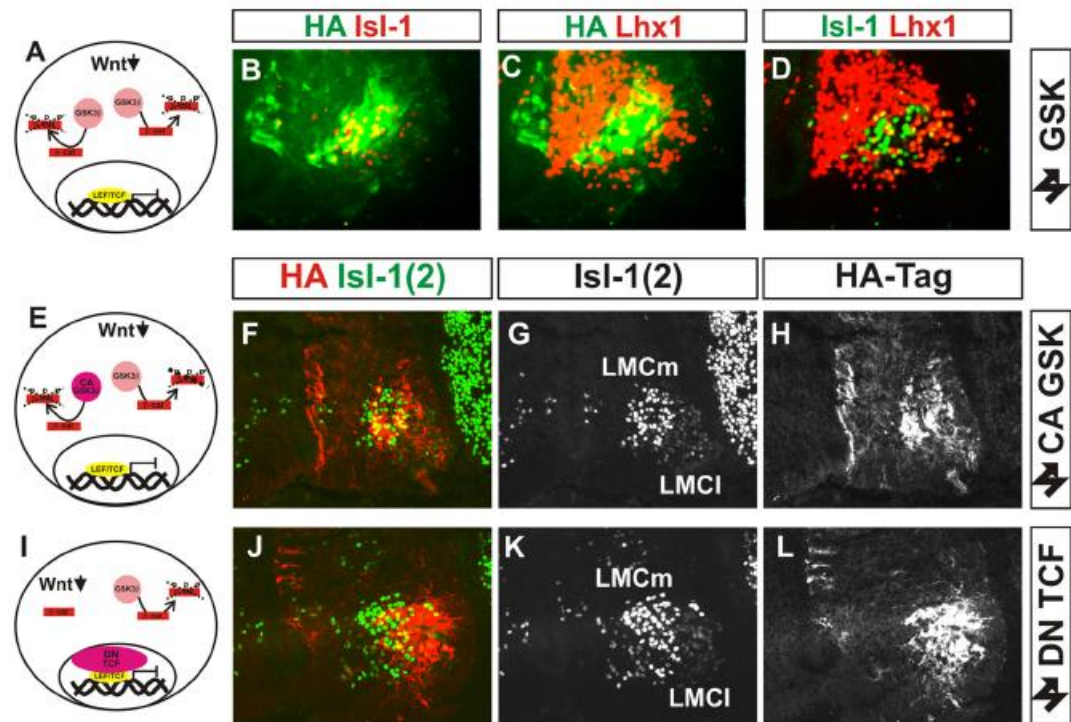
Figure 9. Downregulation of canonical Wnt signaling does not disrupt LMC neuron organization. *A–D*, Lack of effect on LMC organization of expression of wild-type GSK3β. *A*, Schematic of action of the construct. *B–D*, HA-tag (*B, C*, green), Islet-1 (*B*, red; *D*, green) and Lhx1 (*C, D*, red) immunoreactivity following electroporation of the construct. *E–L*, Downregulation of Wnt signaling pathway by expression of constitutively active GSK3β construct (*E–H*) or dominant-negative TCF transcription factor expression (*J–L*). *E, I*, Summary of action of each construct. Islet-1(2) immunohisto-chemistry (*F, G, J, K*) reveals normal motor neuron migration and divisional segregation following expression of the constructs, marked by HA immunoreactivity (*F, H, J, L*). Islet1(2) immunofluo-rescence is lower in LMCl than LMCm.

neuron migration being retarded. Thus, γ(L127A) does not perturb the generation of LMC neurons.

Expression of γ(L127A) resulted in a cell autonomous perturbation of LMC motor neuron position: ~60% of γ(L127A)$^{+ve}$ LMCl MNs were located close to the ventricle with a further ~25% found within the domain occupied by the LMCm. We found that the distances migrated were less than half those compared with control neurons, suggesting that migration of LMC neurons was severely compromised by γ(L127A). Importantly, LMC neurons on the experimental side of the spinal cord that had not acquired γ(L127A) behaved similarly to the control side of the spinal cord. While we cannot rule out an additional role for perturbed β-catenin expression in transitin radial glia in contributing to this migration phenotype, the cell autonomous nature of the effect of γ(L127A) strongly suggests that the predominant role for γ(L127A) is within the motor neurons themselves.

Stalled LMC migration causes buckling of the ventral pax6 progenitor domain

The majority of ventral Pax6 cells express neither β-catenin nor γ-catenin. Instead, transitin radial glia represent ~30% of these progenitor cells and express detectable levels of β-catenin. The general integrity of this progenitor domain and position of generation of motor neurons from it appears normal following NΔ390 or γ(L127A) manipulations. The ventral buckling of the

Pax6 domain was often seen in embryos where the Pax6 cells were not electroporated but was never observed when motor neurons were not electroporated. Further, motor neurons that had not acquired the γ(L127A) manipulation reached a normal settling position. Thus, the motor neurons stalled in their migration probably contribute most to the buckling of the Pax6 domain. We suggest that the force required for the buckling of the progenitor domain could arise from the continued mitotic activity of the ventral Pax6 domain cells. BrdU labeling following γ(L127A) expression demonstrated that cell division is not halted. Additionally, the number of Lhx1 cells arrested close to the ventricle surface was greater than the number of Hb9^{+ve}/Islet-1^{-ve} LMCl cells. Thus, the ventral Pax6 domain continues to generate postmitotic Lhx1 interneurons. This cell division might exert a force rearward away from stalled LMC neurons which would result in the progenitor domain buckling at its ventral extent.

Cadherin involvement in motor neuron migration

Cadherin dominant-negative expression (Fujimori and Takeichi, 1993) caused a similar phenotype to that of γ(L127A). We found that type I cadherins were not expressed in LMC motor neurons. Of the type II classical cadherins, cad-7 was expressed predominantly in most LMC neurons during divisional segregation and downregulated in the vast majority of the LMC thereafter. Downregulation of cad-7 by shRNA resulted in a similar
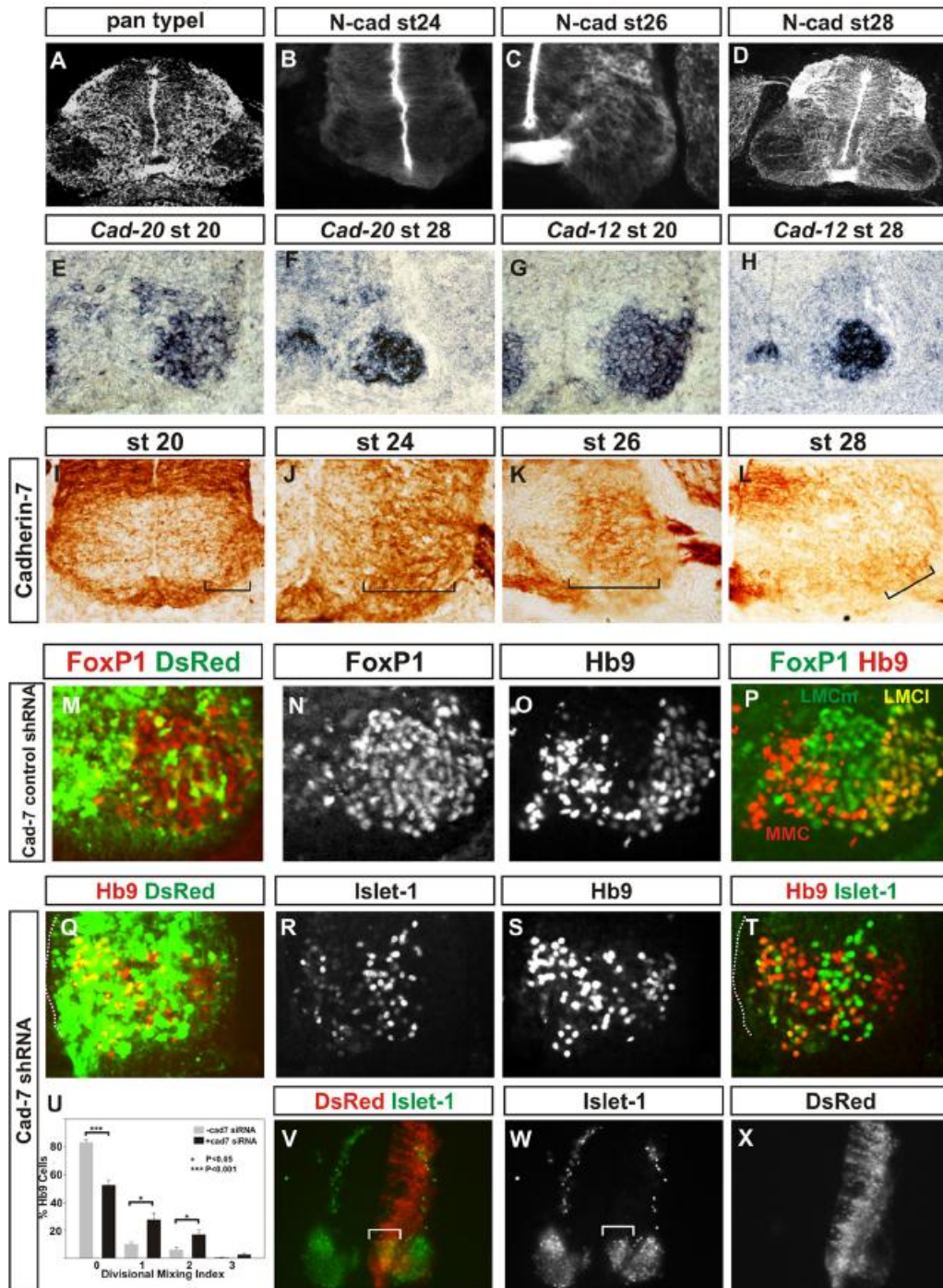
Figure 10. Pan-motor neuron type II cadherin expression and cadherin-7 siRNA restricts LMC neuron migration and divisional segregation. *A*, Pan type I cadherin immunolabeling at st28. *B–D*, N-cadherin immunoreactivity at st24 (*B*), st26 (*C*), and st28 (*D*). *E, F*, Cad-20 *in situ* hybridization in the ventral horn at st20 (*E*) and at caudal lumbar regions of st28 (*Figure legend continues.*)
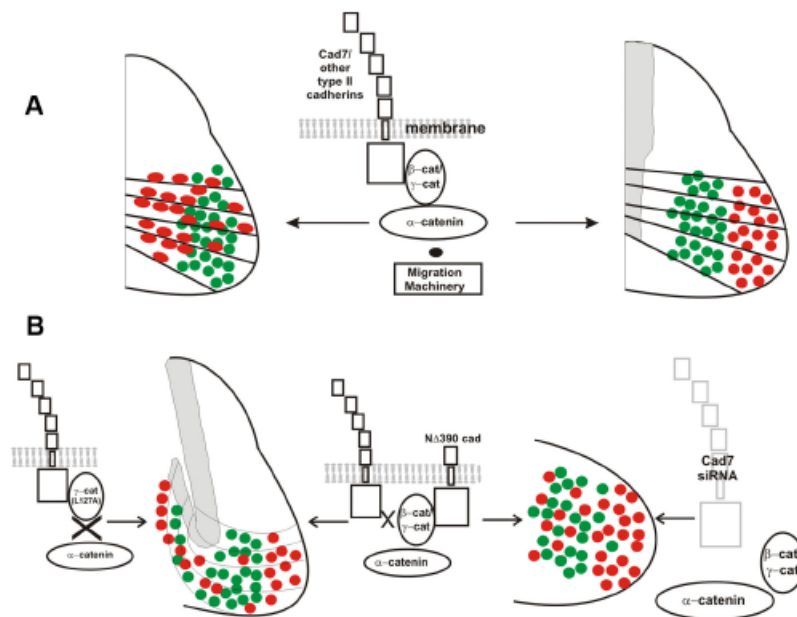
Figure 11. Schematic summary of results. *A*, Schematic of motor neuron migration along pathways of transitin radial glia and divisional segregation and schematic of cadherin–catenin interactions. *B*, Schematic of the effects of γ(L127A) on migration and divisional segregation. Cad-7 shRNA disrupts divisional segregation and NΔ390 cadherin expression results in migration and divisional segregation effects similar to γ(L127A) and the cad-7 shRNA.

←

(Figure legend continued.) (*F*). *G, H,* Cad-12 *in situ* hybridization in the ventral horn at st20 (*G*) and at caudal lumbar regions of st28 (*H*). *I–L,* Cad-7 immunohistochemistry in the ventral spinal cord at st20 (*I*) and in the ventral horn at HH st24 (*J*), st26 (*K*), and st28 (*L*). Cad-7 appears to be expressed in the majority of LMC neurons during their migration (*J–K*) and is weakly expressed in only a small subset of motor neurons subsequently (*L*). *M–P,* Cad-7 control shRNA expression. Foxp1 (*M, N, P*), a pan-LMC marker, and Hb9 immunoreactivity (*O, P*) show normal segregation and positioning of LMCl, LMCm, and medial motor column following control shRNA expression, marked by dsRed fluorescence in *M*. *Q–U,* Cad-7 shRNA perturbs LMC divisional segregation. *Q–T,* HB9 (*Q, S, T*) and Islet-1 (*R, T*) immunohistochemistry at st28 following expression of cad-7 shRNA revealed by dsRed fluorescence (*Q*). *Q, T,* Dotted lines, Ventricle surface. Note that there are motor neurons close to the ventricle surface. *U,* Divisional mixing index following cad-7 shRNA expression compared with cells that had not acquired the construct ($p < 0.001$ for the 0 bin, $p < 0.05$ for the 1 and 2 bins, Student's *t* test; χ^2 analysis, $p < 0.001$ 2df). *V–X,* Islet-1 immunohistochemistry (*V, W*) at st24 reveals a perturbation of LMCm migration following cad-7 shRNA expression (*V, W,* bracket) revealed by dsRed fluorescence (*V, X*); note the paucity of dsRed fluorescence in the lateral LMC.

migration and divisional mixing phenotype to that observed in NΔ390 expression: motor neurons were found close to the ventricle and LMCm and LMCl divisions were mixed. Cad-7 appears not to be expressed in ventral transitin radial glia. This further suggests that the predominant role for cadherins in motor neuron migration is within the motor neurons themselves. Demireva et al. (2011) reported perturbed LMC organization following conditional ablation of both β- and γ-catenin from mouse motor neurons. These findings are in broad agreement with those presented here. However, this conditional ablation approach in mouse revealed a much milder migration phenotype than we show for the chicken. Differences in gene expression, rate of motor neuron generation, and migration between chicken and mouse may underlie differences in severity of catenin and cadherin manipulations in these different species.

How could cadherin and catenin function facilitate motor neuron migration? A model has recently been proposed whereby α-catenin acts as a molecular clutch that links substrate adhesion to retrograde actin flow during cell migration (Bard et al., 2008). Our results are consistent with a model where both γ(L127A) and NΔ390 constructs perturb γ-catenin function intracellularly within motor neurons, disrupting cell migration, likely mediated at least in part through cad-7-based linkage to the migration machinery. Whether retrograde actin flow is a dominant force in motor neuron migration as it is in other cell types will require further characterization of the dynamics of cadherin and catenin linkage (Drees et al., 2005; Yamada et al., 2005) to the actin cytoskeleton during motor neuron migration.

Neuronal nucleus formation through regulated cadherin function

The LMC is organized as a neuronal nucleus. Neuronal nuclei are generally found in more evolutionarily ancient regions of the CNS. It seems likely that the mechanisms of nucleogenesis will reveal similarities and differences with organizational mechanisms in evolutionarily newer regions of the CNS, such as the lamination of the cortex (Rakic, 2006; Lui et al., 2011). Radial glia provide a scaffold for excitatory projection neuronal migration in the cortex and are a major progenitor cell type of the ventricular zone. Additional progenitor cells, generated from radial glia, are found more basally in the subventricular zone (Noctor et al., 2004). Within the spinal cord, radial glia delineate pathways of spinal motor neuron migration, although, in contrast to the cortex, spinal transitin glia represent only a small proportion of the ventral progenitor cells. Additionally, these radial glia are basal to the ventricular progenitor cells. One major difference in the generation of motor neurons from

that observed to drive lamination of the cortex is the rate at which LMC neurons are generated. Rapid LMC generation results in a backlog of neurons waiting to migrate. In contrast, neurons in the cortex destined to populate more superficial layers are born sequentially and migrate in an ordered fashion to generate the layers of the laminated cortex (Noctor et al., 2004). It is likely that the availability of spinal radial glia represents a rate limiting step for motor neuron migration.

We have demonstrated that early, pan-motor neuron cadherin function is required for LMC divisional segregation through neuronal migration. Subsequently, differential type II cadherin function is required for motor neuron pool formation (Price et al., 2002; Patel et al., 2006). Our results therefore suggest a prolonged requirement for cadherin function in all phases of motor neuron cell body organization. How could cadherin-dependent radial LMC migration and later motor pool sorting be coupled? Recent work has suggested that perturbation of reelin signals disrupts later phases of motor neuron organization (Palmesino et al., 2010). Reelin can regulate cadherin function in the control of neuronal migration in the cortex (Franco et al., 2011). Thus, reelin signaling may provide a mechanism for dissociation of cadherin- and catenin-mediated radial migration from a later involvement of cadherin expression in motor pool sorting.

References

Abe K, Takeichi M (2008) EPLIN mediates linkage of the cadherin catenin complex to F-actin and stabilizes the circumferential actin belt. Proc Natl Acad Sci U S A 105:13–19.

Aberle H, Schwartz H, Hoschuetzky H, Kemler R (1996) Single amino acid substitutions in proteins of the armadillo gene family abolish their binding to alpha-catenin. J Biol Chem 271:1520–1526.

Agarwala S, Ragsdale CW (2002) A role for midbrain arcs in nucleogenesis. Development 129:5779–5788.

Bard L, Boscher C, Lambert M, Mège RM Choquet D, Thoumine O (2008) A molecular clutch between the actin flow and N-cadherin adhesions drives growth cone migration. J Neurosci 28:5879–5890.

Barnes SH, Price SR, Wentzel C, Guthrie SC (2010) Cadherin-7 and cadherin-6B differentially regulate the growth, branching and guidance of cranial motor axons. Development 137:805–814.

Barron DH (1946) Observations on the early differentiation of the motor neuroblasts in the spinal cord of the chick. J Comp Neurol 85:149–169.

Briscoe J, Pierani A, Jessell TM, Ericson J (2000) A homeodomain protein code specifies progenitor cell identity and neuronal fate in the ventral neural tube. Cell 101:435–445.

Cajal SR (1995) Histology of the nervous system of man and vertebrates. New York: Oxford UP.

Ciani L, Krylova O, Smalley MJ, Dale TC, Salinas PC (2004) A divergent canonical WNT-signaling pathway regulates microtubule dynamics: dishevelled signals locally to stabilize microtubules. J Cell Biol 164:243–253.

Cole GJ, Lee JA (1997) Immunocytochemical localization of a novel radial glial intermediate filament protein. Brain Res Dev Brain Res 101:225–238.

Das RM, Van Hateren NJ, Howell GR, Farrell ER, Bangs FK, Porteous VC, Manning EM, McGrew MJ, Ohyama K, Sacco MA, Halley PA, Sang HM, Storey KG, Placzek M, Tickle C, Nair VK, Wilson SA. (2006) A robust system for RNA interference in the chicken using a modified microRNA operon. Dev Biol 294:554–563.

Dasen JS, De Camilli A, Wang B, Tucker PW, Jessell TM (2008) Hox repertoires for motor neuron diversity and connectivity gated by a single accessory factor, FoxP1. Cell 134:304–316.

Demireva EY, Shapiro LS, Jessell TM, Zampieri N (2011) Motor neuron position and topographic order imposed by β- and γ-catenin activities. Cell 147:641–652.

Drees F, Pokutta S, Yamada S, Nelson WJ, Weis WI (2005) Alpha-catenin is a molecular switch that binds E-cadherin-beta-catenin and regulates actin-filament assembly. Cell 123:903–915.

Eide AL, Glover JC (1996) Development of an identified spinal commissural interneuron population in an amniote: neurons of the avian Hofmann nuclei. J Neurosci 16:5749–5761.

Franco SJ, Martinez-Garay I, Gil-Sanz C, Harkins-Perry SR, Müller U (2011) Reelin regulates cadherin function via Dab1/Rap1 to control neuronal migration and lamination in the neocortex. Neuron 69:482–497.

Fujimori T, Takeichi M (1993) Disruption of epithelial cell–cell adhesion by exogenous expression of a mutated nonfunctional N-cadherin. Mol Biol Cell 4:37–47.

Haase G, Dessaud E, Garcès A, de Bovis B, Birling M, Filippi P, Schmalbruch H, Arber S, deLapeyrière O (2002) GDNF acts through PEA3 to regulate cell body positioning and muscle innervation of specific motor neuron pools. Neuron 35:893–905.

Hamburger V, Hamilton HL (1992) A series of normal stages in the development of the chick embryo. 1951. Dev Dyn 195:231–272.

Hirano S, Suzuki ST, Redies C (2003) The cadherin superfamily in neural development: diversity, function and interaction with other molecules. Front Biosci 8:d306–d355.

Hollyday M, Hamburger V (1977) An autoradiographic study of the formation of the lateral motor column in the chick embryo. Brain Res 132:197–208.

Imamura Y, Itoh M, Maeno Y, Tsukita S, Nagafuchi A (1999) Functional domains of alpha-catenin required for the strong state of cadherin-based cell adhesion. J Cell Biol 144:1311–1322.

Itoh M, Nagafuchi A, Moroi S, Tsukita S (1997) Involvement of ZO-1 in cadherin-based cell adhesion through its direct binding to alpha catenin and actin filaments. J Cell Biol 138:181–192.

Jessell TM (2000) Neuronal specification in the spinal cord: inductive signals and transcriptional codes. Nat Rev Genet 1:20–29.

Kawakami K, Noda T (2004) Transposition of the Tol2 element, an Ac-like element from the Japanese medaka fish Oryzias latipes, in mouse embryonic stem cells. Genetics 166:895–899.

Kintner C (1992) Regulation of embryonic cell adhesion by the cadherin cytoplasmic domain. Cell 69:225–236.

Krylova O, Messenger MJ, Salinas PC (2000) Dishevelled-1 regulates microtubule stability: a new function mediated by glycogen synthase kinase-3β. J Cell Biol 151:83–94.

Landmesser L (1978) The distribution of motoneurones supplying chick hind limb muscles. J Physiol 284:371–389.

Leber SM, Sanes JR (1995) Migratory pathways of neurons and glia in the embryonic chick spinal cord. J Neurosci 15:1236–1248.

Leber SM, Breedlove SM, Sanes JR (1990) Lineage, arrangement, and death of clonally related motoneurons in the chick spinal cord. J Neurosci 10:2451–2462.

Lin JH, Saito T, Anderson DJ, Lance-Jones C, Jessell TM, Arber S (1998) Functionally related motor neuron pool and muscle sensory afferent subtypes defined by coordinate ETS gene expression. Cell 95:393–407.

Livet J, Sigrist M, Stroebel S, De Paola V, Price SR, Henderson CE, Jessell TM, Arber S (2002) ETS gene Pea3 controls the central position and terminal arborization of specific motor neuron pools. Neuron 35:877–892.

Lui JH, Hansen DV, Kriegstein AR (2011) Development and evolution of the human neocortex. Cell 146:18–36.

Luo J, Ju MJ, Redies C (2006) Regionalized cadherin-7 expression by radial glia is regulated by Shh and Pax7 during chicken spinal cord development. Neuroscience 142:1133–1143.

Momose T, Tonegawa A, Takeuchi J, Ogawa H, Umesono K, Yasuda K (1999) Efficient targeting of gene expression in chick embryos by microelectroporation. Dev Growth Differ 41:335–344.

Nelson WJ, Nusse R (2004) Convergence of Wnt, beta-catenin, and cadherin pathways. Science 303:1483–1487.

Noctor SC, Martínez-Cerdeño V, Ivic L, Kriegstein AR (2004) Cortical neurons arise in symmetric and asymmetric division zones and migrate through specific phases. Nat Neurosci 7:136–144.

Nollet F, Kools P, van Roy F (2000) Phylogenetic analysis of the cadherin superfamily allows identification of six major subfamilies besides several solitary members. J Mol Biol 299:551–572.

Palmesino E, Rousso DL, Kao TJ, Klar A, Laufer E, Uemura O, Okamoto H, Novitch BG, Kania A (2010) Foxp1 and lhx1 coordinate motor neuron migration with axon trajectory choice by gating reelin signalling. PLoS Biol 8:e1000446.

Patel SD, Ciatto C, Chen CP, Bahna F, Rajebhosale M, Arkus N, Schieren I, Jessell TM, Honig B, Price SR, Shapiro L (2006) Type II cadherin ectodomain structures: implications for classical cadherin specificity. Cell 124:1255–1268.

Price SR, De Marco Garcia NV, Ranscht B, Jessell TM (2002) Regulation of

motor neuron pool sorting by differential expression of type II cadherins. Cell 109:205–216.

Rakic P (2006) A century of progress in corticoneurogenesis: from silver impregnation to genetic engineering. Cereb Cortex 16 [Suppl 1]:i3–i17.

Romanes GJ (1964) The motor pools of the spinal cord. Prog Brain Res 11:93–119.

Roose J, Huls G van Beest M, Moerer P, van der Horn K, Goldschmeding R, Logtenberg T, Clevers H (1999) Synergy between tumor suppressor APC and the β-catenin-Tcf4 target Tcf1. Science 285:1923–1926.

Rousso DL, Gaber ZB, Wellik D, Morrisey EE, Novitch BG (2008) Coordinated actions of the forkhead protein Foxp1 and Hox proteins in the columnar organization of spinal motor neurons. Neuron 59:226–240.

Sato Y, Kasai T, Nakagawa S, Tanabe K, Watanabe T, Kawakami K, Takahashi Y (2007) Stable integration and conditional expression of electroporated transgenes in chicken embryos. Dev Biol 305:616–624.

Sockanathan S, Jessell TM (1998) Motor neuron-derived retinoid signaling specifies the subtype identity of spinal motor neurons. Cell 94:503–514.

Tanabe K, Takahashi Y, Sato Y, Kawakami K, Takeichi M, Nakagawa S (2006) Cadherin is required for dendritic morphogenesis and synaptic terminal organization of retinal horizontal cells. Development 133:4085–4096.

Tosney KW, Landmesser LT (1985) Development of the major pathways for neurite outgrowth in the chick limb. Dev Biol 109:193–214.

Tsuchida T, Ensini M, Morton SB, Baldassare M, Edlund T, Jessell TM, Pfaff SL. (1994) Topographic organization of embryonic motor neurons defined by expression of LIM homeobox genes. Cell 79:957–970.

Uemura M, Takeichi M (2006) Alpha N-catenin deficiency causes defects in axon migration and nuclear organization in restricted regions of the mouse brain. Dev Dyn 235:2559–2566.

Watanabe T, Saito D, Tanabe K, Suetsugu R, Nakaya Y, Nakagawa S, Takahashi Y (2007) Tet-on inducible system combined with in ovo electroporation dissects multiple roles of genes in somitogenesis of chicken embryos. Dev Biol 305:625–636.

Weis WI, Nelson WJ (2006) Re-solving the cadherin-catenin-actin conundrum. J Biol Chem 281:35593–35597.

Wentworth LE (1984) The development of the cervical spinal cord of the mouse embryo. I. A Golgi analysis of ventral root neuron differentiation. J Comp Neurol 222:81–95.

Whitelaw V, Hollyday M (1983) Thigh and calf discrimination in the motor innervation of the chick hindlimb following deletions of limb segments. J Neurosci 3:1199–1215.

William CM, Tanabe Y, Jessell TM (2003) Regulation of motor neuron subtype identity by repressor activity of Mnx class homeodomain proteins. Development 130:1523–1536.

Yamada S, Pokutta S, Drees F, Weis WI, Nelson WJ (2005) Deconstructing the cadherin-catenin-actin complex. Cell 123:889–901.

Zhurinsky J, Shtutman M, Ben-Ze'ev A (2000a) Plakoglobin and beta-catenin: protein interactions, regulation and biological roles. J Cell Sci 113:3127–3139.

Zhurinsky J, Shtutman M, Ben-Ze'ev A (2000b) Differential mechanisms of LEF/TCF family-dependent transcriptional activation by β-catenin and plakoglobin. Mol Cell Biol 20:4238–4252.